



UNIVERSITÄT
BAYREUTH

Soil Physics Group

Flow and transport processes as affected by tillage management under monsoonal conditions in South Korea

Dissertation

to obtain the academic degree of Doctor of Natural Science (Dr. rer. nat.)
of the Bayreuth Graduate School for Mathematical and Natural Sciences of the University of Bayreuth

presented by

Marianne C. Ruidisch
born 18th March 1979 in Munich

Bayreuth, September 2012

This doctoral thesis was prepared at the Department of Soil Physics, University of Bayreuth between April 2009 and September 2012. It was supervised by Prof. Dr. Bernd Huwe, Prof. Dr. Stefan Peiffer and Prof. Dr. John Tenhunen.

This is a full reprint of the dissertation submitted to attain the academic degree of Doctor of Natural Sciences (Dr. rer. nat.) and approved by the Bayreuth Graduate School of Mathematical and Natural Sciences (BayNAT) of the University of Bayreuth.

Date of submission: September 28, 2012
Approval by executive committee: October 15, 2012
Date of defense (disputation): January 22, 2013

Director: Prof. Dr. F. X. Schmid

Doctoral Committee:

Prof. Dr. Bernd Huwe, 1st reviewer
Dr. Jan Fleckenstein, 2nd reviewer
Prof. Dr. Thomas Köllner, Chairman
Prof. Dr. John Tenhunen

Summary

A sustainable agriculture, which provides on the one hand enough yields to satisfy the food demand, and on the other hand minimizes the impacts on ecosystem services such as provision of high water quality, is challenging especially in regions with extreme weather conditions. In this thesis, the current status of the dryland farming agricultural practices under monsoonal conditions, namely plastic mulch ridge cultivation, and its impact on flow processes and nitrate transport was investigated in detail.

A variety of field measurements and tracer experiments in combination with process-based numerical modeling techniques were used to identify the main characteristics of soil hydrological processes such as soil water dynamics, preferential flow, surface runoff, soil erosion and fertilizer nitrate leaching. On hillslopes, we investigated surface and subsurface flow processes in four plastic mulched potato fields (*Solanum tuberosum L.*) using a monitoring network of tensiometers and water content sensors as well as runoff collectors in combination with flow dividers. Since these measurements do not consider preferential flow processes, we additionally carried out tracer experiments using the dye Brilliant Blue FCF. The datasets we obtained of matric potentials, surface runoff and sediment concentrations were used to calibrate the HYDRUS 2/3D and the EROSION 3D model in order to quantify drainage water fluxes, surface runoff and erosion rates of plastic mulched ridge tillage (RT_{pm}) compared to ridge tillage without coverage (RT) and conventional flat tillage (CT).

Plastic mulch affects soil water dynamics dominantly during dry periods and during small rain events, when soil in ridge positions was drier compared to furrow positions caused by the protective function of the plastic coverage and root water uptake in ridges. Hence, pressure head gradients induced lateral flow from furrows to ridges in the topsoil. Under RT the differences in soil moisture were caused only by ridge topography. Thus, horizontal pressure head gradients were weakened compared to RT_{pm}. For CT, pressure head gradients were distinct vertically, which forced the water to flow vertically from the topsoil to the subsoil. Under monsoonal conditions, the differences in soil moisture between ridges and furrows were almost absent since the soil was near saturation or fully saturated. During these events, down slope lateral flow occurred in the coarse textured topsoil due to its higher hydraulic conductivity compared to the subsoil. Based on the dye tracer experiments, we found that plastic mulching caused non-infiltration zones, namely plastic mulched ridges and zones of infiltration in furrows and planting holes, where the tracer infiltrates uniformly into the sandy topsoil matrix. Despite management treatments, we found that lateral funnel flow above the tillage pan was the most prominent feature. In contrast to our expectations, macropore flow via fissures and cracks in deeper soil horizons was not detected. The field and modeling studies revealed that surface runoff was substantially increased by plastic mulch compared to RT and CT. However, the field topography primarily controlled surface runoff and erosion rates. The concavity of the field led to flow accumulation and high erosion losses in the center of the field, while a convex shape resulted in less soil erosion, because water was channeled in furrows to the field edges.

In a flat terrain, N fate under varying fertilizer rates was investigated in a plastic mulched radish cultivation (*Raphanus sativus*) using a suction lysimeter study in combination with soil water dynamics measurements and a ¹⁵N tracer experiment. Arranged in a randomized block design, plots were treated with fertilizer rates of 50, 150, 250 and 350 kg NO₃⁻ ha⁻¹. Leaching was found to be the main prominent pathway for NO₃⁻ especially during the early season, when crops had not yet emerged. Furthermore, the biomass production did not significantly differ between fertilizer rates of 150 to 350 kg ha⁻¹. Hence, we recommend the lowest NO₃⁻ fertilizer application of 150 kg ha⁻¹ in combination with a better fertilizer placement and split applications. Based on the obtained datasets of nitrate concentrations and matric potentials we subsequently calibrated a water flow and solute transport model using the numerical code HydroGeoSphere coupled with

ParallelPEST. We simulated whether the given recommendations on fertilizer best management practices (FBMPs), such as a better placement and split application, decreased NO_3^- leaching amounts. Compared to RT under conventional fertilization in ridges and furrows, the simulations showed that NO_3^- leaching can be considerably reduced up to 82% by combining RT_{pm} , fertilizer placement only in ridges and split applications with a total fertilizer NO_3^- amount of 150 kg ha^{-1} .

Based on these findings, the impact of plastic mulched ridge cultivation on flow and transport processes has to be evaluated differently depending on terrain complexity. In a flat terrain, where surface runoff processes are absent or minimal and precipitation contributes entirely to groundwater recharge, RT_{pm} has several advantages. Beside functions such as weed control, and earlier plant emergence due to higher temperatures, plastic mulching decreases drainage water and NO_3^- leaching during the growing season. Thus, RT_{pm} enhances nutrient retention below the plastic coverage and reduces the risk of groundwater contamination by highly mobile agrochemical substances. In a sloped terrain, where precipitation contributes substantially to surface runoff, plastic mulching even increases runoff processes, inducing a high risk of flooding, soil erosion and surface leaching of agrochemicals into aquatic systems.

This thesis provides several recommendations, aiming to minimize environmental impacts and concurrently to decrease costs of fertilizer and herbicide inputs. In order to reduce surface runoff and soil erosion at fields on hillslopes, we suggest applying perforated plastic mulch instead of impermeable plastic mulch and a ridge configuration following contours of the field. Furthermore, we recommend omitting application of herbicides to furrows in order to allow weed growth. This would lead to a higher surface roughness in furrows, which in turn slows down runoff processes. These suggestions would obviously increase infiltration, thus, the subsurface flow processes automatically become more important. However, preferential flow in macropores to deeper soil layers was found to be absent, which is a good indicator for minor groundwater contamination risk. Since funnel flow above the tillage pan was found to be the most important preferential flow path, we propose to protect the river network from contaminant discharge via subsurface lateral flow by the establishment of riparian buffer zones. This would also help to reduce the discharge of sediments, fertilizers and agrochemicals via surface runoff into the streams. Finally, fertilizer best management practices (FBMPs) such as fertilizer placement only in ridges and split applications as well as the combination of both, were found to decrease nitrate leaching considerably. Hence, we suggest applying FBMPs in combination with impermeable plastic mulch in flat terrain, while on hillslopes FBMPs should be applied in combination with perforated plastic mulch. The recommendations imply that the risk of leaching becomes more important after harvest when the plastic mulched ridges are removed and the remaining nitrate is prone to leaching. Therefore, we recommend to cultivate cover crops after harvest to improve N fixation, to reduce NO_3^- leaching, to increase the organic carbon content of the soils as well as to prevent soil erosion in autumn.

Zusammenfassung

Die heutige Landwirtschaft wird durch den Anspruch auf Nachhaltigkeit vor enorme Herausforderungen gestellt. Einerseits müssen hohe Erträge erzielt werden, um die steigende Nachfrage nach landwirtschaftlichen Produkten zu befriedigen. Andererseits sollen jedoch gleichzeitig negative Auswirkungen auf ökosystemare Dienstleistungen wie z.B. Belastungen der Grund- und Fließgewässer minimiert werden. Diese Herausforderungen stellen sich umso dringlicher in Gebieten, die Wetterextremen wie z.B. Starkregenereignissen ausgesetzt sind. In der vorliegenden Studie wurde der Trockenfeldbau im monsungeprägten Haean Einzugsgebiet in Südkorea, der fast ausschließlich als Dammanbau mit Plastikfolienbedeckung praktiziert wird, aus bodenhydrologischer Sicht detailliert auf dessen Auswirkungen auf die Fließ- und Transportprozesse untersucht.

Um die maßgeblichen bodenhydrologischen Prozesse wie die Bodenwasserdynamik, präferentielles Fließen, Oberflächenabfluss, Bodenerosion und Nitrattransport zu identifizieren, wurden zahlreiche Feldmessungen und Tracer-Experimente durchgeführt. Die dabei erhobenen Datensätze dienen u.a. zur Kalibrierung prozess-basierter numerischer Modelle. Die Bodenwasserdynamik, der Oberflächenabfluss und der Sedimenttransport wurden auf Kartoffelfeldern (*Solanum tuberosum* L.) mit typischer Dammkultivierung und Plastikfolienbedeckung in Hanglage mittels eines Messnetzes aus Tensiometern, Wassergehaltssensoren und Oberflächenabflusskollektoren untersucht. Eine Erfassung von präferentiellen Fließwegen war durch diese Messtechniken nicht möglich, sodass zusätzlich Beregnungsexperimente mit dem Tracer Brilliant Blue FCF durchgeführt wurden. Die Modelle Hydrus 2/3D und Erosion 3D wurden mit den erhobenen Datensätzen kalibriert, um die ober- und unterirdischen Flüsse sowie die Erosionsraten beim Dammanbau mit Plastikfolienbedeckung zu quantifizieren und außerdem mit anderen Anbaupraktiken wie der Dammkultivierung ohne Folie und dem konventionellen Anbau auf ebener Oberfläche zu vergleichen. Die Untersuchungen haben gezeigt, dass die Bodenwasserdynamik durch den folienbedeckten Dammanbau maßgeblich in trockenen Perioden bzw. während kleinerer Regenereignisse beeinflusst wird. Die schützende Funktion der Folie sowie die Wasseraufnahme der Wurzeln in den Dämmen verursachen horizontale Druckgradienten, die ein laterales Fließen von den feuchteren Furchen hin zu den trockeneren Dämmen verursachen. Diese horizontalen Druckgradienten waren unter Dammanbau ohne Folie deutlich schwächer ausgeprägt und unter konventionellem Anbau nicht vorhanden, so dass bei einer flachen Oberfläche ein vertikales Fließfeld charakteristisch war. Monsunale Regenereignisse führten demgegenüber zur (fast) vollständigen Sättigung des Bodens. Die Simulationen zeigten weiterhin, dass die grobe Textur des Oberbodens sowie dessen höhere hydraulische Leitfähigkeit gegenüber dem Unterboden einen Zwischenabfluss auf dessen Grenzfläche verursachen.

Die Tracer-Experimente ergaben, dass der Dammanbau mit Folienbedeckung bevorzugt Zonen der Infiltration (Furchen und Pflanzlöcher) hervorruft, in denen der Tracer homogen in die sandige Bodenmatrix infiltrierte. Präferentielles Fließen in Form eines lateralen Fließens auf der Pflugsohle trat bei allen Versuchen unabhängig von den Anbaupraktiken auf. Entgegen unserer Erwartung wurde kein Makroporenfluss in Spalten und Rissen im Unterboden festgestellt. Insgesamt ergaben sowohl die Feldmessungen als auch die Modellierung, dass der Oberflächenabfluss durch den Dammfolienanbau extrem erhöht wird. Ob der Oberflächenabfluss erosionswirksam war, hing von der jeweiligen Topografie des Feldes ab. Eine konkave Form des Feldes führte zur Flussakkumulation in der Mitte des Feldes und verursachte dort erhebliche Bodenerosion. Eine konvexe Form des Feldes leitete hingegen den Oberflächenabfluss in den Furchen zu den Felldrändern, sodass hier nur geringe Erosionsraten simuliert wurden.

In der Beckenebene wurde auf einem Rettichfeld (*Raphanus sativus*) der Verbleib des Stickstoffs anhand ^{15}N markierten Düngers sowie mit Saugkerzen, Tensiometern und Wassergehaltssensoren in Kombination mit vier verschiedenen Düngerraten untersucht. Die Düngerraten mit

50, 150, 250 und 350 kg ha⁻¹ wurden in zufällig angeordneten Parzellen appliziert. Generell wurde festgestellt, dass die Auswaschung des Stickstoffs besonders in der frühen Wachstumsphase der Pflanzen die größte Rolle spielt. Außerdem ergab die Studie, dass sich die Biomasse des Rettichs zwischen den drei höchsten Düngerraten nicht signifikant unterschied. Aufgrund dieser Ergebnisse wurde empfohlen, die Düngerrate auf 150 kg ha⁻¹ zu beschränken, den Dünger besser zu platzieren und ihn in mehreren Raten aufzugeben. Die gemessenen Nitratkonzentrationen und Matrixpotentiale wurden daraufhin verwendet, um ein Wasserdynamik- und Stofftransportmodell zu kalibrieren und um verschiedene Düngermanagement-Szenarien zu simulieren. Die Management-Szenarien wurden in Hinblick auf die kumulative Nitratauswaschung bewertet. Im Vergleich zur Dammkultivierung ohne Folie und einer konventionellen Düngung in Furchen und Dämmen, kann die Nitratauswaschung bei plastikbedeckten Dämmen, einer Gesamtdüngerrate von 150 kg ha⁻¹ aufgeteilt in drei Applikationen und einer Platzierung des Düngers nur in den Dämmen um bis zu 82% reduziert werden.

In Anbetracht der erzielten Ergebnisse muss der folienbedeckte Dammanbau in Abhängigkeit vom jeweiligen Gelände bewertet werden. In der Ebene, wo der Niederschlag fast gänzlich infiltriert und zur Grundwasserneubildung beiträgt, bietet die Dammkultivierung mit Plastikfolienbedeckung große Vorteile. Neben den Funktionen der Unkrautkontrolle und einer früheren Keimung infolge höherer Temperaturen unter der Folie, verringert sie die Entwässerung und die Nitratauswaschung in der Anbauphase erheblich. Somit kann die Nährstoffverfügbarkeit unter der Folie erhöht und gleichzeitig das Risiko einer Grundwasserkontamination aufgrund hochmobiler Düngemittel und Agrochemikalien gesenkt werden. Dagegen wird in Hanglagen ein erheblicher Teil des Niederschlages abflusswirksam. Die Plastikbedeckung auf Hängen steigert zudem den direkten Abfluss, wodurch ein erhöhtes Risiko der Überflutung, der Bodenerosion und des oberflächlichen Stofftransports in die Gewässernetze entsteht.

Die vorliegende Arbeit unterbreiten mehrere Vorschläge, um das Risiko von Umweltbelastungen und die Kosten für Dünger und Herbizide zu reduzieren. Um den direkten Abfluss und Bodenerosion auf den Hängen zu verringern, schlagen wir die Aufbringung einer perforierten Folie vor. Zudem sollten die Dämme exakt entlang der Feldkonturen verlaufen. Die Oberflächenrauigkeit der Furchen könnte durch Unkrautwachstum erhöht werden, wodurch die Kosten für Herbizide eingespart werden könnten. Folgt man diesen Empfehlungen, so wird auch die Infiltration erhöht, sodass den unterirdischen Fließprozessen eine größere Bedeutung zukommen würde. Das Risiko einer Grundwasserkontamination kann dagegen aufgrund fehlender Makroporenflüsse im Unterboden als gering eingestuft werden. Der präferentielle Fluss auf der Pflugsohle würde sich jedoch verstärken. Daher empfiehlt es sich, Pufferzonen zwischen Fließgewässern und landwirtschaftlichen Flächen anzulegen, um den Eintrag von Düngemitteln und anderen Agrochemikalien durch ober- und unterirdische Abflüsse zu minimieren. Durch die Kombination von insgesamt niedrigeren Düngerraten mit einer besseren Platzierung des Düngers nur in den Dämmen und einer mehrfachen Aufbringung von kleineren Düngerraten, kann die Auswaschung der Nährstoffe erheblich reduziert werden. Wir empfehlen daher, das Düngermanagement in Hanglagen in Kombination mit perforiertem Plastik und in der Ebene in Kombination mit undurchlässigem Plastik zu praktizieren. Die diese Maßnahmen aber nach der Ernte und der Entfernung der plastikbedeckten Dämme ein erhöhtes Auswaschungsrisiko implizieren, schlagen wir vor, bodenbedeckende Zwischenfrüchte zu kultivieren, um damit sowohl die Stickstoff-Fixierung und den Anteil an organischer Substanz im Boden zu erhöhen als auch das Risiko der Auswaschung und der Bodenerosion im Herbst zu senken.

Acknowledgements

In the last three and a half years I gained a lot of experiences not only in the fields of research but also in the fields of social and cultural life. During this time I picked up manifold skills from simply radish planting through to complicated numerical modeling. This range indicates the interesting and diversified time, which I experienced during my PhD.

I'm sincerely grateful to my principal supervisor Prof. Dr. Bernd Huwe for giving me the opportunity to do my PhD in such an interesting research field within the Soil Physics Group, for his good ideas and discussions and for his guidance when questions or problems arose but also for the opportunity to work own-initiative. I'm also grateful to the head of TERRECO, Prof. Dr. John Tenhunen, who supported me during my PhD and who recently gave me the opportunity to work for him in the second phase of TERRECO.

Special thanks go to Frau Wittke, Marga Wartinger and Frau Rothe, who supported me by pulling numerous strings behind the scenes. I'm very grateful to our technician Andreas Kolb. Without him the field experiments would not have been possible. It was hard work, but concurrently much fun to "experience the blue miracle" with you. I also would like to thank Iris Schmiedinger for supporting me in the laboratory in Bayreuth.

I gratefully thank Sebastian Arnhold for numerous fruitful discussions and for always finding solutions regardless which kind of problems we faced. Furthermore, I want to thank especially Christina Bogner and Sven Frei, who always kindly granted me their time for teaching patiently image processing, modelling and for the countless and helpful discussions.

I'm thankful to all TERRECO-Members, who supported me during the last three and a half years. Working and occasionally living with all of you was a unique experience and unforgettable time, which I don't want to miss. I also want to thank Frau Kwon and Mr. Park, who allowed us a deep insight in the real korean life by adopting and helping us like family members.

Many thanks go to my friends Janine Kettering, Svenja Bartsch, Eunyoung Jung and Bora Lee, who always enriched my time in Korea and in Bayreuth. A working relationship, which turns out to be a friendship is always special and I'm very grateful for this.

I'm very much thankful to my family, to Sandra Brix, and especially to David, who always encouraged me to keep at it, particularly in periods of difficulty. David, I cannot find words to express my gratitude for supporting me in so many different ways during this challenging time.

Contents

Summary	ii
Zusammenfassung	iv
Acknowledgements	vi
Table of contents	vii
List of figures	ix
List of tables	xi
List of abbreviations	xiii
List of symbols	xv
1 General introduction	1
1.1 Agriculture, ecosystem services and climate change	1
1.2 Water flow and solute transport as affected by tillage in agricultural soils	2
1.3 Methodological approaches in soil hydrology	5
1.4 Objective of the thesis	6
1.5 Study Area	8
1.6 Synopsis	11
1.6.1 Soil water dynamics as affected by tillage management systems (Chapter 2)	11
1.6.2 Preferential flow as affected by tillage management systems (Chapter 3) .	15
1.6.3 Surface runoff and soil erosion as affected by tillage management systems (Chapter 4)	20
1.6.4 N fate in a plastic mulched ridge cultivation system (Chapter 5)	22
1.6.5 Fertilizer best management practices for reducing nitrate leaching: A mod- eling study (Chapter 6)	25
1.6.6 Concluding remarks and further research	30
1.7 List of manuscripts and specification of contribution	31
2 Modeling water flow in a plastic mulched ridge cultivation system on hill- slopes affected by South Korean summer monsoon	35
2.1 Introduction	36
2.2 Materials and methods	38
2.2.1 Study area	38
2.2.2 Field measurements	40
2.2.3 Modeling approach	41
2.2.3.1 Governing flow equations	41
2.2.3.2 Model parameterization	42
2.2.3.3 Initial and boundary Conditions	43
2.2.3.4 Model evaluation statistics	44
2.2.3.5 Sensitivity analysis	45
2.3 Results	46
2.3.1 Model evaluation and parameter optimization	46
2.3.2 Soil water dynamics	48

2.3.3	Flow velocities	49
2.3.4	Water fluxes	52
2.3.5	Sensitivity analysis	53
2.4	Discussion	56
2.5	Conclusions	60
3	Effects of ridge tillage on flow processes in the Haeon catchment, South Korea	63
3.1	Introduction	64
3.2	Materials and methods	66
3.2.1	Study site	66
3.2.2	Experimental set up	66
3.2.3	Statistical analysis	68
3.2.4	Image processing	68
3.2.5	Image index functions	69
3.3	Results and discussion	73
3.3.1	Water balance and water content	73
3.3.2	Analysis of flow patterns	74
3.3.3	The effect of tillage management on flow processes and its ecological implications	77
3.4	Conclusions	81
4	Plastic covered Ridge-Furrow Systems on mountainous farmlands: Runoff patterns and Soil Erosion rates	83
4.1	Introduction	84
4.2	Materials and methods	86
4.2.1	Observation of Runoff and Soil Erosion	88
4.2.2	Simulation of Runoff and Soil Erosion	90
4.3	Results and Discussion	94
4.3.1	Observed Runoff and Soil Erosion	94
4.3.2	Simulated Runoff and Soil Erosion	94
4.4	Summary and Conclusions	100
5	Fate of fertilizer ¹⁵N in intensive ridge cultivation with plastic mulching under a monsoon climate	105
5.1	Introduction	106
5.2	Materials and methods	109
5.2.1	Study site	109
5.2.2	Experimental design	110
5.2.3	Study of soil water dynamics	111
5.2.4	Sampling and Analysis	113
5.2.5	¹⁵ N calculations and tracer recovery	114
5.2.6	Statistical analysis	115
5.3	Results	115
5.3.1	Plant biomass and ¹⁵ N uptake in crops	115
5.3.2	¹⁵ N retention in soil	116
5.3.3	N content in soil solution and N leaching	118
5.4	Discussion	121
5.4.1	Plant biomass and ¹⁵ N uptake by crops	121
5.4.2	N retention and N content in seepage	122
5.4.3	Seepage water fluxes and total leached N	123

5.4.4	^{15}N Budget and simulated budget of fertilizer N	125
5.5	Conclusions	126
6	The effect of fertilizer best management practices on nitrate leaching in a plastic mulched ridge cultivation system	129
6.1	Introduction	130
6.2	Materials and methods	132
6.2.1	Study site	132
6.2.2	Experimental set up	134
6.2.3	Modeling approach	135
6.2.3.1	Model set up	135
6.2.3.2	Governing flow and transport equations	136
6.2.3.3	Initial and boundary conditions	138
6.2.3.4	Model parameterization, calibration and evaluation	139
6.3	Results	141
6.3.1	Model evaluation and parameter optimization	141
6.3.2	The effect of plastic mulch on nitrate dynamics	145
6.3.3	The effect of plastic mulch on nitrate leaching loss	147
6.3.4	Fertilizer best management practices (FBMPs)	148
6.3.4.1	Enhanced fertilizer placement	148
6.3.4.2	Split applications	149
6.3.4.3	Combination of plastic mulching, fertilizer placement and split applications	151
6.4	Conclusion	153

List of Figures

1.1	Agriculture and Ecosystem services after Zhang et al. (2007)	3
1.2	Topographical map of South Korea (left), land use map of the Haean catchment (top right): soil water dynamics, runoff and soil erosion were investigated at field sites 1 and 2, the tracer experiments were carried out at field sites 3 and 4, N leaching experiment and modeling of fertilizer best management practices refers to field site 5, Image of a plastic mulched ridge cultivation (bottom right). . . .	10
1.3	Means of measured matric potentials in ridge and furrow positions in different depths for both monitoring field sites; R: ridge, F: Furrow, 15, 30 and 60 refers to the specific soil depth.	12
1.4	Direction of water movement (arrows) in a ridge cultivation system during dry and wet periods, note that during wet periods water movement strongly depends on soil physical and geological properties.	14
1.5	Steps of image processing from profile images taken in the field towards image index functions.	17
1.6	Time schedule of the field management, NO_3^- measurements and precipitation rate during experiment period 2010.	23
2.1	Topographical map of South Korea (left), land use map of the Haean catchment (top right) and picture of field site 1 (bottom right).	39
2.2	Monitoring network of standard tensiometers, continuously recording tensiometers and FDR sensors; subplots a, b and c refers to different slope locations (a: upper slope, b: middle slope, c: lower slope), 1: field site 1 and 2: field site 2. The distance between subplots was approximately 15 and 30 m on field site 1 and 2, respectively.	40
2.3	Daily precipitation, evaporation and transpiration rates during the growing season 2010; a) Field site 1 and b) Field site 2.	43
2.4	Boundary conditions of the model simulations; note that the bottom boundary varies between the two field sites; vertical meshlines F1-3 and R1-3 were included to calculate lateral water fluxes (Figure 2.9); for simulation of ridges without coverage (RT) and conventional tillage (CT) atmospheric boundary conditions were implemented at the entire surface.	44
2.5	Observed vs. simulated pressure heads in different depth for (a) field site 1 and (b) field site 2; limits of gray area = \pm standard deviation of the observed data, black solid line = simulated pressure heads.	47
2.6	Pressure head (h) and water content (θ) under different management strategies at day 21 for (a) field site 1 and (b) field site 2.	50
2.7	Pressure head (h) and water content (θ) under different management strategies at day 75 during a monsoon event for (a) field site 1 and (b) field site 2.	51

2.8	Flow velocity during a monsoon event (day 75) under different management systems at (a) field site 1 and (b) field site 2, black arrows indicate the main flow direction.	52
2.9	Cumulative water fluxes at the transition from furrows to ridges (F1-3) and from ridges to furrows (R1-3) in slope direction, see also the graphical implementation in Figure 2.4. Due to different bottom boundary conditions at both field sites, only positive cumulative water fluxes are simulated at field site 1 due to mainly lateral water movement, at field site 2 the main vertical water movement results in positive and negative water fluxes: (a) field site 1 and (b) field site 2.	54
3.1	Images processing from a) rectified dye tracer image to b) background image and c) binary image used to calculate image indices.	69
3.2	Left to right: Example of a binary image and three index functions: dye coverage I_D , fragmentation I_F and metric entropy I_{ME8} . The gray background represents the soil profile and the dye stained patterns are shown in black. For explanation of circles and arrows see section 3.2.5.	73
3.3	The dynamics of water content in different depths during the irrigation experiments CT, RT and RT_{pm} . The grey area indicates the time of irrigation.	75
3.4	Example images of excavated soil profiles and their binary images. From top to bottom: CT, RT, RT_{pm} and $RT_{pm+crops}$. Note that the slope orientation differs between field site 1 (CT and RT, slope oriented to the left) and field site 2 (RT_{pm} and $RT_{pm+crops}$, slope oriented to the right). In the colour image of $RT_{pm+crops}$, the white feature on the right hand ridge is a potato cut in half.	78
3.5	Image index functions and their 25% and 75% quantiles (colored ares).	79
4.1	Location of the Haean-Myeon catchment on the Korean peninsula (a) and within the Soyang Lake watershed (b) with locations of the experimental sites conducted for this study (c) ("seminatural areas" include grassland, field margins, riparian areas, small roads and channels).	87
4.2	Experimental design to measure runoff and soil erosion by installation of three runoff collectors (RC) on field 1 and field 2. Fields topography and runoff collector drainage areas were calculated based on surface elevation measurements and generation of digital terrain models of both fields.	89
4.3	Daily precipitation on field 1 and field 2 during the observation time from 5 July to 9 August 2010. The arrows indicate the sampling dates for the associated rainfall periods.	90
4.4	Simulated and observed runoff for field 1 (a) and field 2 (b).	96
4.5	Simulated and observed soil loss for field 1 (a) and field 2 (b).	97
4.6	Simulated runoff for all rainfall periods for field 1 (a) and field 2 (b) for different management practices (RP: ridges with plastic cover, RU: uncovered ridges, SS: smooth soil surface).	98
4.7	Simulated soil loss for all rainfall periods for field 1 (a) and field 2 (b) for different management practices (RP: ridges with plastic cover, RU: uncovered ridges, SS: smooth soil surface).	99
4.8	Simulated sediment concentration over all rainfall periods for field 1 and field 2 for different management practices including main % flow directions (RP: ridges with plastic cover, RU: uncovered ridges, SS: smooth soil surface).	100
4.9	Observed erosion rill formed by ridge breakovers and concentrated flow in the depression line in the center of field 1.	101

5.1	Scheme of a typical ridge cultivation system with plastic mulching in a temperate South Korean area with summer monsoon. Shown are the water fluxes and the distribution of fertilizer N in the system.	107
5.2	Mean daily temperature ($^{\circ}\text{C}$), II. Mean total precipitation amount (mm) for the years 2009 and 2010 as well as the 11-year mean (1999-2009) of the Haean Catchment. Daily precipitation amounts and temperature data have been monitored with an automatic weather station (WS-GP1, Delta-T Devices, Cambridge, UK).	110
5.3	a) ^{15}N uptake by plants (% of ^{15}N applied), b) total crop N uptake (kg N ha^{-1}) and c) dry matter production (kg ha^{-1}) at the four fertilizer N rates after 75 days of growth. Standard error of the mean is given.	116
5.4	Mean soil ^{15}N retention (% of ^{15}N applied) averaged for all three depths at day 75 of growth. Standard error of the mean are shown. Results are given for furrows and ridges separately and in total for the four fertilizer N rates.	117
5.5	Simulated daily seepage water fluxes ($\text{l m}^{-2} \text{d}^{-1}$) at a depth of 45 cm during the 75 day growth period. Daily seepage water was simulated for one plot replicate of each fertilizer N application rate only.	118
5.6	Mean ($n=3$) nitrate concentrations in seepage water (mg l^{-1}) at ridge and furrow positions and two soil depths (15 cm, 45 cm) at the four fertilizer N rates. a) = ridge in 15 cm depth; b) = ridge in 45 cm depth; c) = furrow in 45 cm depth. The graphic top right shows the location of the suction lysimeters for collecting seepage water. Standard error of the mean is given	120
5.7	a) Simulated daily leached NO_3^- ($\text{kg N ha}^{-1} \text{d}^{-1}$) for the four fertilizer N rates and b) simulated cumulative leached NO_3^- (kg N ha^{-1}) for ridges and furrows separately during the growth period of 75 days. Daily leached nitrate was simulated for one plot replicate of each fertilizer N application rate only.	120
6.1	Precipitation rates, time schedule of tillage, crop management and NO_3^- measurements at the experimental site from May to August 2010.	135
6.2	Dimensions of the three-dimensional model	136
6.3	Observed vs. simulated pressure heads in ridge and furrow positions in different depths with evaluation coefficients R^2 (Coefficient of determination) and CE (Nash-Sutcliffe-coefficient), grey area limits: \pm std. dev. of observed data; R and F refers to ridge and furrow position in combination with soil depths 15, 30, 45 and 60 cm.	142
6.4	Observed vs. simulated nitrate concentrations in ridge and furrow positions in different depths with evaluation coefficients R^2 (coefficient of determination) and CE (Nash-Sutcliffe-coefficient), black solid line: simulated nitrate concentrations; error bars with means indicate the measured nitrate concentration; R15: ridge position in 15 cm soil depth, R45: ridge position in 45 cm soil depth, F30: furrow position in 30 cm soil depth; A-D refers to the fertilizer application rates of A 50 kg ha^{-1} , B 150 kg ha^{-1} , C 250 kg ha^{-1} , D 350 kg ha^{-1}	144
6.5	Comparison of simulated nitrate concentrations at days 1, 21, 63 and 75 under RT (ridge tillage without plastic mulch) and RT_{pm} (ridge tillage with plastic mulch).	146
6.6	Precipitation rates and simulated daily nitrate leaching loss in 45 cm soil depth under RT (ridge tillage) and RT_{pm} (plastic mulched ridge tillage) and different fertilizer treatments (A: 50 $\text{kg NO}_3^- \text{ha}^{-1}$, B: 150 $\text{kg NO}_3^- \text{ha}^{-1}$, C: 250 $\text{kg NO}_3^- \text{ha}^{-1}$, D: 350 $\text{kg NO}_3^- \text{ha}^{-1}$).	148

6.7 Simulated cumulative nitrate leaching after 76 days below the root zone for
(a) split application scenarios only and (b) combination of enhanced fertilizer
placement and split applications. 152

List of Tables

1.1	Simulated cumulative NO_3^- leaching rates ($\text{kg NO}_3^- \text{ ha}^{-1}$) below the root zone as affected by plastic mulch and fertilizer placement.	27
1.2	Fertilizer split application scenarios. All values are given in $\text{kg NO}_3^- \text{ ha}^{-1}$	28
1.3	Simulated cumulative NO_3^- leaching rates ($\text{kg NO}_3^- \text{ ha}^{-1}$) below the root zone as affected by plastic mulch, split applications and fertilizer placement.	29
2.1	Soil physical properties of the experimental sites.	39
2.2	Model evaluation coefficients R , R^2 , Nash-Sutcliffe efficiency (NSE), bias (\bar{e}) and percentage bias ($Pbias$) for simulations of both field sites.	46
2.3	Initial estimates (est.) and optimized (opt.) van Genuchten parameters and saturated hydraulic conductivity (K_{sat}) for both field sites.	46
2.4	Water balance of the model flow domain after the simulation period of 86 days. Note that seepage is the only outflow of the flow domain at field site 1 and free drainage is the bottom boundary only at field site 2. P: precipitation (varies between treatments because of differing atmospheric boundary lengths), $\text{WC}_{\text{initial}}$: initial water content (varies between treatments because of differing model volumes), WC_{final} : final water content, T: transpiration, E: evaporation, S: seepage, R: runoff, D: drainage, rel. err.: relative error of the water balance; All values are given in liter and related to the xyz-dimension of the model, the values in braces are associated with an area of m^2 for P, T, E, S, R, D and with a volume of m^3 for $\text{WC}_{\text{initial}}$ and WC_{final}	54
2.5	Sensitivity of cumulative water fluxes and water storage to changes in the spatial distribution of the root system after the simulation period of 86 days; gray: original rooting depth used for model calibration ΔW : change in water storage (l m^{-3}), T: transpiration (l m^{-2}), E: evaporation (l m^{-2}), S: seepage (l m^{-2}), R: runoff (l m^{-2}), D: drainage (l m^{-2}); note that seepage is the only subsurface outflow of field site 1. RT_{pm} : ridge tillage with plastic mulch, RT: ridge tillage without plastic mulch, CT:Conventional tillage with a flat surface.	57
2.6	Sensitivity of cumulative water fluxes and water storage to percentage change of evapotranspiration (ET) after a simulation period of 86 days; grey: original ET rate, which was calculated based on FAO dual crop coefficient approach and used for model calibration; ΔW : change in water storage (l m^{-3}), T: transpiration (l m^{-2}), E: evaporation (l m^{-2}), S: seepage (l m^{-2}), R: runoff (l m^{-2}), D: drainage (l m^{-2}); note that seepage is the only subsurface outflow of field site 1. RT_{pm} : ridge tillage with plastic mulch, RT: ridge tillage without plastic mulch, CT:Conventional tillage with a flat surface.	58
3.1	Soil physical properties of the experimental sites.	67
3.2	Total amount of irrigation and its partitioning into surface runoff and infiltration.	74

4.1	Soil and surface parameter values used for the EROSION 3D simulations, divided into uncovered parts of the field (soil surface) and covered parts (plastic film). The third row shows the horizon names of the soil profiles of both fields (according to FAO, 2006).	93
4.2	Observed data for field 1 and field 2. Rainfall characteristics, runoff volume and sediment mass measured by the runoff collectors (RC 1, RC 2, RC 3), and derived mean runoff and soil loss rates of the whole field.	95
5.1	Physical properties of soils at the experimental field site in the Haean Catchment in 2010. Shown is the sand, silt, and clay content of the soil in %. The texture of the soil taken from the World Reference Base from the IUSS Working Group (2007). The standard error of the mean is given in the parentheses.	109
5.2	Statistical parameters for the evaluation of the simulation of the soil water dynamics. R^2 = coefficient of determination. R = Pearson's correlation coefficient. NSE = Nash-Sutcliffe efficiency. $STDV$ = standard deviation of the mean.	113
5.3	Statistical parameters for the evaluation of the simulation of the nitrate transport. R^2 = coefficient of determination. R = Pearson's correlation coefficient. NSE = Nash-Sutcliffe efficiency. $STDV$ = standard deviation of the mean.	113
5.4	Soil ^{15}N retention (% of ^{15}N applied) in different sampling depths in the ridges and the furrows at day 75 of the growth. The standard error of the mean is given in the parentheses.	117
5.5	Fate of ^{15}N (%) at day 75 of growth for the four fertilizer N rates.	126
6.1	Soil physical properties of the experimental sites.	133
6.2	Initial estimates of water retention and solute transport parameters with θ_s : saturated water content, θ_r residual water content, α and n form parameters of the retention curve, K_{sat} saturated hydraulic conductivity, D_l longitudinal dispersivity, D_t transversal dispersivity, D_{vt} vertical transversal dispersivity.	140
6.3	Optimized solute transport parameters for fertilizer rates A-D.	143
6.4	Simulated cumulative NO_3^- leaching rates below the root zone as affected by plastic mulch and fertilizer placement. All values are given in $\text{kg NO}_3^- \text{ ha}^{-1}$	149
6.5	Fertilizer split application scenarios. All values are given in $\text{kg NO}_3^- \text{ ha}^{-1}$	150
6.6	Simulated cumulative NO_3^- leaching rates below the root zone as affected by plastic mulch, split applications and fertilizer placement. All values are given in $\text{kg NO}_3^- \text{ ha}^{-1}$	152

List of abbreviations

Ap	Ploughed topsoil horizon
BD	Bulk density
Bw	Subsoil horizon
CE	Coefficient of Efficiency (also <i>NSE</i>)
C_{org}	Organic carbon content
CT	Conventional flat tillage
DTM	Digital terrain model
DW	Dry weight of biomass
\bar{e}	Model bias
E	Evaporation
ET	Evapotranspiration
FAO	Food and Agricultural Organization
FDR	Frequency domain reflectometry
FW	Fresh weight of biomass
I_D	Dye coverage index
I_E	Index of run length
I_F	Index of fragmentation
I_{MAX}	Index of maximum run length
I_{ME}	Index of metric entropy
N	Nitrogen
NO_3^-	Nitrate
NSE	Nash-Sutcliffe-coefficient
Pbias	Percentage bias
PE	Polyethylen mulch
R	Pearson's correlation coefficient
R^2	Coefficient of determination
RC	Runoff collector
RDA	Rural Development Administration of South Korea
rel. err.	relative error
RP	Ridge tillage with plastic mulch
RT	Ridge tillage without plastic mulch
RT_{pm}	Ridge tillage with plastic mulch
RSR	RSME-observations standard deviation ratio
SS	Conventional flat tillage
T	Transpiration
WHO	World Health Organization
WRB	World Reference Base for soil resources
Y_i^{obs}	<i>i</i> th value of the observed dataset
Y^{mean}	mean value of the observed dataset
Y_i^{sim}	<i>i</i> th value of the simulated dataset

List of symbols

Symbol	Definition	Dimension
α	form parameter	$[L^{-1}]$
C	sediment concentration	$[M L^{-1}]$
C	solute concentration	$[M L^{-3}]$
d_o	depths of flow	$[L]$
D_l	longitudinal dispersivity	$[L]$
D_t	transversal dispersivity	$[L]$
D_{vt}	vertical transversal dispersivity	$[L]$
E_{can}	canopy evapotranspiration	$[L T^{-1}]$
Γ_o	surface fluid exchange rate with subsurface domain	$[L^3 L^{-3} T^{-1}]$
$h [\psi]$	pressure head [matric potential]	$[L, \text{hPa}]$
l	pore connectivity parameter	$[-]$
l_{exch}	coupling length	$[L]$
LAI	leaf area index	$[-]$
λ	first-order decay constant	$[L^{-1}]$
K_o	surface conductance	$[L T^{-1}]$
K_r	relative hydraulic conductivity	$[L T^{-1}]$
K_s, K_{sat}	saturated hydraulic conductivity	$[L T^{-1}]$
n	form parameter	$[-]$
q	subsurface fluid flux	$[L T^{-1}]$
Q	subsurface fluid source and sink	$[L^3 L^{-3} T^{-1}]$
Q_o	surface fluid source and sink	$[L^3 L^{-3} T^{-1}]$
R	total runoff volume	$[L]$
R	retardation factor $[-]$	
S	sink term	$[-]$
S	total sediment mass	$[M]$
S_p	potential water uptake rate	$[T^{-1}]$
θ_v	volumetric water content	$[L^3 L^{-3}]$
θ_r	residual water content	$[L^3 L^{-3}]$
θ_s	saturated water content	$[L^3 L^{-3}]$
θ_{wp}	water content at the wilting point	$[L^3 L^{-3}]$
θ_{ox}	water content at the oxic limit	$[L^3 L^{-3}]$
θ_{an}	water content at the anoxic limit	$[L^3 L^{-3}]$
T_p	transpiration rate	$[L T^{-1}]$
z	elevation head	$[L]$
z_o	land surface elevation	$[L]$
Ω_{ex}	mass exchange rate of solute between subsurface and surface flow domain	$[M L^{-3} T^{-1}]$

Chapter 1

General introduction

1.1 Agriculture, ecosystem services and climate change

Agricultural practices have opposing effects on ecosystem services. On the one hand agriculture delivers huge benefits in terms of food production, hunger reduction and improvement of public health. On the other hand agricultural practices can reduce the ability of ecosystem services to provide goods and services, due to high inputs of fertilizer and pesticides resulting in lower water quality, water pollution and increasing costs for water purification. Nevertheless population growth coincides with increasing food demand, which results in the necessity of an increased agricultural output (Tilman, Fargione, et al., 2001; Tilman, Cassman, et al., 2002; Spiertz, 2010; Swinton et al., 2007; Dale and Polasky, 2007).

In South Korea the rate of agricultural production per unit area has been sustained at a high level due to the shortage of arable flat land (20% of the total area of Korea), but the application of fertilizer in South Korea is higher than in most other countries. Since the 1950s, chemical fertilizer input has increased from an application rate of 230 kg ha⁻¹ year⁻¹ (1980) to 450 kg ha⁻¹ year⁻¹ (1994) (Bashkin et al., 2002; B. Kim et al., 2001). High fertilizer rates in combination with heavy rainfall events during the East Asian summer monsoon are critical in relation to water pollution and eutrophication. Eutrophication of water reservoirs has become a widely recognized problem of water deterioration in South Korea. Especially the transport of applied phosphorus with sediments in surface runoff during monsoon events significantly impacts South Korean reservoirs (B. Kim et al., 2001; Hwang et al., 2003; S. Kim et al., 2007). Therefore, the frequency and intensity of the monsoon events are of great importance to agriculture, water resources and sustainability (Hong and J. Kim, 2011). The amount and intensity of summer monsoon rainfall have increased over the last decades resulting in high watershed exports of

sediments and nutrients from agricultural areas on steep hillslopes converted from forests (Park et al., 2010). Hence, the degradation of ecosystem services by monsoon activity reinforced by anthropogenic factors in a changing climate is of great concern (Hong and J. Kim, 2011).

Tilman, Cassman, et al. (2002) stated that crop production must increase without an increase of the negative environmental impacts associated with agriculture. The increase in agricultural outputs and a decrease in environmental impacts can be achieved by so called high-precision agriculture (Wallace, 1994). Since only 30-50% of applied nitrogen fertilizer and 45% of phosphorous fertilizer is taken up by plants, further increases in fertilizer application are unlikely to be as effective at increasing yields, because efficiency declines at a higher level of addition. Instead, improved timing of fertilization, fertilizer application during periods of greatest crop demand and only near the crop roots can significantly increase nutrient use efficiency (Tilman, Cassman, et al., 2002; Spiertz, 2010; Wallace, 1994; Dale and Polasky, 2007; Kirchmann and Thorvaldsson, 2000). Thus, precise fertilizer management can reduce substantially the risk of leaching agrochemicals into groundwater bodies or transportation via surface runoff into rivers.

Figure 1.1 provides an overview about the services and dis-services from and to agricultural ecosystems (Zhang et al., 2007). It is evident, that soils play a key role in providing supporting and regulating services such as soil fertility and soil retention, respectively. Appropriately managed agricultural ecosystems can contribute to soil conservation and water supply, while poorly managed systems cause negative effects on ecosystem services by high nutrient runoff and sediment loss from agricultural fields.

1.2 Water flow and solute transport as affected by tillage in agricultural soils

Water flow in soils is complex and depends highly on soil physical properties, topography and agricultural management practices. In general, water flow can be distinguished between uniform matrix flow and non-uniform preferential flow. Uniform flow is described by Green and Ampt (1911) as a stable wetting front parallel to the soil surface, whereas non-uniform preferential flow is characterized by irregular wetting and bypassing areas of the porous soil matrix resulting in faster water and solute movement (Hendrickx and Flury, 2001). Preferential flow is further classified into macropore flow, unstable flow and funnel flow. Macropore flow occurs e.g. in root channels, earthworm burrows, fissures and cracks and is mostly related to fine textured soils. Unstable flow is often triggered in coarser textured soils e.g. by textural layering, water repellency

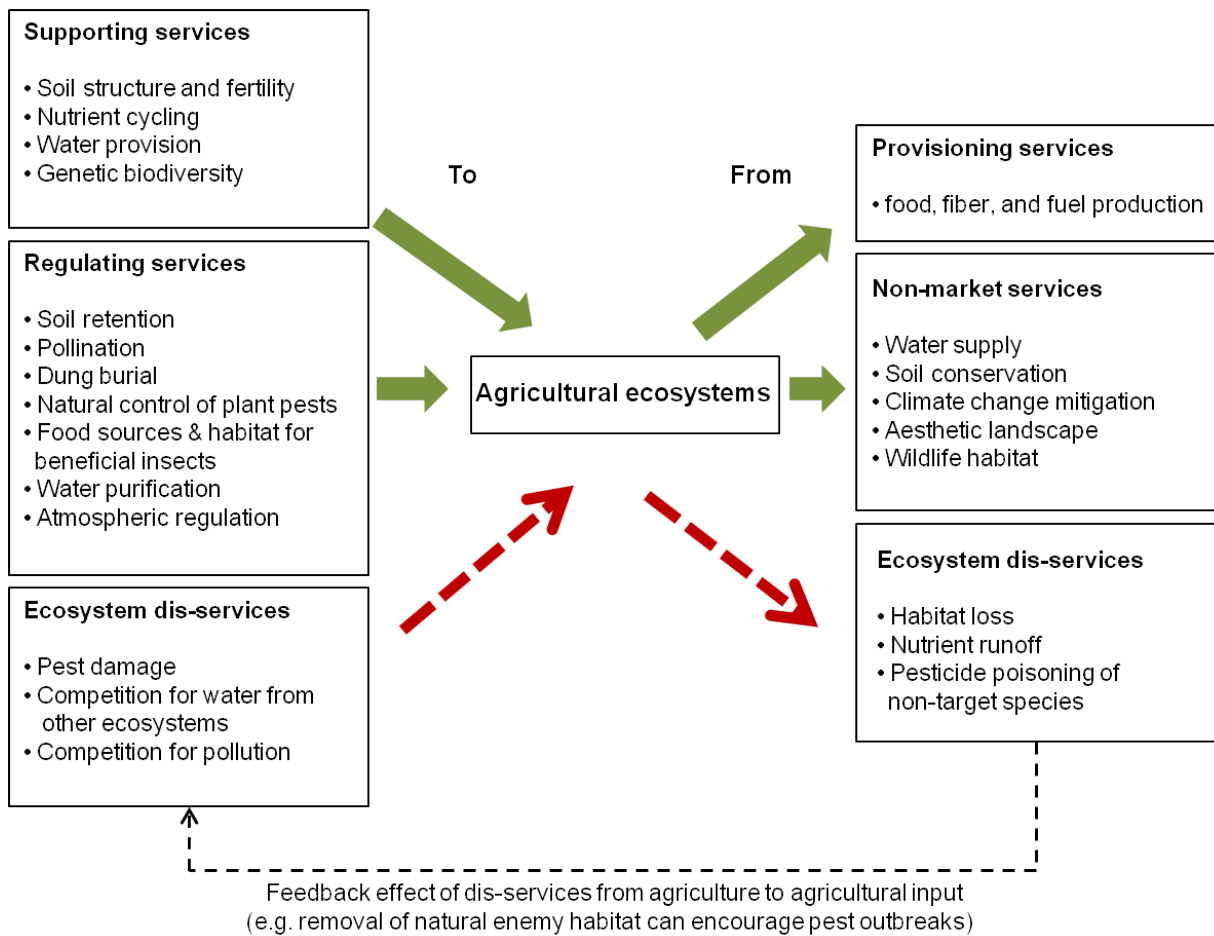


Figure 1.1: Agriculture and Ecosystem services after Zhang et al. (2007)

and air entrapment. Funnel flow occurs due to textural boundaries and redirects water laterally above less permeable layers (Hendrickx and Flury, 2001). The occurrence of non-uniform water flow and solute transport is site specific and depends on the nature of the macropore network, which in turn is determined by factors of structure formation and degradation including soil biota activity (earthworm burrows), soil properties (textural composition), site specific factors such as slope, drying intensity, vegetation and management (cropping, tillage, traffic). Additionally, non-uniform preferential flow is amplified by high rain intensities (Jarvis, 2007).

Agricultural soils exhibiting preferential flow paths are highly susceptible to leach out agrochemicals rapidly to groundwater. However, the susceptibility of soils to leach out agrichemicals does not only depend on soil properties and management practices, it also strongly depends on the sorption characteristics of the applied chemicals. Phosphorous in fertilizer is known for its strong sorption characteristics, thus the transport mainly takes place via surface runoff and erosion and causes significant eutrophication of surface water bodies, whereas nitrate fertilizer is prone to leaching due to its high mobility. The manifold compounds with differing physico-chemical properties exclude generalization about the leaching susceptibility (Jarvis, 2007).

Tillage processes affect soil structure and hydraulic properties in the topsoil. Thus, tillage influences flow patterns, the generation of preferential flow and chemical transport (Petersen et al., 2001). Ridge tillage and its effect on water flow and solute transport was described by several authors. The surface topography in ridge tilled fields was found to channel most of the water via surface runoff into furrows. Hence, soil moisture regime is modified by surface topography with higher soil moisture content in furrows compared to ridges (Saffigna et al., 1976; Leistra and Boesten, 2010; Bargar et al., 1999; Clay et al., 1992). Furthermore, Bargar et al. (1999) reported that water movement below ridges was minimized resulting in a greater solute movement under furrows. Benjamin et al. (1990) found that fertilizer placement in ridges can isolate chemicals from percolating water which decreased the chemical movement to groundwater. That fertilizer injection within the ridge seems to be promising in reducing leaching and in potentially increasing nutrient availability was also found by Jaynes and Swan (1999).

Plastic mulched ridge tillage and its effect on flow and transport processes is sparsely described in literature. In South Korea, plastic mulched ridge tillage is a widespread method to grow vegetables such as radish, cabbage, potatoes and beans. This agricultural method is practiced in order to control weed growth and to induce higher temperatures below the plastic coverage for an earlier plant emergence. Although local farmers reported that the management system is not applied in order to control soil moisture regimes during the East Asian summer

monsoon, plastic mulched ridge cultivation will most likely impact flow pattern and solute transport especially under monsoonal conditions.

1.3 Methodological approaches in soil hydrology

A variety of methods exist to analyze flow processes and solute transport in soils. In field studies, soil water dynamics is commonly investigated using tensiometers in combination with time or frequency domain reflectometry techniques for measuring matric potentials and water contents. Commonly, tensiometer and FDR sensors are connected to dataloggers, which record a high resolution time series of water contents and matric potentials. Retention characteristics (pF curves) of soils can be measured in laboratory using e.g. soil cores in combination with ceramic pressure plates. Monitoring of solute concentrations and solute transport is normally realized using suction lysimeters or field lysimeters. These methods allow a good insight into subsurface water dynamics and solute transport, however, in regions affected by monsoon events, considerably high surface runoff has to be considered as an important component of flow processes. Runoff collectors combined with a flow divider system as described by Bonilla et al. (2006) are valuable to measure surface runoff, sediment transport and solutes in the runoff. However, these measurements are only punctual and cannot cover the entire variability of flow processes e.g. preferential flow in soils. Hence, tracer studies are frequently used to visualize uniform and non-uniform flow. Beside of isotopes tracer such as ^2H , ^3H , ^{18}O , ^{36}Cl and ^{37}Cl , dye tracer such as Brilliant Blue FCF was found to be ideal in compromising properties such as visibility, mobility and toxicity in the field (Flury and Flühler, 1994; Flury and Wai, 2003).

The obtained data sets of field measurements are valuable in calibrating process-based numerical models. Process-based numerical modeling techniques for simulating water flow and solute transport in the unsaturated zone have become popular for a wide range of application in research and management (Simunek, 2006). The need for accurate predictions of subsurface flow and chemical transport to evaluate the effect of management practices and alternatives for contaminant remediation increased widely due to increasing demands on groundwater resources (Kool et al., 1987). Integrating small-scale measurements of soil hydraulic properties in hydrological models that apply across different spatial scales is challenging because of the high nonlinearity of soil hydraulic functions. Therefore the inverse modeling technique is a promising approach to obtain effective hydraulic properties and the best attainable fit between model predictions and observations (Woehling et al., 2008).

It is obvious, that the single application of each method will only deliver an excerpt of water

flow and solute transport processes. Although the application of all mentioned methods is time consuming, cost and labour intensive, their combination will lead to a comprehensive insight in the complexity of water flow and solute transport processes.

1.4 Objective of the thesis

Integrated in the interdisciplinary research project TERRECO (Complex **t**errain and **e**cological heterogeneity) the objective of the thesis was to analyze and model surface and subsurface water flow and solute transport processes as affected by typical plastic mulched ridge cultivation under monsoonal conditions. In order to get a comprehensive understanding of hydrological processes and their effects on ecosystem services in the research area of the Haean-myun catchment, the project was closely linked to related projects dealing with nutrient cycling, soil erosion and catchment hydrology.

Firstly, we analyzed **soil water dynamics** using a monitoring network of tensiometers and water content sensors in two hillslope potato fields which were both characterized by plastic mulched ridge cultivation (RT_{pm}). Subsequently we used the obtained datasets of matric potentials to fit a numerical two-dimensional model using Hydrus2/3D. The soil hydraulic parameters were estimated based on inverse modelling techniques. Afterwards we used the calibrated models to run scenarios regarding water fluxes under ridge tillage without plastic mulch (RT) and conventional tillage with a flat surface (CT). Finally we compared soil water dynamics during drying and wetting cycles and analyzed the differences in water fluxes such as drainage, seepage and runoff between RT_{pm} , RT, and CT (Chapter 2). We hypothesized, that

- Soil water dynamics are strongly influenced by plastic mulching and ridge topography.
- Plastic mulching leads to an increased surface runoff.
- Plastic mulching might decrease drainage water due to higher water retention below plastic mulched ridges.

The monitoring of matric potentials and water contents does not account for non-uniform flow processes, also called preferential flow. **Preferential flow** can lead to a rapid water movement in soils and constitutes a risk to transport agrochemicals fast into deeper soil depths and into groundwater. To analyze whether our sites are affected by preferential flow, we carried out dye tracer experiments using Brilliant Blue FCF at two hillslope potato fields (Chapter 3). According to the scenario procedure in Chapter 2, we conducted four tracer experiments covering a flat

soil surface (CT), ridge tillage without plastic mulch (RT) and plastic mulched ridges (RT_{pm}). Additionally we carried out a fourth experiment in the later season under RT_{pm} with well developed potato crops to investigate the effect of the root system on preferential flow. For partitioning of surface runoff and amounts of infiltrated water, we additionally collected the surface runoff under the different tillage systems (Chapter 3) using an infiltration frame. We hypothesized, that

- Preferential flow is responsible for a rapid transport of agrochemicals and fertilizers, especially highly soluble fertilizer such as nitrate (NO₃⁻) through agricultural soils and to groundwater.
- Under monsoonal conditions the rapid transport via macropore flow to groundwater is enhanced.
- Different tillage management systems induce typical flow patterns.
- Plastic mulching leads to an increased surface runoff.
- Soil physical properties such as bulk density determine flow paths.

To date, the influence of heavy rainstorm events during monsoon season on **surface runoff** and **soil erosion** under RT_{pm} is not well investigated, thus we additionally observed surface runoff and sediment transport using runoff collectors and flow dividers at the hillslope potato fields (Chapter 4), where the monitoring network of tensiometers and water content sensors (Chapter 2) was also installed. Observed data were used to calibrate the process-based erosion model EROSION3D. Complementary to the modeling procedure in Chapter 2, the calibrated model was used to simulate surface runoff and erosion rates under RT_{pm}, RT and CT. We hypothesized, that

- RT_{pm} increases surface runoff and soil erosion due to its topography and impermeable surface.
- At a higher level, the field topography controls the runoff flow patterns generated by the ridge-furrow system and its effects on soil loss.

High mineral fertilizer inputs in combination with monsoon events require knowledge on the fate of the fertilizer components and the main pathways. Therefore we focused on the **N leaching**, **N plant uptake** and **N soil retention** in a typical plastic mulched radish

cultivation under different fertilizer N rates. To get a comprehensive understanding of N cycle under RT_{pm} , we combined several methods. A ^{15}N tracer experiment was applied to trace the fate of N in the biomass and the N retention in the soil. Suction lysimeters, tensiometers and FDR sensors were used to observe soil water dynamics and NO_3^- leaching in seepage water (Chapter 5). We hypothesized, that

- Plastic mulching protects the fertilizer in ridges.
- Plastic mulching increases N retention in soils.
- Nutrient use efficiency (NUE) under RT_{pm} is enhanced.
- Despite its protective function, leaching is the prominent pathway of nitrate (NO_3^-) in a RT_{pm} .
- High fertilizer rates can be decreased without facing substantial losses in biomass production

Finally, the obtained datasets of matric potential and NO_3^- concentrations in the soil solution were used to calibrate the numerical model HydroGeoSphere, which simulates fully-integrated surface and subsurface flow and transport processes. The model was coupled to the parameter estimation software Parallel PEST to estimate the flow and transport parameters using inverse modelling techniques. Based on the findings in Chapter 5, we used the calibrated model to run scenarios with respect to **fertilizer best management practices** such as an enhanced placement of NO_3^- fertilizer as well as split applications (Chapter 6). This modeling approach is used to verify or falsify the following hypotheses:

- Plastic mulching has a positive effect of NO_3^- leaching, thus it reduces leaching and increases retention below the protected ridges compared to RT.
- NO_3^- leaching can be significantly reduced by an appropriate placement only in ridges.
- Split applications in combination with a good timing can avoid high NO_3^- leaching loss.

1.5 Study Area

The Haean-myun catchment, also called Punchbowl, ($128^{\circ}1'33.101''E$, $38^{\circ}28'6.231''N$) is located in the mountainous northeastern part of South Korea 2 km from the border to North Korea (Figure 1.2). The total area is about 64 km². The catchment is characterized by a bowl shape,

which subdivides the catchment into three major land use zones. The steep hillslopes are mostly covered by forest (58%), the moderate hillslopes are dominated by dryland farming (22%). The most cultivated crops on the dryland fields are cabbage, radish, potatoes and beans. A minor percentage of the dryland fields are cultivated with fruit trees, ginseng, vineyards and codonopsis. Rice paddies (8%) are characteristic of the central flat area of the catchment. 12% of the area is occupied by residences, grassland and field margins. The annual precipitation in the Haean catchment is about 1577 mm (11-years average) with 50–60% of the annual rainfall occurring during the monsoon season from June to August. Monsoon events often exceed 100 mm day⁻¹ and generate a considerable amount of annual runoff (Park et al., 2010). Numerous small rivers contribute to the Mandae stream, which is the main stream of the Haean catchment. The Mandae stream in turn contributes to the Soyang Lake, which is the deepest and largest reservoir of South Korea and the main freshwater resource for the capital area of Seoul. The water quality of the Soyang Lake decreased in the last decades due to accelerated eutrophication (B. Kim et al., 2001). The Haean catchment was identified as one of the main non point pollution areas (Park et al., 2010).

The lithology of the catchment is dominated by granitic bedrock material which is strongly weathered due to the high precipitation rates. It constitutes the parent material for Cambisols – the most widely spread soil type. As a consequence of extreme rainfall events during the summer monsoon, the upper soil horizons are often eroded. To compensate this high erosion loss, the local farmers commonly bring sandy soil material at the beginning of the growing season from outside of the catchment and distribute it on their fields.

On the dryland fields, agricultural farming usually starts between April and May depending on the crop type. The common procedure is a primary fertilization using mineral fertilizer in the form of granules and a subsequent ploughing to mix them into the top soil. Therefore, a tillage pan is characteristic for most dryland farming soils. Afterwards, ridges (approx. 15 cm height, 30 cm width) are created perpendicularly to the slope with a ridge to ridge spacing of approx. 70 cm. Typically, the ridges are covered with a black plastic mulch (polyethylen) perforated with planting holes (diameter 5 cm) spaced by 25–30 cm while the furrows remain uncovered. Depending on the crop type, seeds are sowed or juvenile plants are planted after the creation of the ridges. During the growing season herbicides and pesticides are applied several times and fertilizers are spread a second time depending on the crop type. Finally, harvesting usually begins in late August to September.

In order to investigate flow processes as affected by plastic mulched ridge tillage (Chapter 2 and 4) we conducted the soil water dynamics and erosion measurements on two potato fields

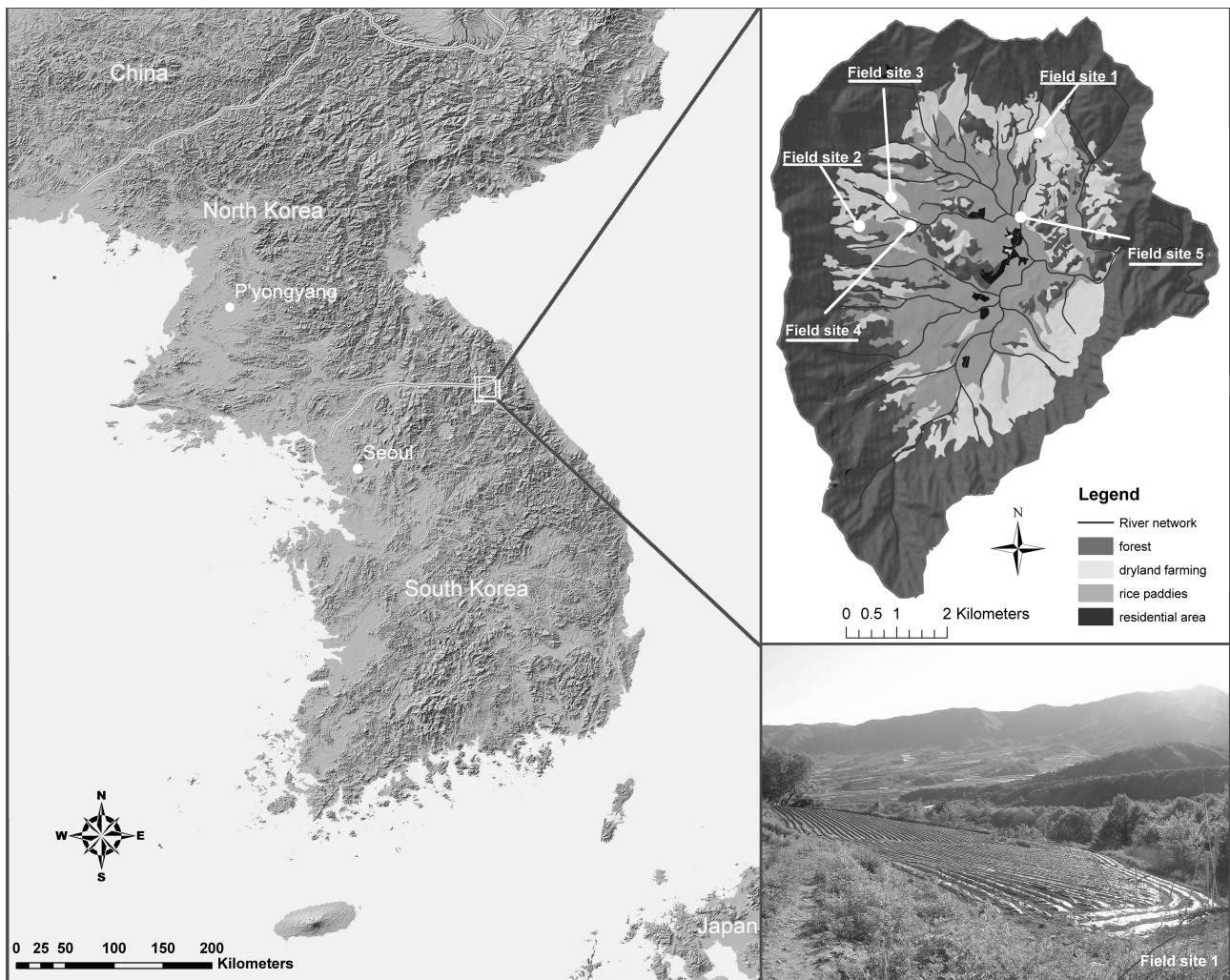


Figure 1.2: Topographical map of South Korea (left), land use map of the Haeam catchment (top right): soil water dynamics, runoff and soil erosion were investigated at field sites 1 and 2, the tracer experiments were carried out at field sites 3 and 4, N leaching experiment and modeling of fertilizer best management practices refers to field site 5, Image of a plastic mulched ridge cultivation (bottom right).

(Field sites 1 and 2), both with an average slope degree of approximately 9° . The dye tracer experiments were also conducted at two hillslope potato fields but slope degree varied among field sites with 8° and 6° for field site 3 and field site 4, respectively (Chapter 3). The nitrate leaching experiment (Chapter 5) was carried out on a flat field site (Field site 5) with plastic mulched radish cultivation in the center of the Haeam catchment (Figure 1.2).

1.6 Synopsis

1.6.1 Soil water dynamics as affected by tillage management systems (Chapter 2)

We combined field observations of soil water dynamics in a plastic mulched ridge cultivation (RT_{pm}) on two hillslope potato fields with a numerical modeling approach using Hydrus 2/3D to investigate soil water dynamics under varying tillage management systems. We hypothesized that plastic mulching has a huge effect on soil water dynamics and strongly influences subsurface water flow because plastic coverage prevents ridges from infiltration. Furthermore, we expected that plastic mulch supports surface runoff generation due to its impermeability. Soil water dynamics in ridge cultivation systems without plastic mulch was previously investigated by several authors (Saffigna et al., 1976; Leistra and Boesten, 2010; Bargar et al., 1999; Clay et al., 1992), while plastic mulched ridge cultivation and its effect on flow processes is rarely described in the literature. Modeling studies are even more rare in literature and most of them are related to furrow irrigation agriculture in arid and semiarid regions. We aimed to evaluate the effect of plastic mulch on soil water dynamics as well as to quantify surface and subsurface water fluxes particularly under monsoonal conditions.

To investigate soil hydrological conditions under RT_{pm} , we installed a monitoring network of tensiometers and soil moisture sensors on both field sites in ridge and furrow positions in 15, 30 and 60 cm soil depth on the upper, middle and lower slope of the fields. The standard tensiometers were read out manually in a two days interval. The continuously recording tensiometers and FDR sensors were connected to a DeltaT datalogger, which recorded matric potentials and water contents half hourly. The monitoring period started from May 31 to August 24 in the growing season 2010. Figure 1.3 shows the time series of calculated means of measured matric potentials in ridge and furrow positions for both field sites. In general, the matric potentials were lower with increasing soil depth. During drying cycles we found the highest matric potential on both fields in ridge positions and 15 cm soil depth due to the root water uptake in the ridges. During monsoon events, the matric potential was almost zero indicating the fully saturation of soils despite of the positions and depths.

Subsequently, we used the datasets of matric potentials for a two-dimensional modeling approach using the numerical model Hydrus 2/3D. The model solves the Richard's equation based on the Galerkin finite element method. The inverse estimation of water retention parameters θ_r , θ_s , α and n and the saturated hydraulic conductivity K_{sat} was accomplished by the Levenberg-

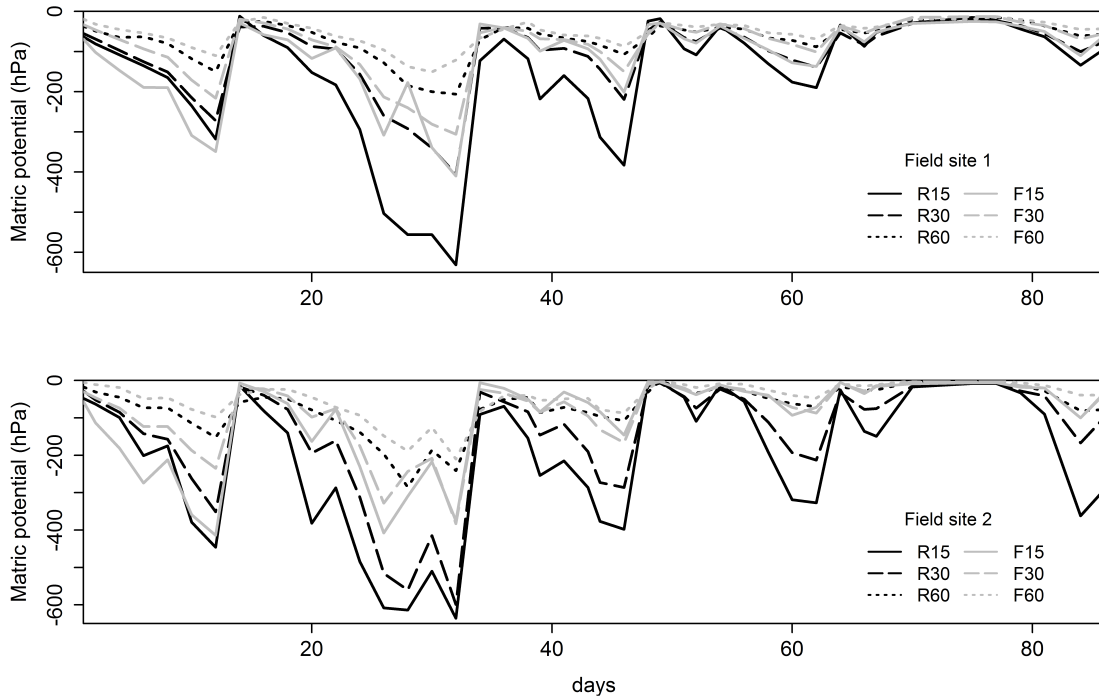


Figure 1.3: Means of measured matric potentials in ridge and furrow positions in different depths for both monitoring field sites; R: ridge, F: Furrow, 15, 30 and 60 refers to the specific soil depth.

Marquardt non-linear minimization method. Afterwards, we used the calibrated models to run scenarios regarding ridge tillage without plastic mulch (RT) and conventional tillage with a flat surface (CT). Evapotranspiration (ET) was included in the model based on the empirical dual crop coefficient approach FAO56 (Allen et al., 1998). To get an deeper understanding, how and to which extend cumulative water fluxes are influenced by ET, we carried out a sensitivity analysis using varying potential ET rates. A dynamic root development was not implemented in the model, thus, we additionally performed a sensitivity analysis using different root depths and investigated the effect on water storage and cumulative water fluxes such as surface runoff and drainage.

To evaluate the models, we used different evaluation coefficients such as the coefficient of determination (R^2), the Nash-Sutcliffe efficiency (NSE), and the percentage bias ($Pbias$). The comparison of observed and simulated pressure heads showed a good agreement for field site 1 ($R^2=0.79$, $NSE=0.79$, $Pbias=2\%$), whereas the agreement for field site 2 was less sufficient ($R^2=0.58$, $NSE=0.48$, $Pbias=12\%$).

During dry periods, the plastic mulch affected soil water dynamics only in the topsoil. The pressure head gradients in this soil horizon were distinct horizontally and forced the water to move laterally from wetter furrows to drier ridges under RT_{pm} . This phenomenon occurred due to the root water uptake and the plastic coverage, which intensified the drying-out of the

ridge soil. The horizontal pressure head gradients were less distinct under RT, where only the topography led to wetter furrow soil compared to ridges. These results coincide with the results of Leistra and Boesten (2010), who investigated soil moisture patterns under RT and found that runoff from ridges resulted in higher soil moisture in furrow positions. The lateral water movement from furrows to ridges was also found by Bargar et al. (1999), who investigated soil water recharge in an uncropped ridges-furrow system. Under CT, vertical pressure head gradients were characteristic, which supported a vertical downward water movement. During monsoon events, the pressure head gradients were not distinct anymore due to the full saturation of the soils. This led to a vertical water movement except for field site 2 under RT_{pm}, where the soil remained slightly unsaturated. Nevertheless, the soil below the plastic coverage was also near saturation at field site 2. Therefore, the weak pressure head gradient did not affect the flow direction as during dry conditions (Figure 1.4).

Additionally, we analyzed simulated flow velocities during a monsoon event and found considerable differences between flow velocities in the topsoil and in the subsoil at field site 1. In the coarse textured topsoil, which was characterized by a high saturated hydraulic conductivity (103 cm d^{-1}), the velocity reached up to 40 cm d^{-1} . In comparison, the saturated hydraulic conductivity in the subsoil were lower (29.4 cm d^{-1}) and flow velocities during the monsoon event reached only 8 cm d^{-1} . The upper part of the ridge was also characterized by low flow velocities about $4\text{-}8 \text{ cm d}^{-1}$ caused by the protective function of the plastic mulch. These results imply that interflow occurred at field site 1 above the interface between the topsoil and subsoil. At field site 2, the velocities were much smaller due to a finer soil texture and a lower hydraulic conductivity in the topsoil (2.9 cm d^{-1}) and the subsoil (15.4 cm d^{-1}).

Furthermore, we investigated the variation of cumulative water fluxes among different tillage treatments and found about 40% higher evaporation rates under RT and CT compared to RT_{pm}. The differences are related to the uncovered surfaces of RT and CT. Transpiration rates as well as cumulative seepage water fluxes were similar between the tillage treatments. Notable differences were found in cumulative drainage and runoff water fluxes. Drainage was 16% less and runoff was 65% higher under RT_{pm} compared to RT and CT.

A dynamic root development was not implemented in the model and a constant average root depth of 30 cm had to be used for model calibration. To analyze, whether the cumulative water fluxes are sensitive to varying rooting depths, we accomplished a sensitivity analysis by varying the rooting depth from 10 cm to 60 cm and analyzed the effect on cumulative water fluxes. The results showed that cumulative seepage, drainage and runoff water fluxes were only slightly affected by varying root depths. The cumulative water fluxes as well as the ratio of

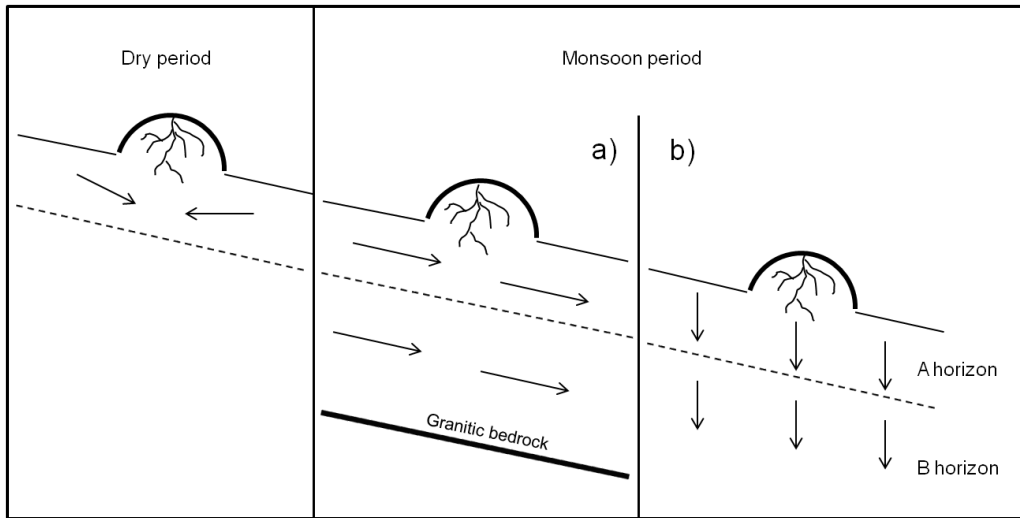


Figure 1.4: Direction of water movement (arrows) in a ridge cultivation system during dry and wet periods, note that during wet periods water movement strongly depends on soil physical and geological properties.

water fluxes between the tillage treatments were found to be robust to varying rooting depths. Moreover, we tested whether the cumulative water fluxes were sensitive to varying potential ET rates. Therefore, the potential ET rates were changed percentagewise by maintaining the calculated ratio between E and T. The sensitivity analysis showed that the cumulative seepage water flux at field site 1 was most sensitive to the variation of potential ET. By reducing the ET to 0%, the cumulative seepage water flux increased between 56-65% dependent on the tillage treatment, whereas a 100% increase of ET led to a decrease of cumulative seepage water of 39%. Runoff was not sensitive to the ET variations and changed merely between 3-6%. The increase of cumulative drainage water was only 14-15% by a ET reduction to zero.

We conclude that soil water dynamics is influenced by plastic mulch mainly during dry periods and small rain events. The important findings are that during drier periods water movement is laterally distinct from furrows to ridges in the top layer due to pressure head gradients, which results from intensive root water uptake in ridges and intensified drying in ridges due to the plastic coverage. During monsoon events the soil was near saturation or fully saturated despite of the tillage management. We found that interflow above the subsoil layer occurred during monsoon events if the granitic bedrock underlays the subsoil (Field site 1), which forced the water to flow laterally downhill. The application of coarse sandy textured soil to the agricultural fields to compensate erosion loss is another important factor, which influence water flow by inducing interflow at the interface between the topsoil and subsoil. This coarse soil texture is associated with a high saturated hydraulic conductivity. Ploughing even more supports the structural differences between both horizons. At field site 2, interflow was

not simulated since the soil was deeper developed and the texture of both horizons was finer compared to field site 1. Therefore a low hydraulic conductivity of both horizons resulted in a vertical flow direction (Figure 1.4).

The sensitivity analyses revealed that the cumulative water fluxes and also the ratio of cumulative water fluxes between the tillage treatments were relatively robust to changes in rooting depth and potential ET rates. Thus, we conclude that plastic mulched ridge cultivation reduces drainage water up to 16% and concurrently increases surface runoff up to 65%. This has important ecological implications in particular under monsoonal conditions. While the reduced drainage water under RT_{pm} might also reduce nitrate leaching, the increased surface runoff results in runoff peak flow, flood risk, erosion. Beside of soil hydrological aspects, RT_{pm} helps to avoid weed growth around the crops and increases the temperature below the plastic coverage which induces a earlier plant emergence.

Considering the advantages and disadvantages of RT_{pm} , we recommend the use of perforated and biodegradable plastic mulch for ridge cultivation systems in areas affected by monsoon season. This seems to be the most promising method to avoid not only high amounts of surface runoff and the decrease of drainage water but also assures a early plant emergence and the suppression of weed growth.

1.6.2 Preferential flow as affected by tillage management systems (Chapter 3)

Flow processes in agricultural soils are highly influenced by tillage, soil properties and surface topography. In the previous chapter we showed that ridge tillage and plastic mulching affects soil water dynamics. However, the observations of soil water dynamics does not account for non-uniform flow processes. Preferential flow like macropore flow is a well known phenomenon, which supports a quick transport of agrochemicals into groundwater. Therefore, the knowledge about the effect of management operations on preferential flow is essential in order to assess its impact on groundwater quality.

Analogously to the modeling procedure in the previous chapter, in which we investigated the effect of management practices like CT, RT and RT_{pm} on soil water dynamics, we conducted four tracer experiments on hillsloped potato fields in the Haean catchment. The first experiment was carried out before ridges were created. This conditions represented conventional tillage (CT). Subsequently the second experiment was conducted at the same field site after the creation of the ridges (RT). In the third and fourth experiment we assessed the influence of plastic mulch

and root systems on preferential flow, so that the third experiment represented RT_{pm} in the early season without crops, while the last experiment were conducted in the later season, when the potato crops were well-developed ($RT_{pm+crops}$).

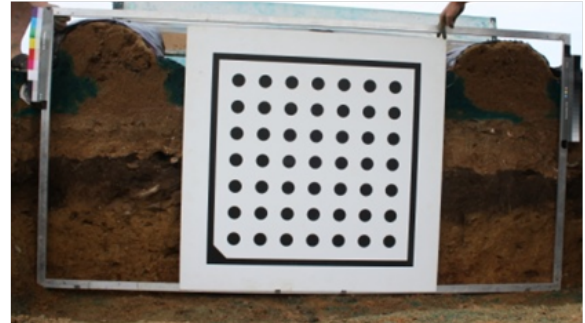
We used the dye tracer Brilliant Blue FCF, which is known for its low toxicology, high mobility and good visibility in the soil (Flury and Flühler, 1995) and irrigated the tracer solution with a sprinkler machine to plots of 2 m². In order to investigate how the applied water contributes to surface runoff and infiltration, we installed a infiltration frame, which channeled the surface runoff in buckets outside of the plot. Additionally we installed soil moisture sensors in 5 and 20 cm soil depth for monitoring the changes in soil water contents during irrigation. After 24 hours, we excavate soil profiles in a distance of approx. 10 cm and photographed them with a metal frame, Kodak color scales and a calibration plate.

Subsequently we rectified the obtained profile images using the software of HALCON ver. 10 (MVTec Software GmbH, Munich, Germany) and converted them into two binary images. The first binary image classified the stained parts of the profiles into black pixels and the non-stained parts into white pixels. The second binary image were coded such that the entire soil profile were coded black and the background was coded white. To analyze flow patterns, we calculated image index functions, namely dye coverage (I_D), Euler number (I_E), fragmentation (I_F), metric entropy (I_{ME8}) and maximum of run length (I_{MAX}) based on both binary images. Besides of the dye coverage function (I_D), these new image index functions were recently introduced by Trancón y Widemann and Bogner (2012) and allow a comprehensive interpretation of image features derived from dye tracer experiments. The commonly used (I_D) represents the percentage of stained pixels compared to the total number of pixels in a image row. The I_E express the number of runs, which are defined by a continuous sequence of stained pixels normalized by the maximum of possible runs, while the I_{MAX} describes the distribution of run lengths by its maximum. The I_F index describes the fragmentation of an image row. The index can be calculated by the inversion of the contiguity index (I_C). Finally, the I_{ME8} originate from information theory and gives the entropy of pixels in words of length 8. Thus, the metric entropy is high, when pixels in words are uncorrelated. The steps of image processing towards the image index functions are shown in Figure 1.5.

In relation to the partitioning of surface runoff and amounts of infiltrated water, we found highest infiltration rates (79%) and lowest surface runoff (21%) under CT. The infiltration rates decreased to 62% and the surface runoff increased to 38% caused by the ridge topography under RT. This trend was amplified under RT_{pm} , when both, infiltration and surface runoff accounted for 50%. These results verified our hypothesis, that plastic mulching of the ridges substantially



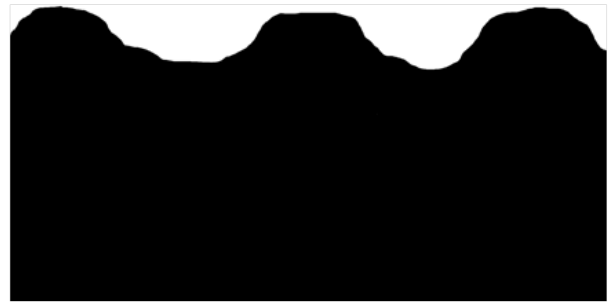
a) Image of the soil profile



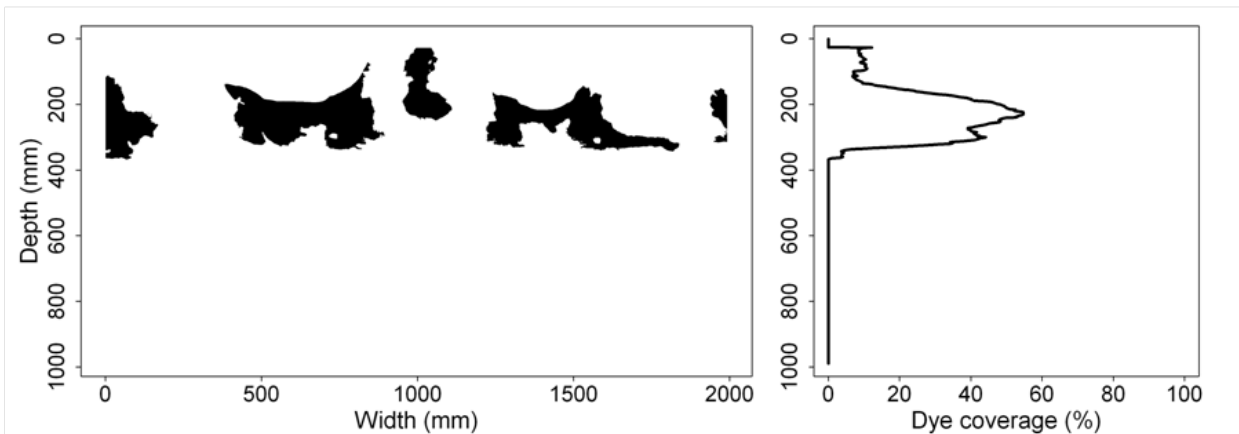
b) Image with calibration plate



c) Image after rectification



d) Binary background image



e) Binary image of stained flow paths

f) Dye coverage function

Figure 1.5: Steps of image processing from profile images taken in the field towards image index functions.

increase surface runoff due to the ridge topography and the impermeable black plastic cover. In the later season, when potato crops were already developed, we found a reversed trend with 69% accounting for infiltration and 31% for surface runoff. This was related to the interception of irrigation water in the crop canopy, the throughfall as well as the stemflow, which channeled the water directly into the planting holes.

The soil water content during irrigation under CT increased primarily in 5 cm depths and about 15 min later in 20 depths, which indicates a homogeneous infiltration front caused by the flat surface of the plot. The sensors which were located downslope of the plot registered higher soil moisture. At the beginning of the experiment, the soil moisture in furrow positions was already higher than in ridge positions under RT. This was presumably due to previous rain events, when water infiltrated preferentially in furrows because of the topography. The water content increased firstly in furrow positions in 5 cm depth because irrigation water accumulated in the depression. The overall increase of soil moisture in 20 cm depth was only small. Under RT_{pm} the soil moisture firstly increased in furrow positions similar to RT. These findings are supported by the research of Leistra and Boesten (2010) and Saffigna et al. (1976), who found also higher water contents in furrow positions due to runoff from ridges to furrows. However, the FDR sensor in 20 cm depth in ridge position showed an increase of soil moisture before the soil moisture increased in 5 cm depth in ridge positions. We relate this finding to water, which infiltrated primarily in furrow positions and moved afterwards laterally to ridges due to horizontal pressure head gradients between wetter furrows and drier ridges. The lateral water movement from furrows to ridges was also confirmed by the field measurements and the modeling study in Chapter 2 and by Bargar et al. (1999).

For all four experiments, the I_E was calculated to be approx. 0.1, which expressed the huge contiguous flow pattern, namely the infiltration in furrows and planting holes. The maximum of 1 would indicate the permanent alternation of black and white pixels in an image row, which is opposed to our findings with a few number of vertical flow pattern. All calculated indices declined to zero in 25-35 cm soil depth. This revealed that the tillage pan was the most important feature in the agricultural soil despite of the management. The tracer solution did not infiltrate deeper than the tillage pan, which is a result of absent macropores and a significantly higher bulk density of the subsoil ($p < 0.05$). Moreover, the water was funneled laterally above the tillage pan in slope direction. Larger fragmentation and metric entropy indices of RT compared to CT showed clearly the topography effects on flow pattern, namely the infiltration in furrows and planting holes alternating with unstained parts of the ridges. Furthermore, the effect of plastic much became evident by comparing the I_D and I_{MAX} of RT to RT_{pm}. The homogeneous

infiltration under RT in the uppermost cm of the soil resulted in a dye coverage of 1 and an I_{MAX} of 0.75, whereas the I_D and I_{MAX} of RT_{pm} was largest in approx. 20 cm soil depth. The influence of the root system on flow pattern was well represented in larger I_D in the rooting depth under $RT_{pm+crops}$ compared to RT_{pm} . Further, the root system led to a redirection of water, which primarily infiltrated in furrows. While water was funneled laterally above the tillage pan in slope direction under RT_{pm} , water flow occurred from furrows to ridges and reversed to the slope direction. This phenomenon can be explained by lower pressure heads in ridge caused by root water uptake.

The findings have important ecological implications for water quality and erosion aspects. On the one hand, the artificial soil layering induced by the application of coarse textured topsoil as well as ploughing activities results in uniform flow through the sandy soil matrix and funnel flow above the tillage pan. Funnel flow above the tillage pan was found to be most important in the early season, when the root water uptake was absent. This implies that the leaching risk of agrochemicals via the interface between topsoil and subsoil is crucial and that the field sites directly next to the rivers are critical locations for discharge of pollutants into the river network. On the other hand, we found that macropore flow in the subsoil was absent, which in turn implies a relative low risk of groundwater pollution by agrochemicals under these specific soil physical properties. Furthermore, we found a substantially increased runoff generation under plastic mulched ridge cultivation. Hence, the management practice supports especially the risk of soil erosion and particle-bound phosphorous leaching via surface runoff. These results are supported by the finding of B. Kim et al. (2001), who reported that the eutrophication of the Soyang Lake originates dominantly from phosphorous and sediment discharge of agricultural fields on steep hillslopes.

We conclude that the impact of plastic mulching on subsurface flow processes is relatively low although it creates respective zones of infiltration and non-infiltration. In contrast, the impact on runoff generation is very high and increases the risk for leaching and soil erosion. Therefore we recommend using perforated plastic mulch. This would retain the positive effects of plastic mulch on weed control and concurrently decreases surface runoff. Additionally, we propose to establish riparian buffer zones to decrease the risk of leaching via lateral subsurface flow above the tillage pan as well as leaching via surface runoff into the river network.

1.6.3 Surface runoff and soil erosion as affected by tillage management systems (Chapter 4)

In this chapter, we assess the influence of a plastic mulched ridge cultivation system in combination with field topography effects on runoff pattern and soil erosion rates using field observations and a process-based modeling approach. The results of several authors, who investigated soil erosion and runoff pattern in plastic mulched plots under varying crop types, contradict tremendously. On the one hand, the authors found that ridge cultivation and plastic mulching increases surface runoff and soil erosion substantially (Wan and El-Swaify, 1999; Rice, McConnell, et al., 2001; Gascuel-Oudoux et al., 2001). In contrast, Stevens et al. (2009) did not detect any differences in soil erosion and runoff between plastic covered and uncovered strawberry cropping systems. Lee et al. (2010) reported even lower runoff and erosion rates under plastic mulched potato and cabbage cultivation. All mentioned studies are limited to the plot scale with similar topography.

In order to investigate the influence of the topographical complexity of the fields but also the topography of the ridge-furrow system on soil erosion loss and runoff, we installed runoff collectors connected to multislot flow dividers at two plastic mulched potato fields. The runoff collectors in combination with multislot flow dividers were designed based on Bonilla et al. (2006) and Pinson et al. (2004). Runoff was observed from July 5 to August 9, 2010. During the observation period seven significant rain events occurred. The collected runoff in the buckets was subsequently sampled to analyze sediment concentrations. To get a high resolution digital elevation map of the field sites, we surveyed intensively the elevation at numerous points in the fields using a tachymeter (Tachymat WILD TC1000). Additionally we measured soil properties such as bulk density, soil texture and organic carbon content in the laboratory.

The process-based, spatial distributed erosion model EROSION 3D (Schmidt, 1991), which requires relatively few input parameters, were calibrated to the observed runoff and erosion rates. Apart from the measured variables, we additionally implemented the initial soil moisture based on simulated values of HYDRUS 2/3D (Chapter 2). The surface roughness (Manning's n) was estimated separately for plastic covered ridges and uncovered furrows based on recommendations in the literature. Additionally we estimated soil coverage by images taken during the measurement period. The parameters skin factor and erodibility were used for model calibration. In accordance to the modeling procedure in Chapter 2, we used the EROSION 3D model to simulate runoff and erosion rates of a ridge tilled field without plastic cover (RT) and a field with a conventional flat surface (CT). The scenarios were subsequently compared to the results

of calibrated model, which considered plastic mulched ridge cultivation (RT_{pm}).

By comparing both field sites, we found differences in measured runoff and soil erosion rates due the variability in rainfall characteristics. The highest daily precipitation amount of 102.5 mm was observed at field site 2, while at field site 1 the highest precipitation event accounted for 76.5 mm. During the observation period, field site 1 received less precipitation (165.2 mm) in total than field site 2 (242.7 mm). The total observed runoff was 80.3 l m^{-2} and 94.1 l m^{-2} for field site 1 and 2, respectively. The measured soil loss differed substantially between both field sites. For field site 1 the overall soil loss was calculated to be $3646.7 \text{ kg ha}^{-1}$, while the total soil loss at field site 2 was only 626.5 kg ha^{-1} . Since the soil properties, slopes and crop management were similar, we address the differences to variations of the field topography and the orientation of the plastic mulched ridges.

The models were evaluated using the *RMSE*-observation standard deviation ratio (*RSR*), the Nash-Sutcliffe efficiency (*NSE*) and the percentage bias (*Pbias*). For runoff, the *NSE* was > 0.91 , *RSR* was < 0.293 and *Pbias* was $< -13.46\%$. For soil loss, the *NSE* was > 0.803 and *RSR* was < 0.444 . The *Pbias* for soil loss was negative for field site 1 indicating an overestimation of soil loss, whereas a positive *Pbias* at field site 2 showed an underestimation of soil loss. With reference to Moriasi et al. (2007), the agreement between observed and simulated runoff and soil loss was satisfying for both field sites.

The comparison of different management practices showed that simulated runoff was highest under RT_{pm} . The simulated runoff was 81.3 l m^{-2} and 106.8 l m^{-2} for field site 1 and field site 2, respectively. Under RT and CT, runoff was 36% and 44% less compared to RT_{pm} . The reduction of surface runoff corresponded to the rainfall intensities and varied strongly between rainfall events. Accordingly, the highest soil loss was also simulated for RT_{pm} accounting for $4178.1 \text{ kg ha}^{-1}$ at field site 1 and 545.8 kg ha^{-1} at field site 2. The scenario RT showed a reduction of 41% and 32% soil loss for field site 1 and field site 2, respectively. Conventional tillage CT showed also lower amounts of soil loss, which equaled a reduction of soil loss by 76% at field site 1. In contrast, the reduction of soil loss under CT at field site 2 was only 14% less compared to RT_{pm} .

The comparison of soil loss showed that the variation among management practices induced by different flow properties due to field topography and ridge orientation was considerably high. RT and RT_{pm} forced water to flow in furrows, while water was triggered to follow the steepest flow paths under CT. Since field site 1 was characterized by a concave shape, the flow accumulation and sediment transport was highest in the depression located in the center of the field, which caused ridge breakovers and the development of a deep erosion rill. In contrast, a convex shape was characteristic for field site 2. These properties resulted in a dominating

flow direction along furrows under RT and RT_{pm} to the field margins. At the bottom of the field site the highest erosion rates were simulated caused by the largest ridge length. Under CT, erosion rates at field site 2 were higher compared to ridge-furrow tillage. These results verified the hypothesis, that the field topography was the most important controlling factor for soil erosion. Thus, ridge-furrow tillage at the concave field site even increased soil erosion, whereas the convex field topography in combination with ridge-furrow tillage led to decreased soil erosion rates.

Based on the findings, we conclude that the configuration of ridge-furrow tillage in order to reduce erosion loss heavily depends on the field topography. Therefore, the topography of the field should be considered before ridge-furrow tillage is practiced. Furthermore, we recommend orientating the ridges exactly along contours and towards the field edges to avoid flow accumulation in field depressions. Additionally, high water flow rates in furrows implies a better protection against soil erosion by decreasing the flow velocities in furrows. This can be achieved by omitting herbicide application in furrows. This was also suggested by Rice, Harman-Fetcho, et al. (2007), who introduced grass cultivation in furrows as "in-field buffers", which increases surface roughness and infiltration rates and reduces flow velocities in furrows.

1.6.4 N fate in a plastic mulched ridge cultivation system (Chapter 5)

In this chapter we determine the N fate in a plastic mulched ridge cultivation system affected by extreme rain events. In contrast to the previous studies, the N fate was investigated in a flat ridge cultivation with radish crops and different soil properties. The study focused on N pathways such as crop N uptake, N retention and N leaching in the soil by using ¹⁵N as a tracer. Additionally, soil water dynamics were monitored using a monitoring network of tensiometers and water content sensors. N concentrations in seepage water were determined using suction lysimeters.

The experiment was conducted at a field site in the flat center of the catchment. Prior to the experiment, the field was fallow over several years. Hence, a basic fertilization of 56 kg NO₃⁻ ha⁻¹ was applied prior to the experimental set up. Afterwards, the field was sectioned into 16 subplots. Four fertilizer rates of 50 (A), 150 (B), 250 (C) and 350 (D) kg NO₃⁻ ha⁻¹ were additionally applied resulting in 4 subplots per fertilizer rate. After the fertilization, fertilizer granules were mixed into 15 cm soil depth by ploughing. Subsequently the ridges were created and covered with black plastic mulch and radish seed were sown. The suction lysimeters were installed in

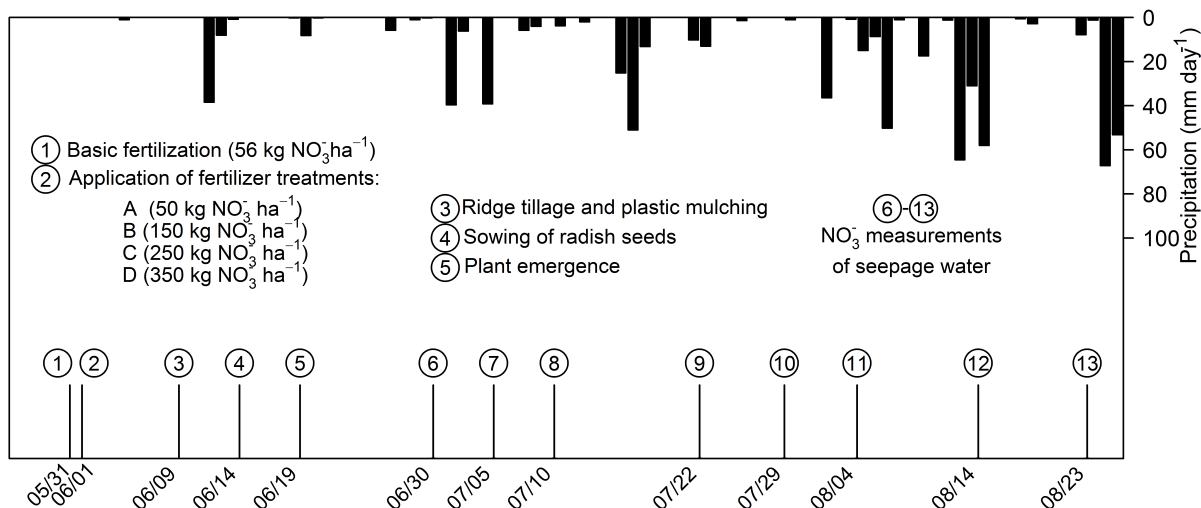


Figure 1.6: Time schedule of the field management, NO₃⁻ measurements and precipitation rate during experiment period 2010.

15 cm and 45 cm in ridges and 30 cm in furrows of the respective surface. In Figure 1.6 the management procedure, the measurement dates of NO₃⁻ in seepage and precipitation rates of the observation period are chronologically shown. At day 25, 50 and 75 after sowing radish plants were partially harvested to determine biomass, total N and ¹⁵N. Accordingly, soil samples were analyzed on total N and ¹⁵N. In an approx. interval of 1 week, soil water samples of the suction lysimeters were measured on NO₃⁻ concentrations using a photometric nitrate test (Nitrate photometric test, Spectroquant, Merck, South Korea). Soil water potential were observed in a two days interval.

¹⁵N uptake by plants showed that uptake rates during the first 25 days of the growing season were low, while the uptake increased significantly during day 25-50 for all fertilizer rates. For the fertilizer rates A and B, the highest ¹⁵N was detected at day 50. After day 50, the only significant increase of ¹⁵N uptake was characteristic for fertilizer rate D. Generally, the mean fertilizer use efficiency (FNUE) at day 25 ranged between 1.7% and 3.8%. Up to day 50, the FNUE increased to 19-36% with a maximum of FNUE for the lowest fertilizer rate A. At harvest day 75, the FNUE was lower and ranged in dependence of fertilizer rates between 20-32%. The biomass production was assumed to increase with increasing fertilizer rates, however, under fertilizer rate B, C and D the biomass production did not significantly differ at the day of final harvest. Hence, the results implies that a similar biomass production can be achieved with the fertilizer rate B of 150 kg NO₃⁻ ha⁻¹. This results coincide with the fact, that the ¹⁵N uptake did not increase significantly between day 50 and day 75. Therefore, it is most likely to assume that fertilizer N for growth was taken up until day 50. Afterwards, the fertilizer N was primarily

accumulated in the root. Furthermore, the low N use efficiency $< 4\%$ in the first third of the growing season implicates, that the leaching risk is particularly high during this early stage of growth.

The overall ^{15}N retention in soil, averaged for all sampling depths, was similar for all fertilizer rates ($p > 0.05$) and ranged between 10-14%. The ^{15}N retention in ridge positions was higher compared to furrow positions. In total, at all three sampling days, decreasing ^{15}N retention was found with increasing soil depth. Due to the repetitive application of coarse sandy soil, low water and nutrient retention was characteristic for the field site. These soil properties increased the risk of ^{15}N leaching into deeper soil layers especially under heavy rainfall. A low N retention in other disturbed ecosystems was also confirmed by Peterjohn and Correll (1984). The higher N retention in the ridge soil was expected since the plastic mulch protected the ridge soil from infiltration. These findings are in accordance to Cannington et al. (1975) who reported that plastic mulch permits a more efficient nutrient use in the root zone.

The mean NO_3^- concentrations in seepage during the season significantly differed among fertilizer rates with A (53 mg l^{-1}), B (67 mg l^{-1}), C (119 mg l^{-1}) and D (122 mg l^{-1}). The mean nitrate concentrations between fertilizer rates differed significantly especially at the end of the experiment from 5-64 mg l^{-1} ($p < 0.05$). At the beginning of the experiment, NO_3^- concentrations in seepage were similar ranging between 138-179 mg l^{-1} . For fertilizer rates A and B, the NO_3^- concentrations in seepage were $< 10 \text{ mg l}^{-1}$ at the day of final harvest, while $> 10 \text{ mg l}^{-1}$ was characteristic for fertilizer rates C and D. Based on the nitrate concentrations and the measured pressure heads, a modeling study was carried out using Hydrus 2/3D. The modeling study exhibited the following limitations. Firstly the calibration was based on only one plot replicate. Secondly, Hydrus 2/3D was not capable to simulate integrated surface-subsurface flow and transport processes directly, so that the precipitation rates for furrow positions were multiplied by a factor of 2 to consider the surface runoff from ridges. Furthermore, it was assumed that the fertilizer was solved from the beginning of the growing season, neglecting that the application was done with fertilizer granules. Finally, the root water uptake parameters for radishes had to be estimated since radish was absent in the crop database of Hydrus 2/3D. Although the agreement between simulated and observed pressure heads was reasonable, the solute transport model resulted in a poor agreement between observed and simulated NO_3^- concentrations. The model showed very high cumulative nitrate leaching rates below the root zone in 45 cm soil depth with A (86 $\text{kg NO}_3^- \text{ ha}^{-1}$) $<$ B (180 $\text{kg NO}_3^- \text{ ha}^{-1}$) $<$ C (260 $\text{kg NO}_3^- \text{ ha}^{-1}$) $<$ D (387 $\text{kg NO}_3^- \text{ ha}^{-1}$) which was equivalent to approximately 95% of the total applied fertilizer, although denitrification and root water uptake was simulated. The low N uptake by

plants in the simulation was related to the plant uptake parameters, which had to be estimated. The denitrification was also simulated to be very low accounting for $< 2\%$. Organic carbon as well as anoxic conditions is necessary to initiate denitrification processes by microorganisms. The low denitrification rates were reliable due to the very low organic carbon content and the high hydraulic conductivity of the coarse textured soil, which in turn led to a quick drainage.

Subsequently, the fate of ^{15}N was determined by calculating the overall budget for each fertilizer rate. Crop ^{15}N uptake accounted for 31.7% (A), 28.1% (B), 20.0% (C) and 29.1% (D). Soil ^{15}N retention was calculated to be 15.1% (A), 11.0% (B), 10.2% (C) and 8.8 % (D). Hence, the remaining percentages constituted the ^{15}N loss, which was 53.2% (A), 60.9% (B), 69.8% (C) and 62.1% (D). The calculated ^{15}N loss contradicted with the simulated high NO_3^- leaching rates. However, the calculated ^{15}N budget as well as the simulated leaching rates revealed, that leaching was the dominant N loss pathway.

Considering the previous findings, it was concluded that $150 \text{ kg NO}_3^- \text{ ha}^{-1}$ should be aimed for a maximum total fertilizer NO_3^- application. Additionally it was recommended to apply the fertilizer in 3-4 applications to meet the crop N needs and to avoid high NO_3^- losses especially at the beginning of the growing season. Finally, it was suggested to distribute the fertilizer only in ridges and to enhance water and nutrient retention by increasing the organic matter content by placing plant residues such as rice straw or soil additives in furrows.

The Hydrus 2/3D model exhibited some limitation in terms of solving surface flow processes, however, in a plastic mulched ridge cultivation system the surface runoff from ridges to furrows plays an important role. Moreover, the agreement between observed and simulated NO_3^- concentrations was not satisfying. Thus, we decided to simulate the NO_3^- leaching experiment using the HydroGeoSphere code, which is capable to solve fully-integrated surface-subsurface water flow and solute transport problems.

1.6.5 Fertilizer best management practices for reducing nitrate leaching: A modeling study (Chapter 6)

The ability of representing physical processes such as surface and subsurface water flow as well as solute transport in a variable saturated media is an advantage of process-based numerical models. In the last decades, it has become a progressively used tool for impact and risk assessment in the field of environmental issues. Therefore, numerical models provide often the basis for conservation planning and decision making. Environmental impacts such as pollution of aquatic systems caused by excessive use of fertilizers, pesticides and herbicides in agriculture constitutes

an increasing problem worldwide. Particularly in South Korea, where the monsoon season coincides with the main growing season, the risk of leaching during heavy monsoon events is amplified compared to other regions.

In this chapter we assess the impact of ridge tillage and plastic mulching on nitrate leaching as well as the potential to decrease the risk of groundwater NO_3^- contamination by applying fertilizer best management practices (FBMPs). High-precision agriculture as proposed by Wallace (1994) includes the correct leveling, draining and contouring of the fields as well as a right timing of application and right placement of fertilizers. The application of FBMPs can therefore be a useful tool to achieve both, economical and environmental benefits.

Based on the NO_3^- leaching experiment as described detailed in the previous section, we carried out a three-dimensional modeling study using the HydroGeoSphere code (Therrien et al., 2010). This code integrates surface-subsurface flow and transport processes and is therefore most suitable to simulate water flow and solute movement in a plastic mulched ridge cultivation system. The datasets of measured pressure heads and NO_3^- concentrations were used to calibrate the water retention and solute transport parameters. We coupled HydroGeoSphere with the powerful parameter estimation software ParallelPEST (Doherty, 2005) to optimize these parameters based on the Gauss-Marquardt-Levenberg non-linear estimation technique. The model was set up with no flux conditions at the left and right hand boundary and a free drainage boundary at the bottom of the flow domain to induce a dominating vertical flow fields. The boundary conditions were chosen based on the assumption, that flat field conditions lead to dominating vertical flow processes and that lateral flow processes are minimal or even absent.

The water flow model was calibrated for the observation period from June 17 to August 27. Since the NO_3^- concentration measurements started approximately one month after the fertilizer application, the calibration period for solute transport was much shorter. We calibrated the solute transport model starting on the day of highest NO_3^- concentrations (July 10). For simulating the for different fertilizer rates with 50 (A), 150 (B), 250 (C) and 350 (D) $\text{kg NO}_3^- \text{ ha}^{-1}$, however, we assumed that the fertilizer, which was applied as granules on May 31 and June 1, had to be solved latest with the first significant rain event, which occurred on June 12 with 38.4 mm day^{-1} . Hence, we implemented the initial NO_3^- concentration in the model beginning on June 13. Fertilizer application was done prior to the creation of the ridges resulting in fertilizer distribution in ridges and furrows. Thus, we set up the initial NO_3^- concentration in the upper 24 cm from the ridge surface in the model domain.

To evaluate the effect of plastic mulch on NO_3^- dynamics and NO_3^- leaching loss below the root zone, we compared the simulation of the calibrated model, which accounts for plastic

mulched ridge cultivation (RT_{pm}), with a simulation of ridge cultivation without coverage (RT). The effect of FBMPs we simulated as follows: Fertilizer placement only in ridges was simulated for all fertilizer rates (A-D). We increased the NO_3^- concentration in the ridges such that the total initial mass ($kg\ NO_3^-$) in the model was equivalent to the previous simulations of fertilizer placement in ridges and furrows. The split application scenarios were all based on a total amount of $150\ kg\ NO_3^-\ ha^{-1}$ as it was recommended in the previous chapter. Based on the findings of the field study, that fertilizer application should be splitted and that the first application amount should be small due to a low fertilizer use efficiency, we set up the split application scenarios as given in Table 1.2. We assumed that the combination of plastic mulch, fertilizer placement and split application will lead to multiplicative effects in reducing NO_3^- leaching below the root zone. Hence, we finally simulated the combination of the FBMPs.

The analysis of simulated NO_3^- concentration pattern differed strongly between RT and RT_{pm} . While the NO_3^- concentration under RT declined fast and relatively homogeneously throughout the soil profile, the concentration pattern under RT_{pm} was clear separated into parts of low concentrations in furrows and planting holes and high concentrations below the plastic coverage. Therefore, the simulation revealed the protection function of plastic mulch, which led to a maximum in NO_3^- concentrations below it, while decreasing NO_3^- concentrations were characteristic in unprotected furrows and planting holes. The findings are in accordance to Locascio et al. (1985) and Cannington et al. (1975), who also reported an enhanced fertilizer retention below the plastic coverage. The protective function of the plastic mulch was also evident by comparing the cumulative NO_3^- leaching loss between RT and RT_{pm} below the root zone (Table 1.1). For all fertilizer rates, the amounts of leached NO_3^- was considerably lower under RT_{pm} compared to RT. Expressed in percentages, the reduction of NO_3^- leaching was 26% less under RT_{pm} and conventional fertilization with NO_3^- fertilizer distributed in ridges and furrows.

The root system of radishes is characterized by the dominating main root and only few fine roots. Hence, we assumed that the fertilizer, which is distributed in furrows, cannot be taken up by the plants and is therefore prone to leaching. Thus, we hypothesized that a better fertilizer placement has the potential to decrease NO_3^- leaching especially when it is placed solely in ridges below the plastic coverage. When fertilizer was placed only in ridges, the simulated total leaching loss was reduced by 15% under RT. Under RT_{pm} , the fertilizer placement only in ridges led to 36% lower leaching rates. Finally, a better fertilizer placement resulted in 44% lower NO_3^- leaching rates under RT_{pm} compared to RT. A decrease of fertilizer leaching by placing the fertilizer only in the elevated part of the ridge was also found in other studies

Table 1.1: Simulated cumulative NO_3^- leaching rates ($\text{kg NO}_3^- \text{ ha}^{-1}$) below the root zone as affected by plastic mulch and fertilizer placement.

	A	B	C	D
	50 kg ha^{-1}	150 kg ha^{-1}	250 kg ha^{-1}	350 kg ha^{-1}
$\text{RT}^{\text{a}} + \text{CF}^{\text{c}}$	23.61	45.83	68.09	90.31
$\text{RT}_{\text{pm}}^{\text{b}} + \text{CF}^{\text{c}}$	17.56	34.08	50.66	67.18
$\text{RT}^{\text{a}} + \text{FP}^{\text{d}}$	20.07	38.96	57.90	76.90
$\text{RT}_{\text{pm}}^{\text{b}} + \text{FP}^{\text{d}}$	11.19	21.71	32.27	42.79

^a ridge tillage without coverage

^b ridge tillage with plastic mulch

^c conventional fertilization in ridges and furrows

^d fertilizer placement only in ridges

Table 1.2: Fertilizer split application scenarios. All values are given in $\text{kg NO}_3^- \text{ ha}^{-1}$.

	Application 1	Application 2	Application 3
Scenario 1	150	-	-
Scenario 2a	75	75	-
Scenario 2b	50	100	-
Scenario 2c	30	120	-
Scenario 3a	50	50	50
Scenario 3b	30	60	60
Scenario 3c	20	80	50

(Hamlett et al., 1990; Waddell and Weil, 2006). Considering the low fertilizer use efficiency at the beginning of the growing season, we reduced successive the fertilizer amount of the first application, but concurrently maintained the total amount of $150 \text{ kg NO}_3^- \text{ ha}^{-1}$ for the split application scenarios (Table 1.2). The influence of split applications in combination with plastic mulch on NO_3^- leaching loss under conventional fertilization in ridges and furrows are shown in (Table 1.3). It was evident, that splitting the fertilizer application reduced NO_3^- leaching considerably. The lowest simulated leaching amount was achieved by applying fertilizer three times throughout the growing season with $20/80/50 \text{ kg NO}_3^- \text{ ha}^{-1}$ (Scenario 3c). This was a maximum total reduction of 59% compared to one-time application (Scenario 1).

As expected, the combination of plastic mulch, split applications and fertilizer placement only in ridges resulted in the lowest NO_3^- leaching loss. Considering the simulation RT and conventional fertilization as the reference ($45.83 \text{ kg NO}_3^- \text{ ha}^{-1}$), the combination of FBMPs resulted in a minimum of $8.14 \text{ kg NO}_3^- \text{ ha}^{-1}$ (Scenario 3c). This was equivalent to total reduction of 82%.

We conclude, that a suitable total amount of $150 \text{ kg NO}_3^- \text{ ha}^{-1}$ as well as each management

Table 1.3: Simulated cumulative NO_3^- leaching rates ($\text{kg NO}_3^- \text{ ha}^{-1}$) below the root zone as affected by plastic mulch, split applications and fertilizer placement.

	$\text{RT}_{pm}^a + \text{CF}^b$	$\text{RT}_{pm} + \text{FP}^c$
Scenario 1	34.1	21.71
Scenario 2a	23.7	14.25
Scenario 2b	19.2	12.25
Scenario 2c	15.7	9.99
Scenario 3a	19.4	11.3
Scenario 3b	23.7	9.13
Scenario 3c	13.9	8.14

^a ridge tillage with plastic mulch

^b conventional fertilization in ridges and furrows

^c fertilizer placement only in ridges

practice, namely plastic mulching, split applications or fertilizer placement, resulted in lower NO_3^- leaching rates, while the lowest leaching rate was achieved by combining all FBMPs. Therefore, the application of combined FBMPs can lead to economic benefits in terms of lower costs for external fertilizer inputs. On the other hand, environmental benefits can be achieved by reducing considerably NO_3^- leaching to groundwater. Furthermore, we conclude, that these positive aspects of plastic mulching are valid for a flat terrain, where the total amount of precipitation contributes to groundwater recharge. Under different topographical conditions such as described in Chapter 2–4, the fertilizer placement and split applications might also be a valuable tool to decrease the risk of NO_3^- leaching. However, plastic mulching on hillslopes increased substantially surface runoff, which in turn may constitute the dominating pathway for leaching fertilizer and other agrochemicals directly into the aquatic systems such as rivers and lakes. Hence, we propose to apply FBMPs in combination with perforated plastic mulch on hillslopes.

1.6.6 Concluding remarks and further research

This study was embedded in an interdisciplinary research project, which aimed to evaluate the status of the dryland agriculture in terms of environmental impacts from several perspectives. The combination of manifold field measurements and process-based modeling studies led to a comprehensive insight of flow and transport processes on dryland agricultural fields in the Haean catchment.

The thesis provides several recommendations for improving the sustainability of agricultural practices, which are dominantly based on the modeling studies. Modeling approaches always simplify the variability of natural systems. In all modeling studies in this thesis, the crop canopy structure e.g. had not been taken into account, which neglects important processes such as stemflow and interception. In the HYDRUS2/3D modeling study the surface runoff could not be directly simulated. This was in contrary an advantage of the HydroGeosphere model, which in turn shows weaknesses in the plant module e.g. solute uptake by plants. Hence, all models have strengths and weaknesses and the outputs are only a more or less good approximation of the reality. The coupling of a crop and root architecture model, the EROSION 3D and the HydroGeoSphere model would therefore be a huge step but also a sophisticated approach towards a better approximation of flow and transport processes in agricultural systems.

Focusing on the dryland agricultural fields and based on the recommendations, it is conceivable, to carry out further field experiments, which test for example the impact of fertilizer best management practices on nitrate leaching. The comparison of flow processes under RT_{pm} , RT and CT is based on modeling scenarios. Further research could also be done e.g. by plot experiments considering these different management practices.

This research and also the linked projects were focusing on dryland farming fields. Since 8% of the total area is occupied by rice paddies, the hydrology of the rice paddies in the catchment should be further investigated. It would be interesting, how and to which extent the rice paddies contribute e.g. to discharge of nutrients into groundwater. However, land use change was found to occur rapidly during the last three years showing a trend for the cultivation of cash crops such as ginseng. In 2011 a considerable area of Haean was covered by ginseng fields, which are roofed. It is obvious, that these ginseng cultivation systems will affect the flow and transport processes. A detailed field study in combination with hydrological modeling of ginseng fields would be interesting.

1.7 List of manuscripts and specification of contribution

The thesis includes five manuscripts. The first manuscript is published online in *Agricultural Water Management*, the second manuscript is submitted to *Hydrological Processes*. The third and fourth manuscript is reconsidered for publication after major revision in *Transactions of ASABE Journal* and *Nutrient Cycling in Agroecosystems*, respectively. The last manuscript is submitted to *Agriculture, Ecosystems and Environment*.

Manuscript 1

Authors	M. Ruidisch, J. Kettering, S. Arnhold, B. Huwe
Title	Modeling water flow in a plastic mulched ridge cultivation system on hillslopes affected by South Korean summer monsoon
Status	published online on August 12, 2012
Journal	<i>Agricultural Water Management</i>
Contributions	M. Ruidisch: idea, methods, data collection, data analysis, modeling, manuscript writing, figures, discussion, editing, corresponding author J. Kettering: data collection, data analysis, manuscript editing S. Arnhold: data collection, discussion B. Huwe: idea, discussion, editing

Manuscript 2

Authors	M. Ruidisch, S. Arnhold, B. Huwe, C. Bogner
Title	Effects of ridge tillage on flow processes in the Haeon catchment, South Korea summer monsoon
Status	submitted
Journal	<i>Hydrological processes</i>
Contributions	M. Ruidisch: idea, methods, data collection, data analysis, modeling, manuscript writing, figures, discussion, editing, corresponding author S. Arnhold: data collection, data analysis, editing, discussion B. Huwe: idea, discussion, editing C. Bogner: idea, data, analysis, discussion, manuscript writing, editing

Manuscript 3

Authors	S. Arnhold, M. Ruidisch, S. Bartsch, C. Shope, B. Huwe
Title	Plastic covered ridge–furrow systems on mountainous farmland: Runoff pattern and soil erosion rates
Status	submitted
Journal	<i>Transactions of ASABE Journal</i>
Contributions	S. Arnhold: idea, methods, data collection, data analysis, modeling, manuscript writing, figures, discussion, editing, corresponding author M. Ruidisch: data collection, data analysis, discussion S. Bartsch: data collection, data analysis, discussion C. Shope: discussion, editing B. Huwe: idea, discussion, editing

Manuscript 4

Authors	J. Kettering, M. Ruidisch, C. Gaviria, Y.-S. Ok, Y. Kuzyakov
Title	Fate of fertilizer ^{15}N in intensive ridge cultivation with plastic mulching under a monsoon climate
Status	reconsidered for publication after major revision
Journal	<i>Nutrient Cycling in Agroecosystems</i>
Contributions	J. Kettering: idea, methods, data collection, data analysis, manuscript writing, figures, manuscript editing, corresponding author M. Ruidisch: data collection, data analysis, modeling C. Gaviria: modeling Y.-S.Ok: editing Y. Kuzyakov: idea, discussion, editing

Manuscript 5

Authors	M. Ruidisch, S. Bartsch, J. Kettering, B. Huwe, S. Frei
Title	The effect of fertilizer best management practices on nitrate leaching in a plastic mulched ridge cultivation system
Status	submitted
Journal	<i>Agriculture, Ecosystems and Environment</i>
Contributions	M. Ruidisch: idea, methods, data collection, modeling, manuscript writing, figures, discussion, editing, corresponding author S. Bartsch: modeling, discussion, manuscript editing J. Kettering: data collection, discussion, editing B. Huwe: idea, discussion, editing S. Frei: modeling, methods, discussion, editing

References

- Allen, R., L. Pereira, D. Raes, and M. Smith (1998). *Crop evapotranspiration. Guidelines for computing crop water requirements*. Rome, Italy: FAO. ISBN: 9789251042199.
- Bargar, B., J. B. Swan, and D. Jaynes (1999). "Soil water recharge under uncropped ridges and furrows". In: *Soil Science Society of America Journal* 63.5, pp. 1290–1299. ISSN: 0361-5995.
- Bashkin, V., S. Park, M. Choi, and C. Lee (2002). "Nitrogen budgets for the Republic of Korea and the Yellow Sea Region". In: *Biogeochemistry* 57/58, pp. 387–403.
- Benjamin, J., A. Blaylock, H. Brown, and R. Cruse (1990). "Ridge tillage effects on simulated water and heat transport". In: *Soil & Tillage Research* 18.2-3, pp. 167–180.
- Bonilla, C. A., D. Kroll, J. Norman, D. Yoder, C. Molling, P. S. Miller, J. C. Panuska, J. B. Topel, P. L. Wakeman, and K. G. Karthikeyan (2006). "Instrumentation for measuring runoff, sediment, and chemical losses from agricultural fields". In: *Journal of Environmental Quality* 35, pp. 216–223.
- Cannington, F., R. B. Duggings, and R. G. Roan (1975). "Florida vegetable production using plastic film mulch with drip irrigation". In: *Proceedings 12th Natl Agr Plastics Congr.*
- Clay, S., D. Clay, W. Koskinen, and G. Malzer (1992). "Agrichemical placement impacts on alachlor and nitrate movement through soils in a ridge tilled system". In: *Journal of Environmental Science and Health* B27.2, pp. 125–138.

- Dale, V. H. and S. Polasky (2007). “Measures of the effects of agricultural practices on ecosystem services”. In: *Ecological Economics* 64.2, pp. 286–296. ISSN: 0921-8009. DOI: 10.1016/j.ecolecon.2007.05.009.
- Doherty, J. (2005). *PEST Model- independent parameter estimation*. 5th. Watermark numerical computing.
- Flury, M. and H. Flühler (1994). “Brilliant Blue FCF as a dye tracer for solute transport studies – a toxicological overview”. In: *Journal of Environmental Quality* 23.5, pp. 1108–1112.
- (1995). “Tracer characteristics of Brilliant Blue FCF”. In: *Soil Science Society of America Journal* 59.1, pp. 22–27. ISSN: 0361-5995.
- Flury, M. and N. Wai (2003). “Dyes as tracers for vadose zone hydrology”. In: *Reviews of Geophysics* 41.1, pp. 1–37.
- Gascuel-Oudou, C., F. Garnier, and D. Heddadj (2001). “Influence of cultural practices on sheet-flow, sediment and pesticide transport: the case of a corn cultivation under plastic mulching”. In: *Sustaining the global farm. Selected papers from the 10th International Soil Conservation Organization Meeting*. Ed. by D. Stott, R. Mohtar, and G. Steinhardt. International Soil Conservation Organization, pp. 300–304.
- Green, H. and G. Ampt (1911). “Studies on Soil Physics”. In: *Journal of Agricultural Science* 4.01, pp. 1–21.
- Hamlett, J., J. Baker, and R. Horton (1990). “Water and anion movement under ridge tillage: a field study”. In: *Transactions of the American Society of Agricultural Engineers* 33, pp. 1859–1866.
- Hendrickx, J. and M. Flury (2001). “Uniform and preferential flow mechanisms in the vadose zone”. In: *Conceptual Models of Flow and Transport in the Fractured Vadose Zone*. Ed. by N. R. Council. Washington and DC: National Academy Press.
- Hong, J. and J. Kim (2011). “Impact of the Asian monsoon climate on ecosystem carbon and water exchanges: a wavelet analysis and its ecosystem modeling implications”. In: *Global Change Biology* 17.5, pp. 1900–1916. ISSN: 1354-1013. DOI: 10.1111/j.1365-2486.2010.02337.x.
- Hwang, S.-J., S.-K. Kwun, and C.-G. Yoon (2003). “Water quality and limnology of Korean reservoirs”. In: *Paddy and Water Environment* 1, pp. 43–52. ISSN: 1611-2490. DOI: 10.1007/s10333-003-0010-7.
- Jarvis, N. J. (2007). “A review of non-equilibrium water flow and solute transport in soil macropores: principles, controlling factors and consequences for water quality”. In: *European*

Journal of Soil Science 58.3, pp. 523–546. ISSN: 1351-0754. DOI: 10.1111/j.1365-2389.2007.00915.x.

Jaynes, D. and J. Swan (1999). “Solute Movement in Uncropped Ridge-Tilled Soil under Natural Rainfall”. In: *Soil Science Society of America Journal* 63, pp. 264–269.

Kim, B., J.-H. Park, G. Hwang, M.-S. Jun, and K. Choi (2001). “Eutrophication of reservoirs in South Korea”. In: *Limnology* 2, pp. 223–229. ISSN: 1439-8621. DOI: 10.1007/s10201-001-8040-6.

Kim, S., J. Yang, C. Park, Y. Jung, and B. Cho (2007). “Effects of winter cover crop of ryegrass (*Lolium multiflorum*) and soil conservation practices on soil erosion and quality in the sloping uplands”. In: *Journal of the Korean Society for Applied Biological Chemistry* 55.1, pp. 22–28.

Kirchmann, H. and G. Thorvaldsson (2000). “Challenging targets for future agriculture”. In: *European Journal of Agronomy* 12.3-4, pp. 145–161. ISSN: 1161-0301. DOI: 10.1016/S1161-0301(99)00053-2.

Kool, J., J. Parker, and M. van Genuchten (1987). “Parameter estimation for unsaturated flow and transport models - A review”. In: *Journal of Hydrology* 91.3-4, pp. 255–293.

Lee, G. J., J. T. Lee, J. S. Ryu, S. W. Hwang, Y. S. Yang, J. H. Joo, and Y. S. Jung (2010). “Loss of soil and nutrient from different soil managements in highland agriculture”. In: *Proc. 19th World Congress of Soil Science. Soil solution for a changing world*. Ed. by R. Gilkes and Prakongkep. International Union of Soil Sciences, pp. 78–81.

Leistra, M. and J. J. T. I. Boesten (2010). “Pesticide Leaching from Agricultural Fields with Ridges and Furrows”. In: *Water Air and Soil Pollution* 213.1-4, pp. 341–352. ISSN: 0049-6979. DOI: 10.1007/s11270-010-0389-x.

Locascio, S. J., J. G. A. Fiskell, D. A. Graetz, and R. D. Hawk (1985). “Nitrogen accumulation by peppers as influenced by mulch and time of fertilizer application”. In: *Journal of the American Society for Horticultural Science* 110, pp. 325–328.

Moriasi, D. N., J. G. Arnold, M. W. van Liew, R. L. Bingner, R. D. Harmel, and T. L. Veith (2007). “Model evaluation guidelines for systematic quantification of accuracy in watershed simulations”. In: *Transactions of the ASABE* 50.3, pp. 885–900. ISSN: 0001-2351.

Park, J.-H., L. Duan, B. Kim, M. J. Mitchell, and H. Shibata (2010). “Potential effects of climate change and variability on watershed biogeochemical processes and water quality in Northeast Asia”. In: *Environment International* 36.2, pp. 212–225. ISSN: 01604120.

Peterjohn, W. and D. Correll (1984). “Nutrient Dynamics in an Agricultural Watershed – Observations on the Role of A Riparian Forest”. In: *Ecology* 65, pp. 1466–1475.

- Petersen, C., H. Jensen, S. Hansen, and C. Bender Koch (2001). “Susceptibility of a sandy loam soil to preferential flow as affected by tillage”. In: *Soil & Tillage Research* 58.1–2, pp. 81–89.
- Pinson, W., D. Yoder, J. Buchanan, W. Wright, and J. Wilkerson (2004). “Design and evaluation of an improved flow divider for sampling runoff plots”. In: *Applied Engineering in Agriculture* 20.4, pp. 433–438.
- Rice, P., J. A. Harman-Fetcho, A. M. Sadeghi, L. L. McConnell, C. B. Coffman, J. R. Teasdale, A. Abdul-Baki, J. L. Starr, G. McCarty, R. R. Herbert, and C. J. Hapeman (2007). “Reducing insecticide and fungicide loads in runoff from plastic mulch with vegetative-covered furrows”. In: *Journal of Agricultural and Food Chemistry* 55.4, pp. 1377–1384. ISSN: 0021-8561. DOI: 10.1021/jf062107x.
- Rice, P., L. L. McConnell, L. Heighton, A. M. Sadeghi, A. Isensee, J. R. Teasdale, A. Abdul-Baki, J. Harman-Fetscho, and C. J. Hapeman (2001). “Runoff loss of pesticides and soil: a comparison between vegetative mulch and plastic mulch in vegetable production systems”. In: *Journal of Environmental Quality* 30, pp. 1808–1821.
- Saffigna, P., C. Tanner, and D. Keeney (1976). “Non-uniform infiltration under potato canopies caused by interception, stemflow, and hilling”. In: *Agronomy Journal* 68, pp. 337–342.
- Schmidt, J. (1991). *A mathematical model to simulate rainfall erosion: in: Erosion, transport and deposition processes. Theories and models*. Cremlingen, Germany.
- Simunek, J. (2006). “Models of Water Flow and Solute Transport in the Unsaturated Zone”. In: *Encyclopedia of Hydrological Sciences*. John Wiley & Sons, Ltd. ISBN: 9780470848944.
- Spiertz, J. H. J. (2010). “Nitrogen, Sustainable Agriculture and Food Security: A Review”. In: *Agronomy for Sustainable Development* 30.1, pp. 43–55.
- Stevens, M., B. Black, J. Lea-Cox, A. M. Sadeghi, J. Harman-Fetscho, E. Pfeil, P. Downey, R. Rowland, and C. J. Hapeman (2009). “A comparison of three cold-climate strawberry production systems: environmental effects”. In: *HortScience* 44.2, pp. 298–305.
- Swinton, S. M., F. Lupi, G. P. Robertson, and S. K. Hamilton (2007). “Ecosystem services and agriculture: Cultivating agricultural ecosystems for diverse benefits”. In: *Ecological Economics* 64.2, pp. 245–252. ISSN: 0921-8009. DOI: 10.1016/j.ecolecon.2007.09.020.
- Therrien, R., R. McLaren, E. Sudicky, and S. Panday (2010). *HydroGeoSphere: A Three-dimensional numerical model describing fully-integrated subsurface and surface flow and solute transport*. University of Waterloo. Waterloo, Canada.
- Tilman, D., K. G. Cassman, P. A. Matson, R. Naylor, and S. Polasky (2002). “Agricultural sustainability and intensive production practices”. In: *Nature* 418.6898, pp. 671–677. ISSN: 0028-0836. DOI: 10.1038/nature01014.

- Tilman, D., J. Fargione, B. Wolff, C. D'Antonio, A. Dobson, R. Howarth, D. Schindler, W. H. Schlesinger, D. Simberloff, and D. Swackhamer (2001). "Forecasting Agriculturally Driven Global Environmental Change". In: *Science* 292.5515, pp. 281–284. ISSN: 0036-8075. DOI: 10.1126/science.1057544.
- Trancón y Widemann, B. and C. Bogner (2012). "Image analysis for soil dye tracer infiltration studies". In: *Proceedings of the 3rd International Conference on Image Processing Theory, Tools and Applications*. (in press).
- Waddell, J. T. and R. R. Weil (2006). "Effects of fertilizer placement on solute leaching under ridge tillage and no tillage". In: *Soil & Tillage Research* 90.1-2, pp. 194–204.
- Wallace, A. (1994). "High-precision agriculture is an excellent tool for conservation of natural resources". In: *Communications in Soil Science and Plant Analysis* 25.1-2, pp. 45–49. DOI: 10.1080/00103629409369002.
- Wan, Y. and S. El-Swaify (1999). "Runoff and soil erosion as affected by plastic mulch in a Hawaiian pineapple field". In: *Soil & Tillage Research* 52.1-2, pp. 29–35.
- Woehling, T., J. A. Vrugt, and G. F. Barkle (2008). "Comparison of three multiobjective optimization algorithms for inverse modeling of vadose zone hydraulic properties". In: *Soil Science Society of America Journal* 72.2, pp. 305–319. ISSN: 0361-5995. DOI: 10.2136/sssaj2007.0176.
- Zhang, W., T. H. Ricketts, C. Kremen, K. Carney, and S. M. Swinton (2007). "Ecosystem services and dis-services to agriculture". In: *Ecological Economics* 64.2, pp. 253–260. ISSN: 0921-8009. DOI: 10.1016/j.ecolecon.2007.02.024.

Chapter 2

Modeling water flow in a plastic mulched ridge cultivation system on hillslopes affected by South Korean summer monsoon

Marianne Ruidisch^{1,a}, Janine Kettering^b, Sebastian Arnhold^a, Bernd Huwe^a

^a Soil Physics Group, BayCEER, University of Bayreuth, 95440 Bayreuth, Germany

^b AgroEcoSystem Research Department, BayCEER, University of Bayreuth, 95440 Bayreuth, Germany

Abstract

Intensive agricultural land use in combination with heavy rain storm events during the summer monsoon season plays a key role in groundwater pollution by nutrients and agrochemicals in agricultural catchments in South Korea. A widespread measure for weed control in this region is plastic mulched ridge cultivation. However, it is not well understood, how and to which extent the water flow regime in sloped fields is hereby modified. To evaluate the effect of plastic mulched ridge cultivation (RT_{pm}) on soil water dynamics, we carried out a two-dimensional process-based modeling study using the numerical model Hydrus 2/3D. Subsequently, RT_{pm} was

¹Correspondence to: Marianne Ruidisch, Soil Physics Group, BayCEER, University of Bayreuth, 95440 Bayreuth, Germany.
E-mail: ruidisch@uni-bayreuth.de

compared to model simulations of ridge cultivation without plastic cover (RT) and flat conventional tillage without ridges and without plastic cover (CT). Datasets of soil water potentials obtained by field measurements at two plastic mulched potato fields (*Solanum tuberosum L.*) provided the basis for optimizing soil hydraulic parameters inversely by the Levenberg-Marquardt algorithm. We found, that plastic mulching induced horizontal pressure head gradients and forced soil water to move laterally from furrows to ridges under normal weather conditions. During monsoon events, soils were fully saturated and interflow occurred in coarse textured and ploughed topsoil. Further, the water balance of the different model scenarios showed that plastic mulching reduced drainage water up to 16% but concurrently increased the surface runoff up to 65%. The consequences are an increase in runoff peak flow, flood risk and erosion. Therefore, we recommend the application of perforated and biodegradable plastic mulch in regions affected by summer monsoon.

Keywords: Polyethylene film, ridge-furrow tillage, extreme rain events, Hydrus 2/3D, potato crop, hillslopes

2.1 Introduction

Agricultural management practices, soil properties and field topography lead to a high variability in soil water movement, solute transport and leaching of nutrients and agrochemicals. In South Korea, ridge tillage with impermeable black plastic mulch covering the ridges is the most common practice for dryland crops such as radish (*Raphanus sativus*), cabbage (*Brassica rapa susp. Pekinensis (lour.) Hanelt*, *Brassica aleracea convar. Capitata var. alba*), beans (*Glycine max. (L.) Merr.*) and potatoes (*Solanum tuberosum L.*), which are predominately grown on slopes. Intense fertilization together with heavy rainfalls during summer monsoon season poses a high risk of groundwater pollution in the Hae-an catchment. Additionally, the discharge of phosphorus associated with sediments from agricultural areas causes eutrophication and deterioration of water quality in downstream reservoirs in South Korea (Kim et al., 2001). This is of major significance because the river system of Hae-an contributes to the Soyang Lake, which is a major source of freshwater for the metropolitan area of Seoul.

The effect of flat row-interrow cultivation on soil water dynamics was investigated for soybean and corn crops in previous studies (Timlin et al., 2001; Wesenbeeck and Kachanoski, 1988; Paltineanu and Starr, 2000). The findings showed increased soil moisture in row positions due

to interception and stemflow. The same effect was also found for potato crops cultivated in ridges (Saffigna et al., 1976), but with the addition of concurrently higher water contents in furrows because of surface runoff from ridges and leaf drip from the outer foliage. Soil and plant biological effects of the plastic mulch were studied by Gürsoy et al. (2011) and Lazlo and Gyuricza (2004), who found favorable physical soil conditions and improved growth and yield of maize and corn crops. Previous research on plastic mulched ridge cultivation focused mainly on rain water harvesting in combination with irrigation techniques in semiarid and arid regions, in which the plastic covered ridges induce runoff to the planted furrow area, leading to an increased crop yield and water availability (Wang et al., 2008; X. Y. Li and Gong, 2002; X.-Y. Li et al., 2008; Tian et al., 2003; Mahajan et al., 2007). In contrast, dryland crops in South Korea are planted in the plastic covered ridges to suppress weed growth and to support early plant emergence due to increased soil temperature in the ridges.

Only a few modeling studies about ridge cultivation systems exist. Solute transport of pesticides in an irrigated potato ridge cultivation system was investigated by Leistra and Boesten (2010). They demonstrated that the risk of pesticide leaching in furrow soil can be substantially higher than in corresponding level field soil. Abbasi et al. (2004) simulated water flow in a long furrow system with furrow irrigation using Hydrus 2/3D to estimate inversely soil hydraulic properties and transport parameters. Dusek et al. (2010) used the S1D and S2D models to simulate water flow and solute transport in a drip irrigated plastic mulched pineapple cultivation.

Since there are no modeling studies about plastic mulched ridge cultivation in mountainous areas affected by extreme rain events, the aim of this study was to evaluate the effect of plastic mulched ridge cultivation on soil water dynamics under a summer monsoonal climate. Therefore, we used a monitoring network of tensiometers and FDR sensors in two potato fields in the mountainous Haean basin in South Korea to observe soil water dynamics in ridge and furrow positions. The field data sets of standard tensiometers were used to estimate soil hydraulic parameters using an inverse modeling approach based on Levenberg-Marquardt nonlinear minimization algorithm. Subsequently we used the optimized parameters of the water flow model to run scenarios regarding ridge tillage without plastic mulch and flat conventional tillage. The comparison of plastic mulched ridge tillage (RT_{pm} , ridge tillage without plastic coverage (RT) and a flat conventional tillage (CT) allows a better understanding of soil water dynamics and water movement influenced by the plastic mulch.

2.2 Materials and methods

2.2.1 Study area

The agriculturally used Haean catchment is located in Gangwon Province in the North-eastern part of South Korea (Figure 2.1). While rice paddies are dominating in the flat parts of the basin, dryland farming is practiced in the hillsloped areas of the catchment. The annual precipitation sum in Haean basin is about 1577 mm (11-years average) with 50-60% of the annual rainfall occurring during summer from June to August. The Korean peninsula is characterized by two rainfall peaks, one in July and one in August. The maximum rainfall, however, shifted in the recent decades from July to August Lee et al. (2010). The precipitation during the 2010 observation period is shown in Figure 2.3.

Plastic mulched ridge cultivation is the common practice to cultivate dryland crops in Haean catchment. Ridges (35 cm width and 15 cm height) are covered with an impermeable black polyethylene film and alternate with uncovered furrows (35 cm width). Planting holes (diameter 5 cm) in the plastic cover are located at the top of the ridges with a plant-to-plant spacing of 25 cm.

Cambisols developed on the granitic bedrock material are widespread over the catchment. Due to high erosion rates, however, the application of sandy soil material before the growing season is a commonly used method to compensate for soil loss. Thus, highly disturbed soil profiles are characterized by light-textured, permeable and ploughed top layers, which are prone to nutrient and pesticide leaching and subjacent B horizons.

Measurements were carried out at two different potato fields (*Solanum tuberosum L.*) within the Haean catchment, each with plastic mulched ridges and similar planting dates as well as slope degrees. The average slope gradient was 11° and 10° at field sites 1 and 2, respectively. Seed potatoes were planted on 5 May at field site 1 and on 10 May at field site 2. Plastic coverage caused higher temperature in soils and therefore crops emerged rapidly. At both field sites plants emerged before the first measurement day (31 May 2010). Mineral fertilizer was applied as granules and mixed into the topsoil layer before ridges were built. During the observation period pesticides were sprayed twice throughout the field sites. Field site 1 was characterized by a granitic bedrock layer at 1 m depth. At field site 2 the soil was deeper developed and the underlying bedrock layer could not be detected by excavation down to 130 cm. Soil physical properties of the experimental sites are given in Table 2.1.

Table 2.1: Soil physical properties of the experimental sites.

	Horizon (WRB)	Sand (%)	Silt (%)	Clay (%)	Bulk density (g cm ⁻³)	Soil texture class (USDA)
Field site 1	Ap	65.72	26.78	7.50	1.28(±0.02)	Sandy loam
	Bw	39.30	51.60	9.10	1.18(±0.05)	Silt loam
Field site 2	Ap	42.65	41.15	16.20	1.27(±0.04)	Loam
	Bwb	22.00	52.90	25.10	1.31(±0.03)	Silt loam

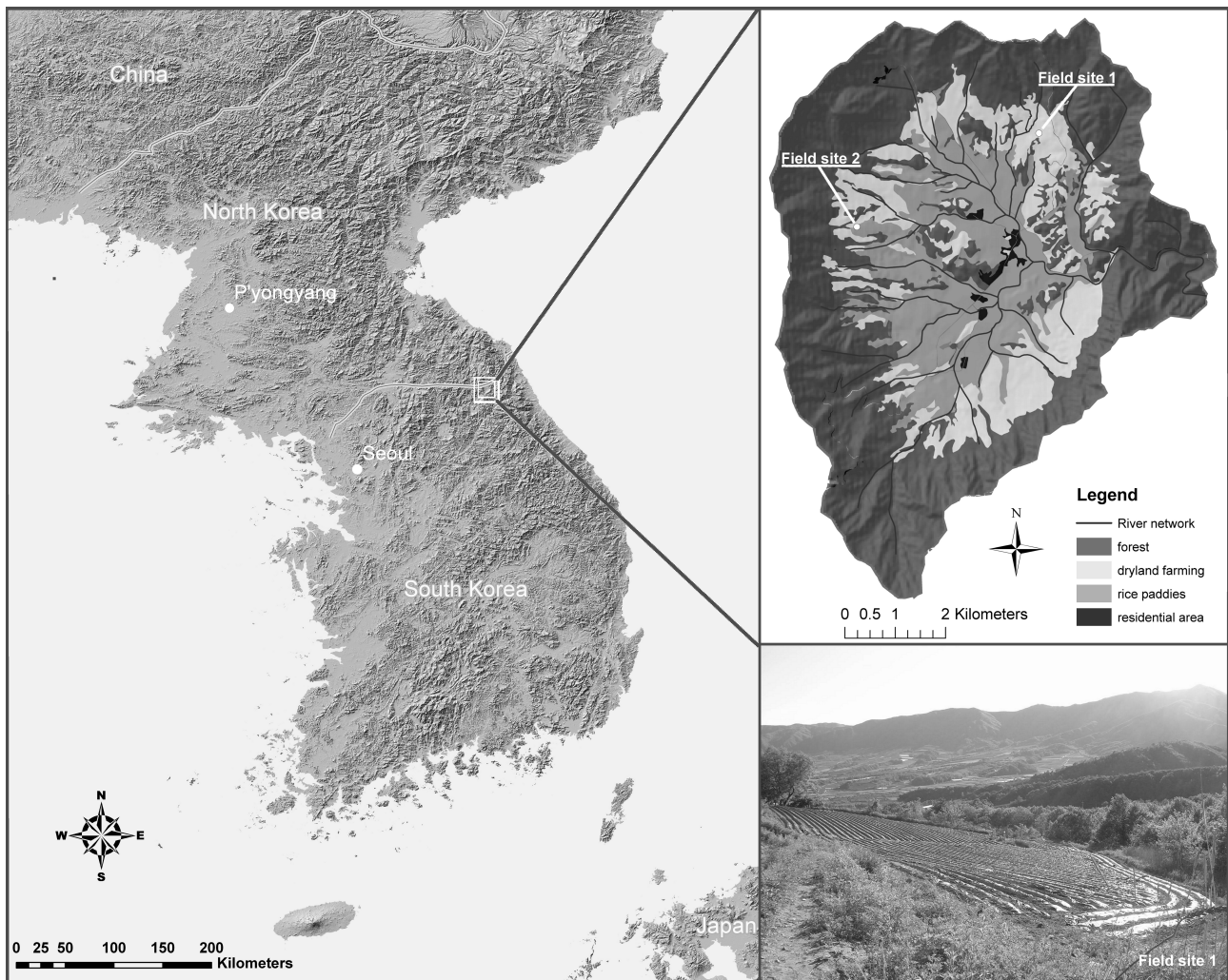


Figure 2.1: Topographical map of South Korea (left), land use map of the Haeon catchment (top right) and picture of field site 1 (bottom right).

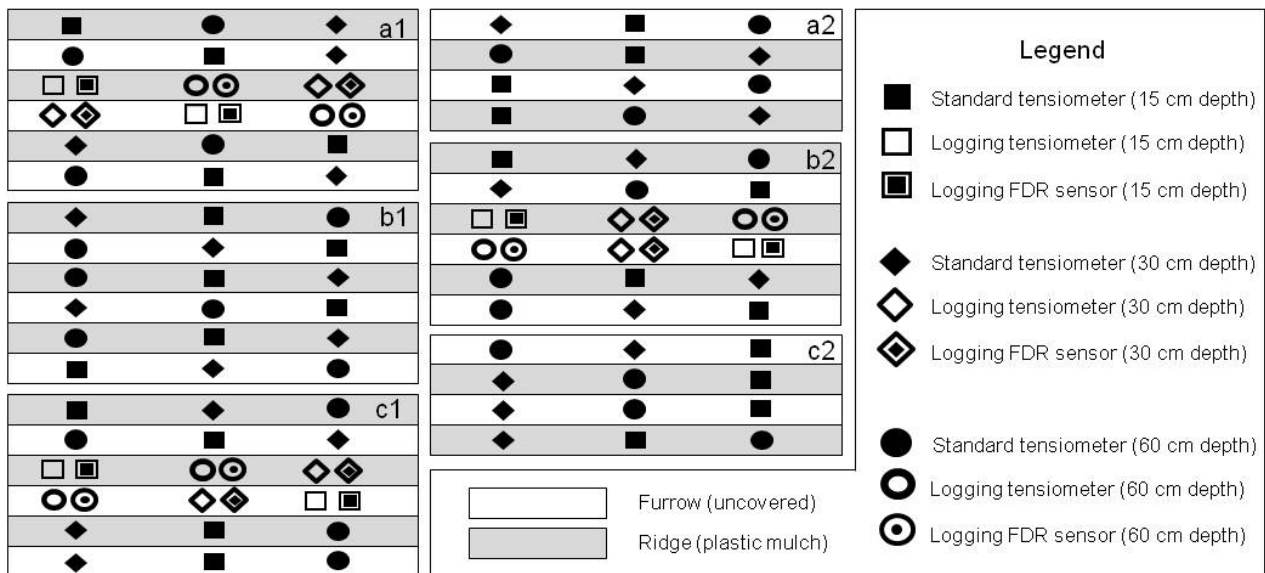


Figure 2.2: Monitoring network of standard tensiometers, continuously recording tensiometers and FDR sensors; subplots a, b and c refers to different slope locations (a: upper slope, b: middle slope, c: lower slope), 1: field site 1 and 2: field site 2. The distance between subplots was approximately 15 and 30 m on field site 1 and 2, respectively.

2.2.2 Field measurements

A field-monitoring network of standard tensiometers, continuously recording tensiometers and FDR sensors (Decagon 10HS moisture sensors at 15 and 30 cm depths, DeltaT ThetaProbe ML2X in 60 cm depths) was set up in the two potato fields on hillslopes on 28 May 2010. At each field site we installed the sensors in three subplots accounting for different slope position (upper, middle and lower slope). In each ridge and each furrow, monitoring devices were installed at 15, 30 and 60 cm depth from the respective soil surface. The location of the respective depth in a ridge or furrow was chosen randomly. The distance between sensors in ridges and furrows was 2 m. All FDR sensors and continuously recording tensiometers were connected to a DeltaT logger, which logged soil water contents and soil water potential in a 30-min interval. Standard tensiometers were read out with a manual pressure reader in a 2-d interval from 31 May to 24 August, 2010. We used only the standard tensiometer data sets for the modeling approach to run simulations on a daily time step. The design of the monitoring set up at both field sites is shown in Figure 2.2.

2.2.3 Modeling approach

2.2.3.1 Governing flow equations

The ability of representing physical processes such as subsurface water flow in variable saturated media is an advantage of process-based numerical models. Previous tracer studies at the selected field sites (unpublished) have shown that preferential flow paths were negligible for soil water movement. Such uniform flow processes can be described using the Richards' equation. Based on the Galerkin finite element method, Hydrus 2/3D solves the Richards' equation for two-dimensional water flow in a variably saturated porous media. The extended Richards' equation incorporates a sink term, which considers the water uptake by roots (Equation (2.1)). All following equations are described in Sejna et al. (2011).

$$\frac{\delta\theta}{\delta t} = \frac{\delta}{\delta x_i} \left[K \left(K_{ij}^A \frac{\delta h}{\delta x_j} + K_{iz}^A \right) \right] - S \quad (2.1)$$

where θ is the volumetric water content ($\text{cm}^3 \text{ cm}^{-3}$), h is the pressure head (cm), S is a sink term (cm d^{-1}), x_i ($i=1,2$) are the spatial coordinates (cm), t is time (days), K_{ij}^A are components of a dimensionless anisotropy tensor K^A , and K is the saturated hydraulic conductivity function (cm d^{-1}) given by

$$K(h, x, y, z) = K_s(x, y, z) K_r(h, x, y, z) \quad (2.2)$$

where K_r is the relative hydraulic conductivity and K_s is the saturated hydraulic conductivity (cm d^{-1}). The sink term S in (1), represents the volume of water removed per unit time from a unit volume of soil due to plant water uptake. Equation (2.3) shows the definitions of the sink term S by Feddes et al. (1978).

$$S(h) = \alpha(h)S_p \quad (2.3)$$

where the water stress response function $\alpha(h)$ is a prescribed dimensionless function of the soil water pressure head ($0 \leq \alpha \leq 1$), and S_p is the potential water uptake rate (d^{-1}). According to Wesseling et al. (1991) root water uptake of potatoes is assumed to be zero if the flow domain is close to saturation (> -10 cm) and if the pressure head becomes lower than the wilting point (< -16000 cm). Water uptake of potatoes is considered optimal for pressure heads between -25 and -320 cm. Within this range, water uptake decreases (or increases) linearly with h . S_p is equal to the water uptake rate during no water stress when $\alpha(h) = 1$. Based on field observations, root water uptake was considered down to 30 cm soil depth. The unsaturated soil hydraulic

properties as well as the hydraulic conductivity are described by the soil hydraulic function model of Genuchten (1980) in equations (2.4) and (2.5).

$$\theta(h) = \begin{cases} \theta_r + \frac{\theta_s - \theta_r}{[1 + |\alpha h|^n]^{1-1/n}} & \text{for } h < 0 \\ \theta_s & \text{for } h \geq 0 \end{cases} \quad (2.4)$$

where $\theta(h)$ is soil water retention, θ_r is the residual water content ($\text{cm}^3 \text{ cm}^{-3}$), θ_s is the saturated water content ($\text{cm}^3 \text{ cm}^{-3}$), α and n are empirical shape parameters

$$K(h) = K_s S_e^l \left[1 - (1 - S_e^{1/(1-1/n)})^{1-1/n} \right]^2 \quad (2.5)$$

where $K(h)$ is hydraulic conductivity (cm d^{-1}), K_s is the saturated hydraulic conductivity (cm d^{-1}), l is the pore connectivity parameter, which was estimated to be about 0.5 (Mualem, 1976).

2.2.3.2 Model parameterization

Two weather stations, both located approximately 750 m from the respective field site, provided daily precipitation data and additional weather parameters for the calculation of soil evaporation and crop transpiration (Figure 2.3). Due to its exposed position in the catchment, field site 2 received approximately 15-20% more precipitation than field side 1. Precipitation data was multiplied by 2 to include the surface runoff from the plastic mulched ridges. This factor was calculated by assuming a permeable area (furrows and planting holes) of 50% of the total area and a plastic covered area (ridges) of 50% in a two-dimensional profile (Dusek et al., 2010). For the model scenario without plastic mulch, the original precipitation data was used.

Soil evaporation and crop transpiration were calculated with the FAO Penman-Monteith equation for potato crops using weather parameters such as solar radiation, air temperature, wind speed, humidity and air pressure, which were measured by the weather stations. A detailed description of the dual crop coefficient approach for separately calculating soil evaporation and crop transpiration is given by Allen et al. (1998). In Figure 2.3, soil evaporation and crop transpiration for both field sites are given separately. Different weather, soil and management conditions at field site 2 lead to lower evaporation and transpiration rates compared to field site 1.

The Van Genuchten parameters saturated and residual water content θ_s , θ_r , α , n and the saturated hydraulic conductivity K_{sat} were initially estimated based on texture and bulk density

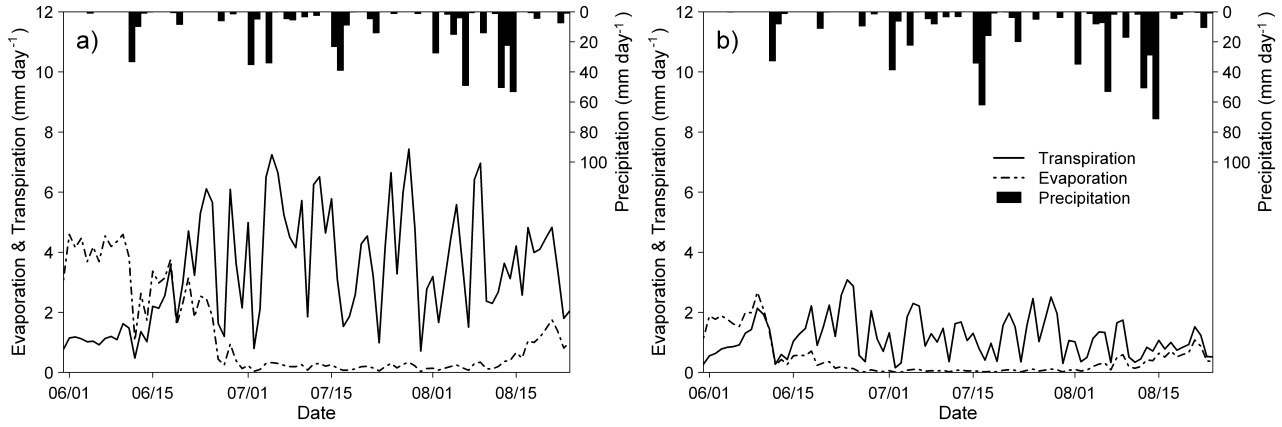


Figure 2.3: Daily precipitation, evaporation and transpiration rates during the growing season 2010; a) Field site 1 and b) Field site 2.

using the neural network pedotransfer functions of Rosetta lite module (Schaap et al., 2001), which is implemented in Hydrus 2/3D. Inverse estimation of soil hydraulic properties are based on time series datasets of pressure heads, which we read out with standard tensiometers. We ran the simulations on a daily timestep with 264 data points in the objective function, which equates 44 pressure head values at each observation point in the model. These 44 pressure head values at each observation point in the model (e.g. ridge 15 cm depth) represented the calculated mean of 7 and 6 tensiometers, which were installed at the same depth (e.g. 15 cm soil depth) and same location (e.g. ridge) at field site 1 and field site 2, respectively. As a first step we fitted the soil hydraulic parameters θ_s and θ_r . Afterwards α , n and K_{sat} were optimized simultaneously. The optimization approach was based on Levenberg-Marquardt non-linear minimization method. Initially estimated soil hydraulic parameters and α , n , θ_s and θ_r and the saturated hydraulic conductivity K_{sat} for both field sites are given in Table 2.3.

2.2.3.3 Initial and boundary Conditions

Pressure head values measured on 31 May 2010 reflecting the beginning of the observation period (31 May to 24 August 2010) were used to adjust the initial conditions in the water flow domain. Surface boundary conditions were set to atmospheric conditions in furrows and planting holes, whereas plastic mulched areas were set to no flux conditions (Figure 2.4). For the scenarios without coverage of the ridges (RT) and flat conventional tillage (CT) atmospheric boundary conditions were applied to the entire surface boundary.

Although the diameter of the planting holes was in fact 5 cm, it was necessary to scale it down to 1 cm width in the two-dimensional model in order to keep the correct dimension, when

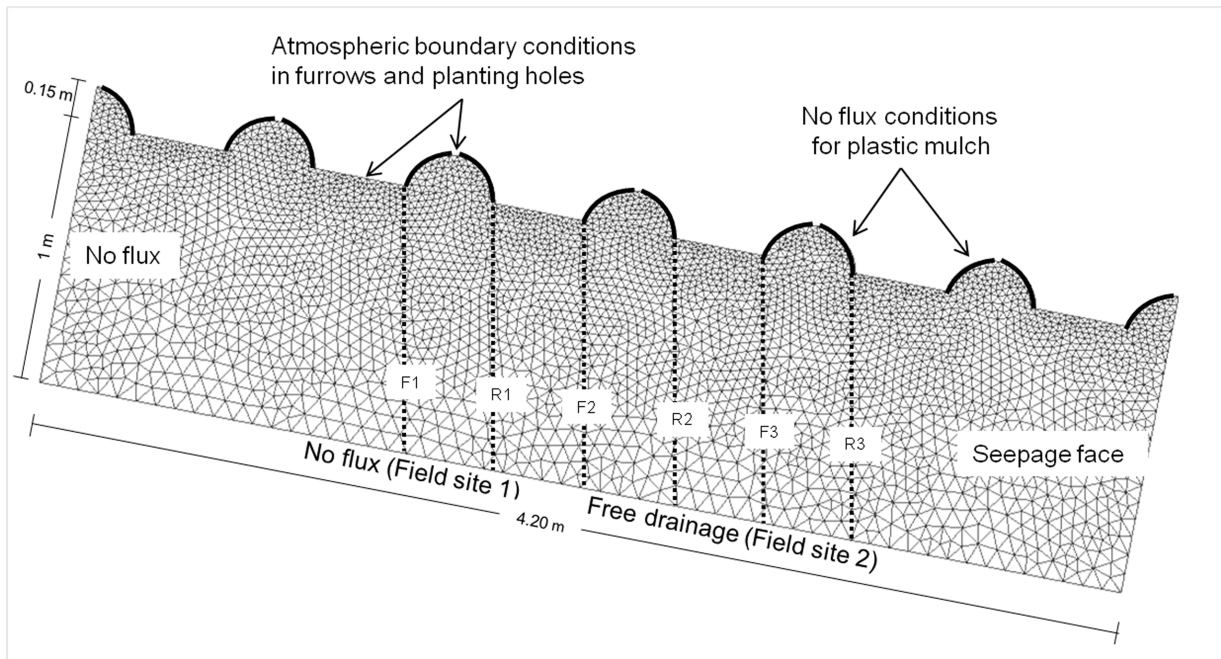


Figure 2.4: Boundary conditions of the model simulations; note that the bottom boundary varies between the two field sites; vertical meshlines F1-3 and R1-3 were included to calculate lateral water fluxes (Figure 2.9); for simulation of ridges without coverage (RT) and conventional tillage (CT) atmospheric boundary conditions were implemented at the entire surface.

calculating, e.g. drainage water fluxes per m^2 . The upper left hand boundary was set to no flux, which marks the transition from the plowed agricultural field to a compacted farm track. The bottom boundary was defined as no flux conditions (field site 1) due to granite parent rock in 1 m depth. At field site 2, free drainage conditions were applied to the bottom boundary, because a soil excavation showed a deeper soil development than 1 m depth. The lower right hand boundary was defined as seepage face. For the calculation of water fluxes at the transition from ridges to furrows and vice versa, meshlines (F1-3 and R1-3) were included in the model. Meshlines F1-3 reflect water fluxes coming from furrows but contribute to ridges. In contrast, meshlines R1-3 represent the transition from ridges to furrows in slope direction (Figure 2.4).

2.2.3.4 Model evaluation statistics

Different statistical techniques such as Pearson's correlation coefficient (R), coefficient of determination (R^2), Nash-Sutcliffe efficiency (NSE), model bias (\bar{e}) and percentage bias ($Pbias$) were used to evaluate the models. A comprehensive overview of the evaluation statistics for hydrological models is provided by Moriasi et al. (2007). Pearson's correlation coefficient and the coefficient of determination range from 0 to 1, where 1 indicates a perfectly linear relationship. The Nash-Sutcliffe coefficient (Equation (2.6)) determines the relative magnitude of the residual

variance compared to the observed data variance. The coefficient of efficiency varies between $-\infty$ and 1, where 1 indicates a perfect model. Model performance is unacceptable when the value is < 0 .

$$NSE = 1 - \left[\frac{\sum_{i=1}^n (Y_i^{obs} - Y_i^{sim})^2}{\sum_{i=1}^n (Y_i^{obs} - Y^{mean})^2} \right] \quad (2.6)$$

McCuen et al. (2006) noted that NSE values also depend on sample size, bias of magnitude and outliers. Therefore he recommended reporting always the bias (Equation (2.7)), in the unit of the variable) along with the NSE , which is computed by

$$\bar{e} = \frac{1}{n} \sum_{i=1}^n (Y_i^{sim} - Y_i^{obs}) \quad (2.7)$$

The percentage bias ($Pbias$) is easier to interpret and is determined by the ratio of the bias (\bar{e}) to the mean of the measured values (Y^{mean}) multiplied by 100. In the case of soil water potentials (negative values), a negative percentage bias indicates higher simulated pressure heads in comparison to observed pressure heads.

2.2.3.5 Sensitivity analysis

Dynamic root development is not implemented in Hydrus 2/3D. Therefore we assumed based on field observations an average rooting depth of 30 cm during the entire simulation period for the model fitting procedure. Plant development to adult stage occurred relatively quickly within approximately 4 weeks after emergence. Within this time period the differing spatial distribution of roots in the soil has an effect on root water uptake and soil water status. We analyzed the sensitivity of the water balance components such as seepage, runoff and drainage water fluxes to differing rooting depths by varying the root depth from 10 cm to 60 cm in an interval of 10 cm. Although the calculation of the FAO56 dual crop coefficients includes actual weather data information, the estimation of evaporation and transpiration rates is empirical and only an approximate determination. We additionally applied a sensitivity analysis of the water balance by changing the evaporation and transpiration rates inputs. Thus we maintained the original calculated ratio of evaporation and transpiration but varied both rates in percentage terms. Therefore we increased the original calculated values up to 100 %. Accordingly we reduced the evaporation and transpiration rates to 0 %. The sensitivity analysis regarding both, root development as well as evaporation and transpiration rates was accomplished for all surface managements RT_{pm} , RT and CT .

Table 2.2: Model evaluation coefficients R , R^2 , Nash-Sutcliffe efficiency (NSE), bias (\bar{e}) and percentage bias ($Pbias$) for simulations of both field sites.

	R	R^2	NSE	\bar{e}	$Pbias$
Field site 1	0.89	0.79	0.79	-1.78	2%
Field site 2	0.76	0.58	0.48	-13.10	12%

Table 2.3: Initial estimates (est.) and optimized (opt.) van Genuchten parameters and saturated hydraulic conductivity (K_{sat}) for both field sites.

		θ_r ($\text{cm}^3 \text{ cm}^{-3}$)		θ_s ($\text{cm}^3 \text{ cm}^{-3}$)		α (cm^{-1})		n (-)		K_{sat} (cm d^{-1})	
		est.	opt.	est.	opt.	est.	opt.	est.	opt.	est.	opt.
Field site 1	Material 1	0.0402	0.071	0.4217	0.313	0.0266	0.046	1.452	1.408	102.9	103.0
	Material 2	0.0471	0.138	0.4121	0.346	0.0057	0.006	1.641	1.2	81.94	29.4
Field site 2	Material 1	0.0574	0.134	0.419	0.301	0.0082	0.014	1.566	1.403	31.02	2.9
	Material 2	0.0767	0.037	0.443	0.393	0.0065	0.006	1.599	1.2	19.13	15.4

2.3 Results

2.3.1 Model evaluation and parameter optimization

The comparison between observed and simulated pressure heads (Figure 2.5) showed a good agreement at field site 1, whereas the agreement at field site 2 was less satisfactory. While, wetting events in particular were simulated reasonably well, the low pressure heads during drying cycles at the beginning of the observation period were underestimated, especially at field site 2. The evaluation coefficients for both field sites are given in Table 2.2.

The optimization of the water retention parameters (Table 2.3) showed an initial overestimation of the saturated water content θ_s , while the residual water content θ_r was underestimated. The n values, which configure the steepness of the water retention curves, were smaller as initially estimated, resulting in a flatter curve characteristic for all horizons at both field sites. Therefore, the water holding capacity was higher in all four horizons and drainage occurred within a wider range of pressure heads. The saturated hydraulic conductivity K_{sat} changed to lower values in the subjacent B-horizon at field site 1 and in both horizons at field site 2.

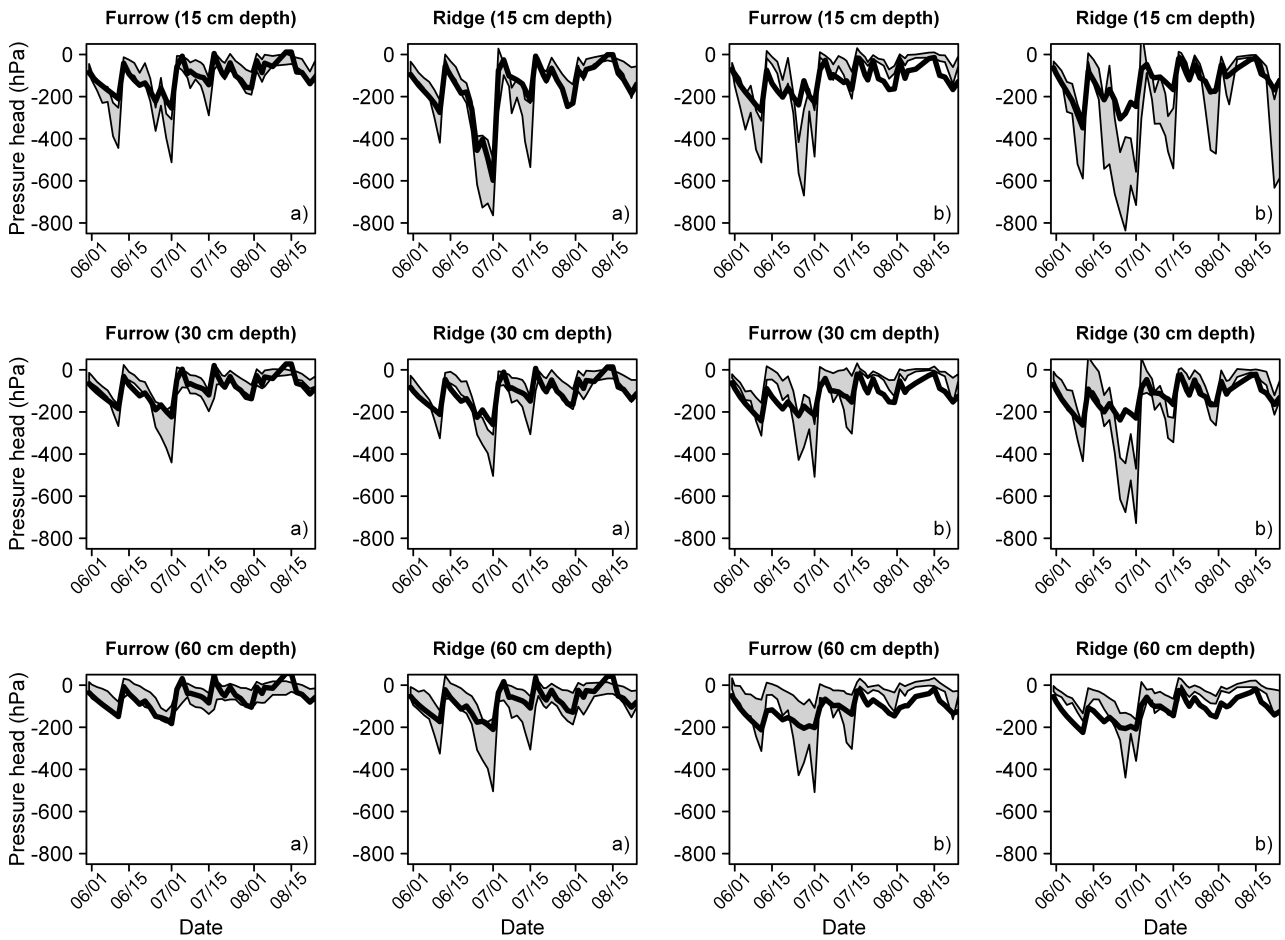


Figure 2.5: Observed vs. simulated pressure heads in different depth for (a) field site 1 and (b) field site 2; limits of gray area = \pm standard deviation of the observed data, black solid line = simulated pressure heads.

2.3.2 Soil water dynamics

Figure 2.6 shows the pressure heads and water contents in the flow domain on day 21 of the simulation period (June 20, 2010) of the growing season. After a dry period of 1 week, a rain event with 8.4 mm and 11 mm at field site 1 and field site 2, respectively, occurred on this day. Pressure heads in the top layer and in ridge positions are lower than in comparable furrow positions under RT_{pm} and RT , indicating that the soil is drier due to intense water uptake by plants during the main growing stage. Differences in pressure heads in the top layer between ridges and furrows are about -70 to -100 cm at field site 1, whereas pressure heads at field site 2 differ between -200 and -40 cm. At both field sites, pressure head gradients are distinct horizontally, which forces soil water to flow laterally from the furrows to the ridges. At field site 1, where the soil texture changes between the A- (sandy loam) and B- (silty loam) horizon, the differences in pressure heads between ridge and furrow positions and the resulting horizontal water flow is only characteristic for the A-horizon. In the subjacent B-horizon the effect of RT_{pm} and RT on pressure heads is negligible. At field site 2, where the A- (loam) and B- (silt loam) horizon are fine-textured, the differences in pressure heads are distinct even in deeper soil layers. Water flow from furrows to ridges due to almost horizontal pressure head gradients was observed down to 50- 60 cm soil depth. Under conventional tillage, pressure head gradients are distinctly vertical to the soil surface at both field sites, which causes a main vertical water flow from the top layer to the sublayer. The differences in pressure heads between the top layer and the sublayer are small at field site 1, whereas at field site 2 differences range between -40 and -160 cm. Although, the simulation of day 21 represents soil hydraulic conditions after a dry period of 7 days, the B-horizons at both field sites are characterized by a high water content ranging between $0.32 \text{ cm}^3 \text{ cm}^{-3}$ and $0.36 \text{ cm}^3 \text{ cm}^{-3}$. Due to an extreme rain event at day 13 and 14 of the simulation with a total amount of precipitation of 43 mm at field site 1 and 33.4 mm at field site 2, drainage processes occurred very slowly due to the finer soil texture of the subsoils.

In comparison to the dry conditions, Figure 2.7 represents soil hydraulic conditions in the flow domain during a monsoon event on simulation day 75 (August 13, 2010) with a total precipitation amount of 50.4 mm and 50.6 mm at field site 1 and field site 2, respectively. The comparison of pressure heads under the different management strategies at field site 1 shows no discrepancy in pressure heads between the ridge and the furrow positions due to the high hydraulic conductivity K_{sat} in the A-horizon. The soil water is quickly and homogeneously distributed in the soil volume. Pressure head gradients are distinct vertically in the soil profile.

However, the effect of plastic mulching on pressure heads during a monsoon event is more evident at field site 2. Due to a lower hydraulic conductivity in the top layer, soil water distribution occurs more slowly compared to field site 1 and a part of the soil remains unsaturated below the plastic film in the top layer as well as in the sublayer of the ridges. RT leads to a more homogeneous infiltration, resulting in a saturated B-horizon and in isolines, which are distinctly parallel to the soil surface.

The simulation showed higher pressure heads at the beginning and at the end of the growing season in the furrow positions, which reflects a smaller transpiration rate in the initial phase of the plant development and in the senescence stage before harvesting, when most of the aboveground plant parts had already died. Smaller transpiration rates coincide with higher evaporation rates resulting in a reversed water flow directed from the ridges to the furrows. However, these simulation results could not be confirmed by field observations. On the contrary, the field measurements revealed that pressure heads in the ridge positions were lower at the beginning as well as at the end of the growing season than in the furrow positions.

2.3.3 Flow velocities

Figure 2.8 shows the effect of tillage management on flow velocities at both field sites. Affected by the bottom boundary conditions, main flow direction is aligned laterally at field site 1 caused by the granite layer at 1 m depth. Field site 2, however, shows a vertical flow direction representing a deeper developed soil. At field site 1, the coarser soil texture of the top layer and the high saturated hydraulic conductivity of 103 cm d^{-1} implicate high flow velocities and interflow above the finer textured subsoil. The bottom of the ridges is only slightly affected by the high velocities. Protected by the plastic coverage, velocities in the entire ridge area are $<8 \text{ cm d}^{-1}$, while the soil water velocities in the top layer below the ridge are 4 to 6-times higher. In general, flow velocities are increasing in slope direction. The flow velocities found at the field site 2 are generally lower than at field site 1. Due to a similar low saturated hydraulic conductivity as well as a similar soil texture in the A- and B-horizon at field site 2, the layer border does not act as an interflow basis. Highest flow velocities (10 cm d^{-1}) are reached at the transition from furrows to ridges. Plastic mulching induces low flow velocities ($0\text{-}1.6 \text{ cm d}^{-1}$) in the ridge area down to 50 cm depth (from top of the ridge surface).

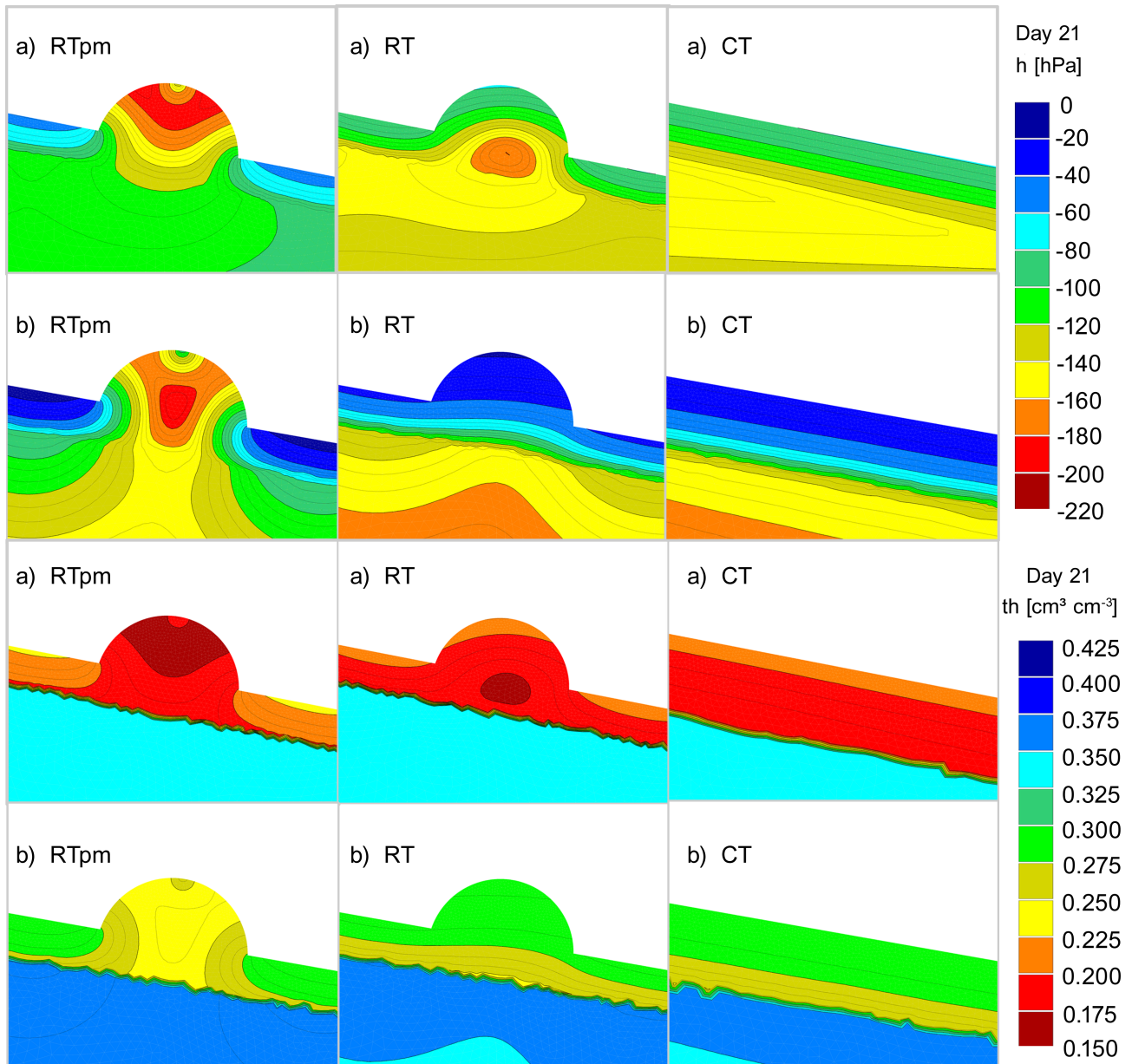


Figure 2.6: Pressure head (h) and water content (θ) under different management strategies at day 21 for (a) field site 1 and (b) field site 2.

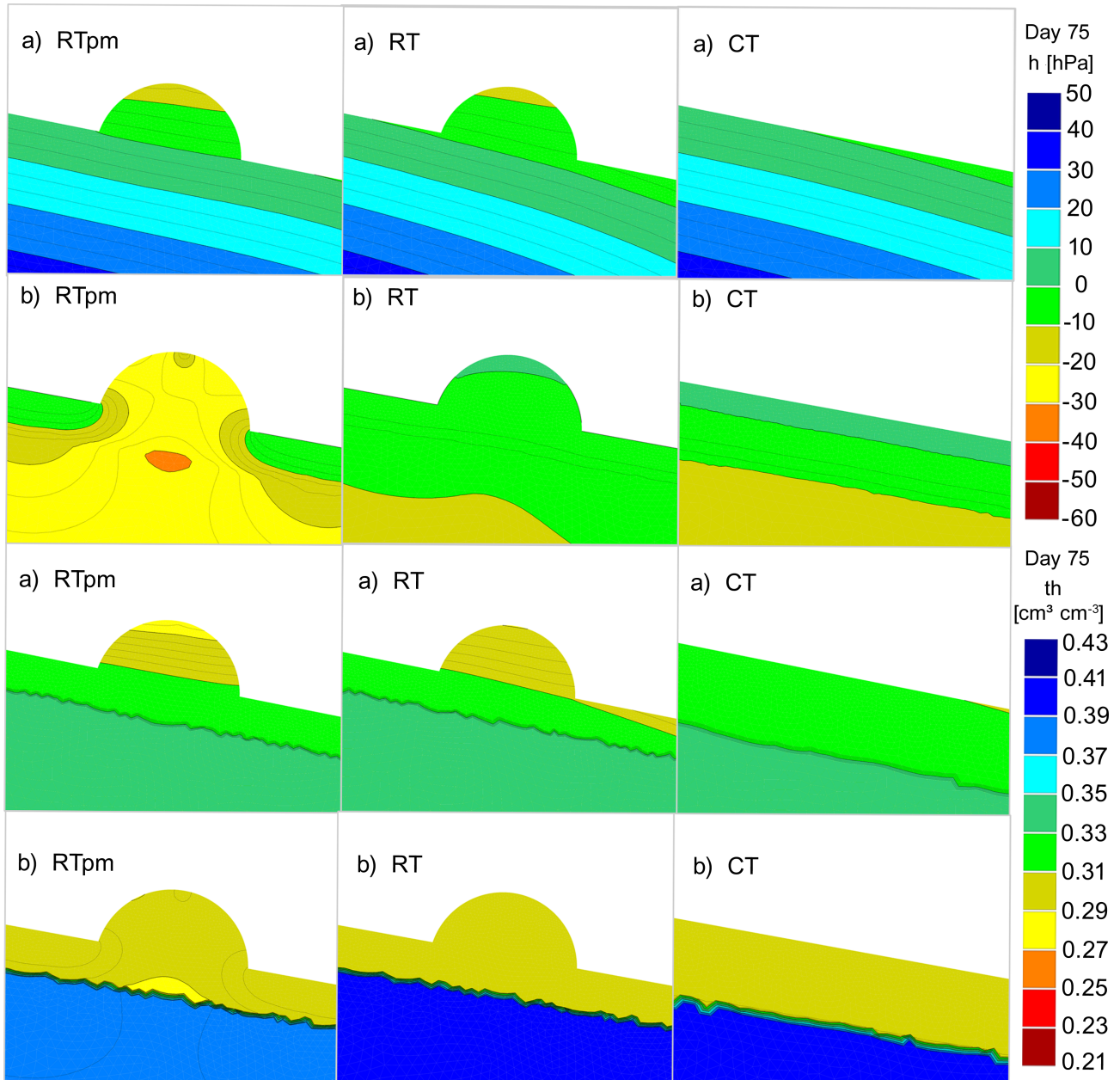


Figure 2.7: Pressure head (h) and water content (θ) under different management strategies at day 75 during a monsoon event for (a) field site 1 and (b) field site 2.

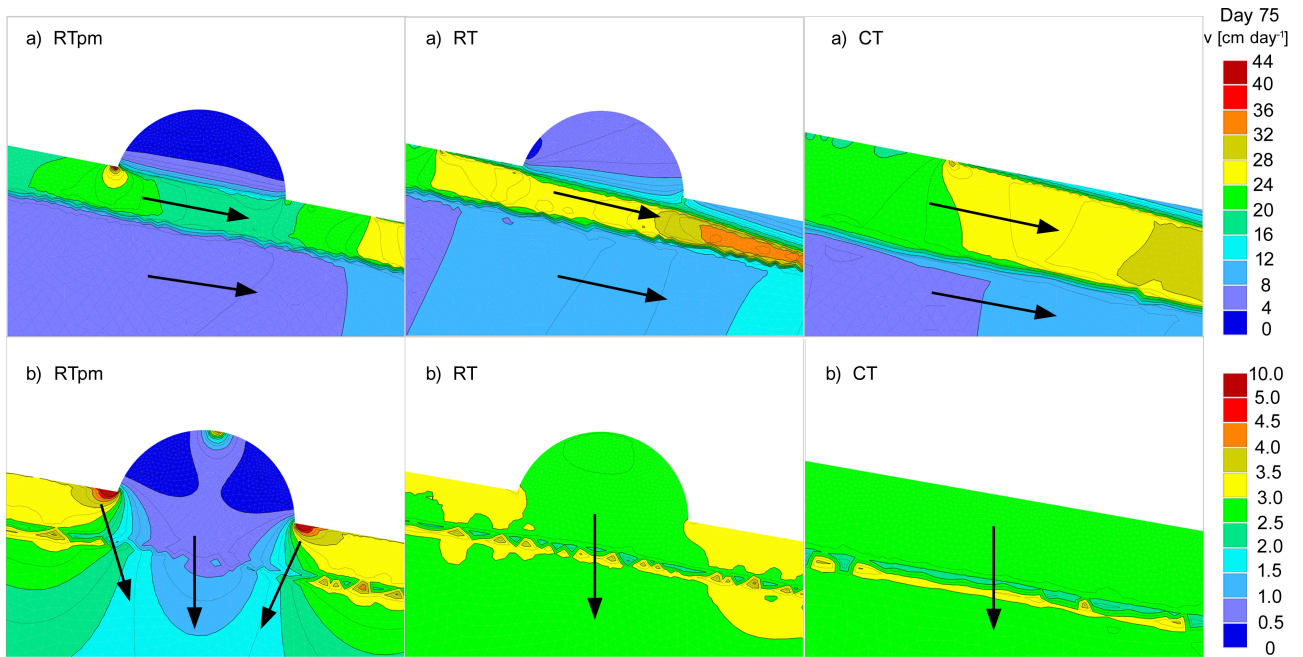


Figure 2.8: Flow velocity during a monsoon event (day 75) under different management systems at (a) field site 1 and (b) field site 2, black arrows indicate the main flow direction.

2.3.4 Water fluxes

To investigate the effect of the different management strategies on water fluxes, cumulative water fluxes at the transitions from furrows to ridges as well as at the transition from ridges to furrows were determined (Figure 2.9). Depending on unequal bottom boundary conditions, cumulative water fluxes varied strongly between both field sites due to different dominant flow directions. At field site 1, where subjacent granite bedrock material forced water to move laterally in slope direction, plastic mulching led to a reduction of water fluxes, whereas water fluxes in simulations without coverage and with a flat surface were high. However, the total amount of water fluxes at R3 after the simulation period only differed slightly between management strategies. In contrast to field site 1, water percolated at the bottom boundary of field site 2, which induced a main vertical water movement, resulting in positive water fluxes at the transition from furrows to ridges and negative water fluxes at the transition from ridges to furrows in slope direction as a result of lower pressure heads below the plastic coverage. Without coverage (RT) the effect was diminished. Under conventional tillage (CT) all values were negative representing the high influence of free drainage conditions at the bottom.

The water balance of the calibrated model with cumulative water fluxes in and out of the flow domain after the simulation period of 86 days is shown in Table 2.4. The water balance error of all simulations was considerably low ($< 0.5\%$). As mentioned before, the differing boundary conditions of both field sites resulted also in large differences in the cumulative water fluxes. At

field site 1 seepage was the only subsurface outflow and the bottom boundary of the model was set to no flux conditions (granitic bedrock). This combination strongly supported the lateral subsurface downhill flow resulting in high seepage water fluxes. On the contrary, the bottom boundary of field site 2 was defined as a free drainage boundary (deeper developed soil), which resulted in a dominating vertical water movement and therefore in high cumulative drainage water fluxes compared to seepage. The runoff was calculated from the amount of water, which ponded theoretically at the surface when the infiltration capacity was exceeded. The difference in runoff rates between both field sites was caused by varying saturated hydraulic conductivity. The transpiration and evaporation rates differed between both field sites because the potential evaporation and transpiration was calculated based on different weather stations (Figure 2.3). Since the potential evaporation and transpiration rates were already low due to a very high average humidity (average humidity of 75% for field site 1 and 91% for field site 2), the actual transpiration rates was determined from the potential ET rates and the soil water status. When the soil was saturated or near saturation in the monsoon season, the root water uptake became zero (Equation (2.3)). The initial and final water content of both field sites were comparable, so that the change in water storage was very low after the simulation period of 86 days.

The comparison among the tillage treatment showed that seepage water was lowest under RT compared to RT_{pm} and CT at field site 1, while the lowest seepage water amount was characteristic for RT_{pm} at field site 2. The simulation at field site 1, however, showed that the differences in seepage water amount were almost negligible, only the flat conventional tillage led to higher amounts of seepage water. Drainage water at field site 2 was about 16% higher without coverage than with coverage. The evaporation rate was 40% higher without coverage at field site 1 and 48% at field site 2, respectively. The transpiration, however, did not vary across the different management strategies. As expected, plastic mulching increased surface runoff. Low runoff rates at field site 1 reflected the high saturated hydraulic conductivity (103 cm d^{-1}) in the top soil. At field site 2, surface runoff was reduced to 65% under RT compared to RT_{pm}.

2.3.5 Sensitivity analysis

A dynamic root development is not implemented in the Hydrus 2/3D model so that the impact on water balance outputs by increasing root water uptake in the first stage of growth could not be captured. Therefore, we analyzed the impact of differing rooting depths on cumulative

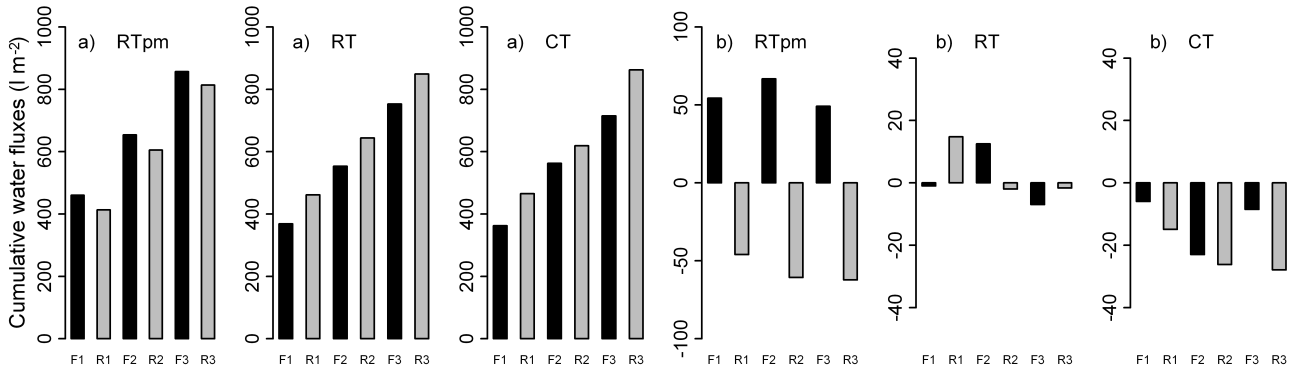


Figure 2.9: Cumulative water fluxes at the transition from furrows to ridges (F1-3) and from ridges to furrows (R1-3) in slope direction, see also the graphical implementation in Figure 2.4. Due to different bottom boundary conditions at both field sites, only positive cumulative water fluxes are simulated at field site 1 due to mainly lateral water movement, at field site 2 the main vertical water movement results in positive and negative water fluxes: (a) field site 1 and (b) field site 2.

Table 2.4: Water balance of the model flow domain after the simulation period of 86 days. Note that seepage is the only outflow of the flow domain at field site 1 and free drainage is the bottom boundary only at field site 2. P: precipitation (varies between treatments because of differing atmospheric boundary lengths), WC_{initial} : initial water content (varies between treatments because of differing model volumes), WC_{final} : final water content, T: transpiration, E: evaporation, S: seepage, R: runoff, D: drainage, rel. err.: relative error of the water balance; All values are given in liter and related to the xyz-dimension of the model, the values in braces are associated with an area of m^2 for P, T, E, S, R, D and with a volume of m^3 for WC_{initial} and WC_{final} .

		P	WC_{initial}	WC_{final}	T	E	S	R	D	rel.err. %
Field site 1	RT _{pm} ^a	20.03 (992)	14.37 (324)	13.96 (315)	5.82 (141)	1.69 (41)	12.65 (1183)	0.15 (4)	-	0.33
	RT ^b	20.49 (992)	14.37 (324)	13.83 (312)	5.79 (140)	2.78 (67)	12.23 (1143)	0.044 (1)	-	0.49
	CT ^c	20.49 (992)	14.28 (321)	13.71 (308)	5.80 (140)	2.63 (64)	12.79 (1306)	0.029 (1)	-	0.47
Field site 2	RT _{pm}	23.85 (1178)	16.81 (379)	15.22 (343)	2.06 (50)	0.64 (15)	0.002 (0)	7.66 (185)	14.99 (367)	0.23
	RT	24.39 (1178)	16.81 (379)	15.18 (342)	1.99 (48)	1.21 (29)	0.094 (8)	4.98 (120)	17.76 (434)	0.03
	CT	24.39 (1178)	16.77 (377)	15.11 (340)	2.00 (48)	1.11 (27)	0.015 (1)	5.56 (134)	17.30 (408)	0.19

^a ridge tillage with plastic mulch

^b ridge tillage without plastic mulch

^c conventional tillage with a flat surface

water fluxes such as seepage, drainage, runoff and water storage by varying the rooting depth from 10 cm to 60 cm (Table 2.5). As expected, with increasing rooting depth the cumulative drainage water fluxes decreased under all tillage management systems due to an increased root water uptake. Furthermore, the increased root depth led to a decrease in seepage water only at field site 1, while the seepage water at field site 2 was consistent. The cumulative runoff did not show a clear trend. At field site 1 seepage water was mostly affected by changes of rooting depth, however, the overall change in seepage water and the influence on water balance was estimated to be low. This was also true for the water balance outputs of field site 2, where cumulative drainage, seepage and runoff water fluxes at the end of the simulation period of 86 days showed only marginal changes as affected by differing rooting depths. Water storage was less after the simulation period, however, the varying rooting depths influenced the change in water storage only marginally. In general, the water balance outputs were robust against varying rooting depths. Further, the ratio between different treatments was also relatively robust. The cumulative runoff under RT at field site 1 was between 64% and 74% less compared to RT_{pm} under varying rooting depth. The difference in runoff between CT and RT_{pm} was about 51 – 81%. At field site 1 the cumulative seepage water fluxes differed only up to 4% between the different treatments. At field site 2 the varying rooting depth affected the total amount of cumulative drainage water only slightly. The ratios between the treatments were constant and the total amount of cumulative drainage water under RT_{pm} was about 15-16% and 13-14% less compared to RT and CT, respectively. The runoff rates at field site 2 were constant as affected by variation of rooting depth.

Table 2.6 shows the cumulative water fluxes after a simulation period of 86 days resulting from the percentage variation of the evapotranspiration (ET) rate. Generally the amounts of cumulative runoff at field site 1 and cumulative seepage at field site 2 were negligible. As we expected, the increase of the ET rate to 100% resulted in decreased cumulative seepage water fluxes at field site 1 and decreased runoff and drainage water fluxes at field site 2. As affected by the variation of ET rates the most sensitive component of the water balance was seepage water at field site 1. By reducing ET to 0%, cumulative seepage increased by 56%, 65% and 61% under RT_{pm}, RT and CT, respectively, whereas the increase of ET to 100% led to a decrease in seepage water up to 39% under RT_{pm} and CT and 41% under RT. By reducing ET to 0%, cumulative drainage water at field site 2 increased between 14% and 15% under all treatments. In the case of increasing ET by 100% the seepage water was reduced to 12-13% under all treatments. Significant runoff rates after a simulation period of 86 days occurred only at field site 2. The results revealed that cumulative runoff was not sensitive to the variation of ET

rates. By reducing ET to 0% the maximum change in runoff was only 3% under all treatments, whereas a 100% increase of ET led to a reduced runoff of 3% under RT_{pm} and RT and 6% under CT. The ratio of the amounts of cumulative water fluxes between the different treatments was also not sensitive to the variation of ET at field site 2. The ratio of cumulative drainage and runoff rates at field site 2 differed only slightly to a maximum of 2%. By increasing ET rates at field site 1, the ratio of seepage water fluxes under RT and RT_{pm} increased from 2% to 8% and from 1% to 6% between RT and CT.

2.4 Discussion

The modeling study showed that the simulation for field site 1 predicted the measured pressure heads reasonably well, whereas pressure head measurements at field site 2 were not well represented by the model simulation.

As the Hydrus 2/3D code does not calculate surface runoff directly, it was necessary to multiply the precipitation data by a factor of 2 for indirectly simulating runoff from plastic mulched ridges to the permeable furrows. This simplified method does not reflect the real field conditions, because ridges were often uneven and small depressions at the top of the ridges support the development of water storage in puddles. However, simulation results between observed and simulated pressure heads showed that the multiplication method was adequate to overcome the problem in calculating surface runoff. This was confirmed by Dusek et al. (2010), who also found that field conditions are better reflected by increased precipitation in comparison to the original data.

Additionally, the simulation neglected that interception on the crop canopy reduces the amount of infiltration water, which plays a relevant role especially during the main growing stage. Field observation showed that the potato canopy covered up to 80% of the surface area. Timlin et al. (2001) confirmed the great influence of water redistribution, which can be caused by crop canopies and suggested to simulate canopy architecture and flow processes.

Finally, root development during growing season could not be simulated and might result in an overestimated root water uptake at the beginning of the growing season. However, the sensitivity analysis revealed the low impact of different rooting depths on water balance components such as drainage, runoff and seepage. The calculation of evaporation and transpiration rates was based on the FAO dual crop coefficient approach by Allen et al. (1998), which uses empirical crop coefficients. It is evident, that this procedure can only be an approximation of evaporation and

Table 2.5: Sensitivity of cumulative water fluxes and water storage to changes in the spatial distribution of the root system after the simulation period of 86 days; gray: original rooting depth used for model calibration ΔW : change in water storage (1 m^{-3}), T: transpiration (1 m^{-2}), E: evaporation (1 m^{-2}), S: seepage (1 m^{-2}), R: runoff (1 m^{-2}), D: drainage (1 m^{-2}); note that seepage is the only subsurface outflow of field site 1. RT_{pm}: ridge tillage with plastic mulch, RT: ridge tillage without plastic mulch, CT: Conventional tillage with a flat surface.

Root depth	RT _{pm}						RT						CT					
	ΔW	T	E	S	R	D	ΔW	T	E	S	R	D	ΔW	T	E	S	R	D
Field site 1																		
10 cm	-9	116	43	1277	3	-	-9	123	86	1241	1	-	-12	140	62	1339	1	-
20 cm	-10	139	40	1197	4	-	-10	138	75	1176	1	-	-13	141	62	1321	2	-
30 cm	-9	141	41	1183	4	-	-9	140	67	1143	1	-	-13	140	64	1306	1	-
40 cm	-9	140	41	1182	4	-	-9	140	68	1146	1	-	-13	140	63	1299	2	-
50 cm	-9	139	42	1183	5	-	-9	139	68	1139	1	-	-13	139	63	1295	1	-
60 cm	-9	138	42	1186	4	-	-9	138	68	1139	1	-	-13	138	64	1302	1	-
mean	-9	135	42	1201	4	-	-9	136	72	1164	1	-	-13	140	63	1310	1	-
std.dev	0	9.47	1.02	37.43	0.58	-	0.39	6.42	7.68	40.17	0.06	-	0.26	1.02	0.80	16.70	0.33	-
Field site 2																		
10 cm	-36	46	16	0	184	372	-37	45	33	8	120	441	-37	47	30	2	134	411
20 cm	-36	49	15	0	185	368	-37	47	31	8	120	437	-37	48	26	2	134	410
30 cm	-36	50	15	0	185	367	-37	48	29	8	120	434	-37	48	27	1	134	408
40 cm	-36	50	16	0	185	365	-37	48	28	8	120	433	-37	49	27	2	131	410
50 cm	-36	50	16	0	186	365	-37	49	29	8	120	431	-37	49	27	1	134	407
60 cm	-36	50	16	0	186	365	-37	49	29	8	120	432	-37	49	28	2	134	406
mean	-36	49	16	0	185	367	-37	48	30	8	120	435	-37	48	27	2	134	409
std.dev	0.20	1.51	0.33	0.00	0.50	2.63	0.17	1.50	1.84	0.05	0.33	3.88	0.12	0.82	1.13	0.03	1.19	2.20

Table 2.6: Sensitivity of cumulative water fluxes and water storage to percentage change of evapotranspiration (ET) after a simulation period of 86 days; grey: original ET rate, which was calculated based on FAO dual crop coefficient approach and used for model calibration; ΔW : change in water storage (1 m^{-3}), T: transpiration (1 m^{-2}), E: evaporation (1 m^{-2}), S: seepage (1 m^{-2}), R: runoff (1 m^{-2}), D: drainage (1 m^{-2}); note that seepage is the only subsurface outflow of field site 1. RT_{pm} : ridge tillage with plastic mulch, RT: ridge tillage without plastic mulch, CT: Conventional tillage with a flat surface.

ET rates	RT_{pm}						RT						CT					
	ΔW	T	E	S	R	D	ΔW	T	E	S	R	D	ΔW	T	E	S	R	D
Field site 1																		
-100%	-3	0	0	1850	6	-	-2	0	0	1883	1	-	-3	0	0	2097	1	-
-80%	-3	28	10	1707	5	-	-3	28	21	1702	1	-	-4	28	21	1898	2	-
-60%	-4	56	21	1566	5	-	-5	56	40	1529	1	-	-5	56	39	1711	1	-
-40%	-6	84	30	1427	6	-	-6	84	52	1382	1	-	-7	84	50	1555	2	-
-20%	-7	113	37	1299	4	-	-9	112	61	1256	1	-	-10	112	56	1427	2	-
0	-9	141	41	1183	4	-	-12	140	67	1143	1	-	-13	140	64	1306	1	-
+20%	-12	169	44	1075	5	-	-16	169	74	1037	1	-	-16	169	69	1190	1	-
+40%	-15	196	47	975	3	-	-19	196	84	936	1	-	-18	197	75	1079	1	-
+60%	-18	223	51	882	3	-	-22	224	94	842	1	-	-21	223	80	978	1	-
+80%	-21	248	53	797	3	-	-25	250	106	753	1	-	-24	249	89	884	1	-
+100%	-23	271	56	721	5	-	-28	275	118	669	1	-	-27	272	102	799	1	-
mean	-11	139	35	1226	4	-	-13	139	65	1194	1	-	-13	139	59	1357	1	-
std.dev	7.23	90.86	18.34	377.66	1.29	-	9.08	91.94	35.71	396.38	0.13	-	8.50	91.32	29.94	423.85	0.40	-
Field site 2																		
-100%	-35	0	0	0	190	421	-36	0	0	9	124	497	-23	0	0	1	138	485
-80%	-35	13	6	0	189	409	-36	12	11	8	123	483	-37	12	11	1	137	471
-60%	-36	22	9	0	188	398	-36	21	17	9	122	468	-37	21	17	1	136	457
-40%	-36	31	11	0	187	387	-37	30	22	8	122	456	-37	30	21	1	134	446
-20%	-36	41	14	0	186	377	-37	39	25	8	120	446	-37	39	24	1	135	434
0	-36	50	16	0	185	367	-37	48	29	8	120	435	-37	48	27	1	134	423
+20%	-36	59	17	0	184	357	-37	57	33	8	119	423	-37	58	30	1	134	412
+40%	-36	69	19	0	183	348	-37	66	37	8	119	412	-37	67	32	1	133	401
+60%	-36	78	20	0	182	339	-37	75	41	8	118	402	-38	76	34	1	132	390
+80%	-36	87	21	0	181	329	-37	84	45	8	118	392	-38	85	39	1	132	380
+100%	-36	97	22	0	180	320	-37	93	48	7	117	382	-38	94	44	1	126	373
mean	-36	50	14	0	185	368	-37	48	28	8	120	436	-36	48	25	1	134	425
std.dev	0.25	31.51	6.96	0.00	3.29	33.14	0.38	30.41	14.81	0.45	2.29	37.51	4.24	30.61	12.64	0.08	3.20	37.30

transpiration rates, however, the sensitivity analysis of water balance components on percentage changes of evaporation and transpiration rates showed that cumulative seepage water flux was sensitive, while drainage and runoff rates were relatively robust. The ratio of cumulative seepage, drainage and runoff water fluxes between the different treatments was also robust to changes in root depth and evaporation and transpiration rates.

During dry periods pressure head gradients were found to deviate horizontally in the case of RT_{pm} indicating a lateral flow direction from the furrows to the ridges in the top layer. These patterns were weakened under RT as only the topography affected soil moisture pattern. Pressure head gradients under RT deviated more vertically, which forced water to flow in a more enhanced vertical than lateral direction. Under conventional tillage (CT), pressure head gradients were found to be exactly vertical to the soil surface inducing a clearly vertical soil water movement.

During monsoon events, however, the dominating flow directions were not as pronounced as during dry conditions. At field site 1, where the top layer was characterized by a coarse sandy loam, ridges were fully saturated in the root zone, even in the case of RT_{pm} . At field site 2, the root zone was protected against full saturation in the case of RT_{pm} because of a less coarse textured top layer and a lower hydraulic conductivity. While drainage in the root zone accelerated, when the topsoil consisted of a coarser-textured material and full saturation occurred only for short after the rain event, the less coarse-textured topsoil was close to full saturation for a much longer time period. However, it has to be considered that monsoon events in the measurement period 2010 were indeed comparatively small with a maximum daily precipitation amount of <80 mm and a relatively low intensity. Precipitation observations of former years indicated that monsoonal events can reach up to 100-150 mm d^{-1} . Taking even higher precipitation amounts into account, even a finer textured top layer would be fully saturated. Hence, the application of sandy soils with a coarse texture, which equals the local method, ensures a rapid drainage of the root zone.

The analysis of flow velocities during monsoon events showed that an interflow phenomenon occurs, when the topsoil is characterized by a coarse soil texture, a high saturated hydraulic conductivity and additionally overlies finer textured subsoil with an underlying compact bedrock material. These conditions are enhanced by ploughing and application of sandy soil material before growing season. Based on these soil properties, flow velocities in the topsoil were simulated to be 6-8 times higher than in the overlying ridge and in the underlying subsoil. Therefore the high flow velocities in the topsoil assure a quick drainage of the root zone particularly at sloped field sites but concurrently might increase the risk of leaching via interflow. In contrast, the soil

properties differed at field site 2 and interflow was not evident in the simulation. A generally finer soil texture in the top layer slows down the drainage process in the root zone but decreases the risk of leaching via interflow.

The comparison of drainage water under different management strategies showed that plastic mulching reduces the amount of drainage water up to 16% and consequently reduces the contribution to the groundwater. Accordingly, plastic coverage might reduce the conservative transport of nitrate to groundwater and might temporally extend the nitrate availability in the root zone below the plastic coverage, but further research on leakage of fertilizer and agrochemicals under plastic mulched ridge cultivation is necessary. Concurrently, the modeling study showed that RT_{pm} increases surface runoff up to 65% compared to RT and CT, which supports a quick water contribution to the river network in the catchment. A substantially increased runoff generation in a plastic mulched pineapple culture was also found by Wan and El-Swaify (1999). The high impact of plastic mulched ridge cultivation in agricultural fields on hillslopes by increasing significantly surface runoff, exacerbates the problem of phosphorous transportation with sediments via overland flow to the stream networks. This is supported by Kim et al. (2001), who found that the discharge of phosphorous associated with sediments from agricultural areas causes eutrophication and deterioration of water quality in downstream reservoirs in South Korea.

2.5 Conclusions

In this study, a combination of field measurements and process-based model simulations was used to evaluate the effect of plastic mulched ridge cultivation in comparison to ridge cultivation without plastic coverage and conventional flat tillage management on soil water dynamics. It was demonstrated that plastic mulching induces typical soil moisture patterns mainly in the topsoil during dry periods compared to the other tillage systems, whereas the impact of tillage management on soil water dynamics in the subsoil was low. During monsoon events, however, no significant soil moisture patterns caused by tillage management could be detected since the soil profile was almost fully saturated, depending on the soil texture.

Summarizing the advantages and disadvantages of the three different management systems on hillslopes in a monsoon climate, conventional tillage (CT) is inadvisable due to the higher amounts of seepage water and the higher rates of surface runoff compared to RT. In addition, a flat surface is predestined for erosive denudation. RT_{pm} was found to have the lowest amount of drainage water and the highest runoff rates. Ridge tillage without coverage (RT) showed

higher amounts of drainage water compared to RT_{pm} as well as the lowest runoff rates of all management practices. Therefore, ridge tillage without coverage (RT) was evaluated as the best management strategy to avoid high amounts of surface runoff. In order to reduce drainage water amounts, however, ridge tillage with plastic mulch (RT_{pm}) showed the best results.

Additionally, it has the advantages of earlier plant emergence and weed control as reported by local farmers. To combine the advantages of both treatments as well as to diminish the negative effects of both, we conclude that the application of perforated and biodegradable plastic mulch seems to be the most promising method in agricultural dryland farming affected by monsoonal climate.

Acknowledgements

This study was carried out as part of the International Research Training Group TERRECO (GRK 1565/1) funded by the Deutsche Forschungsgemeinschaft (DFG) at the University of Bayreuth, Germany and the Korean Research Foundation (KRF) at Kangwon National University, Chuncheon, S. Korea. The author would like to thank especially Andreas Kolb for his technical support during field measurements.

References

- Abbasi, F., J. Feyen, and M. van Genuchten (2004). “Two-dimensional simulation of water flow and solute transport below furrows: Model calibration and validation”. In: *Journal of Hydrology* 290.1–2, pp. 63–79. DOI: 10.1016/j.jhydro.2003.11.028.
- Allen, R., L. Pereira, D. Raes, and M. Smith (1998). *Crop evapotranspiration. Guidelines for computing crop water requirements*. Rome, Italy: FAO. ISBN: 9789251042199.
- Dusek, J., C. Ray, G. Alavi, T. Vogel, and M. Sanda (2010). “Effect of plastic mulch on water flow and herbicide transport in soil cultivated with pineapple crop: A modeling study”. In: *Agricultural Water Management* 97, pp. 1637–1645.
- Feddes, R., P. Kowalik, and H. Zaradny (1978). *Simulation of field water use and crop yield*. New York: John Wiley & Sons. ISBN: 9780470264638.
- Genuchten, M. van (1980). “A closed form equation for predicting the hydraulic conductivity of unsaturated soils”. In: *Soil Science Society of America Journal* 5, pp. 892–898.

- Gürsoy, S., A. Sessiz, E. Karademir, C. Karademir, B. Kolay, M. Urgan, and S. Malhi (2011). “Effects of ridge and conventional tillage systems on soil properties and cotton growth”. In: *International Journal of Plant Production* 5.3, pp. 227–236.
- Kim, B., J.-H. Park, G. Hwang, M.-S. Jun, and K. Choi (2001). “Eutrophication of reservoirs in South Korea”. In: *Limnology* 2, pp. 223–229. ISSN: 1439-8621. DOI: 10.1007/s10201-001-8040-6.
- Lazlo, P. and C. Gyuricza (2004). “Effect of the ridge tillage system on some selected soil physical properties in a maize monoculture”. In: *Acta Agronomica Hungarica* 52, pp. 211–220.
- Lee, S., P. Vinayachandran, K.-J. Ha, and J.-G. Jhun (2010). “Shift of peak in summer monsoon rainfall in Korea and its association with El Nino-Southern Oscillation”. In: *Journal of Geophysical Research-Atmospheres* 115, pp. 1–15.
- Leistra, M. and J. J. T. I. Boesten (2010). “Pesticide Leaching from Agricultural Fields with Ridges and Furrows”. In: *Water Air and Soil Pollution* 213.1-4, pp. 341–352. ISSN: 0049-6979. DOI: 10.1007/s11270-010-0389-x.
- Li, X. Y. and J. D. Gong (2002). “Effects of different ridge: Furrow ratios and supplemental irrigation on crop production in ridge and furrow rainfall harvesting system with mulches”. In: *Agricultural Water Management* 54.3, pp. 243–254. ISSN: 0378-3774. DOI: 10.1016/S0378-3774(01)00172-X.
- Li, X.-Y., W.-W. Zhao, Y.-X. Song, W. Wang, and X.-Y. Zhang (2008). “Rainfall harvesting on slopes using contour furrows with plastic-covered transverse ridges for growing *Caragana korshinskii* in the semiarid region of China”. In: *Agricultural Water Management* 95.5, pp. 539–544. ISSN: 0378-3774. DOI: 10.1016/j.agwat.2007.12.005.
- Mahajan, G., R. Sharda, A. Kumar, and K. G. Singh (2007). “Effect of plastic mulch on economizing irrigation water and weed control in baby corn sown by different methods”. In: *African Journal of Agricultural Research* 2.1, pp. 19–26. ISSN: 1991-637X.
- McCuen, R., Z. Knight, and A. Cutter (2006). “Evaluation of the Nash-Sutcliffe Efficiency Index”. In: *Journal of Hydrologic Engineering* 11.6, pp. 597–602.
- Moriasi, D. N., J. G. Arnold, M. W. van Liew, R. L. Bingner, R. D. Harmel, and T. L. Veith (2007). “Model evaluation guidelines for systematic quantification of accuracy in watershed simulations”. In: *Transactions of the ASABE* 50.3, pp. 885–900. ISSN: 0001-2351.
- Mualem, Y. (1976). “New model for predicting hydraulic conductivity of unsaturated porous media”. In: *Water Resources Research* 12.3, pp. 513–522. ISSN: 0043-1397.

- Paltineanu, I. C. and J. L. Starr (2000). "Preferential water flow through corn canopy and soil water dynamics across rows". In: *Soil Science Society of America Journal* 64.1, pp. 44–54. ISSN: 0361-5995.
- Saffigna, P., C. Tanner, and D. Keeney (1976). "Non-uniform infiltration under potato canopies caused by interception, stemflow, and hilling". In: *Agronomy Journal* 68, pp. 337–342.
- Schaap, M., F. Leji, and M. van Genuchten (2001). "ROSETTA: a computer program for estimating soil hydraulic parameters with hierarchical pedotransfer functions". In: *Journal of Hydrology* 251, pp. 163–176.
- Sejna, M., J. Simunek, and M. van Genuchten (2011). *The HYDRUS Software Package for Simulating the Two-and Three-Dimensional Movement of Water, Heat, and Multiple Solutes in Variably-Saturated Media*. Version 2. PC-Progress. Prague, Czech Republic.
- Tian, Y., Su, F. M. Li, and X. L. Li (2003). "Effect of rainwater harvesting with ridge and furrow on yield of potato in semiarid areas". In: *Field Crops Research* 84.3, pp. 385–391. ISSN: 0378-4290. DOI: 10.1016/S0378-4290(03)00118-7.
- Timlin, D., Y. Pachepsky, and V. R. Reddy (2001). "Soil water dynamics in row and interrow positions in soybean (*Glycine max* L.)". In: *Plant and Soil* 237.1, pp. 25–35. ISSN: 0032-079X.
- Wan, Y. and S. El-Swaify (1999). "Runoff and soil erosion as affected by plastic mulch in a Hawaiian pineapple field". In: *Soil & Tillage Research* 52.1-2, pp. 29–35.
- Wang, Q., E. Zhang, F. Li, and F. Li (2008). "Runoff efficiency and the technique of micro-water harvesting with ridges and furrows, for potato production in semi-arid areas". In: *Water Resources Management* 22.10, pp. 1431–1443. ISSN: 0920-4741. DOI: 10.1007/s11269-007-9235-3.
- Wesenbeeck, I. van and R. Kachanoski (1988). "Spatial and temporal distribution of soil water in the tilled layer under a corn crop". In: *Soil Science Society of America Journal* 52.2, pp. 363–368. ISSN: 0361-5995.
- Wesseling, J., J. Elbers, and B. Kabat P. and van den Broek (1991). "SWATRE: Introductions for Input. Internal Note". In: Wageningen, The Netherlands: Winand Starting Center Alterra.

Chapter 3

Effects of ridge tillage on flow processes in the Haean catchment, South Korea

Marianne Ruidisch^{1,a}, Sebastian Arnhold^a, Bernd Huwe^a, Christina Bogner^b

^a Soil Physics Group, BayCEER, University of Bayreuth, 95440 Bayreuth, Germany

^b Ecological Modelling, BayCEER, University of Bayreuth, Dr.-Hans-Frisch-Straße 1–3, 95448 Bayreuth, Germany

Abstract

The intense agricultural land use has a considerable impact on water quality worldwide. A detailed understanding of the transport of agrochemicals requires knowledge about flow processes and how they are affected by agricultural management operations like tillage. This is especially important in regions influenced by extreme rainstorm events. We carried out four dye tracer experiments on two sloped agricultural dryland fields in South Korea to compare flow processes under (i) conventional tillage, (ii) ridge tillage, (iii) ridge tillage with plastic mulch and (iv) plastic mulched ridge tillage with well developed potato crops. We found that the ridge topography enhanced the infiltration in depression zones like furrows and planting holes. Deeper in the soil the water flow was funnelled preferentially above the tillage pan, however, preferential macropore flow to greater depths was absent. Furthermore, we found substantially higher surface runoff under ridge tillage with plastic mulch before the crop

¹Correspondence to: Marianne Ruidisch, Soil Physics Group, BayCEER, University of Bayreuth, 95440 Bayreuth, Germany.
E-mail: ruidisch@uni-bayreuth.de

canopy was developed. Therefore, to reduce surface runoff, we suggest to encourage crop production in ridge cultivation with perforated plastic mulch. Additionally, to reduce the leaching risk of agrochemicals and fertilizers via subsurface flow above the tillage pan we propose the establishment of riparian buffer zones between dryland fields and the river network.

Keywords: agricultural soils; dye tracers; preferential flow; flow patterns; ridge cultivation; tillage management

3.1 Introduction

Worldwide, intense agriculture is accompanied by increasing use of fertilizers, pesticides and herbicides to meet the food demand of a growing population. This trend has a considerable impact on ecosystem services. In regions like East Asia that are characterized by seasonal extreme rainstorm events, leaching of agrochemicals plays a key role in pollution of freshwater resources. Over the last decades, a substantial increase of extreme rainfall during the summer monsoon has been observed for western, southwestern, and southern parts of China and South Korea (Zhai, Sun, et al., 1999; Zhai, X. Zhang, et al., 2005; Park et al., 2010). Non-point-source pollution like intensified export of sediments and nutrients from agricultural land in combination with these increasing amounts and intensities of precipitation strongly affects the fresh water resources of lakes and reservoirs and results in water quality degradation in these regions (Park et al., 2010; W. Zhang et al., 1996).

To determine the pathways of agricultural pollutants, we have to identify the dominant flow processes in agricultural soils. In general, two major types of water flow in soils can be distinguished: uniform and non-uniform (i.e. preferential) flow. The latter is characterized by water and solute movements bypassing a fraction of the porous soil matrix and can further be classified into a) macropore flow occurring in root channels, earthworm burrows, fissures or cracks, b) unstable flow induced by textural layering, water repellency, air entrapment, or continuous non-ponding infiltration and c) funnel flow describing lateral redirection and funneling of water caused by textural boundaries (Hendrickx and Flury, 2001). Preferential flow paths are responsible for rapid water movement and solute transport to greater soil depths or groundwater (Bogner, Gaul, et al., 2010; Gish et al., 1998; Simunek et al., 2003). Their occurrence in soils depends on soil texture, soil structure, topography, surface microrelief and management as well as on the initial soil water content and the intensity and duration of rainfall (Bachmair et al.,

2009; Jarvis, 2007).

Preferential flow is all the more important when intense agriculture is practiced under the influence of monsoon climate. In South Korea, for instance, a considerable amount of chemical fertilizer of up to 450 kg ha^{-1} is applied yearly on dryland farming fields (Statistics of Korea). Although high rainfall intensities strongly support preferential flow in macropores, the leaching of a particular agrochemical agent depends on its sorption characteristics, nature of biological transformations and the form of its application (Jarvis, 2007).

Agricultural management practices like ploughing, harrowing, drilling and wheel traffic have been identified to strongly affect water flow and infiltrability (Bogner, Mirzaei, et al., 2012; Kulli et al., 2003; Petersen et al., 2001). Both, Bogner, Mirzaei, et al. (2012) and Petersen et al. (2001) found that the tillage pan could initiate water funnelling and disconnect macropores situated below from processes in the ploughed horizon. Furthermore, Kulli et al. (2003) noted in their study that wheel traffic caused soil compaction along with decreased permeability and macroporosity and supported water ponding in the compacted parts of the soil.

Ridge cultivation is another common management practice for example in vegetable production and was found to have positive effects on crop yield and weed control when using plastic mulch (Lament, 1993). Its effects on water flow and solute transport, however, has rarely been investigated and most of the studies concentrated on soil water dynamics in ridge cultivation systems without plastic mulch. Leistra and Boesten (2010), for instance, reported that runoff from ridges to furrows (i.e. induced by surface topography) led to higher soil moisture in furrows. Thus, water movement occurred laterally from furrows to ridges and vertical water flow and solute movement under ridges was minimized (Bargar et al., 1999). However, the effect of plastic mulched ridge cultivation systems on non-uniform flow regimes has not been considered in the literature so far.

In our study, we used the food dye tracer Brilliant Blue FCF to directly visualize flow patterns in irrigation experiments under (i) flat conventional tillage, (ii) ridge tillage, (iii) ridge tillage with plastic mulch and (iv) ridge tillage with plastic mulch cropped with potato plants. Brilliant Blue is often used in tracer studies in soil hydrology and is well known for its low toxicity, relatively high mobility and good visibility against most soil colors (Flury and Flühler, 1995). Our objectives were (i) to compare infiltration and surface runoff under different tillage management systems, (ii) to investigate the effect of ridge tillage, plastic mulch and the crop root system on flow patterns qualitatively using binary images and index functions and (iii) to evaluate the sustainability of the ridge cultivation systems in terms of pollutant transport.

3.2 Materials and methods

3.2.1 Study site

The Haean-myun catchment, also called Punchbowl, ($128^{\circ}1'33.101''\text{E}$, $38^{\circ}28'6.231''\text{N}$) is located in the mountainous northeastern part of South Korea and is approximately 64 km^2 large. The bowl shape is characteristic and subdivides the catchment into three major land use zones. The steep hillslopes are mostly forested (58%) and the more gentle ones are dominated by dryland farming (22%). Rice paddies (8%) are characteristic for the central area of the catchment and the remainder is occupied by residences, grassland and field margins. The annual precipitation in the Haean catchment is about 1577 mm (11-years average) with 50–60% of the annual rainfall occurring during the monsoon season from June to August.

The geology of the catchment is dominated by granite bedrock material which is strongly weathered due to the high precipitation rates. It constitutes the parent material for Cambisols – the most widely spread soil type. As a consequence of extreme rainfall events during the summer monsoon, the upper soil horizons are often eroded. To compensate this high erosion loss, the local farmers commonly bring sandy soil material at the beginning of the growing season from outside of the catchment and distribute it on their fields.

On the dryland fields agricultural farming usually starts between April and May depending on the crop type. The common procedure is a primary fertilization using mineral fertilizer in form of granules and a subsequent ploughing to mix them into the top soil. Therefore, a tillage pan is characteristic for the most dryland farming soils. Afterwards, ridges (approx. 15 cm height, 30 cm width) are created perpendicularly to the slope with a ridge to ridge spacing of approx. 70 cm. Typically, the ridges are covered with a black plastic mulch (polyethylen) perforated with planting holes (diameter 5 cm) spaced by 25–30 cm while the furrows remain uncovered. Depending on the crop type, seeds are sowed or juvenile plants are planted after the creation of the ridges. During the growing season herbicides and pesticides are applied several times and fertilizers spread a second time depending on the crop type. Finally, harvesting usually begins in late August to September.

3.2.2 Experimental set up

We carried out four irrigation experiments at two potato fields (*Solanum tuberosum L.*) on hillslopes. Field site 1 ($128^{\circ}6'32.625''\text{E}$, $38^{\circ}18'4.148''\text{N}$) was located in a distance of approx. 830 m from field site 2 ($128^{\circ}6'54.803''\text{E}$, $38^{\circ}17'43.254''\text{N}$). Both soils can be characterized as strongly

Table 3.1: Soil physical properties of the experimental sites.

	Horizon (WRB)	Depth ^a (cm)	Clay (%)	Silt (%)	Sand (%)	Soil texture class	Bulk density (g cm ⁻³)
Site 1	Ap	0–25	3.2	16.4	80.3	Loamy sand	1.43
	2Apb ^b	25–50	20.2	53.4	26.4	Silt loam	1.45
	Bwb	50–100	24.8	46.6	28.6	Loam	1.38
Site 2	A1	0–35	1.9	14.5	83.6	Loamy sand	1.41
	A2	35–45	8.1	28.9	63.0	Sandy loam	1.66
	A3	45–55	7.6	27.9	64.5	Sandy loam	1.61
	2Apb	55–70	20.9	58.2	20.9	Silt loam	1.28
	2Bwb	70–100	13.6	38.9	47.5	Loam	1.56

^a approximate depth

^b horizon continuous in the second experiment (RT) only.

anthropologically modified Cambisols with eroded A-Horizons. Indeed, intense fertilization and application of pesticides and herbicides have altered the soils chemically. Additionally, allochthonous sandy soil material was spread several times on top of the fields. The soils were classified as a terric Cambisol and a terric Anthrosol over haplic Cambisol (IUSS Working Group WRB, 2006) with a slope of 8° and 6° on field site 1 and 2, respectively. We selected these fields because their slope degrees and soil physical properties were comparable (Table 3.1).

We carried out the first two experiments on field site 1 and the last two at field site 2. The first experiment (CT) took place after ploughing and before ridges were created, so that the soil surface was flat and represented conventional tillage management. The second one (RT) was carried out after the creation of ridges. At field site 2 potato crops were planted in ridges covered with black plastic mulch, and we conducted the third experiment (RT_{pm}) in the early season when seed potatoes were just sowed. Finally, the last irrigation (RT_{pm+crops}) followed in the later season when potato crops and their root system were already well developed. In the following we use CT, RT, RT_{pm} and RT_{pm+crops} to refer to the corresponding experiments or plots.

Before irrigation we installed soil moisture sensors (Decagon devices, Inc., Pullman, WA-99163, USA) to monitor the volumetric water content θ_V . These sensors measure the dielectric constant based on frequency domain technology. On CT, they were placed in 5 and 20 cm depth from the flat soil surface. In experiments RT and RT_{pm}, two sensors were situated in furrows in 5 and 20 cm depth from the furrow surface and another two in ridges in 5 and 20 cm depth from the ridge surface. Due to technical problems, the fourth experiment was carried out without any soil moisture sensors. We recorded the values of soil moisture in a 2 minutes interval on a data logger (Decagon devices, Inc., Pullman, WA-99163, USA).

We irrigated a surface of 2 m² with a tracer solution containing 5 g l⁻¹ of Brilliant Blue FCF using an automated sprinkler. Because this tracer can be retarded compared to infiltrating water (Flury and Flühler, 1995), we added 5 g l⁻¹ potassium iodide on plots CT and RT_{pm} as a reference tracer. To calculate the amount of surface runoff the irrigation area was equipped with an infiltration frame. It channelled the surface runoff via internal tubes into buckets outside of the frame. The total time and amount of irrigation varied among experiments due to technical problems with blocked sprinkler jets. However, the experiments were still comparable (Table 3.2).

One day after the irrigation we excavated 8–10 soil profiles of 1 × 2 m spaced by 10 cm on each plot. For visualization of the iodide tracer, an indicator solution with iron (III) nitrate and starch was prepared (Lu and Wu, 2003) and sprayed onto the excavated soil profiles. All profiles were equipped with a metallic frame of 2 m² and a Kodak color scale and photographed with a digital single lens reflex camera (Canon EOS 1000D). Only the parts of the profiles surrounded by the frame were analyzed.

The soil profiles were sampled systematically in Brilliant Blue stained and non-stained areas to determine soil physical properties. We carefully scraped soil material from different profiles and analyzed the texture in a laser particle size analyzer (Mastersizer S 'MAM 5044', Malvern instruments GmbH, Herrenberg, Germany). Additionally, we took undisturbed samples with small soil core rings (diameter 2.8 cm, height 1 cm) in stained and non-stained parts. They were weighted, dried for 24 hours at 105°C in a drying oven and weighed again to calculate the bulk density.

3.2.3 Statistical analysis

The tillage pan was a prominent feature observed on all experimental sites and might influence the soil physical properties. Therefore, we tested whether the bulk density varied significantly above and below the tillage pan. There were no indications that the distribution of the data was non-normal (quantile-quantile plot and the Shapiro–Wilk test) or that the variance varied from plot to plot (Bartlett's test). Because the sample size differed between soil horizons we performed the Welch *t*-test. All statistical tests were done in R (R Core Team, 2012).

3.2.4 Image processing

We corrected the images for perspective and radial distortion such that they corresponded to pictures taken by an ideal camera looking perpendicularly onto the profiles. The transformation

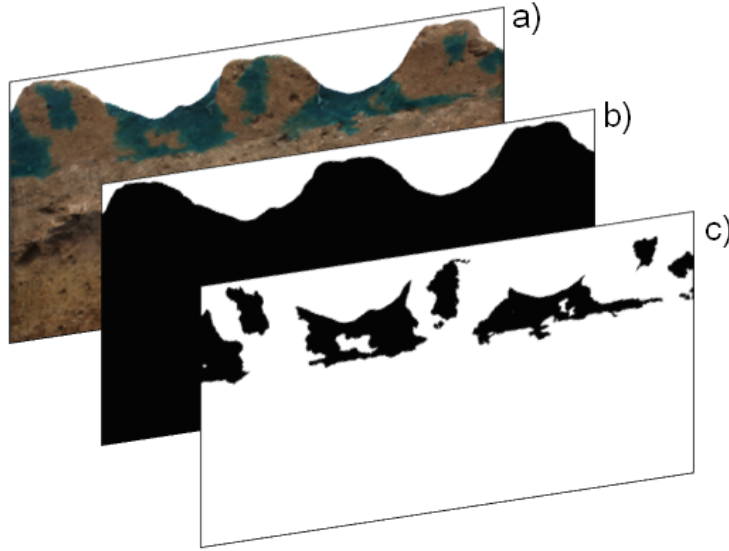


Figure 3.1: Images processing from a) rectified dye tracer image to b) background image and c) binary image used to calculate image indices.

was calculated by

$$\vec{v} = \frac{1}{1 + \kappa \cdot \langle \vec{u}, \vec{u} \rangle} \cdot \vec{u} \quad (3.1)$$

where the parameter κ is the magnitude of the radial distortion, \vec{u} are coordinates of a point in the original image and \vec{v} are coordinates in the corrected one and the brackets $\langle \rangle$ indicate the inner product. If κ is negative, the distortion is barrel-shaped, while for positive κ it is pincushion-shaped (Steger et al., 2008). The parameter κ is obtained in a camera calibration procedure with a special calibration plate. Subsequently, we transformed the images from RGB to HSI (hue, saturation, intensity) color space and classified them into Brilliant Blue stained (black) and non-stained (white) parts resulting in a binary image. Indeed, the HSI color space is more suitable for color-based segmentations of images taken under varying illumination. More details on image transformation and classification are given in Bogner, Gaul, et al. (2010). For the experiments RT, RT_{pm} and RT_{pm+crops} we additionally produced a second binary background image, where soil was coded black and the background between ridges white (Figure 3.1). The correction of distortion and color segmentation were done in Halcon ver. 10.0 (MVTec Software GmbH, Munich, Germany).

3.2.5 Image index functions

We used the binary images to assess differences between the tillage management systems. The first two experiments (CT and RT) show the influence of soil surface topography on flow patterns

in general. By comparing the experiments RT and RT_{pm}, we can infer the effect of plastic mulch. Finally, we can extract information about the impact of the potato root system on flow patterns by comparing the images on plot RT_{pm} with those on RT_{pm+crops}.

To effectively analyze the flow patterns in binary images, we calculate image index functions. An index function is a real-valued function of a row \vec{r} of length m in a binary image (i.e. of a binary vector). These functions are constructed such that they are independent of spatial scale and resolution of the image and confined to the interval $[0, 1]$. They summarize different features of a binary image row by row. Indeed, because the vertical direction is the primary direction of water movement in the vadose zone, these functions summarize the horizontal and emphasize the vertical configuration of patterns. For a detailed mathematical description see (Trancón y Widemann and Bogner, 2012) who we follow closely in the description of image index functions stated below. In the following, we identify stained pixels with the integer 1 and non-stained with 0.

The *dye coverage* is a well-known index function in dye tracer studies. It shows the proportion of stained pixels:

$$I_D(\vec{r}) = \frac{1}{m} \sum_i r_i \quad (3.2)$$

We define contiguous sequences of stained pixels as *runs*. Their lengths represent the width of stained objects in an image row and their number is called the *Euler number*. Normalized by the maximum number of possible runs (i.e. $m/2$) gives:

$$I_E(\vec{r}) = \frac{|\mathcal{R}_1(\vec{r})|}{\lceil m/2 \rceil} \quad (3.3)$$

where \mathcal{R}_1 is a function that calculates the sequence of run lengths and the brackets $\lceil \rceil$ are the ceiling function that rounds up to the nearest integer. $I_E(\vec{r})$ is small if the patterns are dominated by large stained objects and attains its maximum of 1 for a regular sequence of alternating stained and non-stained pixels.

The distribution of run lengths can be summarized by their minimum, *maximum* and median. In our experiments, however, we only used the maximum for the analysis because it was the most suitable index to distinguish between the different tillage managements

$$I_{MAX} = \frac{1}{m} \max(\mathcal{R}_1(\vec{r})) \quad (3.4)$$

Furthermore, we can measure how *contiguous* the runs are by defining:

$$I_C(\vec{r}) = \langle \mathcal{R}_1(\vec{r}), \mathcal{R}_1(\vec{r}) \rangle / (\sum_i r_i)^2 \quad (3.5)$$

The indeterminate case where there are no stained pixels in a row is set to 1. I_C can be interpreted as the reciprocal of a non-integer measure of the number of stained objects weighted by their size. It behaves differently compared to the other index functions because it is 1 for completely stained and completely non-stained rows. Therefore, for an easier interpretation we used $1 - I_C$ (i.e. we flipped it horizontally) and called this new index function *fragmentation*

$$I_F(\vec{r}) = 1 - I_C(\vec{r}) \quad (3.6)$$

In an image row where large stained objects dominate (i.e. contiguous runs), I_F will be smaller compared to an image row with smaller stained objects given the same proportion of staining (i.e. equal I_D). Furthermore, I_F equals 0 for completely stained and non-stained image rows.

Last but not least, we want to assess the information contained in an image row \vec{r} via the metric entropy, a version of the famous Shannon's entropy. Shannon (1948) defined the information content of an outcome x of a discrete random variable as $h(x) = -\log_2 p(x)$, $p(x)$ being the probability of occurrence of the outcome x . It is measured in bits. The average information content (i.e. Shannon's entropy) is defined as

$$H(X) = - \sum_{x \in X} p(x) \cdot \log_2 p(x) \quad (3.7)$$

for a set of events X with probability of occurrence $p(x_1), p(x_2), \dots, p(x_n)$. Among all distributions with n possible events, H attains its maximum of $\log_2 n$ for the uniform distribution. This is intuitively clear for the average information content is equivalent to our uncertainty about which event will occur. In other words Shannon's entropy measures how much information is "produced" by the random variable. For an event that will certainly occur H is equal to 0.

Now let's consider the staining of a pixel as realization of a binary random variable (i.e. possible outcomes are stained or non-stained). In this case H is maximum for $p(1) = p(0) = 0.5$ and is called the binary entropy function. Replacing the theoretical probabilities in (3.7) by empirical frequencies, $p(0)$ and $p(1)$ we can calculate Shannon's entropy via

$$H(\vec{r}) = -(p(0) \cdot \log_2 p(0) + p(1) \cdot \log_2 p(1)) \quad (3.8)$$

Often, it is more informative to consider the entropy of substrings or words (\vec{w}) of length L in a binary vector (**Ebeling1995**). Normalizing by L yields the metric entropy:

$$I_{\text{ME}L}(\vec{r}) = \frac{1}{L} \cdot H(\mathcal{W}_L(\vec{w})) \quad (3.9)$$

where H is the generalization of Shannon's entropy for words of length L . In other words, the random variable X from equation (3.7) is defined to pick an arbitrary word of length L from \vec{r} . For our images we chose $L = 8$. \mathcal{W}_L is a sliding window function that moves through the image row \vec{r} to produce the different words. The metric entropy gives useful values only if $m \gg L$. Compared to Shannon's entropy in equation (3.7), the metric entropy allows to assess the correlation structure inside words. Indeed, metric entropy attains its maximum when single pixels in the words are uncorrelated and decreases for correlated pixels. For binary sequences $I_{\text{ME}L}$ is confined to the interval $[0, 1]$.

Special care should be taken when calculating image index functions for soils with an uneven soil surface. Therefore, to differentiate between soil and non-soil on the ridged surface of RT, RT_{pm} and RT_{pm+crops}, we used the background binary images (Figure 3.1b). Areas identified as non-soil were omitted. Additionally, we discarded the first and the last profiles completely because of edge effects and used 8 images for CT, RT and RT_{pm} and 5 images for RT_{pm+crops}. The image index functions were calculated in R (R Core Team, 2012).

The interpretation of differences in tillage management systems is based on median values of image index functions. To better understand which features of flow patterns are reflected by these functions we first give an example of a single profile from RT_{pm} (Figure 3.2). As indicated by circles and arrows, the index functions are sensible to different relevant features and complement each other. In fact, the dye coverage I_D increases when the stained objects become larger (red arrow), however, it is not sensitive to different pattern configurations. By contrast, I_F increases when smaller stained objects appear and the pattern is fragmented. The metric entropy $I_{\text{ME}8}$ indicates that at the scale of 8 pixels we find a strong correlation in our patterns. In other words, there are only few different words of length 8 (namely predominantly those with 1s only or 0s only) because large stained and non-stained areas alternate.

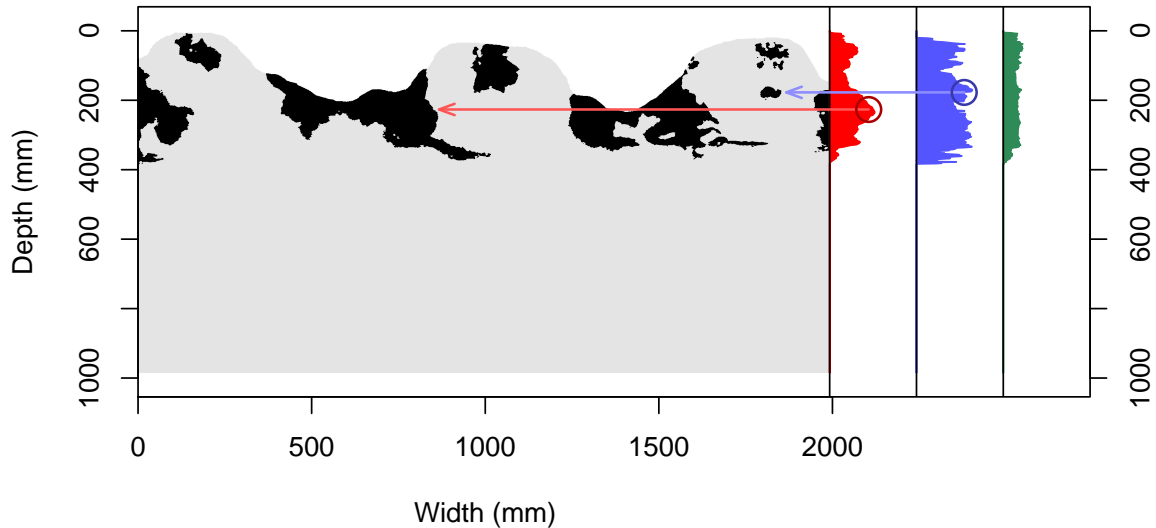


Figure 3.2: Left to right: Example of a binary image and three index functions: dye coverage I_D , fragmentation I_F and metric entropy I_{ME8} . The gray background represents the soil profile and the dye stained patterns are shown in black. For explanation of circles and arrows see section 3.2.5.

3.3 Results and discussion

3.3.1 Water balance and water content

We observed the largest infiltration and the smallest runoff on plot CT (Table 3.2). The amount of infiltrated water decreased and the surface runoff increased from CT to RT and further to RT_{pm} due to the surface topography and plastic mulching of the ridges. In experiment RT_{pm} , approx. 50% of the total amount of irrigation water contributed to the runoff. By contrast, on $RT_{pm+crops}$ the infiltration increased again and the surface runoff decreased to 31% compared to RT_{pm} probably due to the well developed crop canopy. Indeed, interception and throughfall of irrigated water might have reduced the formation of surface runoff. Our results agree well with Saffigna et al. (1976) who investigated non-uniform infiltration patterns caused by hilling and potato canopy. These authors also found an increased runoff from ridges.

At the beginning of experiment CT the water content in 5 cm depth was lower compared to 20 cm depth (Figure 3.3). Approx. 15 minutes after the start of irrigation, the sensors placed in 5 cm depth registered an increase of water content, while the dynamics in 20 cm depth was delayed. Although flat the soil surface was inclined which explains larger soil moisture values measured by the FDRs situated downslope (FDR 2 and FDR 4).

On plots RT and RT_{pm} we found higher water contents in furrows at the beginning of irrigation. This was probably caused by previously preferentially infiltrated water due to topography effects. Indeed, higher soil moisture in furrows due to runoff from ridges was also found by

Table 3.2: Total amount of irrigation and its partitioning into surface runoff and infiltration.

Experiment	Total amount of irrigated water (l)	Infiltration		Runoff	
		(l)	(%)	(l)	(%)
CT ^a	87	69	79	18	21
RT ^b	74	46	62	28	38
RT _{pm} ^c	81	41	50	41	50
RT _{pm+crops} ^d	91	63	69	28	31

^a Conventional flat tillage

^b Ridge tillage

^c Ridge tillage with plastic mulch

^d Ridge tillage with plastic mulch and potato crops

Leistra and Boesten (2010) and Saffigna et al. (1976). In 5 cm depth in RT the water content went up first in furrows, since the runoff from the ridges accumulated here, and then in ridges. It increased only slightly in 20 cm depth.

In experiment RT_{pm} the dynamics was comparable to RT except on ridges that were covered with plastic mulch. The increase in water content in ridges in 20 cm depth was probably related to water which infiltrated primarily in the furrows and was subsequently funnelled laterally above the tillage pan to the ridges. Furthermore, the initial soil moisture differed between furrows and ridges so that pressure head gradients caused lateral water movement from furrows to ridges (Ruidisch et al., 2012). These findings are in accordance with results by Bargar et al. (1999). They investigated soil water recharge and infiltration patterns in an uncropped ridge–furrow formation without plastic mulch and found lateral water flow from furrows to ridges.

3.3.2 Analysis of flow patterns

The experiments revealed that firstly, tillage produced zones of preferential infiltration, namely furrows and planting holes and zones of no infiltration, namely plastic mulched ridges (Figure 3.4). Therefore, the patchiness of the patterns and the occurrence of preferential flow is a result of the soil surface topography. Figure 3.5 shows the image index functions. In all four experiments I_E was approx. 0.1, which is quite small and reflects the few vertically stained patterns. Secondly, the tillage pan was the most important feature for water movement in these agricultural soils which was clearly evident by the decrease of all the indices to zero in approx. 25–35 cm depth. Furthermore, we found that the bulk density differed significantly ($p < 0.05$) above and below the tillage pan on RT_{pm} and RT_{pm+crops} (i.e. between the horizons Ap and Bwb and between the horizons Ap1 and Ap2, respectively). However, we could not detect any difference ($p > 0.05$)

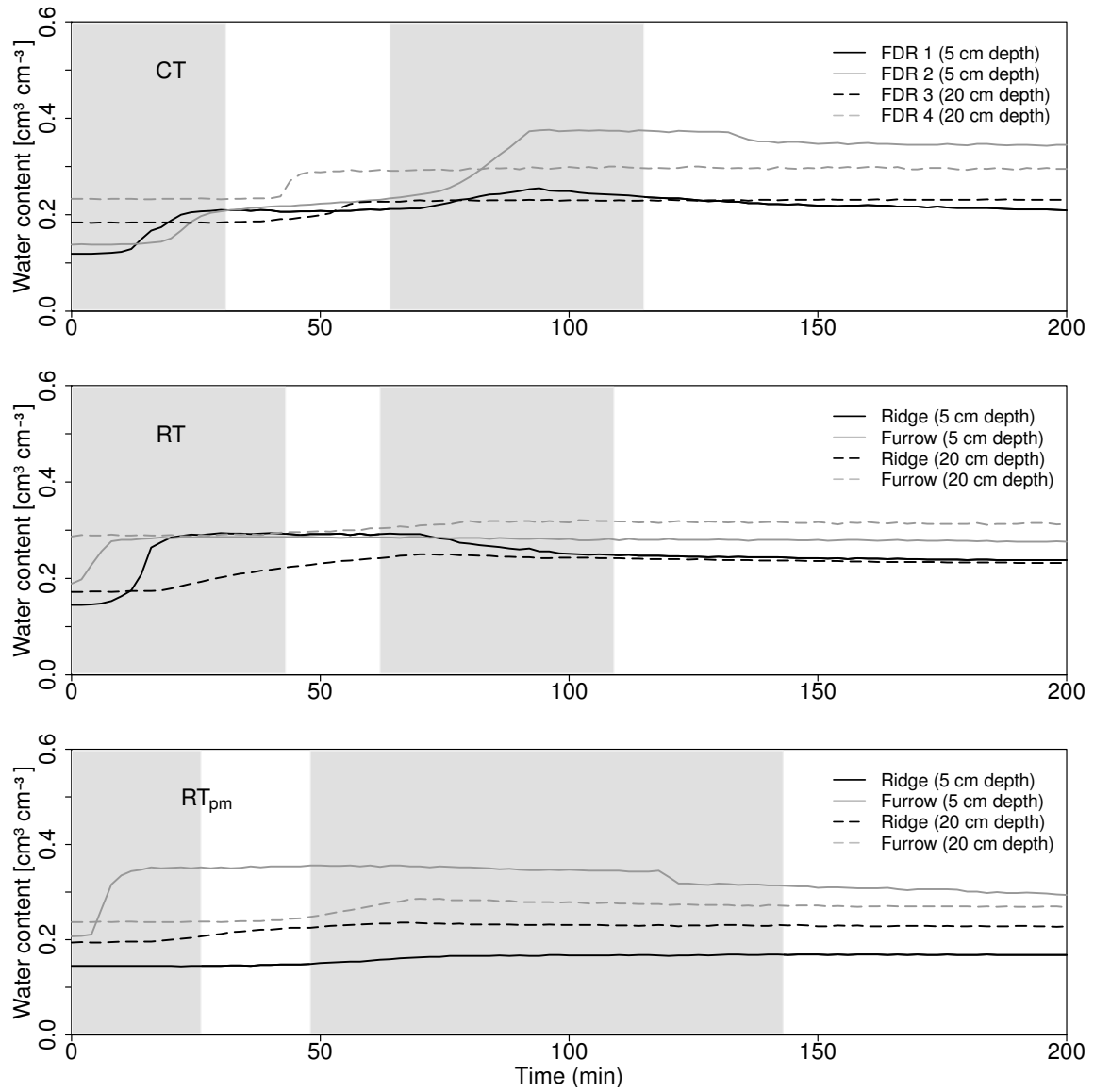


Figure 3.3: The dynamics of water content in different depths during the irrigation experiments CT, RT and RT_{pm}. The grey area indicates the time of irrigation.

between Ap and 2Apb on RT despite the visible funnel flow (Figure 3.4) due to textural differences (Table 3.1). Thirdly, the shape of the index curves shows that in our experiments water flow occurred in the topsoil and was funneled preferentially above the tillage pan. Indeed, the vertical propagation to the deeper soil horizons via macropores was absent. This was also confirmed by comparing the Brilliant Blue stained patterns to the iodide patterns. The propagation of the iodide tracer solution was exactly equivalent to that of Brilliant Blue FCF. This result contradicts the findings by Flury and Flühler (1995) who reported that Brilliant Blue FCF was retarded by a factor of 1.2 compared to the iodide tracer. We explain this disagreement by the sandy texture of the top soil and thus its large hydraulic conductivity.

The effect of the *ridge topography* in experiment RT was well represented by the indices I_D , I_F , I_{ME8} and I_{MAX} . Both, I_F (max = 0.64) and I_{ME8} (max = 0.35) were larger on RT compared to CT (max(I_F) = 0.48 and max(I_{ME8}) = 0.21), which reflected the typical dye pattern induced by topography effects. Indeed, the alternation between stained furrows, stained inner parts of the ridges due to infiltration in planting holes and unstained parts on the inner sides of the ridges are the prominent features (Figure 3.4). The index I_{MAX} with a maximum of 1 reflected the homogeneous and continuous infiltration on CT. It remained large down to the depth of the tillage pan indicating homogeneous matrix flow. Similarly, looking at the uppermost cm of RT, where the tracer infiltrated homogeneously as well, we also find a large I_{MAX} (max = 0.75).

The effect of *plastic mulch* can be best extracted by comparing I_D and I_{MAX} on RT and RT_{pm}. On RT, I_D was largest (max = 1) in the uppermost cm as a result of homogeneous infiltration. In contrast, I_D on RT_{pm} increased to a maximum of 0.53 in 20 cm soil depth reflecting the high surface runoff rates from the plastic mulched ridges into furrows where most of the irrigated water infiltrated preferentially. Additionally, the blockage of tracer infiltration caused by plastic mulch was well mirrored by I_{MAX} . In fact, the homogeneous matrix flow in the upper cm of RT was reflected by a large I_{MAX} (max = 0.75), whereas the largest I_{MAX} (max = 0.22) on RT_{pm} marked the depth of laterally funnelled water above the tillage pan.

The effect of the *root system* on dye patterns was only slightly apparent in larger I_D in approx. 20 cm soil depth on RT_{pm+crops} compared to RT_{pm}. The stem flow funnelled the irrigation water to the planting holes and therefore caused an additional ponding. After infiltration the tracer solution was preferentially channelled along living roots, which resulted in a maximum of I_D (0.66) in the root zone depth. In contrast, the maximum of I_D on RT_{pm} without crop roots occurred in the depth of the tillage pan (0.53). Similarly, the largest I_{MAX} on RT_{pm} (0.22) and RT_{pm+crops} (0.25) reflected the funnel flow above the tillage pan under RT_{pm} and the highly stained root zone on RT_{pm+crops}, respectively. We observed another important factor which was

best visible in the profile pictures (Figure 3.4). On $RT_{\text{pm+crops}}$ water movement in slope direction was not longer pronounced compared to RT_{pm} . Instead, water was primarily redirected from furrows to ridges (i.e. up slope). We attribute this lateral flow to the hydraulic gradient with lowest pressure heads found in the inner part of the plastic mulched ridges where root water uptake took place. A similar phenomenon was observed by Ruidisch et al. (2012), who found that plastic mulched ridge cultivation led to lateral flow driven by a pressure head gradient between furrows and the relatively drier ridges.

3.3.3 The effect of tillage management on flow processes and its ecological implications

First we want to highlight the tillage operations, which take place regardless of ridge cultivation with or without plastic mulch, namely the distribution of sandy soil material on agricultural fields prior to planting and the subsequent ploughing. Indeed, the distribution of sandy soil material to counterbalance erosion loss in the Haean catchment strongly influences the flow processes. This management practice leads to an artificial layering with different soil physical properties. A cohesive, denser and finer textured subsoil is overlain by a topsoil consisting of a non-cohesive and coarse material. As a result an important textural boundary is created with clearly contrasting hydraulic conductivities between the horizons above and below it. Additionally, ploughing activities create a tillage pan and thus further support the structural differences between the horizons. We identified these structural features to be responsible for the initiation of the rather uniform flow through the sandy toplayer as well as for the funnel flow on the tillage pan.

Several authors reported that fissures, cracks and earthworm burrows could act as preferential flow paths especially in fine textured subsoils (Weiler and Naef, 2003; Bachmair et al., 2009). Although ploughing activities lead to a discontinuity of macropores between topsoil and subsoil (Gjettermann et al., 1997), preferential flow paths in the deeper subsoil can still conduct water (Bogner, Mirzaei, et al., 2012). In our experiments, we could not detect any macropore flow neither in the topsoil nor in the subsoil. This can be related to the fact that the non-cohesive sandy toplayer does not have any macropores even before ploughing. Simultaneously, the denser and finer textured subsoil lacked macropores like fissures or cracks which could initiate preferential flow. Additionally, we did not observe any soil fauna on our field sites, which could build a network of macropores.

Ecologically our findings imply that the risk of a vertical propagation of agrochemicals to

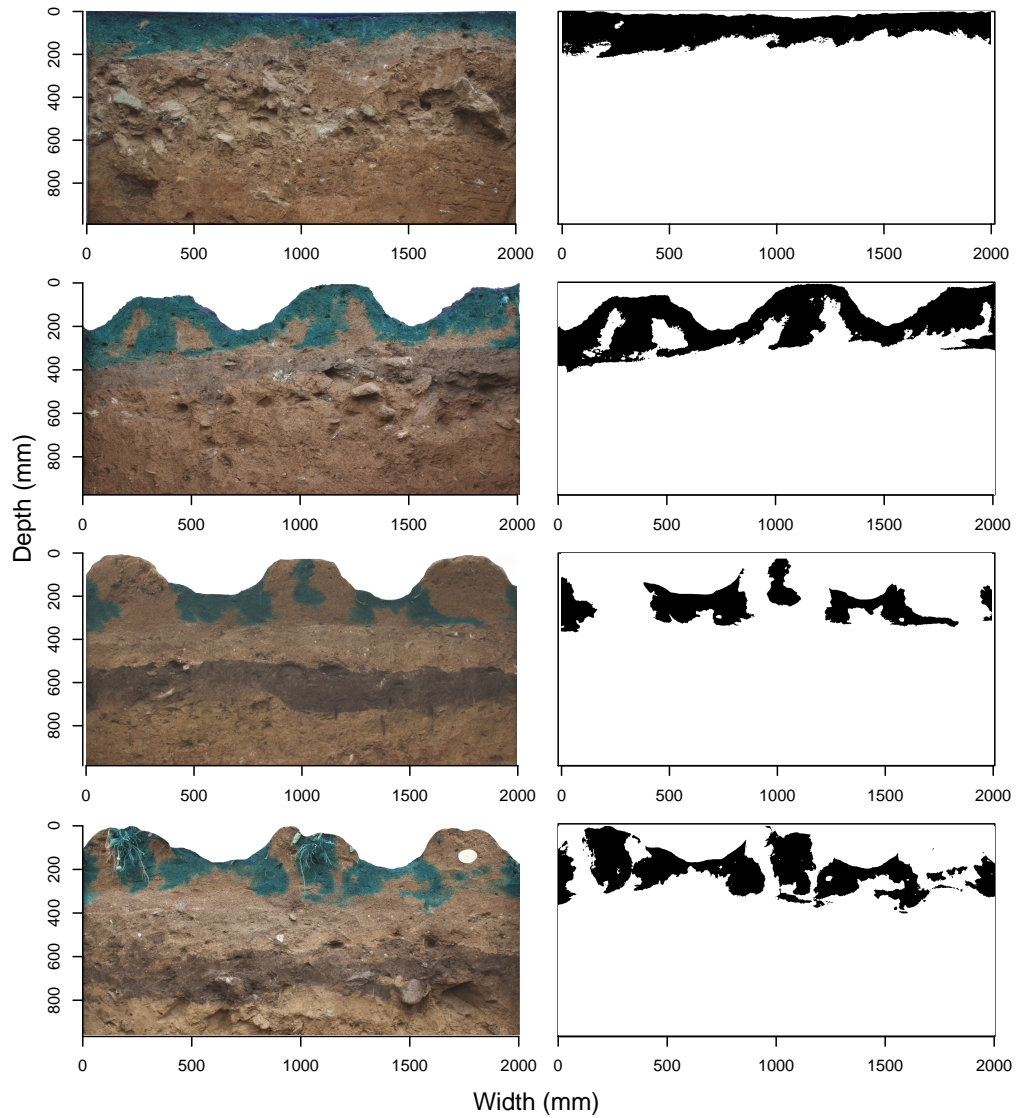


Figure 3.4: Example images of excavated soil profiles and their binary images. From top to bottom: CT, RT, RT_{pm} and $RT_{pm+crops}$. Note that the slope orientation differs between field site 1 (CT and RT, slope oriented to the left) and field site 2 (RT_{pm} and $RT_{pm+crops}$, slope oriented to the right). In the colour image of $RT_{pm+crops}$, the white feature on the right hand ridge is a potato cut in half.

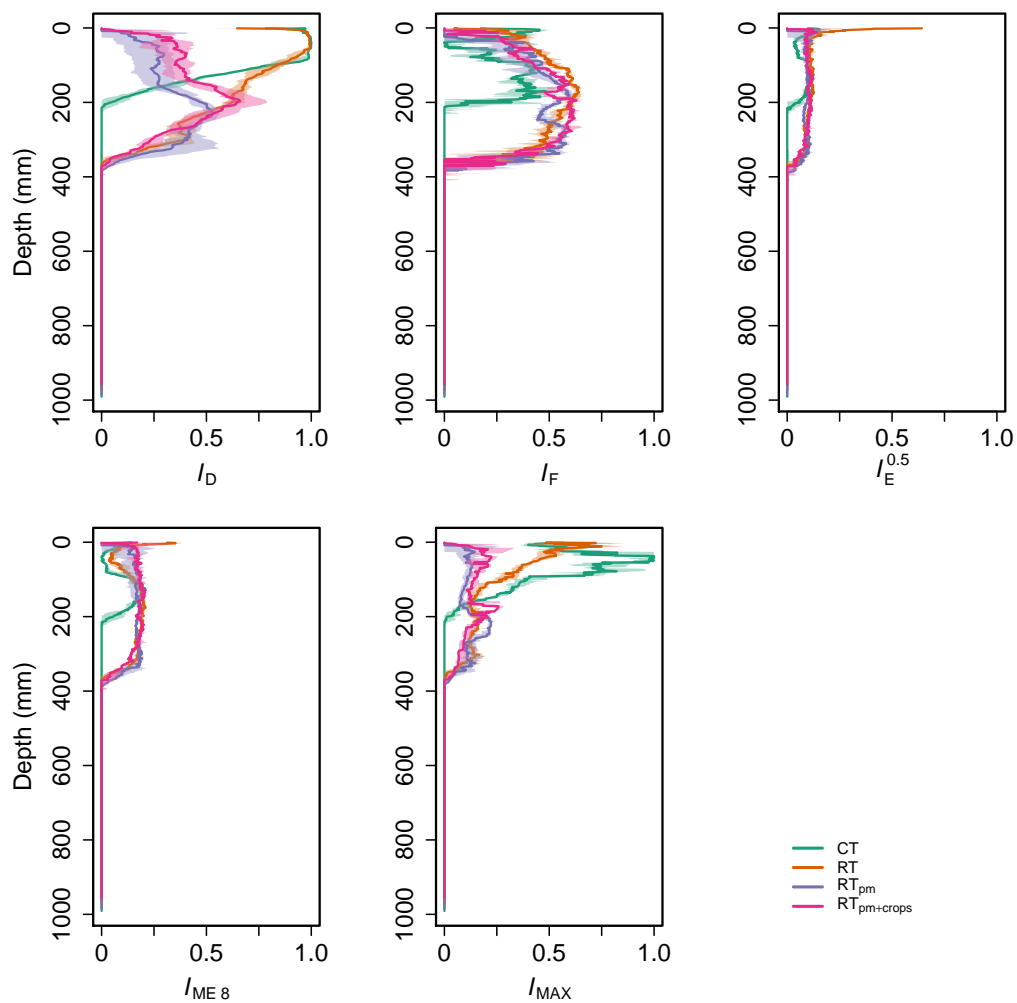


Figure 3.5: Image index functions and their 25% and 75% quantiles (colored ares).

groundwater is generally relatively low. On the other hand the lateral downhill water flow above the tillage pan seems to be the most crucial process to which we should pay particular attention. Especially during the East Asian summer monsoon, when rain events can reach more than 100 mm per day, the fast flow through a coarse textured top soil laterally down the slope seems to play a key role in the transport of agrochemicals. Therefore, the field sites which are located next to the river system should be recognized as critical locations for pollutants entering the water bodies.

Additionally, the temporal aspect plays an important role. We found that in the later season the developed potato crop canopy decreased surface runoff due to interception and throughfall. Additionally a developed root system has the potential to interrupt the subsurface funnel flow above the tillage pan because root water uptake induced pressure head gradients and therefore influenced water movement. Hence, the leaching risk via surface runoff and subsurface water flow is reduced in the adult stage of the crop development. On the other hand it means that the leaching risk is especially high at the beginning of the growing season when the plants are juvenile and the fertilizers are recently applied, because in this juvenile stage the interception and root water uptake are very low. However, the potential for interrupting lateral subsurface flow due to pressure head gradients depends presumably on the intensity and amount of rainfall. We can relate the occurrence only to the irrigation rates which equaled moderate rain events of 37–45 l m⁻².

Our results suggest that differences between tillage management systems have to be considered when evaluating the impact of agricultural land use on ecological services. The important amount of runoff generated under ridge tillage cultivation with plastic mulching can increase the risk of surface water pollution and soil erosion. In fact, even in the later season, when the crop canopy was well developed, the runoff still constituted one third of the total irrigation in our experiments. Arnhold (personal communication) compared CT, RT and RT_{pm} plots using the process-based model EROSION 3D (von Werner, 1995) and found the highest runoff and erosion rates under ridge tillage with plastic mulching. Additionally, we assume that the widespread usage of plastic mulching in combination with heavy monsoon events is partly responsible for higher phosphorous leaching in the Haean catchment, which is predominately transported via surface runoff. This is supported by Kim et al. (2001) who found that eutrophication and deterioration of water quality in in downstream reservoirs in South Korea is associated with discharge of phosphorous.

3.4 Conclusions

Different tillage management practices created typical infiltration zones (i.e. furrows and planting holes) and non-infiltration zones (i.e. plastic covered ridges). However, the impact of ridge cultivation with or without plastic mulch on the predominant subsurface flow processes is relatively low compared to the impact on surface runoff generation. Therefore, to reduce surface runoff, we suggest (i) to encourage crop production in ridge cultivation with perforated plastic mulch. On the one hand, perforated plastic mulch should decrease the amount of surface runoff and thus diminish the risk of erosion and leaching of agrochemicals, especially in the early season when crops are juvenile. On the other hand, it maintains a positive effect on crop yield and weed control. Furthermore, particular attention should be paid to the lateral leaching risk of agrochemicals and fertilizers above the tillage pan particularly on field sites located directly next to the stream network. Hence, we propose (ii) to promote the establishment of riparian buffer zones between dryland farming fields and the rivers.

Acknowledgements

We are grateful to Dr. Baltasar Trancón y Widemann for technical assistance and intense discussions. We would like to thank Andreas Kolb for his invaluable technical support during the irrigation experiments. Furthermore, we thank Bora, Heera and Eun-Young for translating and Farmer Shin for giving us the opportunity to carry out the experiments on his fields. This study was carried out as part of the International Research Training Group TERRECO (GRK 1565/1) funded by the Deutsche Forschungsgemeinschaft (DFG) at the University of Bayreuth, Germany and the Korean Research Foundation (KRF) at Kangwon National University, Chuncheon, South Korea.

References

- Bachmair, S., M. Weiler, and G. Nuetzmann (2009). “Controls of land use and soil structure on water movement: Lessons for pollutant transfer through the unsaturated zone”. In: *Journal of Hydrology* 369.3-4, pp. 241–252. DOI: 10.1016/j.jhydro1.2009.02.031.
- Bargar, B., J. B. Swan, and D. Jaynes (1999). “Soil water recharge under uncropped ridges and furrows”. In: *Soil Science Society of America Journal* 63.5, pp. 1290–1299. ISSN: 0361-5995.

- Bogner, C., D. Gaul, A. Kolb, I. Schmiedinger, and B. Huwe (2010). “Investigating flow mechanisms in a forest soil by mixed-effects modelling”. In: *European Journal of Soil Science* 61.6, pp. 1079–1090. ISSN: 1351-0754. DOI: 10.1111/j.1365-2389.2010.01300.x.
- Bogner, C., M. Mirzaei, S. Ruy, and B. Huwe (2012). “Microtopography, water storage and flow patterns in a fine-textured soil under agricultural use”. In: *Hydrological Processes*. ISSN: 0885-6087. DOI: 10.1002/hyp.9337.
- Flury, M. and H. Flühler (1995). “Tracer characteristics of Brilliant Blue FCF”. In: *Soil Science Society of America Journal* 59.1, pp. 22–27. ISSN: 0361-5995.
- Gish, T. J., D. Gimenez, and W. J. Rawls (1998). “Impact of roots on ground water quality”. In: *Plant and Soil* 200.1, pp. 47–54. ISSN: 0032-079X. DOI: 10.1023/A:1004202013082.
- Gjettermann, B., K. L. Nielsen, C. T. Petersen, H. E. Jensen, and S. Hansen (1997). “Preferential flow in sandy loam soils as affected by irrigation intensity”. In: *Soil Technology* 11.2, pp. 139–152. ISSN: 0933-3630. DOI: 10.1016/S0933-3630(97)00001-9.
- Hendrickx, J. and M. Flury (2001). “Uniform and preferential flow mechanisms in the vadose zone”. In: *Conceptual Models of Flow and Transport in the Fractured Vadose Zone*. Ed. by N. R. Council. Washington and DC: National Academy Press.
- IUSS Working Group WRB (2006). *World reference base for soil resources 2006 – A framework for international classification, correlation and communication*. World Soil Resources Reports No. 103. Rome: FAO. URL: <ftp://ftp.fao.org/agl/agll/docs/wsrr103e.pdf>.
- Jarvis, N. J. (2007). “A review of non-equilibrium water flow and solute transport in soil macropores: principles, controlling factors and consequences for water quality”. In: *European Journal of Soil Science* 58.3, pp. 523–546. ISSN: 1351-0754. DOI: 10.1111/j.1365-2389.2007.00915.x.
- Kim, B., J.-H. Park, G. Hwang, M.-S. Jun, and K. Choi (2001). “Eutrophication of reservoirs in South Korea”. In: *Limnology* 2, pp. 223–229. ISSN: 1439-8621. DOI: 10.1007/s10201-001-8040-6.
- Kulli, B., M. Gysi, and H. Flühler (2003). “Visualizing soil compaction based on flow pattern analysis”. In: *Soil & Tillage Research* 70.3, pp. 29–40.
- Lament, W. J. (1993). “Plastic mulches for the production of vegetable crops”. In: *HortTechnology* 3.1, pp. 35–39.
- Leistra, M. and J. J. T. I. Boesten (2010). “Pesticide Leaching from Agricultural Fields with Ridges and Furrows”. In: *Water Air and Soil Pollution* 213.1-4, pp. 341–352. ISSN: 0049-6979. DOI: 10.1007/s11270-010-0389-x.

- Lu, J. H. and L. S. Wu (2003). “Visualizing bromide and iodide water tracer in soil profiles by spray methods”. In: *Journal of Environmental Quality* 32.1, pp. 363–367. ISSN: 0047-2425.
- Park, J.-H., L. Duan, B. Kim, M. J. Mitchell, and H. Shibata (2010). “Potential effects of climate change and variability on watershed biogeochemical processes and water quality in Northeast Asia”. In: *Environment International* 36.2, pp. 212–225. ISSN: 01604120.
- Petersen, C., H. Jensen, S. Hansen, and C. Bender Koch (2001). “Susceptibility of a sandy loam soil to preferential flow as affected by tillage”. In: *Soil & Tillage Research* 58.1–2, pp. 81–89.
- R Core Team (2012). *R: A Language and Environment for Statistical Computing*. ISBN 3-900051-07-0. R Foundation for Statistical Computing. Vienna, Austria. URL: <http://www.R-project.org/>.
- Ruidisch, M., J. Kettering, S. Arnhold, and B. Huwe (2012). “Modeling water flow in a plastic mulched ridge cultivation system on hillslopes affected by South Korean summer monsoon”. In: *Agricultural Water Management*. DOI: 10.1016/j.agwat.2012.07.011.
- Saffigna, P., C. Tanner, and D. Keeney (1976). “Non-uniform infiltration under potato canopies caused by interception, stemflow, and hilling”. In: *Agronomy Journal* 68, pp. 337–342.
- Shannon, C. E. (1948). “A mathematical theory of communication”. In: *Bell System Technical Journal* 27, pp. 379–423.
- Simunek, J., N. J. Jarvis, M. T. van Genuchten, and A. Gardenas (2003). “Review and comparison of models for describing non-equilibrium and preferential flow and transport in the vadose zone”. In: *Journal of Hydrology* 272.1-4, pp. 14–35.
- Steger, C., M. Ulrich, and C. Wiedemann (2008). *Machine Vision Algorithms and Applications*. Weinheim, Germany: Wiley-VCH.
- Trancón y Wiedemann, B. and C. Bogner (2012). “Image analysis for soil dye tracer infiltration studies”. In: *Proceedings of the 3rd International Conference on Image Processing Theory, Tools and Applications*. (in press).
- von Werner, M. (1995). “GIS-orientierte Methoden der digitalen Reliefanalyse zur Modellierung von Bodenerosion in kleinen Einzugsgebieten”. PhD thesis. Berlin, Germany: Free University of Berlin, Department of Earth Science.
- Weiler, M. and F. Naef (2003). “An experimental tracer study of the role of macropores in infiltration in grassland soils”. In: *Hydrological Processes* 17.2, pp. 477–493. ISSN: 0885-6087. DOI: 10.1002/hyp.1136.
- Zhai, P., A. Sun, F. Ren, X. Liu, B. Gao, and Q. Zhang (1999). “Changes of Climate Extremes in China”. In: *Climatic Change* 42, pp. 203–218.

- Zhai, P., X. Zhang, H. Wan, and X. Pan (2005). “Trends in Total Precipitation and Frequency of Daily Precipitation extremes over China”. In: *Journal of Climate* 18, pp. 1096–1108.
- Zhang, W., Z. Tian, N. Zhang, and X. Li (1996). “Nitrate pollution of groundwater in northern China”. In: *Agriculture, Ecosystems and Environment* 59, pp. 223–231.

Chapter 4

Plastic covered Ridge-Furrow Systems on mountainous farmlands: Runoff patterns and Soil Erosion rates

Sebastian Arnhold^{1,a}, Marianne Ruidisch^a, Svenja Bartsch^b, Christopher L. Shope^b,
Bernd Huwe^a

^a Soil Physics Group, BayCEER, University of Bayreuth, 95440 Bayreuth, Germany

^b Department of Hydrology, BayCEER, University of Bayreuth, 95440 Bayreuth, Germany

Abstract

Plastic covered ridge furrow systems can substantially influence runoff and soil erosion on agricultural land. However, the impact of this management practice in combination with a complex farmland topography has not been thoroughly investigated and is still poorly understood. The goal of this study was to identify how topography influences the runoff patterns and erosion rates of plastic covered ridge-furrow systems. We measured runoff and sediment transport on two mountainous fields in South Korea, one with a concave and one with a convex topography, during monsoonal rain events. We used the EROSION 3D model to compare flow and sediment transport differences between the plastic covered system, uncovered ridges, and a smooth soil surface. We found the highest runoff and erosion rates from both of the

¹Correspondence to: Sebastian Arnhold, Soil Physics Group, BayCEER, University of Bayreuth, 95440 Bayreuth, Germany.
E-mail: sebastian.arnhold@uni-bayreuth.de

plastic covered fields, due to the impermeable surface. For the uncovered ridges, we identified a 140% higher erosion compared to the smooth surface on the concave field, although a reduction of 20% on the convex field. The simulated sediment transport patterns showed that the ridge-furrow system concentrated the flow on the concave field resulting in high erosion rates. On the convex field, the ridge-furrow system prevented flow accumulation and erosion. Our results demonstrate that the effect of ridge-furrow systems on erosion is controlled primarily by the topography. These results have practical consequences for watershed conservation planning and the application of large-scale erosion models. Nevertheless, further research is needed to fully understand the impact of this management system on erosion on mountainous farmland.

Keywords: Complex landscape; Erosion; Furrows; Korea; Plastic mulch; Ridges; Runoff; Topography

4.1 Introduction

Intensive agriculture in mountainous landscapes can cause severe soil erosion, resulting in irreversible loss of fertile farmland soil and decrease water quality in streams and lakes. Tillage and crop cultivation practice instituted by the farmers has a substantial influence on the amount of erosion on steep farmland areas. Important cultivation practices for vegetable production are ridge-furrow systems covered with plastic films (plastic mulch) accounting for 3 to 4 million hectares worldwide (Dilara and Briassoulis, 2000), with an increasing trend, particularly in China (Espí et al., 2006). Plastic mulch has increased crop yields, reduced evaporation losses, reduced nutrient leaching, and limited weeds (Lament, 1993). Plastic mulching is a common management practice on most of the agricultural areas in South Korea (except for rice paddies). Agricultural areas in mountainous landscapes, such as the Kangwon Province in the northeast of South Korea, are cultivated predominantly by cash crops like cabbage, radish and potato (S. Kim et al., 2007; Lee et al., 2010b; Y. S. Park et al., 2010). These mountainous agricultural areas are characterized by steep slopes and complex field topographies. The ridge-furrow system is predominantly oriented perpendicular to the main slope direction of field sites, but often not parallel with the contours. In many cases, the tillage directions vary across individual field sites. The distance between the center of two ridges is approximately 70 cm and the ridges are usually between 30 to 40 cm wide and 15 cm higher than the furrows. The ridges are covered with a

black plastic film with regularly spaced, 5 cm diameter, planting holes, and the film is buried on either side of the ridge several centimeters deep. Furrows are conventionally treated with herbicides in order to eliminate weeds during the growing season. Therefore the soil surface between the ridges typically remains uncovered until crops reach their adult stage and start covering parts of the furrows. During rain events, ridge-furrow systems basically drain runoff from ridges into the furrows, producing concentrated overland flow with higher erosive power than without ridges (Wan and S. El-Swaify, 1999). The impermeable plastic film produces higher surface runoff and can therefore, intensify the concentrated flow. Even though the plastic cover protects the surface from raindrop impacts and eliminates ridge erosion, the remaining exposed soil surface in the furrows can have significantly increased erosion losses due to elevated runoff amounts (Wolfe et al., 2002).

Several studies have previously investigated the effect of plastic covered ridge-furrow systems on runoff and soil erosion for a variety of different crops. Wan and S. El-Swaify (1999) analyzed plastic mulch pineapple plantations by using rainfall simulator experiments on field plots. They found substantially higher runoff generation and soil erosion on plastic mulch plots relative to bare plots. Although the authors also observed that plastic mulch in combination with a vegetative crown reduces runoff and soil loss, because water is ponded in the pineapple crowns and funneled into the planting holes. Rice, McConnell, et al. (2001) measured the amount of runoff, sediment and pesticides from tomato plots with plastic mulch in comparison to vegetative mulch. They found increased runoff and at least three times higher soil loss for plastic mulch plots. In another example higher surface runoff contributed to four times higher erosion rates for corn cultivation with plastic mulch than without plastic during field experiments (Gascuel-Odoux et al., 2001). Stevens et al. (2009) measured runoff, soil loss, transported pesticides, and nitrogen in plot experiments for a variety of strawberry cultivation practices including plastic mulch. In contrast to the other studies, they did not identify large differences in surface runoff between plastic mulch and uncovered management strategies. Moreover, they found that plastic mulch significantly reduced soil erosion during select rainfall events. In lysimeter plot studies in South Korea, Lee et al. (2010a) analyzed the effect of contour farming with plastic mulch on runoff, soil losses and nutrient losses for cabbage and potato. They found that both, runoff and erosion was reduced by plastic mulch compared to the non-covered plots.

These studies showed that plastic mulch can have contrary effects, which may be a result of crop type or different ridge-furrow system design and dimension. In addition, these studies also varied in their experimental design, particularly in plot size and orientation of the ridge-furrow system in relation to the plot direction. However, each of the described studies used plots or

delimited sections of a field site with a defined size and uniform topographical conditions. Complex topography, which dominates in mountainous areas of South Korea, remains particularly absent in the literature. The combination of the ridge-furrow system and the shape of a field with its internal topographical variations influence overland flow patterns and can affect the overall soil loss from a field. Runoff flows along the furrows to lower areas in the field where ridge breakovers can occur (Renard et al., 1997). Wischmeier and Smith (1978) have described that for high slope lengths, the soil loss from a contoured field can exceed that from a field without contouring, because of concentrated flow due to breakovers. Higher erosion damage caused by the breakover of contour ridges has also been reported by Stocking (1972), S. A. El-Swaify et al. (1982), and Hagmann (1996). Plastic mulch is typically resistant to raindrop impact and overland flow and provides ridge protection. Although, our field observations indicated, that during peak events, concentrated flow can also wash out the plastic film and erode the ridges. Concentrated overland flow and breakovers within a field, primarily depends on the topography (convex or concave slopes, plains, depressions) and the orientation of the ridge-furrow system. In order to evaluate those systems in complex landscapes, the entire field site should be considered to take into account all possible flow paths that contribute to concentrated overland flow.

The goal of this study was to investigate the role of plastic covered ridge-furrow management on runoff patterns and soil erosion in two mountainous agricultural fields in South Korea. Therefore, we quantified runoff and erosion from fields with plastic mulch, and subsequently applied a model to simulate the response without plastic and ridges. We implemented a novel measurement method, which is not limited to defined plot dimensions and is able to better represent the complex structure of those fields. We used a process-based erosion model, which describes the spatial runoff and erosion patterns affected by ridge-furrow systems and terrain topography.

4.2 Materials and methods

Study Area

This study was conducted in the Haeon-Myeon catchment in the Kangwon Province in the northeast of South Korea (Figure 4.1). The catchment is part of the watershed of Soyang Lake, which is the largest reservoir in South Korea (B. Kim et al., 2000). The Haeon catchment is a key contributor of agricultural water pollution with substantial impacts on the trophic state of the lake (J.-H. Park et al., 2010). Total catchment area is 64 km² with 58% of the catchment

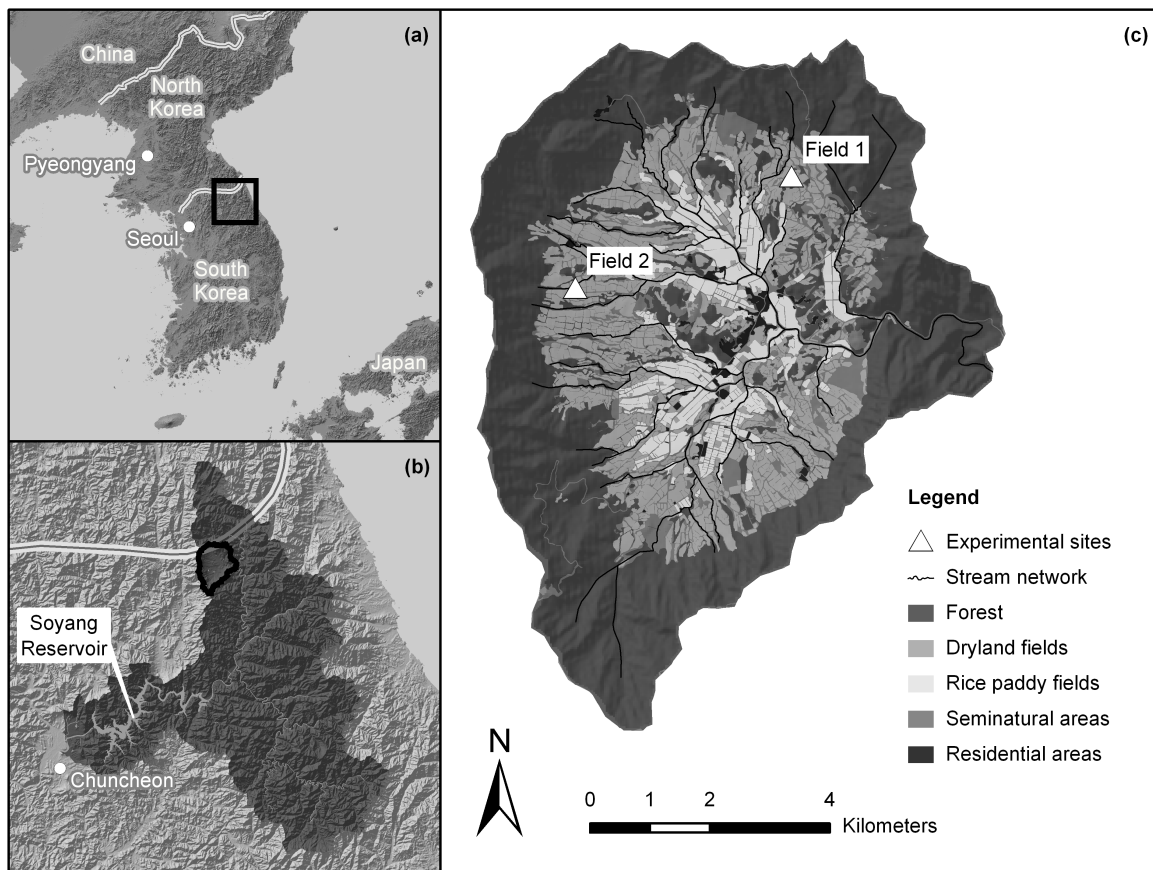


Figure 4.1: Location of the Haeon-Myeon catchment on the Korean peninsula (a) and within the Soyang Lake watershed (b) with locations of the experimental sites conducted for this study (c) ("seminatural areas" include grassland, field margins, riparian areas, small roads and channels).

classified as forested mountains and 30% as agricultural areas (22% dryland fields and 8% rice paddies). The remaining 12% are residential and seminatural areas including grassland, field margins, riparian areas, small roads and channels. The soil landscape is dominated by *Cambisols* formed from weathered granite. Soils are strongly influenced by human disturbance, especially on cropland through replenishment with excavated soils from nearby mountain slopes (J.-H. Park et al., 2010). Haeon average annual precipitation of 1514 mm (2009 and 2010) was approximately 200 mm higher than the average precipitation of the Soyang Lake watershed described in J.-H. Park et al. (2010). Nearly 65% of the total rainfall in Haeon is concentrated in July, August and September.

We selected two typical dryland fields on steep slopes located in the northeastern and western part of the catchment (Figure 4.1c). The topographical shape of field 1 was concave, characterized by a depression line going through the field's center and field 2 was convex without topographical depressions. Both fields had an average slope of about 9 degrees. The soil type of field 1 was a haplic Cambisol (Ap-Bw-BwC-C) and the soil of field 2 was a leptic terric Cambisol (Ap-2Apb-2Bwb-2C), both formed from weathered granite material. The total area

of field 1 was 2133 m² and the total area of field 2 1825 m². The crop type planted during our study period for each of the fields was potato *Solanum tuberosum* L., which was conventionally cultivated with plastic mulch.

4.2.1 Observation of Runoff and Soil Erosion

The experimental design for runoff and erosion measurement is shown in Figure 4.2. On each field site we installed three runoff samplers designed according to Bonilla et al. (2006). Each sampler consisted of a runoff collector (RC) connected with a PVC pipe to a multislot flow divider designed by Pinson et al. (2004) (Figure 4.2 only shows the positions of the collectors). The runoff collectors were located at positions where large amounts of runoff from the field sites were expected, without artificial enclosure of the contributing areas. The only variations from the Bonilla et al. (2006) design were that the collector width was changed to exactly five meters and no mesh at the transition between the collector and the PVC pipe was used to prevent blockage. For the flow divider, the "mid-size-fields" configuration after Bonilla et al. (2006) was used, which included four 20-Liter buckets, one with a 1:12 divisor head and two with 1:24 divisor heads and one without a head, resulting in a total runoff sampling capacity of 144 m³ for each collector. The flow dividers were installed in buried wooden boxes similar to those described in Bonilla et al. (2006). A PVC pipe was buried and connected to the bottom of the wooden box for removal of excessive water to the field's edge. After a rainfall period we measured the water level and calculated the runoff volume for each bucket. We took samples from each bucket (three replicates with 0.12 L) of the homogenized suspension and determined the sediment concentration by evaporation and weight measurement. The sediment concentration was calculated as the average of three replicates. For very high sediment yields during peak events the sediment concentration of bucket 1 was estimated from the sediment level. The dry bulk density was estimated through a general relationship between bulk density and organic carbon content for sediments (Avnimelech et al., 2001). Organic carbon content was estimated by measuring the weight loss after organic matter destruction in the laboratory. The total runoff sampled by each collector was calculated by the following equation (modified after Bonilla et al., 2006),

$$R = V_1 + 12 \cdot V_2 + 288 \cdot V_3 + 6912 \cdot V_4 \quad (4.1)$$

where R is the total runoff volume (L) and V_1 to V_4 the volumes (L) collected in the buckets 1 to 4, respectively. The associated sediment mass was then calculated by (modified after Bonilla

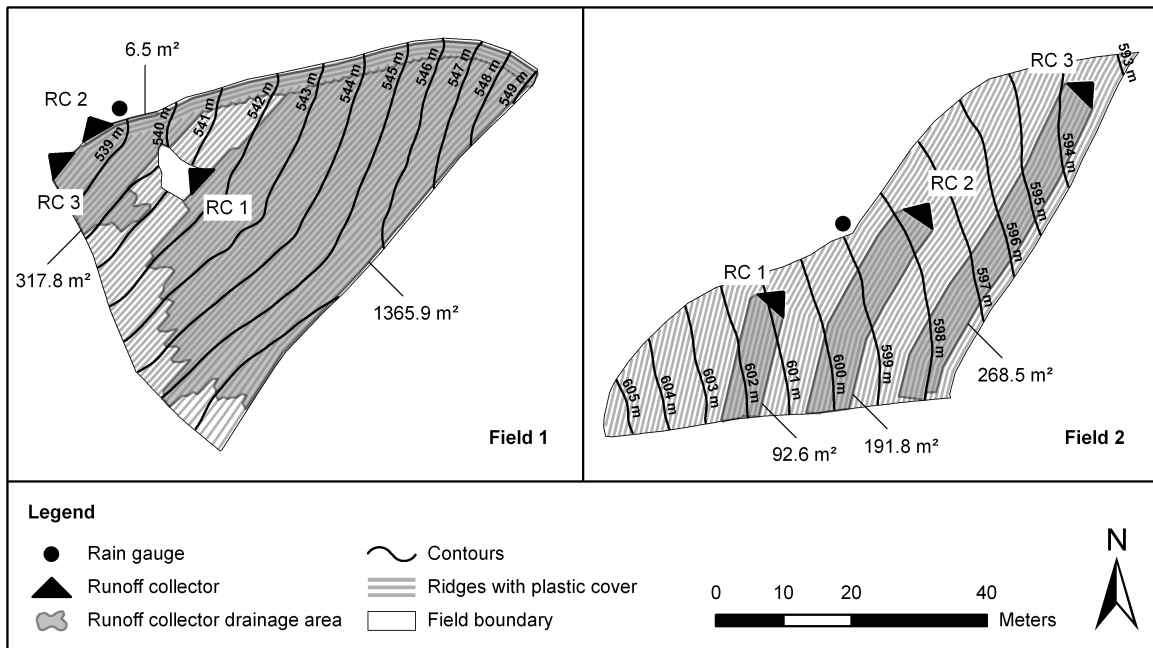


Figure 4.2: Experimental design to measure runoff and soil erosion by installation of three runoff collectors (RC) on field 1 and field 2. Fields topography and runoff collector drainage areas were calculated based on surface elevation measurements and generation of digital terrain models of both fields.

et al. (2006))

$$S = V_1 \cdot C_1 + 12 \cdot V_2 \cdot C_2 + 288 \cdot V_3 \cdot C_3 + 6912 \cdot V_4 \cdot C_4 \quad (4.2)$$

where S is the total sediment mass (kg) and C_1 to C_4 the sediment concentration (kg L^{-1}) measured for bucket 1 to 4, respectively.

Observation time was within the Korean summer monsoon period from 5 July to 9 August 2010. We measured seven rainfall periods with different rainfall characteristics over variable time intervals (Figure 4.3). On each of the field sites we installed rain gauges, which recorded precipitation during all seven rainfall periods at 10 minute resolution. Due to limited rain gauge malfunctions, gap filling was completed to generate continuous precipitation data sets. The rainfall records of adjacent Haeon weather stations displayed linear correlations to our field data. These records were multiplied by the slope of the linear regression functions and added to our data sets to fill those gaps. Total amount of rainfall, rainfall intensity and rainfall erosivity (EI30) calculated after Renard et al. (1997) for each period were derived.

To transform the total sediment mass measured at each collector to the soil loss per area, it was necessary to define the size of the drainage area for each collector. We used a tachymeter (Tachymat WILD TC1000) to create a gridded mesh of elevation points at approximately two by two meter intervals over the entire field area. Furthermore, we counted the number of ridges and

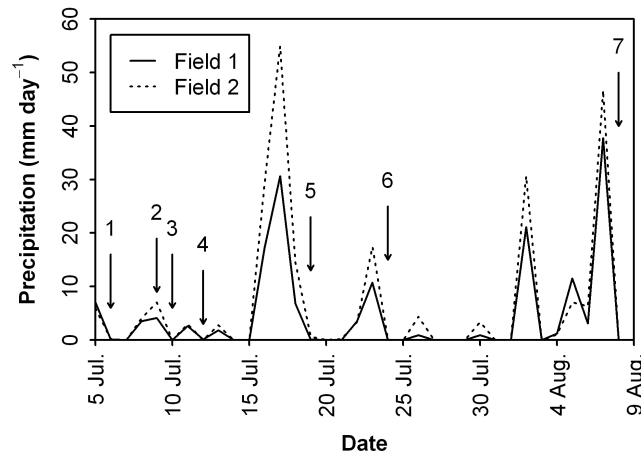


Figure 4.3: Daily precipitation on field 1 and field 2 during the observation time from 5 July to 9 August 2010. The arrows indicate the sampling dates for the associated rainfall periods.

measured their orientation and dimensions (average height, width and spacing) on both fields. In a first step, the elevation points were interpolated to create surfaces representing the basic field topography (indicated by the contours in Figure 4.2). In a second step, we added ridges to the interpolated surfaces assuming semicircular ridge profiles with the same dimensions (15 cm high and 40 cm wide) throughout the field area. Finally, we created two digital terrain models (DTMs) with 25 cm spatial resolution for the fields, one representing the basic topography with a smooth surface and one representing the actual field shape with ridges. By using those DTMs we could delineate the drainage area to each collector and calculate the area (Figure 4.2). The fields were enclosed by elevated mounds and drainage ditches, which minimized the probability of an additional runoff contribution from outside. Nevertheless, in two cases ditch overflow and external runoff contribution was observed. Therefore, the measured runoff and sediment mass during these periods were eliminated from the data set. In all other cases, runoff and soil loss per unit area was quantified by calculating the quotient of runoff volume and sediment mass and the drainage area at each collector. To quantify the mean runoff and soil loss from each field site, the single values for the collectors were averaged and weighted to the drainage area size. The weighted average was used instead of the normal average to account for a higher field representation of RCs covering large areas and for reducing the effect of RCs covering only a small part (e.g. Field 1 RC 2). Because of external runoff contributions and additional damages caused by intense rain events, we could not measure all rainfall periods with all three runoff collectors. In those cases the mean runoff and soil loss rates were calculated only based on the available data of the functioning collectors.

4.2.2 Simulation of Runoff and Soil Erosion

We used the EROSION 3D model (von Werner, 1995) to compare runoff and soil erosion for the plastic covered ridge-furrow management (RP - Ridges with Plastic) to the runoff and erosion for ridge-furrow cultivation without plastic film covers (RU - Ridges Uncovered), and cultivation using a smooth soil surface (SS - Smooth Surface) as it is usually applied for grain crops in many countries. EROSION 3D is a process-based, spatially distributed, erosion model based on the physical principles developed by Schmidt (1991). EROSION 3D describes overland flow distribution and diversion as affected by terrain morphology, as well as the associated erosion and sediment transport. Compared to other process-based erosion models such as WEPP (NEARING1989) or LISEM (Roo et al., 1996), EROSION 3D requires a relatively small number of input variables (Wickenkamp et al., 2000), and most of them are directly related to measured soil, slope and rainfall properties (Schmidt, 1991). Nevertheless, the relatively simple physical approach has some limitations. Soil erodibility and surface roughness, which can vary in the course of rain events, are assumed to be constant throughout the calculations (Wickenkamp et al., 2000). EROSION 3D does not differentiate between rill and inter-rill detachment and when applied to small spatial resolutions, can therefore overestimate soil erosion rates (von Werner, 1995).

The EROSION 3D input parameters can be summarized into three groups, relief parameters, precipitation parameters and soil-surface parameters (Schmidt et al., 1999). For the relief parameters we used the measured 25 cm resolution DTMs. We used the DTM including ridges for the RP and RU scenarios and we used the measured base DTM without ridges to represent a smooth soil surface (SS). Precipitation parameters for each of the seven rainfall periods were provided by the on-site rain gauge records at 10 minute resolution. Soil and surface parameters used for the simulations are shown in (Table 4.1). Layer thickness, texture, bulk density and organic carbon content for the different soil horizons were derived from field measurements and laboratory analysis. For the different management practices the parameters in (Table 4.1) were assigned as follows. For RP, parameters specified for "plastic film" were applied for ridges, and parameters specified for "soil surface" were used for the furrows. For RU and SS the parameters specified for "soil surface" were applied to the entire field area (ridges, furrows as well as the smooth surface). The initial soil moisture at the beginning of each rainfall period was derived from HYDRUS 2/3D (Šimůnek et al., 2011) simulations. The HYDRUS 2/3D model was calibrated to pressure heads measured from May to August 2010 on field 1 and field 2 and used to analyze soil water dynamics due to plastic mulch management. Surface roughness (Manning's n)

was obtained from recommended literature values. Huggins and Monke (1966) (cited in Vieux, 2001, p. 129) give Manning's n values for row crops of 0.07 to 0.2 s m^{-1/3} and the EROSION 3D parameter catalogue (Michael et al., 1996) recommend values for potato fields of 0.08 to 0.09 s m^{-1/3}. These recommendations represent average field conditions including the roughness of the soil surface and the roughness caused by plant stems and leaves. To take into account the different surface conditions between the plastic covered ridges and the uncovered furrows, plastic film and soil surface were treated separately. For the plastic film cover a Manning's n value of 0.01 s m^{-1/3} was selected (Montes, 1998; Chanson, 2004). Potato stems are embedded in small planting holes within the plastic film on the top of the ridges and rarely influence flow along the ridge flanks. For the bare sandy soil surface Engman (1986) (cited in Vieux, 2001, p. 130) recommend values of 0.01 to 0.016 s m^{-1/3}. Nevertheless, due to the fact that potatoes were at a mature stage during our observations and their leaves partially touched the ground, we used a Manning's n value for the soil surface of 0.035 s m^{-1/3} (Chow, 1959), cited in Sturm, 2001, p. 118, Vieux, 2001, p. 130). Percentage soil cover during each rainfall period was estimated by photographs taken during the field measurements. Plastic covered ridges were considered to cover the soil to 100%. Although the plastic film contains planting holes, it was assumed that they were completely covered by crop leaves.

EROSION 3D was calibrated to observed runoff and erosion rates for the plastic covered ridge-furrow system and then used to simulate runoff and erosion for the other management practices (RU and SS). The two last parameters in Table 4.1 (skin factor and erodibility) were used for the calibration. The skin factor is used in EROSION 3D to manipulate the infiltration capacity, as predicted by an empirical approach after Campbell (1985) in order to take into account preferential flow and soil surface conditions, such as crusting. The skin factor for plastic film was defined as 1.3% of the soils value to consider the planting holes which made up approximately 1.3% of the ridge's area. The plastic itself was considered as impermeable. The erodibility parameter is defined as the critical momentum flux, which has to be exceeded by the momentum flux of rainfall and overland flow to generate erosion (Schmidt, 1991) and was calibrated only at the soil surface. The plastic film material was considered as non-erodible (1000 N m⁻²). We used three performance statistics as evaluation criteria for the quality of model calibration, the Nash-Sutcliffe efficiency (NSE), the $RMSE$ -observations standard deviation ratio (RSR) and the Percent bias ($Pbias$). According to Moriasi et al. (2007) satisfactory model performance can be assumed if NSE is larger than 0.5, RSR smaller or equal to 0.7, and if $Pbias \pm 25\%$ or less. Positive values of $Pbias$ indicate model underestimation, and negative values indicate model overestimation (Gupta et al., 1999).

Table 4.1: Soil and surface parameter values used for the EROSION 3D simulations, divided into uncovered parts of the field (soil surface) and covered parts (plastic film). The third row shows the horizon names of the soil profiles of both fields (according to FAO, 2006).

Input parameters	Field 1						Field 2					
	Soil surface			Plastic film			Soil surface			Plastic film		
	Ap	Bw	BwC	Ap	Bw	BwC	Ap	2Apb	2Bwb	Ap	2Apb	2Bwb
Soil parameters:												
Layer thickness (m)	0.20	0.80	0.10	0.20	0.80	0.10	0.20	0.08	0.62	0.20	0.08	0.62
Clay (%)	9	9	9	9	9	9	11	24	25	11	24	25
Silt (%)	33	55	38	33	55	38	36	59	57	36	59	57
Sand (%)	58	36	53	58	36	53	53	17	18	53	17	18
Bulk density (kg m^{-3})	1279	1178	1183	1279	1178	1183	1269	1146	1309	1269	1146	1309
Organic carbon (%)	1.8	0.0	0.0	1.8	0.0	0.0	1.7	2.0	0.0	1.7	2.0	0.0
Initial moisture (%)												
Period 1	33	36	37	26	36	37	32	44	44	29	40	44
Period 2	27	36	36	23	36	36	28	39	44	26	37	44
Period 3	28	36	37	23	36	36	29	40	44	26	38	44
Period 4	27	36	36	23	35	36	28	39	44	26	37	44
Period 5	24	35	36	22	35	36	27	37	43	24	35	43
Period 6	27	36	36	23	35	36	29	41	46	28	41	46
Period 7	25	35	36	23	35	36	29	42	46	28	40	46
Surface parameters:												
Roughness ($\text{s m}^{-1/3}$) ^a	0.035						0.035			0.010		
Soil cover (%)												
Period 1	65						100			100		
Period 2	73						100			100		
Period 3	75						100			100		
Period 4	79						100			100		
Period 5	85						100			100		
Period 6	75						100			100		
Period 7	50						100			100		
Skin factor (-) ^b	0.00250						0.01000			0.00013		
Erodibility (N m^{-2}) ^b	0.07						1000.00			1000		

^a Manning's roughness coefficient derived from literature values (Chow, 1959; Montes, 1998; Vieux, 2001; Chanson, 2004)

^b Skin factor and erodibility values optimized after model calibration to total observed runoff volume and sediment mass

4.3 Results and Discussion

4.3.1 Observed Runoff and Soil Erosion

The measured runoff and soil erosion was highly variable during the observation time due to the rainfall characteristics and varied strongly between field 1 and field 2 (Table 4.2). Precipitation amounts ranged from 2.6 mm to 76.5 mm on field 1 and from 3.0 mm to 102.5 mm on field 2. Total precipitation over all periods of field site 2 (242.7 mm) was higher than field site 1 (165.2 mm). The highest precipitation was recorded for the periods 5 and 7 on both fields. Even though precipitation amounts were similar in both periods, rainfall erosivity was much higher in period 7, due to higher rainfall intensities. On both fields, two of the seven rainfall periods (2 and 3) did not produce appreciable runoff and sediment and the associated soil loss rate for those periods was zero. As expected, runoff and transported sediment correlated positively with precipitation and the highest amounts of runoff and sediment were found on both field sites in periods 5 and 7. The soil loss rate predominantly corresponded with rainfall erosivity within each field, although, the magnitude of difference between fields was large. Even though erosivity was usually higher on field 2, soil loss was always higher on field 1, except during period 3 (Table 4.2). The largest difference between both field sites was observed for period 7. The total observed runoff over all seven rainfall periods was 80.3 L m^{-2} on field 1 and 94.1 L m^{-2} on field 2. The ratio of total runoff to the amount of rainfall was higher on field 1 (0.49) compared to field 2 (0.39), indicating a lower infiltration capacity of field 1. Total soil loss was $3646.7 \text{ kg ha}^{-1}$ on field 1 and 626.5 kg ha^{-1} on field 2. The large differences in soil loss may not be explained by the soil characteristics, slope and crop conditions only, which were relatively similar for both fields. It is expected that soil loss may be affected primarily by the differences in the field topography and the orientation of the ridge-furrow system.

4.3.2 Simulated Runoff and Soil Erosion

The optimized values for the skin factor resulting in the best fit between observed and simulated runoff were 0.0025 for field 1 and 0.01 for field 2 for soil surface, and 0.00003 and 0.00013 for plastic film, respectively (Table 4.1). The optimized values for soil surface erodibility with the best fit between observed and simulated soil loss was N m^{-2} for field 1 and 0.11 N m^{-2} for field 2 (Table 4.1). The optimized values of erodibility were relatively high and out of the range suggested by Michael et al. (1996). These high values indicate a strong erosion overestimation of the model due to the high DTM resolution (von Werner, 1995), which had

Table 4.2: Observed data for field 1 and field 2. Rainfall characteristics, runoff volume and sediment mass measured by the runoff collectors (RC 1, RC 2, RC 3), and derived mean runoff and soil loss rates of the whole field.

Site	Period	Rainfall		Rainfall erosivity ^a		RC1		RC2		RC3		Mean	Mean
		(mm)	intensity (mm h ⁻¹)	(MJ mm ha ⁻¹ h ⁻¹)	erosivity ^a (h ⁻¹)	Runoff (L)	Sediment (kg)	Runoff (L)	Sediment (kg)	Runoff (L)	Sediment (kg)	runoff (L m ⁻²)	soil loss ^b (kg ha ⁻¹)
Field 1	1	7.2	7.2	19.4	-	-	10.9	0.06	246.2	4.23	0.8	132.2	
	2	3.5	1.4	0.8	0.1	0.00	0.3	0.00	0.5	0.00	0.0	0.0	
	3	4.2	2.3	1.3	3.7	0.01	1.1	0.00	9.1	0.03	0.0	0.2	
	4	2.6	1.0	0.2	0.0	0.00	0.0	0.00	0.0	0.00	0.0	0.0	
	5	56.8	2.4	40.9	-	-	84.5	0.15	6457.6	10.66	20.2	333.3	
	6	14.3	2.7	8.1	2245.4	0.89	33.4	0.05	1935.4	2.02	2.5	17.5	
	7	76.5	4.3	293.3	-	-	150.4	0.24	18268.7	102.35	56.8	3163.5	
Field 2	1	6.2	7.4	13.9	41.2	0.37	126.6	0.67	165.7	0.17	0.6	21.9	
	2	4.2	1.7	1.2	1.8	0.00	0.2	0.00	0.0	0.00	0.0	0.0	
	3	6.9	4.1	4.8	14.9	0.01	64.4	0.08	4.6	0.00	0.2	1.7	
	4	3.0	1.2	0.3	1.1	0.00	3.1	0.00	0.0	0.00	0.0	0.0	
	5	102.1	3.3	167.0	4635.7	2.35	-	-	-	-	50.1	254.2	
	6	20.9	3.6	27.5	148.0	0.15	634.1	0.46	101.1	0.04	1.6	11.9	
	7	99.5	4.5	373.4	5393.8	3.04	6457.6	6.54	-	-	41.7	336.8	

^a Rainfall erosivity calculated after Renard et al. (1997)

^b Mean runoff and soil loss calculated as average of the runoff collector values weighted to their drainage area size

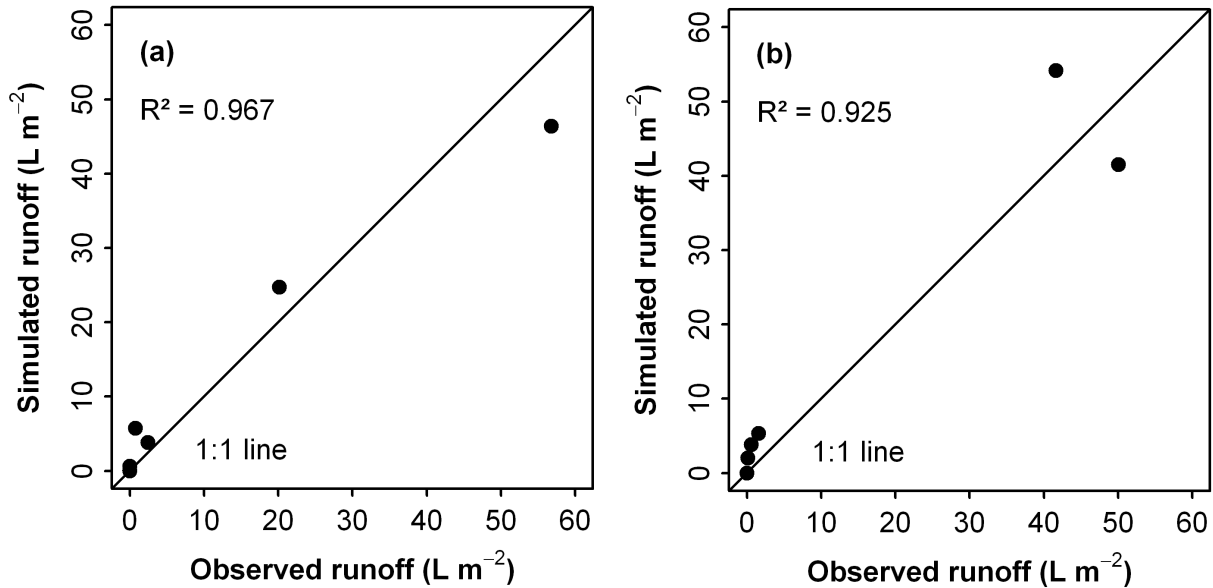


Figure 4.4: Simulated and observed runoff for field 1 (a) and field 2 (b).

to be compensated during the calibration. However, the comparison between simulated and observed runoff (Figure 4.4) and soil loss (Figure 4.5) shows acceptable results. For runoff the model performance was slightly better for field 1 ($NSE = 0.943$, $RSR = 0.239$) than for field 2 ($NSE = 0.914$, $RSR = 0.293$). The model overestimated runoff for both fields with higher magnitude for field 2 ($Pbias = -13.462$) compared to field 1 ($Pbias = -1.275$). Also for soil loss the model performed better for field 1 ($NSE = 0.976$, $RSR = 0.154$) than for field 2 ($NSE = 0.803$, $RSR = 0.444$). The percent bias values showed an overestimation of soil loss for field 1 ($Pbias = -14.571$) and an underestimation of soil loss for field 2 ($Pbias = 12.879$). Satisfactory representations were achieved for both, runoff and soil loss for field 1 and field 2 (Moriasi et al., 2007).

Among the three different management practices, we found the highest simulated runoff for both fields for the ridges with plastic cover (RP) over each rainfall period (Figure 4.6). The total runoff simulated for RP for field 1 and field 2 over all seven rainfall periods was 81.3 L m⁻² and 106.8 L m⁻², respectively. Without plastic cover, the total runoff was reduced to 52.1 L m⁻² (36%) on field 1 and 60.2 L m⁻² (44%) on field 2. The higher runoff amounts for RP are a direct result of the high spatial area associated with the impermeable plastic film. This was also found by HYDRUS 2/3D simulations at both fields, which calculated up to 70% more runoff for plastic mulch than without plastic cover. For all periods, EROSION 3D predicted the same runoff amount for RU and SS, because soil properties were not changed between the management practices. For both RU and SS, the model estimated the same hydraulic conductivity, resulting in the same runoff amount from the entire field. Only the runoff distribution changed due to

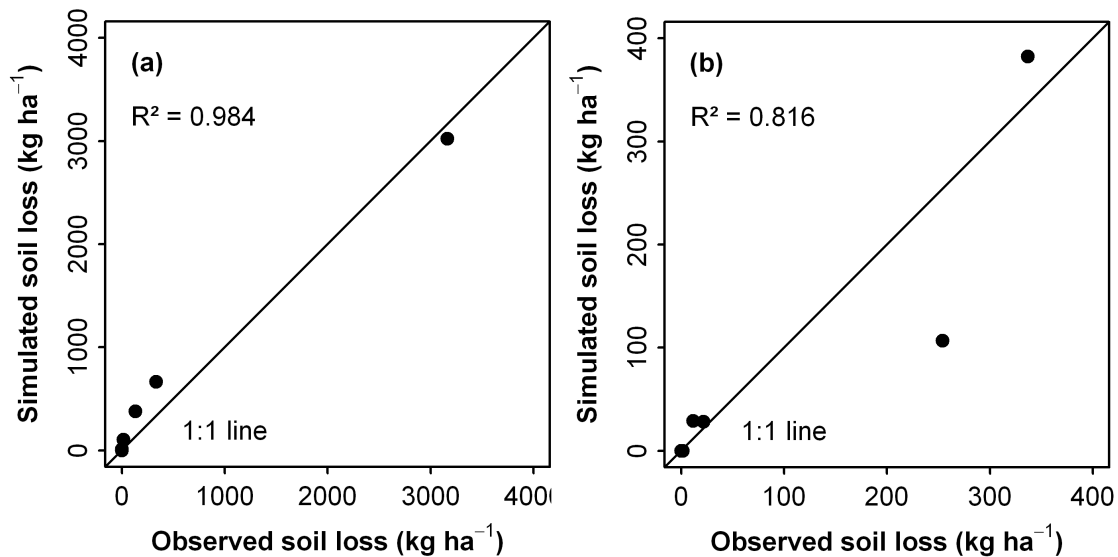


Figure 4.5: Simulated and observed soil loss for field 1 (a) and field 2 (b).

different surface conditions. The amount of runoff reduction by removal of the plastic cover largely varied between the different rainfall periods, and corresponded with the rainfall intensity. The lowest runoff reduction was simulated for period 1 (10% reduction for field 1 and 21% reduction for field 2). Period 1 was characterized by one very short rain event with average intensities of 7.2 mm h⁻¹ and 7.4 mm h⁻¹ on field 1 and field 2, respectively. For period 7 with average intensities of 4.3 mm h⁻¹(field 1) and 4.5 mm h⁻¹(field 2) runoff was reduced by 23% on field 1 and 28% on field 2. The highest runoff reduction was predicted for field 1 (79%) for period 6 (average intensity of 2.7 mm h⁻¹) and for field 2 (61%) for period 5 (average intensity of 3.3 mm h⁻¹). For small rainfall intensities lower than the infiltration capacity of the soil the impermeable plastic cover largely increases the total runoff of the field sites. For high intensities exceeding the soil's infiltration capacity this effect is much smaller, because of high runoff generation on both, plastic and bare soil. This effect was previously described also by Wolfe et al. (2002). Nevertheless, canopy interception and stem flow were not considered in the simulations, because we did not have information about the infiltration amounts caused by stem flow on plastic covered ridge-furrow systems. After plant emergence, stem flow leads to local infiltration of precipitation water around the stems (Leistra and Boesten, 2010; Saffigna et al., 1976) and Jefferies and MacKerron (1985) cited in Leistra and Boesten (2010) found that for potato plants, the percentage of stem flow of the above-crop rainfall can account for up to 46% and 87%, respectively. During the mature crop stage, stem flow could potentially result in higher infiltration and less soil erosion (Wan and S. El-Swaify, 1999). Therefore, the runoff effect of plastic mulch may be slightly overestimated for the rainfall periods throughout this study. However, stem flow is only relevant for infiltration rates, when a high covering crop

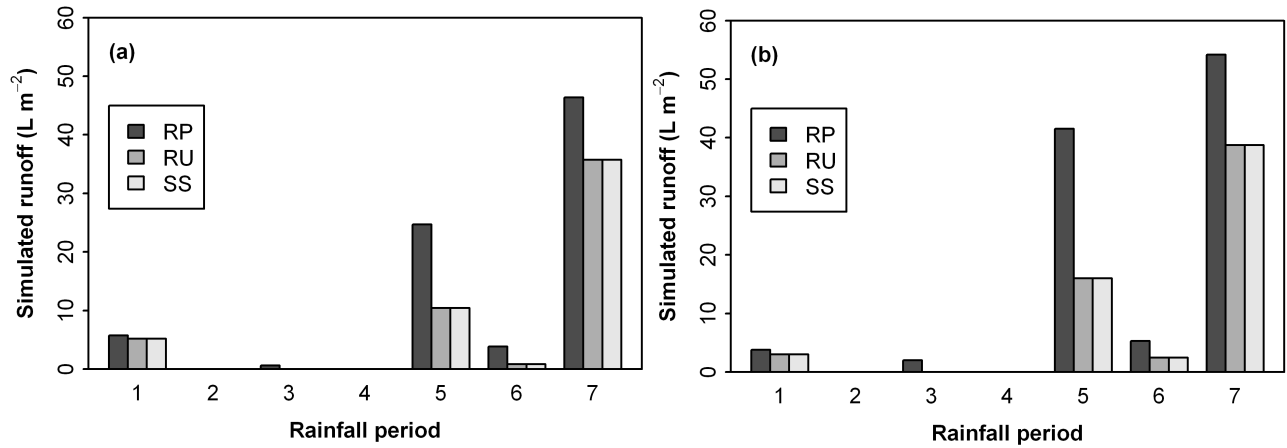


Figure 4.6: Simulated runoff for all rainfall periods for field 1 (a) and field 2 (b) for different management practices (RP: ridges with plastic cover, RU: uncovered ridges, SS: smooth soil surface).

crowns are developed. For the time between field preparation and maturity and after senescence, when most of the aboveground biomass is dead, the stem flow effect is negligible. Therefore, we believe that the model assumptions are reasonable for evaluating the principle effects of plastic mulch on runoff and erosion over the season.

The highest soil loss was simulated for ridges with plastic cover (RP) at both fields caused by the higher rate of surface runoff compared to RU, but for SS we found contrary effects between the fields (Figure 4.7). The total soil loss simulated for RP for field 1 and field 2 over all seven rainfall periods was 4178.1 kg ha⁻¹ and 545.8 kg ha⁻¹, respectively. Total soil loss was reduced to 2469.9 kg ha⁻¹ (41%) on field 1 and 371.7 kg ha⁻¹ (32%) on field 2 by removal of plastic from the ridges (RU). The highest reduction was predicted for both fields for period 6 with 79% on field 1 and 82% on field 2. The lowest soil loss reduction was simulated for field 1 for period 1 (30%) and field 2 for period 7 (25%). For smooth soil surface conditions (SS), the model predicted an additional soil loss reduction for field 1 to 1017.3 kg ha⁻¹ (76% reduction compared to RP), but for field 2 an increase in soil loss compared to RU to 467.5 kg ha⁻¹, which is only 14% reduction compared to RP. Soil loss reduction by SS on field 1 and the soil loss increase on field 2 compared to RU was predicted for all periods. The highest soil loss reduction for SS occurred during period 6 at both fields with 89% reduction compared to RP on field 1 and 42% reduction compared to RP on field 2. The lowest soil loss reduction for field 1 was period 1 (72% compared to RP) and for field 2 period 5 (9% compared to RP). Correlation between measured rainfall characteristics and the effects of the three management practices as described for surface runoff and rainfall intensity were not detected.

Due to field topography and ridge orientation, both fields show totally different flow char-

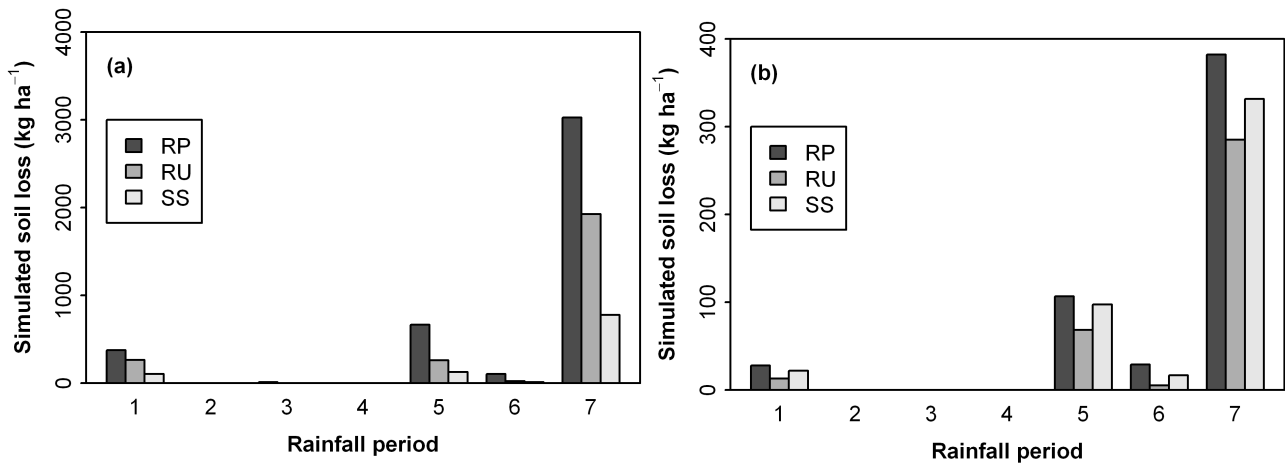


Figure 4.7: Simulated soil loss for all rainfall periods for field 1 (a) and field 2 (b) for different management practices (RP: ridges with plastic cover, RU: uncovered ridges, SS: smooth soil surface).

acteristics, which caused the differences in soil loss for RP, RU and SS. Figure 4.8 shows the flow patterns and spatial distribution of the simulated sediment concentrations. The magnitude of increase in sediment concentration represents the amount of erosion at a particular location. Runoff flow direction (indicated by the arrows) for RP and RU is primarily controlled by the ridges. Therefore water is routed in the furrows parallel to ridges instead of moving along the steepest flow paths. The spatial patterns of erosion for RP and RU are basically the same. With increasing flow length sediment concentration becomes higher. The reason is the increasing runoff rate, which provides higher erosive energy in the furrows (Wolfe et al., 2002). The RU scenario shows slightly higher sediment concentration than RP because of additional soil erosion from the uncovered ridges. The total sediment mass transported from the field sites was higher for RP because of higher amounts of runoff. Water is flowing along the furrows until it reaches the field's edge or a topographical depression. On field 1, runoff is trapped and accumulating in such depressions due to the field concavity and routed across the ridges. As a consequence, lines of concentrated flow are formed perpendicular to the ridge orientation, especially in the field's center and on the bottom (Figure 4.8). For those concentrated flow lines, the model predicted much higher soil erosion rates than for the surrounding areas. During our field measurements, we observed ridge breakovers with a deep erosion rill formed by concentrated flow in the center of field 1 (Figure 4.9). The plastic film was washed out and ridges were destroyed by water flow, forming a permanent channel partially deeper than 10 cm. On field 2, such concentrated flow lines were not formed because of its convex shape. Water was routed along the furrows and leaving the field at its edge without accumulation. Row lengths are relatively high especially at the field bottom, which results in higher erosion rates at the lower parts of the furrows.

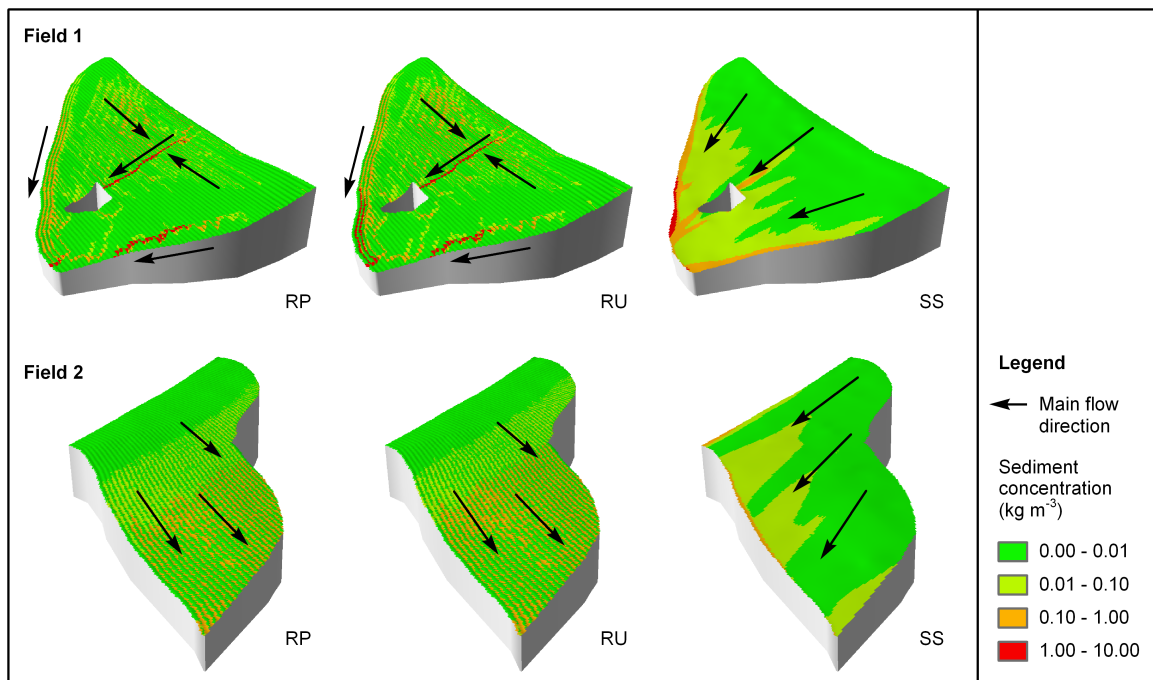


Figure 4.8: Simulated sediment concentration over all rainfall periods for field 1 and field 2 for different management practices including main % flow directions (RP: ridges with plastic cover, RU: uncovered ridges, SS: smooth soil surface).

Nevertheless, the predicted sediment concentration at those locations remained lower than for the concentrated flow lines on field 1. Management without ridges (SS) produced entirely different runoff flow patterns and erosion rates. For the SS scenario, water was routed directly along the steepest flow paths and solely controlled by field topography. Runoff was more evenly distributed over the surface without high flow concentration. For field 1, part of the runoff was still accumulating in the field's center and at the edges, although with less erosive power than predicted for RP and RU, as indicated by lower sediment concentrations for SS throughout the field. The absence of ridges on field 2 resulted in routing along a steeper slope and flow accumulation at field's edges where higher erosion was predicted.

These results demonstrate that the effect of the ridge-furrow system on erosion is controlled primarily by the topography of the fields. Because of its concave shape, field 1 generated a 140% higher erosion for the ridge-furrow system compared to a smooth surface due to ridge breakovers, as previously described (Wischmeier and Smith, 1978; Stocking, 1972; S. A. El-Swaify et al., 1982; Hagmann, 1996). The ridge-furrow system on the convex field 2 separated runoff and constrained flow to the furrows, which prevented flow accumulation and resulted in 20% lower soil erosion rates.



Figure 4.9: Observed erosion rill formed by ridge breakovers and concentrated flow in the depression line in the center of field 1.

4.4 Summary and Conclusions

In this study, we analyzed the effect of plastic covered ridge-furrow systems on runoff and erosion in combination with the complex field topography of a mountainous landscape in South Korea. We installed runoff collectors on two field sites managed with plastic mulch and measured runoff and sediment loss during monsoonal rain events in 2010. The measured differences in soil loss between both fields suggested that soil erosion may be primarily affected by the field's topography and the orientation of the ridge-furrow system. We used observed field data to calibrate the EROSION 3D model and subsequently applied the model to investigate runoff and erosion for an uncovered ridge-furrow system and a smooth soil surface on the same fields. Model performance statistics demonstrate that EROSION 3D can be applied successfully on high spatial resolutions when calibrated to available measured data.

The model results for different management practices showed much higher surface runoff produced by plastic film covers. The percent difference between plastic mulch and uncovered management was strongly influenced by the average intensities of the rain events. Simulated soil loss was also highest on both fields for plastic mulch ridges as a result of higher runoff rate produced by the impermeable plastic film. The effect of the plastic film on surface runoff may be slightly overestimated for the rainfall periods throughout this study, because stem flow effects on the infiltration rate were not considered. However, for evaluating the principle effects of plastic mulch on runoff and erosion, we believe that the model assumptions were reasonable. Nevertheless, additional research is necessary in order to identify the effect of interception and stem flow on the infiltration rate in plastic mulch systems for different crops during the growing season.

The effect of the ridge-furrow system on soil erosion compared to the smooth soil surface was very different between fields. The ridge-furrow system increases soil erosion of field 1, however, it potentially prevents erosion on field 2 when not covered with plastic film. The predicted flow patterns and spatial distribution of sediment concentration demonstrated that the effect is primarily controlled by the field topography. Because of the concave shape of field 1, ridges lead to flow accumulation causing breakovers and concentrated flow with high erosive power and resulting in higher total erosion from the field. Although ridges on convex field 2 prevent runoff routing along the steepest slope and accumulation at the edges, which resulted in reduced total erosion from the field. These results show that ridge-furrow systems can increase soil erosion dramatically on one field, but have contrary effects on another field, simply depending on the topography.

Our results have practical consequences for planning and implementation of best management practices for watersheds. Especially in mountainous areas, where the topography within and between fields can be strongly variable, ridge-furrow cultivation should be performed carefully. The ridge-furrow system should be preferable located parallel with the contours, or oriented towards the edges in order to drain runoff away from depressions and to prevent concentrated flow within fields. To prevent flow accumulation and high erosion rates at the field edges, also the transition zones between the field and the surrounding margins have to be considered. Our results show that in any case the furrows between the ridges need to be better protected against soil erosion. Conventional herbicide applications eliminate the development of a plant cover in the furrows. Even though the vegetative cover of adult crops can protect soil from raindrop impact, the furrows remain susceptible to erosion by overland flow during the entire growing season. In order to reduce soil erosion on crop fields in South Korea we recommend organic farming practices without herbicide application, which supports the development of weeds in the furrows. Another effective erosion control measure can be cereal grass cultivation in the furrows as suggested by Rice, Harman-Fetcho, et al. (2007). Vegetative-covered furrows are functioning as "in-field buffers", which can increase infiltration capacity and reduce runoff flow velocity due to higher surface roughness (Rice, Harman-Fetcho, et al., 2007). Reducing the runoff flow rate along the furrows could also help to prevent the severe damages caused by ridge breakovers. Another important issue is the application of large-scale erosion models to those areas dominated by ridge-furrow cultivation. Erosion prediction on watershed-scale is usually conducted on the basis of relatively coarse digital elevation models and often do not account for special tillage and cropping systems and their orientation. The models can strongly over- and underestimate soil erosion rates especially for complex landscapes and should be corrected for ridge-furrow systems. However, this study analyzed only two field sites with a specific topography and ridge orientation. In order to identify general patterns, which can be used for large-scale model applications, additional research studies are necessary to account for a variety of different field topographies and ridge-furrow systems.

Acknowledgements

This study was carried out within the framework of the International Research Training Group TERRECO, funded by the German Research Foundation (DFG) and the Korea Science and Engineering Foundation (KOSEF). The authors thank Andreas Kolb, Steve Lindner and Bongjae Kwon for their technical support during the field installations.

References

- Avnimelech, Y., G. Ritvo, L. Meijer, and M. Kochba (2001). “Water content, organic carbon and dry bulk density in flooded sediments”. In: *Aquacultural Engineering* 25, pp. 25–33. ISSN: 0144-8609. DOI: 10.1016/S0144-8609(01)00068-1.
- Bonilla, C. A., D. Kroll, J. Norman, D. Yoder, C. Molling, P. S. Miller, J. C. Panuska, J. B. Topel, P. L. Wakeman, and K. G. Karthikeyan (2006). “Instrumentation for measuring runoff, sediment, and chemical losses from agricultural fields”. In: *Journal of Environmental Quality* 35, pp. 216–223.
- Campbell, G. (1985). *Soil Physics with BASIC. Transport models for soil-plant systems*. Amsterdam, The Netherlands.
- Chanson, H. (2004). *The hydraulics of open channel flow. An Introduction*. 2nd ed. Oxford, Great Britain: Elsevier Butterworth Heinemann.
- Chow, V. T. (1959). *Open-channel hydraulics*. New York, USA: McGraw-Hill.
- Dilara, P. A. and D. Briassoulis (2000). “Degradation and stabilization of low-density polyethylene films used as greenhouse covering materials”. In: *Journal of Agricultural Engineering Research* 76.4, pp. 309–321. ISSN: 0021-8634. DOI: 10.1006/jaer.1999.0513.
- Engman, E. (1986). “Roughness coefficients for routing surface runoff”. In: *Journal of Irrigation and Drainage Engineering* 112.1, pp. 39–53.
- Espí, E., A. Salmeron, A. Fontecha, Y. Garcia, and A. I. Real (2006). “Plastic films for agricultural applications”. In: *Journal of Plastic Film & Sheeting* 22.2, pp. 85–102. ISSN: 8756-0879. DOI: 10.1177/8756087906064220.
- Gascuel-Oudou, C., F. Garnier, and D. Heddadj (2001). “Influence of cultural practices on sheet-flow, sediment and pesticide transport: the case of a corn cultivation under plastic mulching”. In: *Sustaining the global farm. Selected papers from the 10th International Soil Conservation Organization Meeting*. Ed. by D. Stott, R. Mohtar, and G. Steinhardt. International Soil Conservation Organization, pp. 300–304.
- Gupta, H. V., S. Sorooshian, and P. O. Yapo (1999). “Status of automatic calibration for hydrological models: Comparison with multilevel expert calibration”. In: *Journal of Hydrologic Engineering* 4.2, pp. 135–143. ISSN: 1084-0699. DOI: 10.1061/(ASCE)1084-0699(1999)4:2(135).
- Hagmann, J. (1996). “Mechanical soil conservation with contour ridges: Cure for, or cause of, rill erosion?” In: *Land Degradation & Development* 7.2, pp. 145–160. ISSN: 1085-3278. DOI: 10.1002/(SICI)1099-145X(199606)7:2<145::AID-LDR224>3.0.CO;2-Z.

- Huggins, L. and E. Monke (1966). *The mathematical simulation of the hydrology of small watersheds*. Tech. rep. 1. West Lafayette, USA: Water Resources Research Center, Purdue University.
- Jefferies, R. and D. MacKerron (1985). “Stemflow in potato crops”. In: *Journal of Agricultural Science* 105, pp. 205–207.
- Kim, B., K. Choi, C. Kim, U. H. Lee, and Y. H. Kim (2000). “Effects of the summer monsoon on the distribution and loading of organic carbon in a deep reservoir, Lake Soyang, Korea”. In: *Water Research* 34.14, pp. 3495–3504. ISSN: 0043-1354. DOI: 10.1016/S0043-1354(00)00104-4.
- Kim, S., J. Yang, C. Park, Y. Jung, and B. Cho (2007). “Effects of winter cover crop of ryegrass (*Lolium multiflorum*) and soil conservation practices on soil erosion and quality in teh sloping uplands”. In: *Journal of the Korean Society for Applied Biological Chemistry* 55.1, pp. 22–28.
- Lament, W. J. (1993). “Plastic mulches for the production of vegetable crops”. In: *HortTechnology* 3.1, pp. 35–39.
- Lee, G. J., J. T. Lee, J. S. Ryu, S. W. Hwang, Y. S. Yang, J. H. Joo, and Y. S. Jung (2010a). “Loss of soil and nutrient from different soil managements in highland agriculture”. In: *Proc. 19th World Congress of Soil Science. Soil solution for a changing world*. Ed. by R. Gilkes and Prakongkep. International Union of Soil Sciences, pp. 78–81.
- (2010b). “Status and Soil management problems of highland agriculture of the main mountainous region in the South Korea”. In: *Proc. 19th World Congress of Soil Science. Soil solution for a changing world*. Ed. by R. Gilkes and Prakongkep. International Union of Soil Sciences, pp. 154–157.
- Leistra, M. and J. J. T. I. Boesten (2010). “Pesticide Leaching from Agricultural Fields with Ridges and Furrows”. In: *Water Air and Soil Pollution* 213.1-4, pp. 341–352. ISSN: 0049-6979. DOI: 10.1007/s11270-010-0389-x.
- Michael, A., J. Schmidt, and W. Schmidt (1996). *EROSION 2D/3D: A computer model for the simulation of soil erosion by water. Parameter catalog application (2D)*. Freiberg, Germany.
- Montes, S. (1998). *Hydraulics of open channel flow*. Reston, USA: ASCE Press.
- Moriasi, D. N., J. G. Arnold, M. W. van Liew, R. L. Bingner, R. D. Harmel, and T. L. Veith (2007). “Model evaluation guidelines for systematic quantification of accuracy in watershed simulations”. In: *Transactions of the ASABE* 50.3, pp. 885–900. ISSN: 0001-2351.
- Park, J.-H., L. Duan, B. Kim, M. J. Mitchell, and H. Shibata (2010). “Potential effects of climate change and variability on watershed biogeochemical processes and water quality in Northeast Asia”. In: *Environment International* 36.2, pp. 212–225. ISSN: 01604120.

- Park, Y. S., J. Kim, N. W. Kim, S. J. Kim, J.-H. Jeon, B. A. Engel, W. Jang, and K. J. Lim (2010). “Development of new R, C and SDR modules for the SATEEC GIS system”. In: *Computers & Geosciences* 36.6, pp. 726–734. ISSN: 0098-3004. DOI: 10.1016/j.cageo.2009.11.005.
- Pinson, W., D. Yoder, J. Buchanan, W. Wright, and J. Wilkerson (2004). “Design and evaluation of an improved flow divider for sampling runoff plots”. In: *Applied Engineering in Agriculture* 20.4, pp. 433–438.
- Renard, K. G., G. R. Foster, G. A. Weesies, D. K. McCool, and D. C. Yoder (1997). *Predicting soil erosion by water. A guide to conservation planning with the Revised Universal Soil Loss Equation (RUSLE)*. Washington D.C. , USA.
- Rice, P., J. A. Harman-Fetcho, A. M. Sadeghi, L. L. McConnell, C. B. Coffman, J. R. Teasdale, A. Abdul-Baki, J. L. Starr, G. McCarty, R. R. Herbert, and C. J. Hapeman (2007). “Reducing insecticide and fungicide loads in runoff from plastic mulch with vegetative-covered furrows”. In: *Journal of Agricultural and Food Chemistry* 55.4, pp. 1377–1384. ISSN: 0021-8561. DOI: 10.1021/jf062107x.
- Rice, P., L. L. McConnell, L. Heighton, A. M. Sadeghi, A. Isensee, J. R. Teasdale, A. Abdul-Baki, J. Harman-Fetscho, and C. J. Hapeman (2001). “Runoff loss of pesticides and soil: a comparison between vegetative mulch and plastic mulch in vegetable production systems”. In: *Journal of Environmental Quality* 30, pp. 1808–1821.
- Roo, A. P. J. de, C. G. Wesseling, and C. J. Ritsema (1996). “LISEM: A single-event physically based hydrological and soil erosion model for drainage basins. I: Theory, Input and Output”. In: *Hydrological Processes* 10.8, pp. 1107–1117. ISSN: 1099-1085. DOI: 10.1002/(SICI)1099-1085(199608)10:8<1107::AID-HYP415>3.0.CO;2-4.
- Saffigna, P., C. Tanner, and D. Keeney (1976). “Non-uniform infiltration under potato canopies caused by interception, stemflow, and hilling”. In: *Agronomy Journal* 68, pp. 337–342.
- Schmidt, J. (1991). *A mathematical model to simulate rainfall erosion: in: Erosion, transport and deposition processes. Theories and models*. Cremlingen, Germany.
- Schmidt, J., M. von Werner, and A. Michael (1999). “Application of the EROSION 3D model to the CATSOP watershed, The Netherlands”. In: *Catena* 37.3–4, pp. 449–456. ISSN: 0341-8162. DOI: 10.1016/S0341-8162(99)00032-6.
- Šimůnek, J., M. Šejna, and M. Van Genuchten (2011). *The Hydrus software package for simulating two- and three-dimensional movement of water, heat, and multiple solutes in a variably-saturated media: Technical Manual*. 2.0. Prague and Czech Republic.

- Stevens, M., B. Black, J. Lea-Cox, A. M. Sadeghi, J. Harman-Fetscho, E. Pfeil, P. Downey, R. Rowland, and C. J. Hapeman (2009). "A comparison of three cold-climate strawberry production systems: environmental effects". In: *HortScience* 44.2, pp. 298–305.
- Stocking, M. (1972). "Aspects of the role of man in Rhodesia". In: *Zambezia* 2.2, pp. 1–10.
- El-Swaify, S. A., E. W. Danglar, and C. L. Armstrong (1982). *Soil Erosion by Water in the Tropics*. Honolulu, USA: College of Tropical Agriculture and Human Resources, University Hawaii.
- Vieux, B. (2001). *Distributed hydrological modeling using GIS*. Dordrecht, The Netherlands: Kluwer Academic Publisher.
- von Werner, M. (1995). "GIS-orientierte Methoden der digitalen Reliefanalyse zur Modellierung von Bodenerosion in kleinen Einzugsgebieten". PhD thesis. Berlin, Germany: Free University of Berlin, Department of Earth Science.
- Wan, Y. and S. El-Swaify (1999). "Runoff and soil erosion as affected by plastic mulch in a Hawaiian pineapple field". In: *Soil & Tillage Research* 52.1-2, pp. 29–35.
- Wickenkamp, V., R. Duttmann, and T. Mosimann (2000). *A multiscale approach to predicting soil erosion on cropland using empirical and physically based soil erosion models in a geographic information system: in: Soil erosion. Application of physically based models*. Berlin: Springer, pp. 109–134.
- Wischmeier, W. H. and D. D. Smith (1978). *Predicting rainfall erosion losses. A guide to conservation planning: Agricultural Handbook 537*. Washington D.C., USA.
- Wolfe, M. L., B. B. Ross, J. F. Diem, T. A. Dillaha, and K. A. Flahive (2002). *Protecting water quality: best management practices for row corn crops grown on plastic mulch in Virginia*. Blacksburg, USA.

Chapter 5

Fate of fertilizer ^{15}N in intensive ridge cultivation with plastic mulching under a monsoon climate

Janine Kettering^{1,a}, Marianne Ruidisch^b, Camila Gaviria^b, Yong Sik Ok^c, Yakov Kuzyakov^{a,d}

^a Department of Agroecosystem Research, University of Bayreuth, 95440 Bayreuth, Germany

^b Soil Physics Group, BayCEER, University of Bayreuth, 95440 Bayreuth, Germany

^c Department of Biological Environment, Kangwon National University, Chuncheon 200-701, Korea

^d Department Soil Science of Temperate Ecosystems, University of Göttingen, 37077 Göttingen, Germany

Abstract

Reduction of nitrogen (N) leaching to groundwater requires an improved understanding of the effect of microtopography on N fate. Because of the heterogeneity among positions, ridge tilled fields, frequently used in intensive agriculture, should be treated as two distinct management units. In this study, we identified N dynamics for plastic-mulched ridges and bare furrows with the goal of developing more sustainable agricultural practices with optimal gains, namely crop production versus

¹Correspondence to: Janine Kettering, Department of Agroecosystem Research, BayCEER, University of Bayreuth, 95440 Bayreuth, Germany.
E-mail: janine.kettering@uni-bayreuth.de

limited impacts on water quality. We investigated: (1) biomass production; (2) crop N uptake; (3) N retention in soil; and (4) N leaching using ^{15}N fertilizer in a radish cultivation. Broadcast mineral N fertilizer application prior to planting resulted in high total leaching losses (up to 390 N kg ha^{-1}). The application of plastic mulch in combination with local fertilizer management did not help to reduce N leaching. At all fertilizer N rates, the mean nitrate concentrations in seepage water were found to be above the WHO drinking water standard of $50 \text{ mg NO}_3^- \text{ l}^{-1}$. To reduce nitrate leaching, we recommend: 1) decreasing the fertilizer N rates to a maximum of 150 kg N ha^{-1} ; 2) applying fertilizer N in 3 to 4 split applications according to the plant's N needs; 3) applying fertilizer N to the ridges (after their formation) to avoid losses from the furrows; and 4) increasing the soil organic matter content to enhance the water and nutrient retention by covering the furrows with plant residues, i.e., rice straw or soil additives.

Keywords: N leaching ; N retention ; sandy soil ; N use efficiency ; stable isotope ; suction lysimeter

5.1 Introduction

N leaching from agricultural fields is considered a major source of water pollution (Buczko et al., 2010; Zotarelli et al., 2007) and considerable levels can be reached, especially in intensively cultivated areas with high precipitation and coarse-textured soils. N leaching depends on the amount of water percolating through the soil and the N concentration in the seepage water (Sieling and Kage, 2006), which is strongly influenced by local factors such as climate (arid < humid), soil type (fine-textured soil < coarse-textured soil), and land use system (natural system < agricultural system) (Boumans et al., 2005; Di and Cameron, 2002). N leaching is difficult to control because it is often derived from large areas of land and losses mostly occur intermittently with rainfall events (Barton and Colmer, 2004). Another factor that complicates the measurement and the interpretation of N leaching, however, is the soil structure, which might induce preferential flow. This uneven and often fast flow of water and solutes through the soil causes that a small fraction of the media participates in most of the flow, allowing much faster transport of nutrients. N leaching processes have been measured using different methods in various crop systems and pastures that had a relatively homogenous spatial distribution of water and N (Di and Cameron, 2002; Nyamangara et al., 2003; Zotarelli et al., 2007).

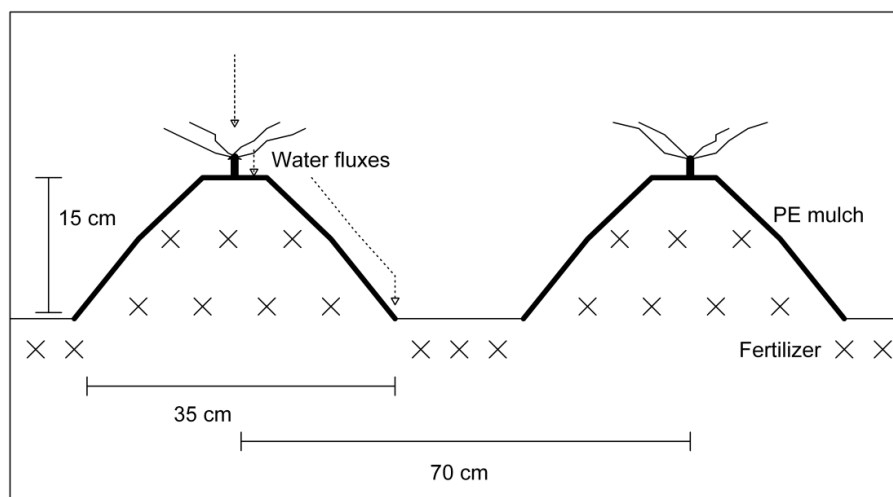


Figure 5.1: Scheme of a typical ridge cultivation system with plastic mulching in a temperate South Korean area with summer monsoon. Shown are the water fluxes and the distribution of fertilizer N in the system.

Polyethylene (PE) mulch has been used to cover soil surfaces in South Korea for ridge cultivation of vegetable crops (Figure 5.1). When this method is practiced, the ridges are covered with a plastic film, but the furrows are left uncovered which should diminish N leaching (Henriksen et al., 2006; Islam et al., 1994; Romić et al., 2003). However, the soil surface microtopography associated with this practice involves a non-uniform distribution of water and N. Previous studies focused on comparing total N leaching amounts between flat tillage, ridge cultivation, and/or ridge cultivation with plastic mulching (Drury et al., 1993; Romić et al., 2003; Vázquez et al., 2005). The potential differences in N fate between plastic-mulched ridges and bare furrows in dryland agriculture have not been extensively evaluated. Many processes, such as water flow and solute transport, are different in the ridge and furrow zones. Additionally, such a microrelief might even increase the total leaching as both sites are interrelated, and the water volume in furrows increases in the presence of ridges (Leistra and J. Boesten, 2008). The PE mulch protects the ridges from direct infiltration, and hence, the fertilizer N beneath the ridge is protected against percolation with seepage water. It consequently intensifies percolation in the furrows (Bargar et al., 1999; Henriksen et al., 2006; Islam et al., 1994), which in turn can lead to water ponding on the furrow surface after heavy rainfall. However, due to the lower fertilizer N concentrations in the furrows, the total amount of N leaching is assumed to decrease. Consequently, N retention in ridge soil and N uptake by plants is expected to increase.

In the mountainous highlands of Gangwon Province in South Korea, the agricultural systems have shifted over the last 40 years towards intensive management that depends heavily on high

mineral N fertilizer inputs. Recommendations for highland summer radishes provided by the Rural Development Administration of South Korea (RDA) amounted to 252 kg N ha⁻¹ (RDA, 2006), while local farmers have adopted N application rates of up to 400 kg N ha⁻¹.

Due to the high soil erosion loss from mountainous cropland areas, local farmers use a management practice of frequently adding sandy soil to the top layer of agricultural fields to compensate for soil loss. Excessive N fertilization and the predominantly sandy soils, together with heavy summer monsoon rainfalls, result in high N losses, which lead to surface and groundwater pollution in many of the thousands of small agricultural watersheds in South Korea. Our study site, Haeon Catchment, is a subcatchment of the Lake Soyang watershed, which is a major drinking water reservoir in South Korea and is known as a hot spot of agricultural non-point pollution (Jung et al., 2009; Kim et al., 2006). It is a typical basin with representative characteristics of South Korean agricultural areas such as the following: (1) high N inputs exceeding crop demands; (2) cultivation on sandy soils; (3) dependence on monsoon rainfall; (4) a high percentage of vegetable production; and (5) specific management practices such as ridge cultivation with black PE mulch.

The purpose of this study was to identify the N dynamics for plastic-mulched ridges and bare furrows with the goal of developing more sustainable agricultural practices to reduce non-point pollution of water resources. Using ¹⁵N, we investigated the budget of fertilizer N, including the following: (1) the N uptake by crops; (2) the N retention in soil; and (3) the N downward movement with percolation in a radish (*Raphanus sativus L.*) system under conventional local management. ¹⁵N isotopes are an invaluable tool to trace the fate of fertilizer N in soil/plant systems (Xu et al., 2008) because ¹⁵N undergoes the same chemical and microbial transformations as ¹⁴N in the soil. Hence, analysis of the ¹⁵N content in plant parts and soil was evaluated at selected times during the growing season, and ¹⁵N content was used as a measure of the actual ¹⁵N recovery and ¹⁵N loss derived from the fertilizer (Buresh et al., 1982; Vlek and Byrnes, 1986). To evaluate the effect of plastic mulched ridges on N leaching, a two-dimensional process-based modeling study was carried out using the numerical model Hydrus 2/3D. To assess productivity implications versus environmental impacts of N fertilizer use, namely impacts on water quality, N dynamics were examined at fertilizer N application rates from 50 to 350 kg N ha⁻¹ on top of the basal fertilization rate of 56 kg N ha⁻¹. Because N leaching was absent during the dry and cold winter, we conducted the field and the modeling study only during the growing season.

Table 5.1: Physical properties of soils at the experimental field site in the Haeon Catchment in 2010. Shown is the sand, silt, and clay content of the soil in %. The texture of the soil taken from the World Reference Base from the IUSS Working Group (2007). The standard error of the mean is given in the parentheses.

Soil depth cm	Sand %	Silt %	Clay %	Texture	Bulk density g cm ⁻³
0-20	81 (± 0.8)	16 (± 0.7)	3.0 (± 0.2)	Loamy sand	1.22(± 0.07)
20-40	77 (± 1.5)	19 (± 1.2)	3.6 (± 0.3)	Loamy sand	1.43(± 0.06)
40-60	73 (± 1.5)	22 (± 1.2)	4.4 (± 0.4)	Sandy loam	1.27(± 0.01)

5.2 Materials and methods

5.2.1 Study site

The field experiment was conducted on a typical Korean terric cambisol or even anthrosol (WRB, 2007) (Table 5.1) because of the artificial long-term addition of sandy soil on the top of the fields at the Punchball Tongil Agricultural Experimental Farm (38.3°N, 128.14°E, 420 masl) in the Haeon-myun Catchment in Yanggu County, Gangwon Province, South Korea. The experiment went from June 1 to August 28, 2012.

The study area falls within the East-Asian monsoon climate and has an 11-year (1999-2009) average annual air temperature of 8.5°C and an annual precipitation of approximately 1577 mm, with 70% of the precipitation occurring as heavy rainfall between June and August (Figure 5.2). In recent decades, a shortening of the monsoon season, as well as an increase in the amount of precipitation, and the number of heavy rainfall days, was observed (Chung et al., 2004). However, the months of June and July in 2010 had precipitation amounts of only 67 mm and 216 mm, respectively, which were exceptionally low compared to the 11-year averages. Very dry periods, each with less than 20 mm precipitation in total, were observed from June 14 to July 1, July 6 to July 15, and from July 19 to August 1. In contrast, the months of August and September were extremely wet, with precipitation amounts of 458 mm and 415 mm, respectively. The heaviest rainfall during the experiment was 150 mm in the three days from August 13 to 16. Although no runoff was observed throughout the experimental period, water sometimes ponded on the furrow surface after a heavy rainfall. However, rainfall events in the experiment period (2010) were comparatively small, with a maximum daily precipitation of less than 70 mm. For March, April and May, the temperature was colder than the 11-year mean. This led to a delay in the start of cropping by approximately two to four weeks.

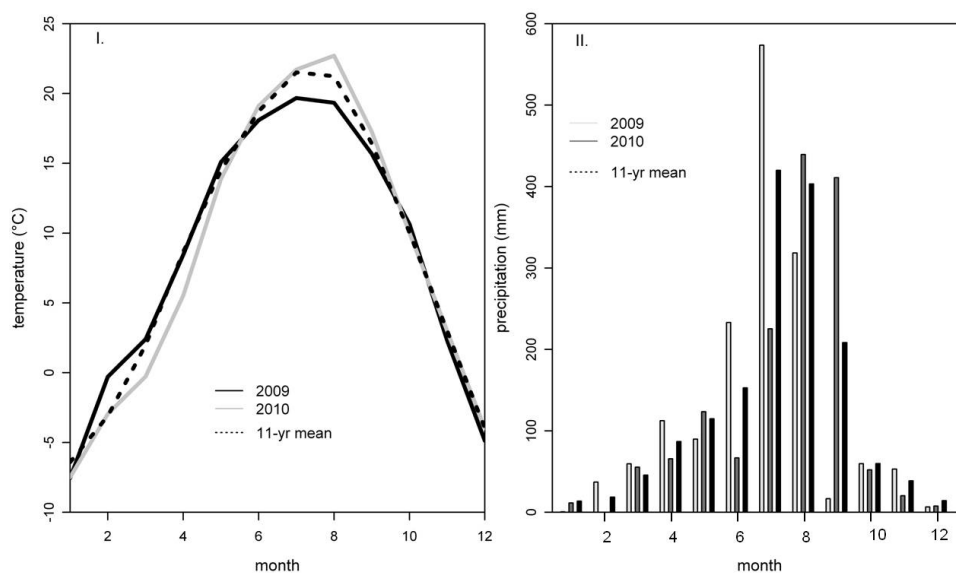


Figure 5.2: Mean daily temperature ($^{\circ}\text{C}$), II. Mean total precipitation amount (mm) for the years 2009 and 2010 as well as the 11-year mean (1999-2009) of the Haeon Catchment. Daily precipitation amounts and temperature data have been monitored with an automatic weather station (WS-GP1, Delta-T Devices, Cambridge, UK).

5.2.2 Experimental design

Before the experiment started, commonly used fertilizer (30% mineral NPK fertilizer with 4.2-2-2, 70% organic fertilizer with C/N ratio 50:1, SamboUbi, South Korea) was applied as granules at the rate of $56 \text{ kg NO}_3^- \text{ ha}^{-1}$ on May 31, 2010, and mixed in the top 0.15 m of the soil to enhance soil fertility of the previously fallow field. On June 1, NO_3^- was applied as a one-time top dressing (mineral NPK fertilizer 11-8-9 +3MgO+0.3B, KG Chemicals, South Korea) at four fertilizer N rates: N50, N150, N250, and N350, reflecting the application of 50, 150, 250, and $350 \text{ kg NO}_3^- \text{ ha}^{-1}$. The N250 treatment satisfied the recommendations for highland radishes provided by the RDA (RDA, 2006). Each treatment was applied to a plot (7x7 m) and replicated three times at the field site. A randomized block design was used for the experimental layout. On June 9, the top 0.2 m of the soil was ploughed, and the ridge system (35 cm width and 10-15 cm height) was implemented with a distance of 70 cm between the rows. The ^{15}N labeling experiment was performed in microplots (125x75 cm), each containing one bare furrow and one ridge with six labeled radish plants. Each plot included three microplots, one for each sampling day (day 25, 50, and 75). $\text{K}^{15}\text{NO}_3^-$ (10 at%) was applied as a tracer to the microplots on June 10. After application of the tracer, the ridges were covered with impervious black PE mulch on June 11. Finally, radishes were sowed on the top ridges on June 14 at a plant density of 25 cm (Hungnong Seeds, South Korea). June 14, the day of the planting, is therefore set as day 0 of the experiment. Weeding during the experiment was performed manually without the application

of herbicides. The plots were harvested after 75 days of growth on August 28.

5.2.3 Study of soil water dynamics

To estimate N loss in seepage water, suction lysimeters combined with a soil hydrological monitoring network of standard tensiometers were installed. The suction lysimeters consisted of a ceramic cup, a PVC tube, and a PE suction tube. The latter was connected to samplers (brown glass bottles), which were connected through a network of high-density tubing to a vacuum pump (KNF Neuberger, Type N86KNDCB 12v, Freiburg i.Br., Germany). In each microplot, two suction lysimeters were placed in the ridge (15 cm and 45 cm from the top of the ridge), and one was placed in the furrow (45 cm from the top of the ridge). The suction lysimeters were installed by following the recommendations of DGFZ and HLUG (2004) and UMS GmbH (2008). Quantifying N losses with downward percolation is highly challenging due to uncertainties associated with estimating drainage fluxes and solute concentrations in the seepage (Van der Laan et al., 2010). Suction lysimeters can be used to determine the nitrate concentrations in seepage but provide no information on water fluxes. Hence, a process-based numerical model was used for the inverse simulation of water flow and the estimation of N leaching (Hydrus 2/3D, (Simunek, 2006)). The ability of representing physical processes such as subsurface water flow in variable saturated media is an advantage of process-based numerical models. Uniform flow processes in a variably saturated porous media without preferential flow pathways can be described using the extended Richards' equation based on the Galerkin linear finite element method. The extended Richards' equation for water flow incorporates a sink term, which considers the root water uptake. We used the data defined for sugar beet from the Hydrus 2/3D data base because radish data was not available. Surface boundary conditions were set to atmospheric conditions in furrows and planting holes, whereas plastic mulched areas were set to no flux conditions. Soil evaporation and crop transpiration were calculated with the FAO-56 dual crop coefficient approach using weather parameters such as solar radiation, air temperature, wind speed, humidity and air pressure, which were measured by the weather station at the experiment site. The amount of precipitation was multiplied by 2 to include the surface runoff from the plastic mulched ridges to the furrows (Dusek et al., 2010). The Van Genuchten parameters, the saturated and the residual water content θ_s , θ_r , α and n , and the saturated hydraulic conductivity (K_{sat}) were initially estimated based on texture and bulk density using the Rosetta lite DLL module, which is implemented in Hydrus 2/3D. The optimization of the Van Genuchten parameters was performed based on the Levenberg-Marquardt algorithm using

the measured pressure head values in the field, which is a parameter estimation technique for inverse estimation of selected soil hydraulic and/or solute transport and reaction parameters from measured data.

Hydrus 2/3D numerically solves Fickian-based advection-dispersion equations for solute transport in variably saturated porous media using the Galerkin linear finite element method. To solve the advection-dispersion equations, water content and volumetric flow need to be defined. Therefore, Hydrus 2/3D first solves the Richards' equation and subsequently simulates the solute transport. To adjust the simulation of the solute transport to the measured nitrate concentrations in the seepage water, the solute reaction parameters longitudinal dispersion D_L and denitrification rate k were inverse optimized. Because Hydrus 2/3D is not able to invers simulate several solutes at the same time, the simulation was kept fairly simple and was carried out only for nitrate. Other N forms were therefore not included in the simulation. N uptake by crops takes place passively in the simulation and is linked to the water uptake by crops. The nitrate concentration at the start of the simulation was calculated from the N application rates N50, N150, N250, and N350 and defined up to the soil depth of 24 cm. For the solute transport simulation, we assumed that a) all applied fertilizer N was applied as nitrate, b) N mineralization, N fixation, and atmospheric N deposition during the 75 days of growth were negligible, and c) the N fertilizer granules were directly dissolved in the soil water all at once. Denitrification, however, was included in the simulation because the soil in a depth of 50 cm and deeper was often saturated and anaerobic conditions were assumed. Denitrification was the only unmeasured sink term for nitrate in soil and was simulated invers as a first order kinetic process. The simulation of the water flow as well as of the solute transport was carried out for one of the three replicates of each N application rate.

The simulation of the water flow was carried out for 74 days and started at the time of planting at June 14, 2010 (day 0). The simulation of the nitrate transport, however, was carried out for 78 days and started at June 10, 2010. Different statistical techniques such as Pearson's correlation coefficient (R), coefficient of determination (R^2) and Nash-Sutcliffe efficiency (NSE) were used to evaluate the models. The water flow models achieved a good agreement between measured and simulated pressure heads (Table 5.2). To examine the influence of differing Van Genuchten parameters or differing saturated hydraulic conductivities on the amount of percolated water, we tested the simulations with two methods (Monte Carlo simulation with random combinations of the parameters and gradually modified parameters). The sensitivity analysis showed that the water fluxes were robust against changes in the hydraulic parameters.

The inverse simulation of the nitrate transport, however, showed a less good agreement

Table 5.2: Statistical parameters for the evaluation of the simulation of the soil water dynamics. R^2 = coefficient of determination. R = Pearson's correlation coefficient. NSE = Nash-Sutcliffe efficiency. $STDV$ = standard deviation of the mean.

N application rate	R^2 (-)	R (-)	NSE (-)	$STDV$ (-)
N50	0.6366	0.7979	0.6026	7.4884
N150	0.6483	0.8052	0.5216	10.833
N250	0.7385	0.8594	0.6122	8.8381
N350	0.6654	0.8157	0.6325	11.436

Table 5.3: Statistical parameters for the evaluation of the simulation of the nitrate transport. R^2 = coefficient of determination. R = Pearson's correlation coefficient. NSE = Nash-Sutcliffe efficiency. $STDV$ = standard deviation of the mean.

N application rate	R^2 (-)	R (-)	NSE (-)	$STDV$ (-)
N50	0.3174	0.5634	0.2451	$3.13 \cdot 10^{-5}$
N150	0.5033	0.7094	0.3927	$-1.42 \cdot 10^{-5}$
N250	0.3508	0.5923	-0.034	$4.69 \cdot 10^{-5}$
N350	0.1354	0.3680	-0.1817	$0.61 \cdot 10^{-5}$

between the measured and the simulated nitrate concentrations in seepage water (Table 5.3) and underestimated the nitrate concentrations at the fertilizer application rates N50, N250, and N350 and overestimated the nitrate concentrations at the fertilizer N application rate N150, respectively.

5.2.4 Sampling and Analysis

Above-ground and below-ground biomass was measured gravimetrically in each microplot at day 25, 50, and 75 after sowing. Four ^{15}N labeled plants in each plot were harvested to determine the fresh weight (FW) and dry weight (DM) of shoots and roots (Wu et al., 2012) and to analyze ^{15}N excess (at%). Immediately after separation of the plant parts, the FW was measured, and DM was determined after drying at 70°C for at least 48 h. An aliquot of each plant part was ground with a ball mill (≤ 0.25 mm) (Brinkman Retsch, MM2 Pulverizer Mixer Mill, Germany) for isotopic analysis and stored until further analysis. Soil samples (0-20, 20-40, 40-60 cm) with three replicates each were collected at day 25, 50, and 75 after sowing with a soil corer (diameter: 5 cm). Soil sampling and analysis were conducted separately for ridges and furrows. The soil samples were dried at 60°C , mixed, and sieved (< 2 mm). An aliquot of each soil sample was ground with a ball mill (< 0.25 mm) (Brinkman Retsch, MM2 Pulverizer Mixer Mill, Germany) for isotopic analysis and stored until further analysis. Total N content and ^{15}N in soil and plant samples

were determined using an elemental analyzer (NC 2500, CE Instruments, Italy) coupled with an isotope mass spectrometer (delta plus, Thermo Fisher Scientific, Germany) through a ConFlo III open split interface (Thermo Fisher Scientific, Germany) as further specified in Bidartondo et al. (2004). To determine N loss through seepage water, the soil water samplers at each depth (15 cm, 45 cm) and position (ridge, furrow) were separately sampled for chemical analysis approximately on a weekly basis (30.06.2010, 05.07.2010, 10.07.2010, 22.07.2010, 29.07.2010, 04.08.2010, 14.08.2010, 23.08.2010). Samples were refrigerated at 5°C within 2 h of collection and analyzed within 24 h in the field laboratory with Spectroquant® quick tests based on the photometric method (Nitrate test photometric, DMP 0.10 - 25.0 mg/l NO₃⁻-N 0.4 - 110.7 mg/l NO₃ Spectroquant®, MERCK, South Korea) and by using a photometer (LP2W Digital Photometer, Dr. Lange, Germany).

5.2.5 ¹⁵N calculations and tracer recovery

¹⁵N concentration in dry plant and soil material (¹⁵N/¹⁴N at%) was corrected for natural ¹⁵N abundance (at%). ¹⁵N concentrations were then converted to an area basis (mg ¹⁵N m⁻²) using in equations (5.1), (5.2) and (5.3) (Buchmann et al., 1995):

$$[^{15}\text{N}] = \text{}^{15}\text{N}/^{14}\text{N at\%} / 100 * [\text{N}] \quad (5.1)$$

with [N] = N concentration.

$$\textit{Plant samples} : \text{}^{15}\text{N g m}^{-2} = [^{15}\text{N}] * \textit{bio g m}^{-2} \quad (5.2)$$

with bio m⁻² = biomass (g) per unit ground area (m⁻²)

$$\textit{Soil samples} : \text{}^{15}\text{N g m}^{-2} = [^{15}\text{N}] * d_B * s \quad (5.3)$$

with d_B = bulk density of each soil layer, s = soil volume of soil horizon in m³.

A ¹⁵N budget was calculated for each fertilizer N level. The ¹⁵N uptake by crops was expressed as the percentage of applied ¹⁵N fertilizer taken up by the above- and below-ground plant parts and reflects the fertilizer N use efficiency of the plants. The ¹⁵N retention in soil was described as the percentage of applied ¹⁵N fertilizer recovered in the top 60 cm of the soil profile. Only the upper 60 cm of the soil was used for the calculations because more than 90% of the roots were found in the upper 30 cm and N that leached deeper than 60 cm was lost to groundwater. ¹⁵N recovery was calculated as the percentage of ¹⁵N uptake by plants and the ¹⁵N retention in soil.

The ^{15}N loss was calculated by subtracting the uptake by plants and retention in soil from 100.

5.2.6 Statistical analysis

Statistical analysis was carried out using the statistical software R (version 2.13.2), with a significance level of $p \leq 0.05$. All variables were tested for normal distribution. Mean values are presented in the figures, if not stated differently. Differences in the central location (median) of independent samples (DM, crop N uptake, ^{15}N uptake) were analyzed using the Kruskal-Wallis non-parametric analysis of variance and pairwise comparisons using the Wilcoxon rank sum test with Bonferroni correction. Differences in the central location (median) for dependent samples (seepage nitrate concentration, ^{15}N retention) were analyzed using the Friedman non-parametric ANOVA and pairwise comparisons using the Wilcoxon matched pair test. Different statistical techniques such as Pearson's correlation coefficient (R), coefficient of determination (R^2) and Nash-Sutcliffe efficiency (NSE) were used to evaluate the models.

5.3 Results

5.3.1 Plant biomass and ^{15}N uptake in crops

The total DM at final harvest increased with an increase in the fertilizer N application rate, with a significantly lower DM at the N application rate N50 ($p < 0.05$). The maximum DM production was achieved at N350 (5.5 Mg ha $^{-1}$). For N50, a significantly lower final DM production was observed (4 Mg ha $^{-1}$). While the DM increased significantly from day 25 to day 50 at all N application rates, it did not increase at all at any N application rate for the last 25 days of the growth period (Figure 5.3).

The highest ^{15}N uptake by crop was observed at N50 and was 36% at day 50. The N application rate N150 was also at its highest at day 50. Over the entire 75 days of growth, the ^{15}N uptake by crop increased only for the higher fertilizer N rates (N250, N350). In addition, the increase in ^{15}N from day 25 to day 50 was significant at all N application rates. However, the increase for the last 25 days was only significant at N350. At day 75, the total crop ^{15}N uptake ranged between 20% (N250) and 32% (N50), and this difference was significant. The ^{15}N uptake by crops reflects the fertilizer N use efficiency of the plants. At the first sampling day, the order of the mean fertilizer N use efficiency was as follows: 3.8% (N150) > 3.7% (N50) > 2.7% (N250) > 1.7% (N350). The mean fertilizer N use efficiency of all fertilizer N rates at final harvest was found to be 27%.

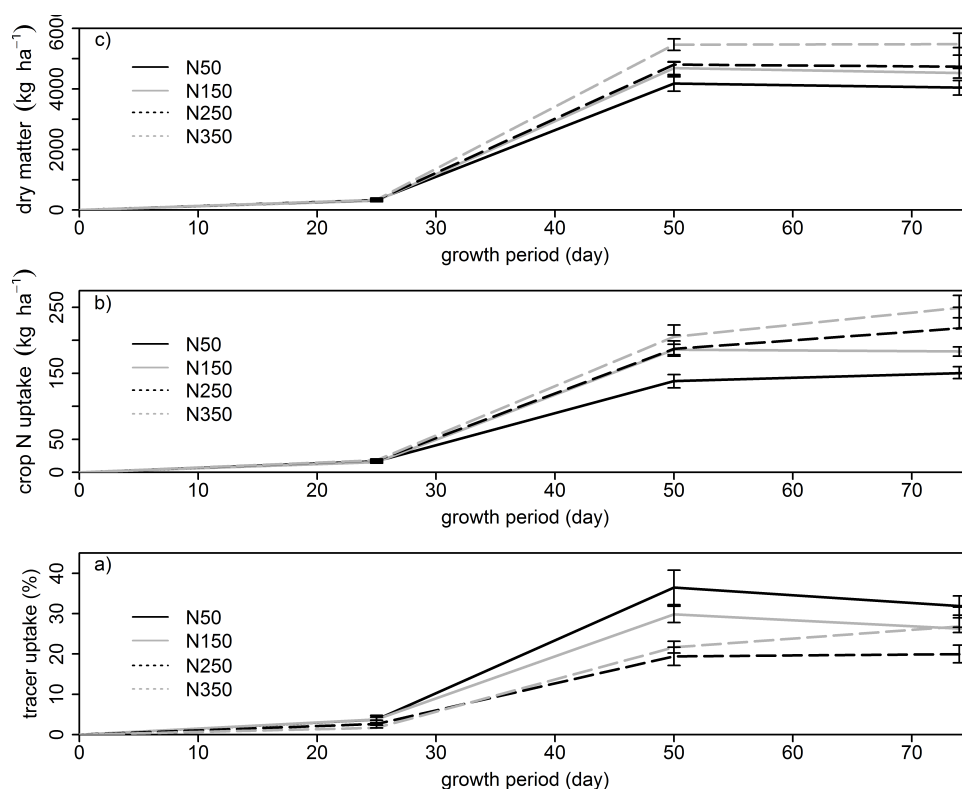


Figure 5.3: a) ^{15}N uptake by plants (% of ^{15}N applied), b) total crop N uptake (kg N ha^{-1}) and c) dry matter production (kg ha^{-1}) at the four fertilizer N rates after 75 days of growth. Standard error of the mean is given.

The total crop N uptake increased linearly with an increase in the fertilizer N application rate at day 75 ($R^2 = 0.97$), while in the first 50 days of the growing period, the N application rates N150 and N250 were still within the same range. The crop N uptake at the two lower fertilizer N rates (N50, N150) stagnated from day 50 to day 75, whereas the uptake continued to increase at the two higher N application rates, leading to the highest final crop N uptake of all four N application rates. The increase in N uptake by crops, however, was only significant from day 25 to day 50 at all four N application rates.

5.3.2 ^{15}N retention in soil

The order of the final ^{15}N retention (% of ^{15}N applied), averaged for all sampling depths, was as follows: 14% (N50) > 13% (N250) > 11% (N150) > 10% (N350), and these differences were not statistically significant. Ridges showed higher soil ^{15}N retention than furrows but again no significant differences were found ($p > 0.05$) (Figure 5.4). In the ridge position as well as in the furrow position, the final soil ^{15}N retention decreased with increasing soil depth at all three sampling days ($p > 0.05$) (Table 5.4).

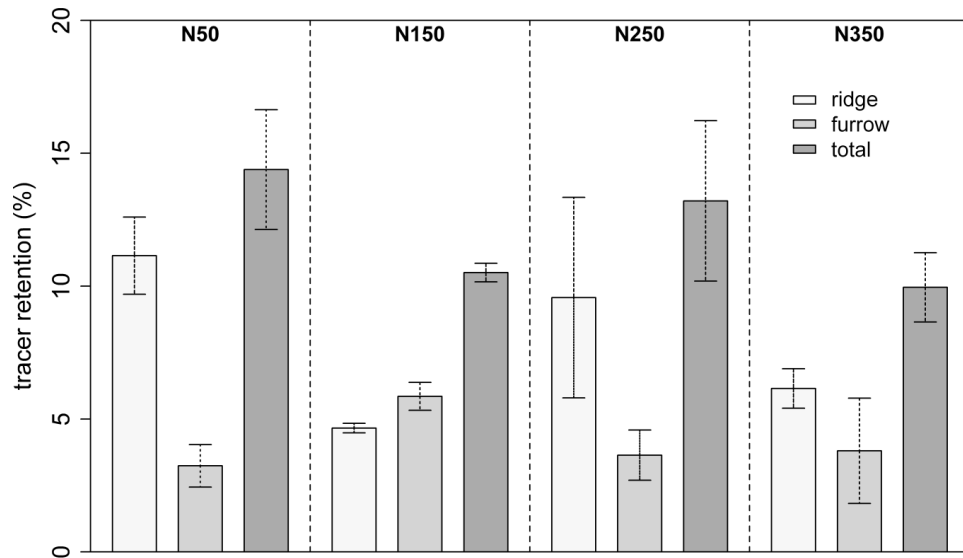


Figure 5.4: Mean soil ^{15}N retention (% of ^{15}N applied) averaged for all three depths at day 75 of growth. Standard error of the mean are shown. Results are given for furrows and ridges separately and in total for the four fertilizer N rates.

Table 5.4: Soil ^{15}N retention (% of ^{15}N applied) in different sampling depths in the ridges and the furrows at day 75 of the growth. The standard error of the mean is given in the parentheses.

N application rate	Ridge 0-20cm	Ridge 20-40cm	Ridge 40-60cm	Furrow 0-20cm	Furrow 20-40cm
N50	9.19 (0.84)	6.81 (0.75)	3.67 (1.00)	2.71 (0.63)	0.53 (0.11)
N150	3.7 (0.25)	0.96 (0.95)	0.51 (0.16)	4.70 (0.15)	1.15 (0.43)
N250	8.29 (2.82)	1.28 (0.68)	0.97 (0.27)	3.12 (0.55)	0.52 (0.12)
N350	5.03 (0.54)	1.12 (0.86)	0.57 (0.10)	3.18 (1.26)	0.63 (0.14)

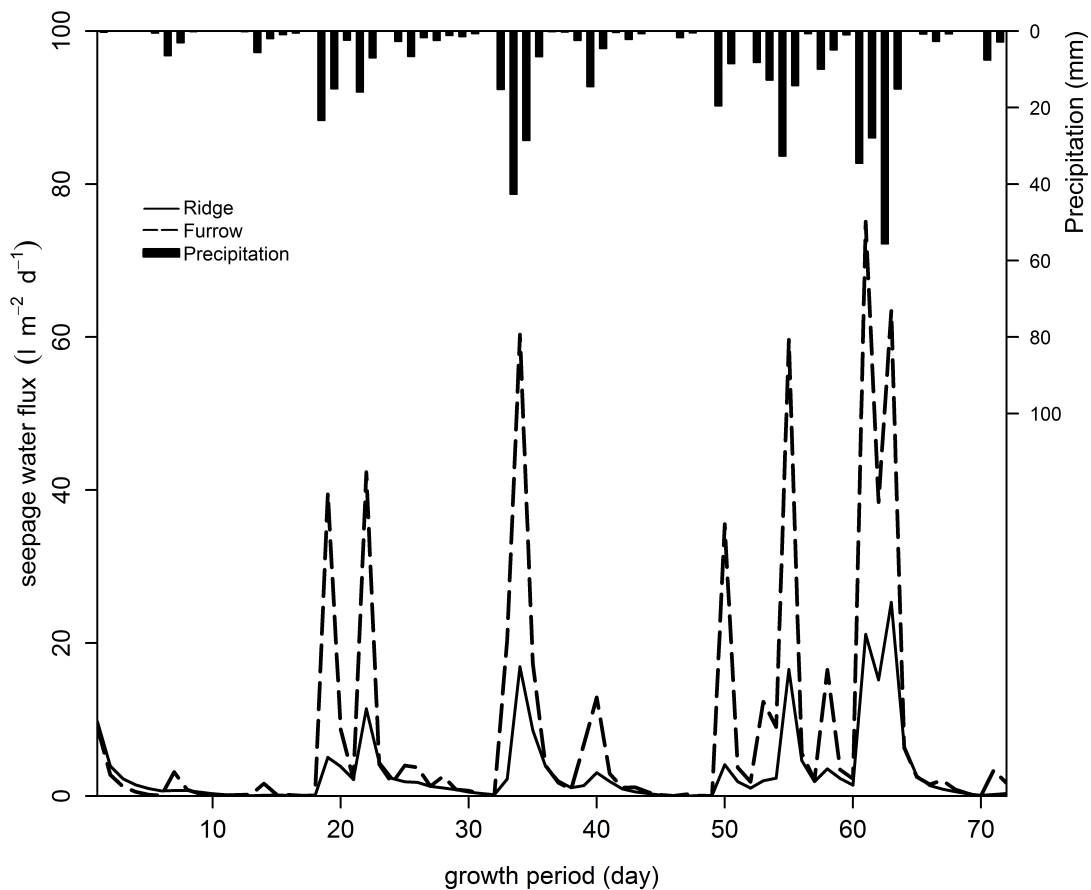


Figure 5.5: Simulated daily seepage water fluxes ($l\ m^{-2}\ d^{-1}$) at a depth of 45 cm during the 75 day growth period. Daily seepage water was simulated for one plot replicate of each fertilizer N application rate only.

5.3.3 N content in soil solution and N leaching

The total added amount of water in the simulation consisted of precipitation amount and soil water content at the beginning of the simulation. The amount of water, which was discharged in the simulation, consisted of the amount of water percolated deeper than 45 cm and the amount of water lost by transpiration and evaporation. The simulated amounts of total seepage water percolating deeper than 45 cm during the 75 days of growth increased in the order: $774\ l\ m^{-2}$ (N350) < $796\ l\ m^{-2}$ (N50) < $853\ l\ m^{-2}$ (N150) < $887\ l\ m^{-2}$ (N250). The water dynamics were only simulated for one plot replicate per fertilizer N application rate in the model. In the simulation, the furrows contributed 1.5 to 3 times more than the ridges to the total amount of seepage water (Figure 5.5). Simulated seepage water fluxes were strongly affected by rainfall and increased considerably with each heavy rain event at all N application rates. Accordingly, the highest seepage water fluxes were simulated on July 16, August 10, and August 13-16, 2010, when the measured precipitation was high, while the dry periods of June 14-30 and July 25 to August 2, 2010 showed low seepage water fluxes.

Mean seasonal nitrate concentrations in seepage water increased with an increase in fertilizer N rate in the following order: N50 (53 mg l⁻¹) < N150 (67 mg l⁻¹) < N250 (119 mg l⁻¹) < N350 (122 mg l⁻¹) (p < 0.05). This order was common at all sampling depths as well as for ridge positions and furrow positions. Differences in the mean nitrate concentrations between the four fertilizer N rates were not significant at the beginning of the experiment (138-179 mg NO₃⁻ l⁻¹) but increased at the end of the experiment (5-64 mg NO₃⁻ l⁻¹) (p < 0.05). Nitrate concentrations in seepage water showed no significant differences between the two sampling depths of 15 cm and 45 cm (p > 0.05). The nitrate concentrations separately sampled at a soil depth of 45 cm in the ridges and in the furrows, in each case measured from the top of the ridge, did also show no significant differences (Figure 5.6).

The continuous and quick decline of nitrate concentrations in seepage water at N50 and N150 resulted in concentrations lower than 10 mg NO₃⁻ l⁻¹ at the end of July (day 45-50 after sowing). In contrast, the slower and discontinuous decrease of nitrate concentrations at N250 and N350 resulted in higher concentrations at the end of July (> 40 mg l⁻¹) and at the final harvest (> 10 mg l⁻¹). The concentration pattern at the beginning of the measurements was unexpected. Although the fertilizer was applied four weeks before the first seepage water sampling, the peak concentrations did not occur at the beginning of the seepage water measurements but around day 21 for the ridge position at a depth of 15 cm and around day 28 for the ridge position and furrow position at a depth of 45 cm.

Because ¹⁵N in seepage water was not measured to determine the proportion of mineral N fertilizer that leached deeper than the rooting zone, simulation results of one plot replicate per fertilizer N application rate from Hydrus 2/3D were used. The simulated total amount of nitrate that leached deeper than 45 cm during the growing season increased linearly ($R^2=0.99$) with an increase in fertilizer N rate: 86 kg NO₃⁻ ha⁻¹ (N50) < 180 kg NO₃⁻ ha⁻¹ (N150) < 260 kg NO₃⁻ ha⁻¹ (N250) < 387 kg NO₃⁻ ha⁻¹ (N350) (Figure 5.7). Additionally, the simulation showed that nitrate leaching was strongly affected by the amount of rainfall. The daily amount of leached nitrate increased considerably at days with high precipitations amounts, while at days with low or no precipitation the daily amount of leached nitrate was found to decrease and to be fairly low. Accordingly, the peaks of high daily nitrate leaching were all found on days with high rainfall amounts. The pattern of the daily N leaching was therefore highly consistent with the pattern of the seepage water fluxes. The ridges and furrows, however, contributed equally to the total amount of leached nitrate at all fertilizer N application rates.

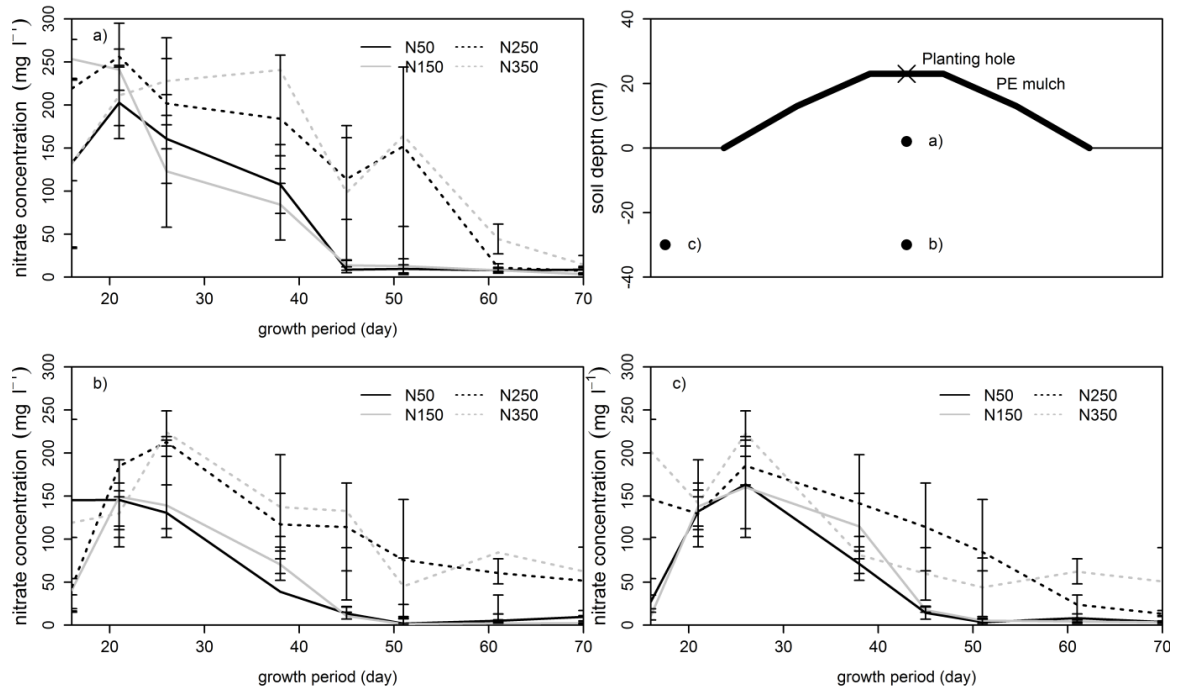


Figure 5.6: Mean ($n=3$) nitrate concentrations in seepage water (mg l^{-1}) at ridge and furrow positions and two soil depths (15 cm, 45 cm) at the four fertilizer N rates. a) = ridge in 15 cm depth; b) = ridge in 45 cm depth; c) = furrow in 45 cm depth. The graphic top right shows the location of the suction lysimeters for collecting seepage water. Standard error of the mean is given

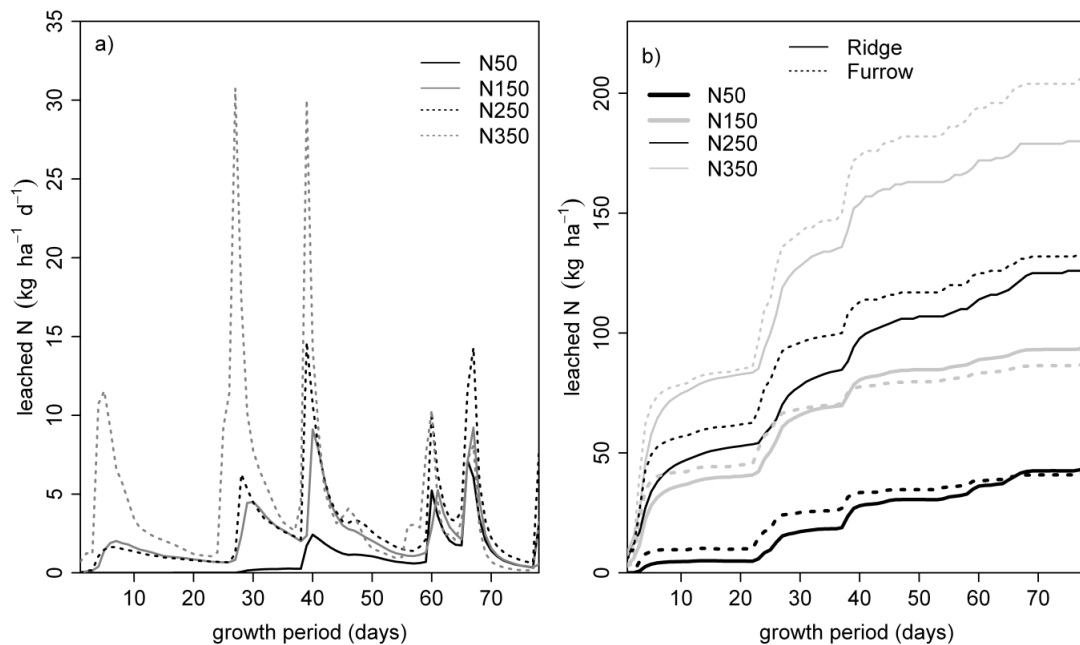


Figure 5.7: a) Simulated daily leached NO_3^- ($\text{kg N ha}^{-1} \text{d}^{-1}$) for the four fertilizer N rates and b) simulated cumulative leached NO_3^- (kg N ha^{-1}) for ridges and furrows separately during the growth period of 75 days. Daily leached nitrate was simulated for one plot replicate of each fertilizer N application rate only.

5.4 Discussion

5.4.1 Plant biomass and ^{15}N uptake by crops

The results for DM production were supported by earlier findings that showed that the highest biomass production for radishes was recorded at the highest rates of fertilizer N (Guvenc, 2002). However, the lack of significant differences in DM production between N150, N250 and N350 indicates that similar crop yields can be achieved with lower fertilizer N rates. In contrast, a significantly lower DM production was observed at N50 when compared to the higher N application rates, which implies that an N fertilizer rate of 150 kg N ha⁻¹ is adequate to achieve maximum biomass production.

The highest ^{15}N uptake by plants of all sampling days was observed at day 50 at the fertilizer N rates N50 and N150, and accordingly, no significant ^{15}N uptake occurred in the final 25 days of growth at these rates. These findings suggest that most of the fertilizer N was either taken up by crops or lost from the soil by day 50 and that only a small amount of ^{15}N was taken up by the crops after this day. A significant ^{15}N uptake between day 50 and 75 was recorded at the N application rate N350. However, because the fertilizer N application rate did not have a significant effect on the final ^{15}N crop uptake, a majority of the fertilizer N was taken up by the plant and used for biomass production in the first 50 days of growth at all fertilizer N rates. This was highly consistent with the fact that no significantly greater biomass production was observed in the last 25 days of growth at any of the four N application rates. Furthermore, the total N content of the plants increased with an increase in the N application rate, as did the nitrate content of the radish (root) (Guvenc, 2002). According to Guvenc (2002), N taken up after day 50 accumulated mostly in the root, rather than being used for further growth. The final mean fertilizer N use efficiency of all 4 N application rates was as low as 27%. ^{15}N isotopes are an invaluable tool to estimate fertilizer N use efficiency, but studies with ^{15}N fertilizers have often shown that fertilizer ^{15}N application increased plant uptake of unlabeled soil N due to mineralization-immobilization turnover (Jenkinson et al., 1985; Kuzyakov et al., 2000). Hence, for soils low in native N, ^{15}N uptake by crops may be lower if immobilization of fertilizer ^{15}N occurs to a significant extent. This pool substitution could lead to an underestimation of the fertilizer ^{15}N uptake by plants (Eviner et al., 2000; Vlek and Byrnes, 1986). Taking this underestimation into account, although the effect was probably of secondary importance for the sandy soils of the experimental field, the calculated mean fertilizer N use efficiency was still fairly low. The low fertilizer N use efficiency of < 4% in the first third of the growing season

was responsible for this poor performance. The crop was unable to utilize all available N at the beginning of the growing season, and hence, the excess fertilizer N applied at the beginning of the growing season had a high potential of being lost to the groundwater in the sandy soils.

5.4.2 N retention and N content in seepage

The percolation risk increased with increasing amounts of precipitation at the beginning of the monsoon season, which usually starts at the end of June. In fact, the precipitation level in June (67 mm) was exceptionally low in 2010, but a rain event with 42 mm of precipitation occurred shortly after the tracer application. The sandy soils with their low water and nutrient retention capacity are extremely susceptible to the rainfall events occurring early in the season, especially when the crops have not yet emerged.

The final ^{15}N retention in soil showed no significant differences between the four N application rates. The final ^{15}N retention in soil showed also no significant differences for the different sampling depths. The coarse texture of the upper 60 cm of the homogenous sandy soils and the poor sorption characteristics increased the risk of ^{15}N percolating quickly to deeper layers instead of accumulating in the soil (Shrestha et al., 2010). The low final ^{15}N retention in soil was consistent with that of other disturbed ecosystems (Peterjohn and Correll, 1984). A higher ^{15}N retention was expected in the covered ridges compared to the bare furrows based on the procedure used for the fertilizer application. While the fertilizer was uniformly distributed at the application, a majority of the fertilizer N accumulated in the ridges during their creation. In addition, the ridges were covered with plastic mulch, which is assumed to protect the soil from direct infiltration of excessive precipitation and accordingly is supposed to reduce the possibility of N loss by leaching (Leistra and J. J. T. I. Boesten, 2010; Romić et al., 2003). However, no statistically significant differences in ^{15}N retention were observed between the ridges and the furrows at all N application rates at the final harvest. This unexpected behavior was most likely due to the ^{15}N uptake by crops in the ridges compared to no ^{15}N uptake by crops in the furrows. Another potential reason might be the stemflow of precipitation water through the canopy leading to local infiltration and preferential flow in the ridge soil, which was observed in other field studies (Leistra and J. J. T. I. Boesten, 2010; Saffigna et al., 1976). This might reverse the protecting effect of the PE cover. A modeling study on water flow in ridges and furrows in South Korean agriculture found another explanation. Pressure head gradients during dry periods were found to deviate horizontally, indicating a lateral flow direction from the furrows to the ridges. However, during monsoon events, the dominating flow directions were less pronounced because

ridges were also fully saturated due to the high hydraulic conductivity of the soils (Ruidisch et al., 2012). This study also showed that there is no protective function of the PE mulch during heavy rain events or during drier periods.

Seepage water was only collected weekly. The effect of single rain events on nitrate concentration in seepage water, such as the rain event shortly after the tracer application, could therefore not be captured experimentally. The nitrate concentration in seepage was highest during the first 25-35 days of growth for all four N addition rates. We hypothesized that the nitrate concentrations were highest at the time of the first seepage water measurements because the seepage water sampling started 3 weeks after the tracer was applied and even 4 weeks after the fertilizer was applied. The highest nitrate concentrations, however, were found a couple of weeks after the first measurements. This behavior might be explained by the fact that the fertilizer N did not dissolve in the soil water immediately and at once and therefore was not immediately susceptible for percolation but to a later point of time. Nitrate concentration in seepage water also decreased with an increase in soil depth in the ridges, but the differences between the furrows and ridges in the same sampling depths were not significant ($p > 0.05$). This implies that the plastic mulch, which covered the ridges, did not protect the ridges from N leaching as we would have expected due to the assumed protection of the soil from the direct infiltration of excessive precipitation. This, however, is highly consistent with the results presented for the ^{15}N retention in ridges and furrows. Moreover, the PE mulch did not seem to influence the nitrate concentrations at all because the patterns of the nitrate concentrations over the season were identical for the ridges and the furrows. These results additionally support the assumption that the major portion of the fertilizer N at N50 and N150 was either taken up by the crop or lost from the soil by day 50. The decrease in nitrate concentrations in seepage water at N50 and N150 occurred quicker and more continuously than at N250 and N350, resulting in nitrate concentrations $< 10 \text{ mg l}^{-1}$ around days 45-50 after sowing. In contrast, nitrate concentrations in seepage water at N250 and N350 were still $> 10 \text{ mg l}^{-1}$ at day 75. However, we found that the seasonal mean nitrate concentrations in seepage did not meet the WHO water quality standards of $50 \text{ mg NO}_3 \text{ l}^{-1}$ for any of the fertilizer N rates (WHO, 2011). This is even more remarkable as the nitrate concentrations of the seepage water were strongly diluted by the massive rainfall.

5.4.3 Seepage water fluxes and total leached N

Simulated seepage water fluxes were highly affected by heavy rain events and increased at days with high rainfall amounts. The furrows had a clearly higher contribution to the amount of

seepage water than ridges at all four N application rates, because the amount of precipitation in the furrows was multiplied by 2 to include the surface runoff from the plastic mulched ridges to the furrows. This procedure was successfully used in other modeling studies (Dusek et al., 2010). Several studies proved experimentally that infiltration and initial water movement occurred largely in the furrows mainly due to surface runoff (Bargar et al., 1999; Hamlett et al., 1990; Leistra and J. J. T. I. Boesten, 2010). Li et al. (2000) compared runoff from bare ridges to runoff from plastic mulched ridges. Runoff from the latter showed an average runoff efficiency (runoff/rainfall) of 87%, with the maximum efficiency being close to 100%. Additionally, the plastic mulched ridges were able to generate runoff even under low intensity of the rainfall. Hamlett et al. (1990) additionally observed ponding of water in the furrows, when rainfall exceeded infiltration capacity. Ponding water in the furrows was also observed in our field study. In addition, no water was taken up by plants in the furrows, which also led to higher seepage water fluxes in the furrows than in the ridges. The water dynamics, however, were only simulated for one plot replicate per fertilizer N application rate in the model. Influencing parameters like biomass production and soil texture of the simulated plots were fairly homogeneous. While biomass production did not show a significant difference between the N application rates N150, N250, and N350, the soil texture was homogeneous even in soil depths up to 60 cm because of the regular addition of sandy soil to the top layer of the field by the local farmers. The model showed a good agreement between the measured and the simulated pressure heads. Additionally, the sensitivity analysis showed that the water fluxes were robust against changes in the hydraulic parameters. The simulations of the water dynamics presented therefore a good foundation for the simulations of the nitrate transport.

In the analysis of the simulated nitrate leaching deeper than 45 cm throughout the growing season, we observed very high values of up to 387 kg N ha⁻¹. These N leaching losses were extremely high and amounted up to 95% of the applied fertilizer N. To interpret these results, one has to consider the application of the basal fertilizer at the rate of 56 kg N ha⁻¹, which was additionally applied prior to the start of the experiment. However, the total amounts of leached N increased linearly with an increase in the N application rate, while biomass production did not significantly increase with increasing fertilizer N rates. Accordingly, the negative effect of water pollution at N250 and N350 was greater than the positive effects of the higher biomass production, indicating high environmental costs caused by exceeding optimum fertilizer N rates. Rapidly increasing amounts of leached N at increasing N application rates for ridge tillage on sandy soils have also been reported in studies conducted in ridge cultivations with uncovered ridges (Errebhi et al., 1998; Shrestha et al., 2010). In this experiment, the ridges were covered

with PE mulch but the application of PE mulch on the ridges did not clearly prevent the linear or rapid increase observed in the other studies. In contrast, high N leaching losses from the plastic-mulched ridges was observed in our study despite the assumed protection from local infiltration and preferential flow in the ridge soil. Additionally, the contribution of nitrate leaching from the ridges and from the furrows was fairly similar at all N application rates. Previous studies showed that fertilizer N should be placed in the active water and nutrient uptake zone and, hence, away from the furrows (Hatfield et al., 1998; Jaynes and Swan, 1999) because all fertilizer N, which was placed in the furrows, had a very high risk of being leached. The contribution to the total amount of leached nitrate increased considerably in the ridges and in the furrows during heavy rain events, especially early in the growing season. This again indicated that the PE mulch provided little protection of the ridge soil from N leaching. However, the increase in N leaching during heavy rain events confirmed that the excess N applied prior to planting had a higher probability of percolating deeper than the root zone with the beginning of the summer monsoon season. The summer monsoonal precipitation over Korea has recently increased due to a higher occurrence of heavy rainfall ($\geq 30 \text{ mm d}^{-1}$) events and an increase in the total summertime precipitation (Ho et al., 2003). This change in rainfall intensity, and total amount as well as the high inter-annual variability (Ho et al., 2003) amplifies the N leaching problem. However, the inverse simulation of the nitrate transport showed a less good agreement between the measured and the simulated nitrate concentrations in seepage water than the simulation of the water flow did. The nitrate concentrations at the fertilizer application rates N50, N250, and N350 were underestimated, while the nitrate concentrations at the fertilizer N application rate N150 were overestimated.

5.4.4 ^{15}N Budget and simulated budget of fertilizer N

A ^{15}N budget of the top 60 cm soil layer was calculated for each fertilizer N treatment for the 2010 cropping season (Table 5.5). The ^{15}N loss at the end of the cropping season averaged to 63%. The highest ^{15}N recovery was observed at N50 (47%), followed by N150 (38%), and the fate of the lost tracer was unaccounted for. When simulated values of leached nitrate were expressed in relation to applied fertilizer N (basal fertilizer included), N losses with leaching amounted to 81%, 87%, 85% and 95% at N50, N150, N250, and N350, respectively. Simulated N losses with leaching were therefore approximately 25% higher than the N losses calculated by the ^{15}N budget. This difference arises from some uncertainties of the simulations. The underestimation of plant N uptake in the simulation was for example partly responsible for the overestimation of

Table 5.5: Fate of ^{15}N (%) at day 75 of growth for the four fertilizer N rates.

N fate	N50	N150	N250	N350
^{15}N recovery	46.8	39.1	30.2	37.9
Crop ^{15}N uptake	31.7	28.1	20.0	29.1
Soil ^{15}N retention	15.1	11.0	10.2	8.8
^{15}N loss	53.2	60.9	69.8	62.1

the N leaching losses and was consistently observed in other studies (Doltra and Muñoz, 2010). The simulated mean N uptake by crops accounted to $\sim 15\%$ compared to the measured mean N uptake of 27% in our field study. This underestimation arises from the fact that the N uptake by crops is linked to the water uptake by the crops and therefore takes place passively. An underestimation of crop N uptake leads subsequently to higher amounts of mineral N left in the soil, which is in turn prone to leaching. Another factor of uncertainty in the simulation is denitrification, which is the only unmeasured sink term in the study. Denitrification accounted for at most 2% in the simulations. This finding was not consistent with other calculations for Korea (Bashkin et al., 2002). However, the microorganisms, which are responsible for the denitrification processes need easily available or decomposable carbon (C_{org}) as an energy source. The denitrification rate in soils with low C_{org} content was therefore found to be very low. As the C_{org} content of the experimental field was also measured to be very low, we assume that a low denitrification rate is in this case plausible.

To carry out the simulations we had to make some assumptions, e.g. that N fertilizer granules were directly dissolved in the soil water all at once. The measured results of the nitrate concentrations in the seepage water reflected that this assumption was not sustainable in the field study. Additionally, the simulations have been carried out only for one plot replicate per N application rate and no statistically significant differences could therefore be identified. However, the simulation in combination with the ^{15}N budget showed that N leaching can be definitely seen as the dominant N loss pathway in this ridge cultivation system for both of the zones, the ridges and furrows.

5.5 Conclusions

Excessive application of mineral N fertilizer to ridge cultivation with PE mulch on sandy soils resulted in high N leaching losses in ridges and furrows, when fertilizer application was broadcast prior to planting. Based on the finding that soil ^{15}N retention and nitrate concentration in

seepage water decreased similarly for ridges and furrows during the entire growing season, we conclude that the PE mulch had no significant effect on ^{15}N retention in soil and on nitrate concentration in seepage water and did therefore not effectively protect the fertilizer in the ridges from percolation. Accordingly, the ridges and furrows contributed approximately an equal amount of leached N to the total amount. Based on the simulation results, we observed that the risk of N leaching during heavy rain events was pronounced in both the furrow and the ridge zones. We therefore conclude that the PE mulch provided little protection for the fertilizer N in the ridges during heavy rainfall. Consequently, the ^{15}N uptake was found to be low at all N application rates. N leaching amounts were further found to increase linearly with an increase in N addition rate as it is well known for R/F cultivations without PE mulch. The PE mulch did therefore not prevent the linear increase in leaching with an increase in fertilizer N addition. We summarize that without the use of additional measures, the application of PE mulch combined with the local fertilizer application practices did not reduce N leaching rates and groundwater pollution in Haean Catchment. At all the fertilizer N rates, mean nitrate concentrations in seepage water were found to be above the WHO drinking water standard of $50 \text{ mg NO}_3 \text{ l}^{-1}$.

To reduce nitrate leaching, we recommend the following management strategies in addition to the application of plastic mulch: 1) decreasing the fertilizer N rates to a maximum of 150 kg N ha^{-1} ; 2) applying fertilizer N in 3 to 4 split applications according to the plant's N needs; 3) applying fertilizer N only to the ridges (after their formation) to avoid losses from the furrows; and 4) increasing the soil organic matter content to subsequently enhance water and nutrient retention by covering the furrows with plant residues, i.e., rice straw or soil additives. Splitting the applications helps to protect the fertilizer N against the temporal and quantitative variability of the heavy rainfalls, especially at the beginning of the growing season, when the crop N uptake is small. However, split applications might be impractical or more costly in plastic covered R/F cultivations because mechanical equipment is required to apply fertilizer under the PE mulch. The proposed fertilizer N application rate of 150 kg N ha^{-1} equals a N reduction of 40% compared to the current recommendation of the RDA. The N application rate N150 resulted in a similar biomass production to those with higher fertilizer N rates, while lower nitrate amounts in the radishes and significantly lower N leaching losses were observed.

Finally, the reasons for the high N leaching losses from covered ridges are not completely understood. Further field studies will have to concentrate more on the processes in the plastic-mulched ridges and the subsequent N fate in those ridges to further adjust the management strategies.

Acknowledgements

This study was carried out as part of the International Research Training Group TERRECO (GRK 1565/1) funded by the Deutsche Forschungsgemeinschaft (DFG) at the University of Bayreuth, Germany and the Korean Research Foundation (KRF) at Kangwon National University, Chuncheon, S. Korea. We thank the Punchball Tongil Agricultural Experimental Farm in Haean for providing an agricultural field site as well as advice on local practices. We also want to thank Andreas Kolb for his help in designing the suction lysimeter study. Soil analysis is partly supported by the Cooperative Research Program for Agricultural Science & Technology Development (PJ9070882011) of the RDA in Korea.

References

- Bargar, B., J. B. Swan, and D. Jaynes (1999). “Soil water recharge under uncropped ridges and furrows”. In: *Soil Science Society of America Journal* 63.5, pp. 1290–1299. ISSN: 0361-5995.
- Barton, L. and T. Colmer (2004). “Irrigation and fertilizer strategies for minimising nitrogen leaching from turfgrass, 26 Sep – 1 Oct 2004, Brisbane, Australia”. In: *Proceedings of the 4th International Crop Science Congress*.
- Bashkin, V., S. Park, M. Choi, and C. Lee (2002). “Nitrogen budgets for the Republic of Korea and the Yellow Sea Region”. In: *Biogeochemistry* 57/58, pp. 387–403.
- Bidartondo, M., B. Burghardt, G. Gebauer, T. Bruns, and D. Read (2004). “Changing partners in the dark: isotopic and molecular evidence of ectomycorrhizal liaisons between forest orchids and trees”. In: *Proceedings of the Royal Society Biological Sciences* 271, pp. 1799–1806.
- Boumans, L., D. Fraters, and G. van Drecht (2005). “Nitrate Leaching in Agriculture to Upper Groundwater in the Sandy Regions of the Netherlands during 1992-1995 Period”. In: *Environmental Monitoring and Assessment* 102, pp. 225–241.
- Buchmann, N., E. Schulze, and G. Gebauer (1995). “¹⁵N-ammonium and ¹⁵N-nitrate uptake of a 15-year-old *Picea abies* plantation”. In: *Oecologia* 102, pp. 361–370.
- Buczko, U., R. Kuchenbuch, and B. Lennartz (2010). “Assessment of the predictive quality of simple indicator approaches for nitrate leaching from agricultural fields”. In: *Journal of Environmental Management* 93, pp. 1305–1315.
- Buresh, R., E. Austin, and E. Craswell (1982). “Analytical methods in ¹⁵N research”. In: *Fertilizer Research* 3, pp. 37–62.

- Chung, Y., M. Yoon, and H. Kim (2004). "On Climate Variations and Changes observed in South Korea". In: *Climatic Change* 66, pp. 151–161.
- DGFZ and HLUG (2004). *Handlungsempfehlung für Sickerwasseruntersuchungen im Altlastenbereich mit Saugkerzen für organische Schadstoffe am Beispiel PAK*. accessed 21 June 2011. Dresdner Grundwasserforschungszentrum, Hessisches Landesamt für Umwelt und Geologie. <http://www.hlug.de/fileadmin/dokumente/altlasten/empfsaug2004.pdf>.
- Di, H. and K. Cameron (2002). "Nitrate leaching in temperate agroecosystems: sources, factors and mitigating strategies". In: *Nutrient Cycling in Agroecosystems* 46, pp. 237–256.
- Doltra, J. and P. Muñoz (2010). "Simulation of nitrogen leaching from a fertigated crop rotation in a Mediterranean climate using the EU-Rotate-N and Hydrus-2D models". In: *Agricultural Water Management* 97, pp. 227–285.
- Drury, C., D. McKenney, W. Findlay, and J. Gaynor (1993). "Influence of Tillage on Nitrate Loss in Surface Runoff and Tile Drainage". In: *Soil Science Society of America Journal* 57, pp. 797–802.
- Dusek, J., C. Ray, G. Alavi, T. Vogel, and M. Sanda (2010). "Effect of plastic mulch on water flow and herbicide transport in soil cultivated with pineapple crop: A modeling study". In: *Agricultural Water Management* 97, pp. 1637–1645.
- Errebhi, M., C. Rosen, S. Gupta, and D. Birong (1998). "Potato yield response and nitrate leaching as influenced by nitrogen management". In: *Agronomy Journal* 90, pp. 10–15.
- Eviner, V., F. Chapin III, and C. Vaughn (2000). "Nutrient manipulations in terrestrial ecosystems". In: *Methods in Ecosystem Science*. Springer, New York.
- Guvenc, I. (2002). "Effect of Nitrogen on growth, yield and nitrogen contents of radishes". In: *Gartenbauwissenschaft* 67, pp. 23–27.
- Hamlett, J., J. Baker, and R. Horton (1990). "Water and anion movement under ridge tillage: a field study". In: *Transactions of the American Society of Agricultural Engineers* 33, pp. 1859–1866.
- Hatfield, J., R. Allmaras, G. Rehm, and B. Lowery (1998). "Ridge Tillage for corn and soybean production: environmental quality impacts". In: *Soil & Tillage Research* 48, pp. 145–154.
- Henriksen, C., J. Rasmussen, and J. Mølgaard (2006). "Ridging in autumn as an alternative to mouldboard ploughing in a humid-temperate region". In: *Soil & Tillage Research* 85, pp. 27–37.
- Ho, C., J. Lee, M. Ahn, and H. Lee (2003). "A sudden change in summer rainfall characteristics in Korea during the late 1970s". In: *International Journal of Climatology* 2, pp. 117–128.

- Islam, T., I. Hasegawa, K. Ganno, N. Kihou, and T. Momonoki (1994). “Vinyl-film mulch: a practice for sweet potato (*Ipomoea Batatas* Lam. Var. *Edulis* Makino) cultivation to reduce nitrate leaching”. In: *Agricultural Water Management* 26, pp. 1–11.
- Jaynes, D. and J. Swan (1999). “Solute Movement in Uncropped Ridge-Tilled Soil under Natural Rainfall”. In: *Soil Science Society of America Journal* 63, pp. 264–269.
- Jenkinson, D., R. Fox, and J. Rayner (1985). “Interactions between fertilizer nitrogen and soil nitrogen - the so-called ‘priming’ effect”. In: *Soil Science* 36, pp. 425–444.
- Jung, S., C. Jang, J. Kim, and B. Kim (2009). “Characteristics of Water Quality by Storm Runoffs from Intensive Highland Agricultural Area in the Upstream of Han River Basin”. In: *Journal of Korean Society on Water Quality* 25, pp. 102–111.
- Kim, B., S. Jung, Y. Kim, J. Kim, and S. Sa (2006). “The effect of nutrients discharged from agricultural watershed upon the eutrophication of reservoirs in Korea”. In: *Proceeding of the International Symposium on Water Conservation and Management in Coastal Area Nov. 11-16, 2006*.
- Kuzyakov, Y., J. Friedel, and K. Stahr (2000). “Review of mechanisms and quantification of priming effects”. In: *Soil Biology & Biochemistry* 32, pp. 1485–1498.
- Leistra, M. and J. Boesten (2008). *Movement of bromide-ion and carbofuran in the humic sandy soil of a potato field with ridges and furrows – Measurements in the field and computations with the PEARL model*. Tech. rep. Alterra Report.
- Leistra, M. and J. J. T. I. Boesten (2010). “Pesticide Leaching from Agricultural Fields with Ridges and Furrows”. In: *Water Air and Soil Pollution* 213.1-4, pp. 341–352. ISSN: 0049-6979. DOI: 10.1007/s11270-010-0389-x.
- Li, X., J. Gong, and X. Wei (2000). “In-situ rainwater harvesting and gravel mulch combination for corn production in the semi-arid region of China”. In: *Journal of Arid Environments* 46, pp. 371–382.
- Nyamangara, J., L. Bergström, M. Piha, and K. Giller (2003). “Fertilizer Use Efficiency and Nitrate Leaching in Tropical Sandy Soil”. In: *Journal of Environmental Quality* 32, pp. 599–606.
- Peterjohn, W. and D. Correll (1984). “Nutrient Dynamics in an Agricultural Watershed – Observations on the Role of A Riparian Forest”. In: *Ecology* 65, pp. 1466–1475.
- RDA (2006). “The standard rate of chemical fertilizer for crops”. In: Rural Development Administration of Korea.

- Romic, D., M. Romic, M. Borosic, and M. Poljak (2003). “Mulching decreases nitrate leaching in bell pepper (*Capsicum annuum* L.) cultivation”. In: *Agricultural Water Management* 60, pp. 87–97.
- Ruidisch, M., J. Kettering, S. Arnhold, and B. Huwe (2012). “Modeling water flow in a plastic mulched ridge cultivation system on hillslopes affected by South Korean summer monsoon”. In: *Agricultural Water Management*. DOI: 10.1016/j.agwat.2012.07.011.
- Saffigna, P., C. Tanner, and D. Keeney (1976). “Non-uniform infiltration under potato canopies caused by interception, stemflow, and hilling”. In: *Agronomy Journal* 68, pp. 337–342.
- Shrestha, R., L. Cooperband, and A. MacGuidwin (2010). “Strategies to reduce Nitrate Leaching into Groundwater in Potato Grown in Sandy Soils: Case Study from North Central USA”. In: *American Journal of Potato Research* 87, pp. 229–244.
- Sieling, K. and H. Kage (2006). “N balance as an indicator of N leaching in an oilseed rape – winter wheat – winter barley rotation”. In: *Agriculture, Ecosystems & Environment* 115, pp. 261–269.
- Simunek, J. (2006). “Models of Water Flow and Solute Transport in the Unsaturated Zone”. In: *Encyclopedia of Hydrological Sciences*. John Wiley & Sons, Ltd. ISBN: 9780470848944.
- UMS GmbH, (M. S. (2008). *Empfehlungen zur Bodenwasserprobennahme. Version 11/2008*. Tech. rep. UMS, München.
- Van der Laan, M., R. Stirzaker, J. Annandale, K. Bristow, and C. du Preez (2010). “Monitoring and modelling drainage and resident soil water nitrate concentrations to estimate leaching losses”. In: *Agricultural Water Management* 97, pp. 1779–1786.
- Vázquez, N., A. Pardo, M. Suso, and M. Quemada (2005). “A methodology for measuring drainage and nitrate leaching in unevenly irrigated vegetable crops”. In: *Plant and Soil* 269, pp. 297–308.
- Vlek, P. and B. Byrnes (1986). “The efficiency and loss of fertilizer N in lowland rice”. In: *Fertilizer Research* 9, pp. 131–147.
- WHO (2011). *Guidelines for Drinking-water Quality*. Geneva: WHO (World Health Organization).
- WRB, I. W. G. (2007). *World Reference Base for Soil Resources 2006 first update 2007. World Soil Resources Reports No. 103*. Tech. rep. Rome, Italy: Food and Agriculture Organization of the United Nations.
- Wu, L., Y. Ok, X. Xu, and Y. Kuzyakov (2012). “Effects of anionic polyacrylamide on maize growth: a short term ¹⁴C labeling study.” In: *Plant and Soil* 350, pp. 311–322.

- Xu, X., F. Stange, A. Richter, W. Wanek, and Y. Kuzyakov (2008). “Light affects competition for inorganic and organic nitrogen between maize seedlings and soil microorganisms”. In: *Plant and Soil* 304, pp. 59–72.
- Zotarelli, L., J. Scholberg, and R. Dukes M.D. and Munez-Carpena (2007). “Monitoring of Nitrate Leaching in sandy Soils: Comparison of three methods”. In: *Journal of Environmental Quality* 36, pp. 953–962.

Chapter 6

The effect of fertilizer best management practices on nitrate leaching in a plastic mulched ridge cultivation system

Marianne Ruidisch^{1,a}, Svenja Bartsch^b, Janine Kettering^c, Bernd Huwe^a, Sven Frei^b

^a Soil Physics Group, BayCEER, University of Bayreuth, 95440 Bayreuth, Germany

^b Department of Hydrology, BayCEER, University of Bayreuth, 95440 Bayreuth, Germany

^c AgroEcoSystem Research Department, BayCEER, University of Bayreuth, 95440 Bayreuth, Germany

Abstract

Groundwater pollution by fertilizer NO_3^- is a major problem recognized in many parts of the world. The excessive use of mineral fertilizers to assure high yields in agricultural production intensifies the leaching problem especially in regions affected by a monsoon climate as in South Korea. To which extend leaching occurs, depends on several factors such as climatic conditions, agricultural management practices, soil properties and the sorption characteristics of fertilizers and agrochemicals. In

¹Correspondence to: Marianne Ruidisch, Soil Physics Group, BayCEER, University of Bayreuth, 95440 Bayreuth, Germany.
E-mail: ruidisch@uni-bayreuth.de

the South Korean monsoon season 2010, NO_3^- concentrations under varying nitrogen fertilizer rates were monitored in a plastic mulched ridge cultivation (RT_{pm}) with radish crops (*Raphanus sativus L.*). Based on these findings we calibrated a three-dimensional water flow and solute transport model using the numerical code HydroGeoSphere in combination with the parameter estimation software ParallelPEST. Subsequently, we used the calibrated model to investigate the effect of plastic mulch as well as different fertilizer best management practices (FBMPs) on NO_3^- leaching. We found that cumulative NO_3^- leaching under RT_{pm} was 26% lower compared to ridge tillage without coverage (RT). Fertilizer placement confined to the ridges resulted in 36% lower cumulative NO_3^- -leaching rates compared to broadcast applied fertilizer. Splitting the total amount of $150 \text{ kg NO}_3^- \text{ ha}^{-1}$ per growing season into three fertilizer applications (20 kg/ 80 kg /50 kg) led to a reduction of NO_3^- leaching of 59% compared to the one-top dressing at the beginning of the growing season. However, the combination of a fertilizer rate of $150 \text{ kg NO}_3^- \text{ ha}^{-1}$, plastic mulched ridges, fertilizer placement only in the ridges and split applications of fertilizer resulted in the lowest cumulative leaching rate ($8.14 \text{ kg NO}_3^- \text{ ha}^{-1}$) during the simulation period, which is equivalent to 5.4% of the total NO_3^- fertilizer input. Compared to RT with conventional fertilization in ridges and furrows, the NO_3^- leaching was reduced by 82%. Therefore, the combination of all FBMPs is highly recommendable to decrease economical costs for fertilizer inputs as well as to minimize nitrate leaching and its impact on groundwater quality. Finally, we recommend cultivating cover crops after harvest to increase N fixation after harvest, to increase N_{min} for the following growing season and to reduce the risk of leaching and soil erosion in autumn.

Keywords: nitrate leaching, numerical modeling, fertilizer best management practices, ridge tillage, plastic mulch, groundwater

6.1 Introduction

Agricultural productivity is under considerable strain to meet the food demand of a growing population. This pressure causes high external inputs such as fertilizer and pesticides into the agricultural systems. Thus, the ongoing degradation of water resources by agricultural practices constitutes a challenging problem worldwide (Spiertz, 2010; Danielopol et al., 2003; Tilman

et al., 2002; Matson et al., 1997; Ongley, 1996). The risk of fertilizer and pesticides leaching via surface runoff into rivers and lakes or percolation through the unsaturated zone into groundwater is especially high in regions affected by East Asian summer monsoon due to the high frequency and intensity of rainfalls. In China and South Korea, intensively used agricultural areas were identified as hotspots of non-point pollution, which cause water deterioration and eutrophication of important freshwater resources such as lakes and reservoirs (Park et al., 2010; Kim et al., 2001; Zhang et al., 1996).

Apart from manifold agrochemicals, NO_3^- fertilizer is one of the most critical pollutants due to its excessive input and the low N use efficiency of crops (Spiertz, 2010). A concentration maximum of 50 mg $\text{NO}_3^- \text{ l}^{-1}$ in drinking water was recommended by the World Health Organization, while in the USA and South Korea the official regulations are even less with 10 mg $\text{NO}_3^- \text{ l}^{-1}$ (Choi et al., 2007). Nevertheless, the worldwide observation of water quality in surface water and groundwater showed that the NO_3^- concentrations exceed the WHO recommendations by far (Liu et al., 2005). In South Korea, especially in areas intensively used for agriculture, elevated nitrate concentrations in groundwater often exceeding the national drinking water standard (Min et al., 2002; Koh, Ko, et al., 2007; Koh, Chae, et al., 2009).

To minimize the leaching risk of agrochemicals, precision agriculture was found to be a valuable tool. Wallace (1994) proposed economic and environmental benefits by an adjusted fertilizer placement, an adapted timing of fertilizer application to the plant's needs and an adapted leveling, draining and contouring of agricultural fields. Furthermore, the effect of ridge tillage on solute movement was investigated by several authors. They found, that ridge tillage provides potential to decrease NO_3^- leaching by isolating NO_3^- from the percolating water, especially if fertilizer is placed only in the upper part of the ridge (Bargar et al., 1999; Benjamin et al., 1990; Clay et al., 1992; Hamlett et al., 1990; Jaynes and Swan, 1999; Waddell and Weil, 2006).

Plastic mulching of the ridges is practiced for many crop types worldwide for several reasons. Lament (1993) found an increased temperature in the ridge soil, which in turn induces earlier plant emergence. Furthermore plastic mulching was shown to be useful in terms of weed suppression and reducing evaporation loss. In general an earlier and higher overall yield was found for several crop types. Besides, Locascio et al. (1985) and Cannington et al. (1975) found that plastic mulch protects the fertilizer from infiltrating water and consequently enhances the nutrient retention in the ridge soil and the nutrient use efficiency of crops. Accordingly, uncovered furrow positions are more prone to agrichemical leaching compared to ridge positions due to higher infiltration rates caused by the surface runoff from the ridges to the furrows (Clay

et al., 1992; Leistra and Boesten, 2010).

Intensive agriculture in the highlands of Gangwon Province, South Korea depends heavily on high mineral N fertilizer inputs. Vegetable production in plastic mulched ridge cultivation is practiced widespread over the region on dominating sandy soils with poor sorption characteristics (Kettering et al., 2012). However, the influence of plastic mulched ridge cultivation in regions affected by monsoon climates on water flow and nitrate leaching has not been investigated yet. Based on the findings of a ^{15}N field experiment and the monitoring of nitrate concentrations in soil water during the growing/monsoon season 2010 in a plastic mulched radish cultivation (*Raphanus sativus L.*) in the Haean catchment in South Korea (Kettering et al., in review), we set up a three-dimensional numerical model using HydroGeoSphere (Therrien et al., 2010), which simulates fully-integrated surface-subsurface flow and solute transport processes. The model was coupled with ParallelPEST (Doherty, 2005) to calibrate soil hydraulic and solute transport parameters based on the Gauss-Marquardt-Levenberg nonlinear estimation technique. Our objective was to quantify and evaluate the potential of fertilizer best management practices to decrease NO_3^- leaching losses to groundwater under monsoonal conditions. Thus, the calibrated model was used to run scenarios in terms of precision agriculture such as an enhanced fertilizer placement and fertilizer split applications as well as the combination of both. We hypothesized, that (i) plastic mulching reduces NO_3^- leaching losses compared to uncovered ridge cultivation, (ii) fertilizer placement only in ridges decreases NO_3^- - leaching losses compared to the conventional fertilization in ridges and furrows, (iii) NO_3^- leaching losses could be reduced by the right timing and the splitting of fertilizer application.

6.2 Materials and methods

6.2.1 Study site

The Haean catchment ($128^\circ 1' 33.101''\text{E}$, $38^\circ 28' 6.231''\text{N}$, approx. 420-1000 masl) is located in the mountainous northeastern part of South Korea. The basin, which is situated at the upper reach of the Mandae stream, has been identified as a main non-point source pollution area. The Mandae Stream contributes to the Soyang Lake (Park et al., 2010), which in turn constitutes the main fresh water reservoir for the metropolitan area of Seoul. The annual precipitation amount of 1577 mm (11-years average) is characteristic for the catchment. During the East Asian summer monsoon, which occurs usually between June and August, the catchment receives 50-60% of the annual precipitation sum. Furthermore, the catchment is characterized by three

Table 6.1: Soil physical properties of the experimental sites.

	Clay (%)	Silt (%)	Sand (%)	Bulk density (g cm ⁻³)	Soil texture class (USDA)
Topsoil A	2.72	15.19	82.09	1.48	Loamy sand
Subsoil B	3.28	19.16	77.56	1.54	Loamy sand

major land use types, namely forested land, agriculture and residential area. The steep hillslopes are covered by forest accounting for 58% of the total area. Dry land agriculture is practiced mainly on moderate hillslopes with 22% of the total area. Rice paddies in the center of the catchment occupy 8%. The remaining area of 12% constitutes of residential area, grassland and field margins.

Depending on the crop type, the growing period starts usually between April and June. In order to suppress weed growth and to ensure an early plant emergence, ridge tillage with plastic mulching is a widespread practice for cultivating dryland crops such as radish (*Raphanus sativus* L.), potatoes (*Solanum tuberosum* L.), cabbage (*Brassica rapa* *susp. Pekinensis* (lour.), Hanelt, *Brassica aleracea* *convar. Capitata* *var. alba*) and beans (*Glycine max.* (L.) Merr.). Before ridges are created, fertilizer is commonly applied to the fields and mixed into the upper part of the soil by ploughing. Afterwards the ridges are created and concurrently covered by plastic mulch. The crops are sowed as seeds or planted as juvenile plants in the planting holes at the top of the ridges. During the growing season, herbicides and pesticides are sprayed several times throughout the fields. The harvest normally takes place from late August to October.

Based on a soil survey, the soil type Cambisol, which is developed on weathered granite bedrock material, was found widespread within the catchment. The physical and chemical properties of most soils are strongly anthropogenically modified due to the repetitive application of sandy soil material and excessive fertilizer, pesticides and herbicides input. Soil application is a common method to compensate the erosion loss of topsoil occurring during the monsoon season. Although the dryland crops are primarily grown on hillslopes, a flat field site in the center of the catchment was selected for the leaching experiment in order to exclude surface runoff (Kettering et al., unpublished data). The soil at the experimental field site was classified as an Anthrosol (IUSS Working group WRB, 2007) due to the long-term application of sandy soil. Soil samples for texture analysis were taken up to 2 m soil depth. Two horizons were identified in the field mainly because of their differing soil color, but the soil texture analysis showed only marginal differences between both horizons. In Table 6.1 the soil physical properties of the experimental field are shown.

6.2.2 Experimental set up

Before conducting the experiment, an automatic weather station (WS-GP1, Delta-T devices, Cambridge, UK) was installed at the field margin of the experimental field. Weather parameters such as precipitation, solar radiation, wind speed, air temperature, humidity and air pressure were logged in a 5 min interval and provided the basis for calculating evapotranspiration rates using the dual crop coefficient approach based on FAO-56 for crops. A detailed description of the calculation procedure is given by Allen et al. (1998). In Figure 6.1 the precipitation rates during the experiment are given. The set up of the field experiment is chronologically shown in Figure 6.1. Before we set up the experiment, the selected field site was fallow. Therefore, granulate mineral fertilizer of $56 \text{ kg NO}_3^- \text{ ha}^{-1}$ was applied as a basic fertilizer to enhance soil fertility. Afterwards the field was sectioned into 16 square subplots, each with an area of 49 m^2 . Additionally to the basic fertilization, four fertilizer rates with 50 (A), 150 (B), 250 (C) and 350 (D) $\text{kg NO}_3^- \text{ ha}^{-1}$ were applied on June 1, 2010. Each fertilizer rate was applied to 4 of the 16 square subplots and arranged in a randomized block design. At June 9 the ridges were created and covered with black plastic mulch. The plastic covered ridges (35 cm width, 15 cm height) alternated with uncovered furrows with a ridge-to-ridge spacing of approximately 70 cm. The plastic cover at the top of the ridge was perforated with planting holes (5 cm diameter) with a plant to plant spacing of 25 cm. At June 14 radish seeds were sowed in the planting holes. Harvesting was accomplished on August 28. For monitoring soil water dynamics, each subplot was equipped with standard tensiometers and volumetric water content sensors (5TM soil moisture sensors, Decacon devices, Pullman WA, USA) in plastic mulched ridges (15, 45 and 60 cm depth) and in uncovered furrows (15 and 30 cm depth). 30 cm depth in furrow positions is equivalent to 45 cm in ridge positions. In order to measure NO_3^- concentrations in seepage, suction lysimeter were additionally installed in ridges (15 and 45 cm depth) as well as in furrows (30 cm depth) and connected to a vacuum pump (KNF Neuberger, Type N86KNDCB12v, Freiburg i.Br. Germany). The collected water samples were kept refrigerated at $< 5^\circ\text{C}$ and analyzed within 24 hours for NO_3^- using Spectroquant quick tests (Nitrate test photometric, MERCK, South Korea) and a photometer (LP2W Digital Photometer, Dr. Lange, Germany). The observation period started on June 30 and ended with harvest on August 28, 2010.

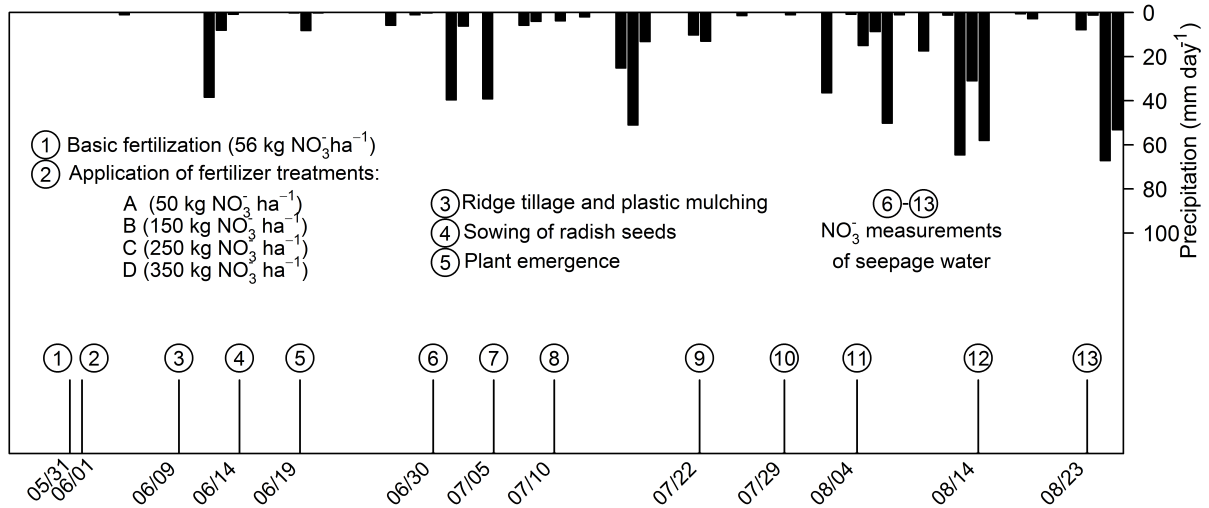


Figure 6.1: Precipitation rates, time schedule of tillage, crop management and NO_3^- measurements at the experimental site from May to August 2010.

6.2.3 Modeling approach

6.2.3.1 Model set up

To describe flow processes in a plastic mulched ridge cultivation system influenced by monsoonal events, surface and subsurface flow processes have to be considered. The process-based numerical code HydroGeoSphere is capable to solve fully-integrated surface and subsurface water flow and solute transport problems in a variable saturated media. Due to the coarse sandy texture of the field site, we assumed that preferential flow paths like macropore flow are negligible for soil water movement. Absent preferential flow was confirmed by Brilliant Blue tracer experiments at different field sites in the catchment (Ruidisch, in review). Therefore we simulated water flow based on finite element method as an uniform flow process, which can be described by the Richards' equation (6.1). The dimensions of the three-dimensional model are shown in Figure 6.2. The groundwater depth was calculated to be in approximately 4.5 m depth by interpolation of groundwater levels measured in the surrounding fields. Thus, we set up the model with a depth of 4.65 m. The model dimensions were chosen for several reasons. In general, we assumed that the flat field exhibited a dominating vertical flow field. These conditions exclude lateral flow processes such as downhill water flow. Furthermore, a high spatial resolution was necessary to implement small features such as planting holes. The high spatial resolution required in turn long computational time. In order to capture the most important flow and transport processes and to save computational time, we kept the model dimensions therefore as small as possible.

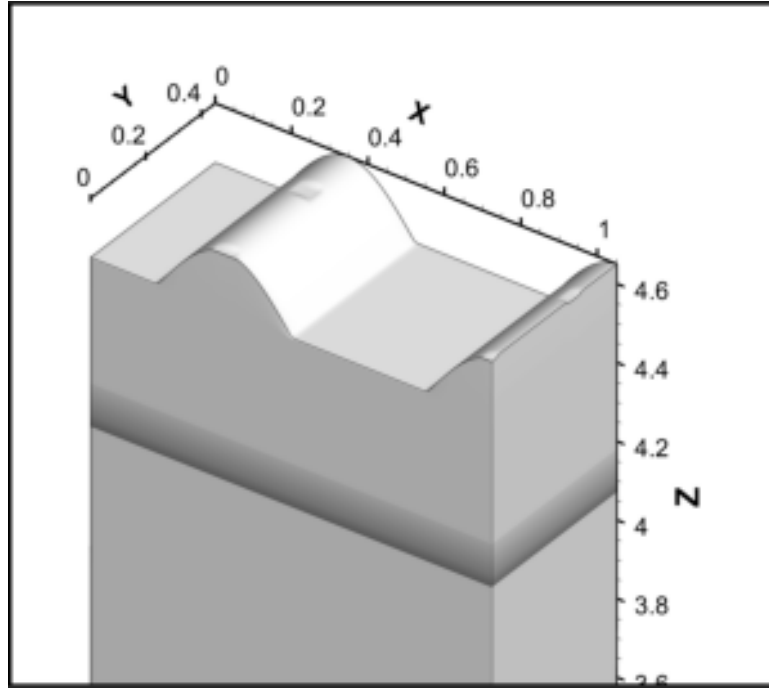


Figure 6.2: Dimensions of the three-dimensional model

6.2.3.2 Governing flow and transport equations

The governing flow and transport equations are given in Therrien et al. (2010). The units meter [L], day [T] and kg [M] were used for the simulations. Three dimensional subsurface flow in variable saturated porous media is described by a modified form of the Richards' equation (Equation (6.1)).

$$-\nabla \cdot \omega_m (-\bar{K} \cdot k_r \nabla(\varphi + z)) + \sum \Gamma_{\text{ex}} \pm Q = \omega_m \frac{\delta}{\delta t} (\theta_s S_w) \quad (6.1)$$

where ω_m [-] is the volumetric fraction of the total porosity occupied by the porous medium, \bar{K} is the hydraulic conductivity tensor [L T⁻¹], k_r is the relative permeability of the medium [-], φ is the pressure head [L], z is the elevation head [L], Γ_{ex} is the volumetric subsurface fluid exchange rate with the surface domain [L³ L⁻³ T⁻¹], Q is a subsurface fluid source or a sink [L³ L⁻³ d⁻¹], θ_s is the saturated water content [-] and S_w is degree of water saturation [-].

Surface flow in HydroGeoSphere is considered by a two-dimensional depth-averaged flow equation, which is the diffusion-wave approximation of the St. Venant equation.

$$-\nabla \cdot (d_o q_o) - d_o \Gamma_o \pm Q_o = \frac{\delta \phi_o h_o}{\delta t} \quad (6.2)$$

where the fluid flux q_o [$L T^{-1}$] is given by

$$q_o = -K_o \cdot k_{ro} \nabla(d_o z_o) \quad (6.3)$$

where ϕ_o is the surface flow domain porosity, h_o is the water surface elevation [L] ($h_o = d_o - z_o$) with d_o is the depth of flow [L] and z_o is the land surface elevation [L], K_o is the surface conductance [$L T^{-1}$], k_{ro} [-] is a factor that accounts for the reduction in horizontal conductance from obstruction storage exclusion, Γ_o is the volumetric surface fluid exchange rate with the subsurface domain [$L^3 L^{-3} T^{-1}$], Q_o is a surface fluid source or a sink [$L^3 L^{-3} T^{-1}$].

The surface–subsurface coupling is given by the exchange term

$$d_o \Gamma_o = \frac{k_r K_{zz}}{l_{\text{exch}}} (h - h_o) \quad (6.4)$$

where a positive Γ_o represents flow from the subsurface system to the surface system [$L^3 L^{-3} T^{-1}$], h_o is the surface water head [L], h is the subsurface water head [L], k_r is the relative permeability for the exchange flux [-], K_{zz} is the vertical saturated hydraulic conductivity of the underlying porous medium [$L T^{-1}$] and l_{exch} is the coupling length [L].

Transpiration takes place within the root zone and the transpiration rate (T_p) [$L T^{-1}$] based on (Kristensen and Jensen, 1975) is estimated as follows

$$T_p = f_1(LAI) f_2(\theta) RDF [E_p - E_{\text{can}}] \quad (6.5)$$

where f_1 (LAI) is a linear function of the leaf area index [-], f_2 (θ) is a function of nodal water content [-], and RDF is the time-varying root distribution function, E_{can} is the canopy evapotranspiration [$L T^{-1}$].

$$f_2(\theta) = \begin{cases} 0 & \text{for } 0 \leq \theta \leq \theta_{\text{wp}} \\ f_3 & \text{for } \theta_{\text{wp}} \leq \theta \leq \theta_{\text{fc}} \\ 1 & \text{for } \theta_{\text{fc}} \leq \theta \leq \theta_o \\ f_4 & \text{for } \theta_o \leq \theta \leq \theta_{\text{an}} \\ 0 & \text{for } \theta_{\text{an}} \leq \theta \end{cases} \quad (6.6)$$

where θ_{wp} , θ_{fc} , θ_o and θ_{an} is the moisture content [-] at the wilting point, field capacity, oxic and anoxic limit, respectively.

The three-dimensional transport of solutes considering advection, dispersion, retardation

and decay processes in a variably-saturated porous matrix is described in HydroGeoSphere as follows:

$$-\nabla \cdot (\omega_m(qC - \theta_s S_\omega D \nabla C)) + [\omega_m \theta_s S_\omega R \lambda C]_{par} + \sum \Omega_{ex} \pm Q_c = \omega_m \left[\frac{\delta(\theta_s S_\omega R C)}{\delta t} + \theta_s S_\omega R \lambda C \right] \quad (6.7)$$

where ω_m is the subsurface volumetric fraction of the total porosity [-], q is the subsurface fluid flux [$L T^{-1}$], C is the solute concentration [$M L^{-3}$], θ_s is the subsurface saturated water content [-], S_ω is the subsurface water saturation [-], D is subsurface hydrodynamic dispersion tensor [$L^2 T^{-1}$], Ω_{ex} is the mass exchange rate of solutes between subsurface and surface flow domain and Q_c is the fluid source or sink [$M L^3 T^{-1}$], λ is the first-order decay constant [L^{-1}] and R is the retardation factor [-]. In our modeling study, we only considered a conservative transport of NO_3^- and neglected retardation and decay. The hydrodynamic dispersion tensor D is given by Bear (1972):

$$\theta_s S_\omega D = (\alpha_l - \alpha_t \frac{qq}{|q|}) + \alpha_t |q| I + \theta_s S_\omega \tau D_{free} I \quad (6.8)$$

where α_l and α_t are the longitudinal and transversal dispersivities [L], $|q|$ is the magnitude of the Darcy flux, τ is the matrix tortuosity [-], D_{free} is the free-solution coefficient [$L^2 T^{-1}$] and I is the identity tensor. The product τD_{free} represents an effective diffusion coefficient for the matrix.

6.2.3.3 Initial and boundary conditions

The initial pressure head conditions in the model flow domain were adjusted to the observed pressure head using a steady state solution with a constant precipitation flux of 0.04 m day^{-1} . The solute transport simulation started on the day of the highest measured NO_3^- concentrations (July 10). The water flow model delivered the initial pressure head conditions for this simulation day. The initial concentration in the models was adjusted to the measured NO_3^- values on July 10 for all fertilizer rates. Indeed, we fixed NO_3^- concentrations with 160, 125-150, 200 and 230 $NO_3^- \text{ mg l}^{-1}$ corresponding to the fertilizer rate A 50 kg, B 150 kg, C 250 kg and D 350 kg $NO_3^- \text{- ha}^{-1}$ plus basic fertilizer ($56 \text{ kg } NO_3^- \text{- ha}^{-1}$), respectively. The bottom boundary condition of the models was specified as a free drainage boundary in 4.65 m depth. The left and right hand boundary was set to no flux conditions since the flat field conditions led to a mainly vertical flow field. For the scenarios with specified fertilizer placement we defined the initial concentration

of the fertilizer placement scenarios in a way that the initial mass of nitrate was exactly the same to the previous simulations regarding the different fertilizer rates. Hence, we increased the initial concentration in the ridges, while the initial mass in the model was equivalent to the fertilizer rates A 50 kg, B 150 kg, C 250 kg and D 350 kg $\text{NO}_3^- \text{ ha}^{-1}$.

The split applications were implemented in the modeling approach as follows: For the first application, the initial NO_3^- concentrations related to the specific fertilizer rate were included in the upper part of the model down to approximately 24 cm depth measured from the ridge surface. This translates to the local method of fertilizer application in the upper 15 cm of the soil before the ridges are created. The concentration and head conditions of June 25 were subsequently extracted and used as initial conditions to run the scenarios with a second application. The second application for each scenario was implemented by assuming that the fertilizer rate is solved in 0.25 liter water and applied only to the planting holes. Therefore we defined an initial water depth of 3.1 cm at the surface of the planting holes which equals 0.25 liter and implemented the initial concentration for each scenario at the surface of the planting holes. The third application for the model scenarios 3a, 3b and 3c was implemented in an analogous manner but using the initial head and concentration outputs from July 6 of the second application simulations.

6.2.3.4 Model parameterization, calibration and evaluation

In order to estimate pressure heads and nitrate concentrations using inverse modeling techniques, we coupled the HydroGeoSphere model with the Parallel PEST Version 12.1.0 (Doherty, 2005). PEST uses a nonlinear estimation technique known as the Gauss-Marquardt-Levenberg method. We derived the initial estimates of the Van Genuchten parameter based on measured texture and bulk density data (Table 6.1) using the ROSETTA model (Schaap et al., 2001), which estimates soil hydraulic parameters with hierarchical pedotransfer functions. The Van Genuchten parameters α and n and saturated hydraulic conductivity K_{sat} were estimated simultaneously for the measurement period of 17 June to 23 August 2010.

Based on the water flow model we subsequently implemented the solute transport. We initially estimated the transport parameters longitudinal, transversal and vertical transversal dispersivity based on literature values (Rausch et al., 2005) and optimized them for all fertilizer rates A-D. Initial estimated parameters are given in Table 6.2. We estimated the longitudinal dispersivity for both horizons in a range between 0.1 m and 1 m according to the findings of Gelhar et al. (1985), who showed that longitudinal dispersivity is scale-dependent. According to Pickens and Grisak (1981) the ratio of longitudinal and transversal dispersivity is between 0.01

Table 6.2: Initial estimates of water retention and solute transport parameters with θ_s : saturated water content, θ_r residual water content, α and n form parameters of the retention curve, K_{sat} saturated hydraulic conductivity, D_l longitudinal dispersivity, D_t transversal dispersivity, D_{vt} vertical transversal dispersivity.

	θ_s ($\text{m}^3 \text{ m}^{-3}$)	θ_r ($\text{m}^3 \text{ m}^{-3}$)	α (m^{-1})	n [-]	K_{sat} (m d^{-1})	D_l (m)	D_t (m)	D_{vt} (m)
Topsoil A	0.3855	0.0386	4.31	1.94	1.74	0.1	0.01	0.01
Subsoil B	0.3662	0.0366	4.55	1.71	0.97	0.1	0.01	0.01

and 0.3. Therefore, we initially estimated the transversal and vertical transversal dispersivity to be 0.01 and optimized them in a range between 0.1 and 0.001. The solute transport parameters were estimated for the observation period from July 10 to August 23. The first two observation dates were excluded from the optimization due to increasing concentrations at these dates. We affiliated these conditions to the stabilization phase of the suction lysimeters because the first two measurements were done shortly after the installation.

At the surface of the model, we implemented zones of infiltration (uncovered furrows and planting holes) and non-infiltration zones (plastic mulched ridges) using the model parameter coupling length. A coupling length of 0.1 m and 1000 m was defined for the infiltration zones and non-infiltration zones, respectively. For the simulation of RT (ridge tillage without plastic mulch) we defined a coupling length of 0.1 m for the entire surface of the model domain. The potential evaporation and transpiration rates were calculated based on the dual crop coefficient approach proposed by Allen et al. (1998) using the measured weather parameters like rainfall, temperature, humidity, solar radiation and wind speed.

For the evaluation of the models we used the coefficient of determination (R^2) and the Nash-Sutcliffe-Efficiency (CE). Moriasi et al. (2007) provided a comprehensive overview of the evaluation statistics for hydrological models. The coefficient of determination ranges from 0 to 1, where 1 indicates the total agreement between measured and simulated values. The Nash-Sutcliffe coefficient (Equation (6.9)) determines the relative magnitude of the residual variance compared to the observed data variance. The Nash-Sutcliffe-Efficiency varies between $-\infty$ and 1, where 1 indicates a perfect model. Model performance is unacceptable when the value is < 0 .

$$CE = 1 - \frac{\left[\sum_{i=1}^n (Y_i^{obs} - Y_i^{sim})^2 \right]}{\left[\sum_{i=1}^n (Y_i^{obs} - Y^{mean})^2 \right]} \quad (6.9)$$

where Y^{mean} indicates the mean of the observed data, Y_i^{obs} is the i th observation of the

observed and Y_i^{sim} is the i th observation of the simulated dataset, n is the total number of observations.

6.3 Results

6.3.1 Model evaluation and parameter optimization

The simultaneous estimation of soil hydraulic parameters n , α and K_{sat} resulted in similar n values compared to the initially estimated values with $n=1.92$ and $n=1.85$ for the topsoil and subsoil, respectively. In contrast, α values were estimated to be smaller than initially estimated with 2.89 m^{-1} for the topsoil and 2.97 m^{-1} for the subsoil. Relatively large n values lead to a quick drainage, which is characteristic for coarse textured material, whereas small α values indicate drainage under relatively low pressure head conditions, which is more common for finer soil texture. This combination of α and n was also found in a two-dimensional simulation study investigating water flow in sloped potato fields in the Haean catchment (Ruidisch et al., 2012). The saturated hydraulic conductivity (K_{sat}) was optimized to be 2.99 m d^{-1} and 1.88 m d^{-1} for the topsoil and subsoil, respectively, which is higher than the initially estimated K_{sat} values obtained by the ROSETTA model. In Figure 6.3 the comparison of simulated and measured pressure heads in different depths of ridge and furrow positions as well as evaluation coefficients R^2 and Nash-Sutcliffe efficiency (CE) are shown. In all depths and positions, the lowest pressure heads during drying cycles were underestimated by the model. In contrast, wet periods during monsoon were reasonable simulated except in furrow positions (30 cm depth), where pressure heads were underestimated during the entire simulation period.

The optimization of the solute transport parameters (longitudinal, transversal and vertical transversal dispersivity) showed that the parameters were similar among the fertilizer rates (Table 6.3). The highest longitudinal dispersivity was found for the lowest fertilizer rate but in general the differences to the other fertilizer rates were small. The longitudinal dispersivity for the subsoil was in a range between 0.012 m and 0.051 m, which was much smaller than longitudinal dispersivity for the top soil. The transversal and vertical transversal dispersivity for the subsoil was comparable with the optimized dispersivity for the topsoil. Due to the similarity of optimized dispersivity among fertilizer treatments, we calculated the mean for each parameter and used the mean parameter set for subsequent model simulations regarding the effect of different fertilizer rates, fertilizer placement and split applications on NO_3^- leaching loss. Although the agreement between measured and simulated pressure heads of the water

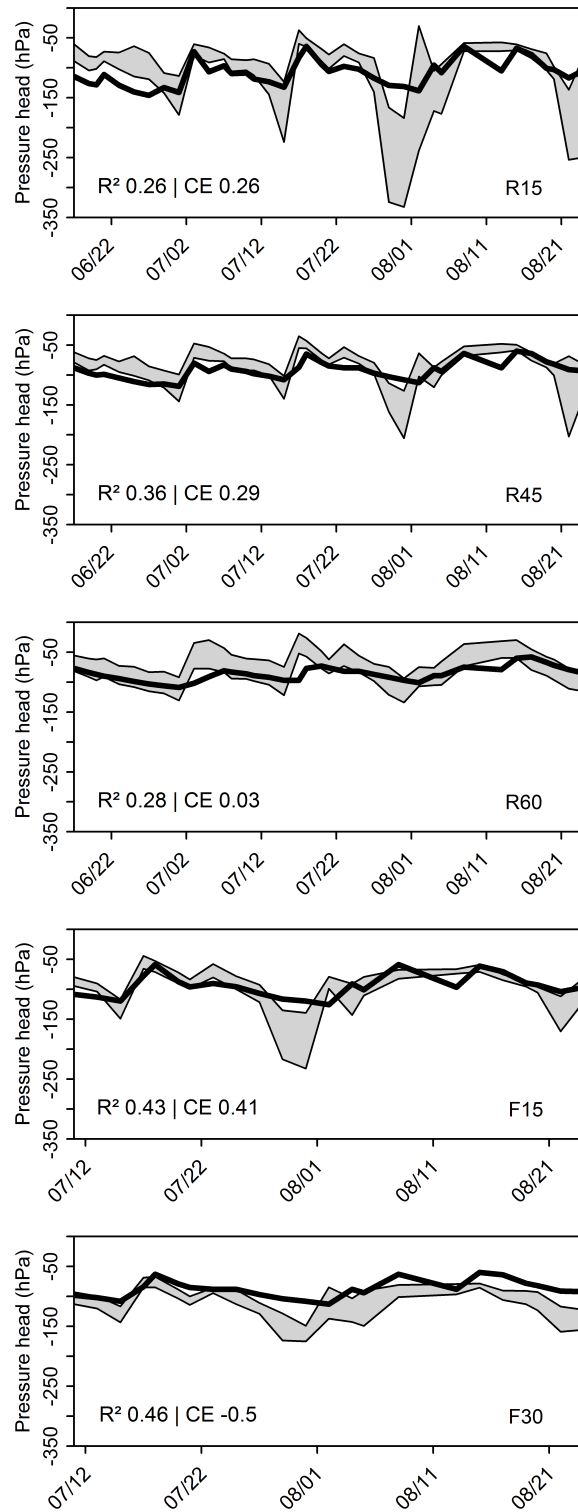


Figure 6.3: Observed vs. simulated pressure heads in ridge and furrow positions in different depths with evaluation coefficients R^2 (Coefficient of determination) and CE (Nash-Sutcliffe-coefficient), grey area limits: \pm std. dev. of observed data; R and F refers to ridge and furrow position in combination with soil depths 15, 30, 45 and 60 cm.

Table 6.3: Optimized solute transport parameters for fertilizer rates A-D.

	Dispersivity (m)	A (50 kg ha ⁻¹)	B (150 kg ha ⁻¹)	C (250 kg ha ⁻¹)	D (350 kg ha ⁻¹)	mean (m)
Topsoil A	D _l ^a	0.28	0.26	0.16	0.19	0.2225
	D _t ^b	1.0E-03	4.89E-02	1.0E-03	1.0E-02	0.01523
	D _{vt} ^c	5.57E-02	4.72E-02	5.15E-03	1.14E-03	0.02729
Subsoil B	D _l	5.10E-02	1.18E-02	1.49E-02	4.98E-02	0.03188
	D _t	1.0E-02	1.0E-03	8.99E-03	1.0E-02	0.0075
	D _{vt}	6.59E-03	1.0E-02	1.0E-03	9.94E-02	0.02925

^a longitudinal dispersivity

^b transversal dispersivity

^c vertical transversal dispersivity

flow model was not satisfying, the optimization for the solute transport model resulted in a reasonable agreement between measured and simulated NO₃⁻ concentrations (Figure 6.4). At all observation points the Nash Sutcliffe coefficient (CE) was ≥ 0.50 except under fertilizer rate C in the furrow position (30cm depth) and the coefficient of determination (R^2) was ≥ 0.54 for all observation points.

The fertilizer had been applied approximately one month before the NO₃⁻ concentration measurements. Hence, the measured NO₃⁻ concentrations on July 10 did not reflect the original applied fertilizer rates. For the subsequent modeling we therefore assumed that the applied granule fertilizer was latest solved with the first significant rain event after the application, which occurred on June 12 with a total precipitation amount of 38.4 mm. Hence, we implemented the respective NO₃⁻ concentrations on the following day (June 13) for the fertilizer rates and tested, whether the NO₃⁻ concentration of the simulation day 28, which equals the first measurement day (July 10), corresponds to the measured concentrations. The simulated concentrations were comparable to those measured on July 10. This seconds the assumption that the dissolution of granules with the first rain event was reliable and that the solute transport parameters reflected reasonably the distribution of NO₃⁻ in the soil profile. In the modeling study, we simulated a conservative transport and neglected decay processes such as denitrification. Denitrification depends on factors such as aeration, saturation and organic carbon content. Thus, anoxic conditions in combination with high carbon contents initiate denitrification processes. Due to the characteristics of the experimental field site with coarse textured sandy soil, high permeability and additionally low carbon content, denitrification processes at the experimental field site are assumed to be minimal or even absent. Although during monsoon events the soil was saturated short in time, the high saturated hydraulic conductivity of the soil led to fast drainage and oxic conditions after a monsoon event so that we excluded decay as a possible N pathway.

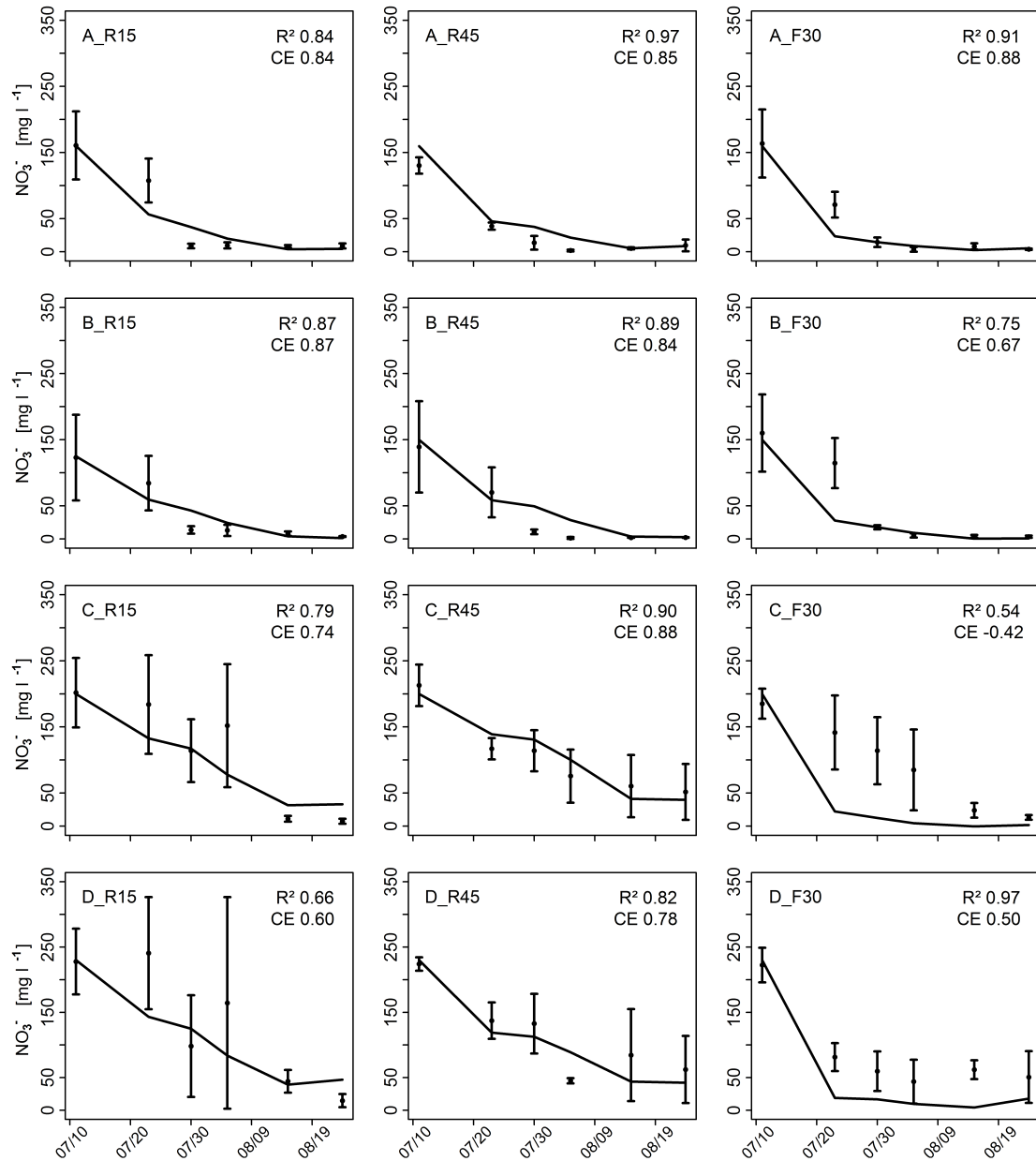


Figure 6.4: Observed vs. simulated nitrate concentrations in ridge and furrow positions in different depths with evaluation coefficients R^2 (coefficient of determination) and CE (Nash-Sutcliffe-coefficient), black solid line: simulated nitrate concentrations; error bars with means indicate the measured nitrate concentration; R15: ridge position in 15 cm soil depth, R45: ridge position in 45 cm soil depth, F30: furrow position in 30 cm soil depth; A-D refers to the fertilizer application rates of A 50 kg ha^{-1} , B 150 kg ha^{-1} , C 250 kg ha^{-1} , D 350 kg ha^{-1} .

6.3.2 The effect of plastic mulch on nitrate dynamics

To evaluate the effect of plastic mulching on nitrate dynamics, we compared the nitrate concentrations of the calibrated model (RT_{pm}) with a model simulation without plastic mulch (RT) using the fertilizer rate B (150 kg ha^{-1}). The comparison of the NO_3^- concentrations between the management treatments RT and RT_{pm} during the simulation period of 76 days are shown in Figure 6.5.

NO_3^- concentrations of about $2000\text{-}2200 \text{ mg l}^{-1}$ at the beginning of the simulation represented identical conditions for both treatments. Day 21 indicated the first significant rain event with a precipitation amount of about 40 mm d^{-1} . Under RT, the NO_3^- concentration decreased relatively homogeneously within the soil profile with slightly higher NO_3^- concentration in the inner part of the ridge. Compared to these conditions, RT_{pm} showed a clearly different behavior for the distribution of NO_3^- concentrations. The highest NO_3^- concentrations remained below the plastic coverage, while the lowest concentrations were simulated at the transition from ridges to furrows and in the area of the planting hole. This shows clearly, that surface runoff from the plastic covered ridge infiltrated in the furrow soil next to the ridge, which resulted in high NO_3^- leaching amounts at this part of the soil profile. In the middle part of the upper ridge, NO_3^- concentrations also decreased considerably under RT_{pm} due to the infiltration of water into the planting hole. At this simulation stage, only the NO_3^- concentration of about $1000\text{-}1500 \text{ mg l}^{-1}$ in the furrow soil was comparable between the management treatments. By comparing the simulated concentration on day 63, it was evident that the ridge topography led to a higher concentration of NO_3^- in the ridge soil compared to the furrow soil. The concentration front moved homogeneously deeper into the soil profile. Under RT_{pm} the NO_3^- concentration patterns at day 63 were still similar to day 21 except that the previously preferential leached areas at the transition of furrows to ridges and in the planting hole extended and the area of high NO_3^- concentrations below the plastic coverage narrowed. Until the end of the simulation NO_3^- concentrations further decreased, but generally it remained at a high level especially under the plastic coverage during the entire simulation.

These results showed that not only the plastic coverage but also the topography of the ridges potentially increased the nitrate availability in the root zone since surface runoff was channeled into the furrows and nitrate in the ridge soil was therefore protected. The results are in accordance to Locascio et al. (1985) and Cannington et al. (1975), who found that the plastic coverage led to enhanced fertilizer retention underneath the ridges and protected the fertilizer from leaching.

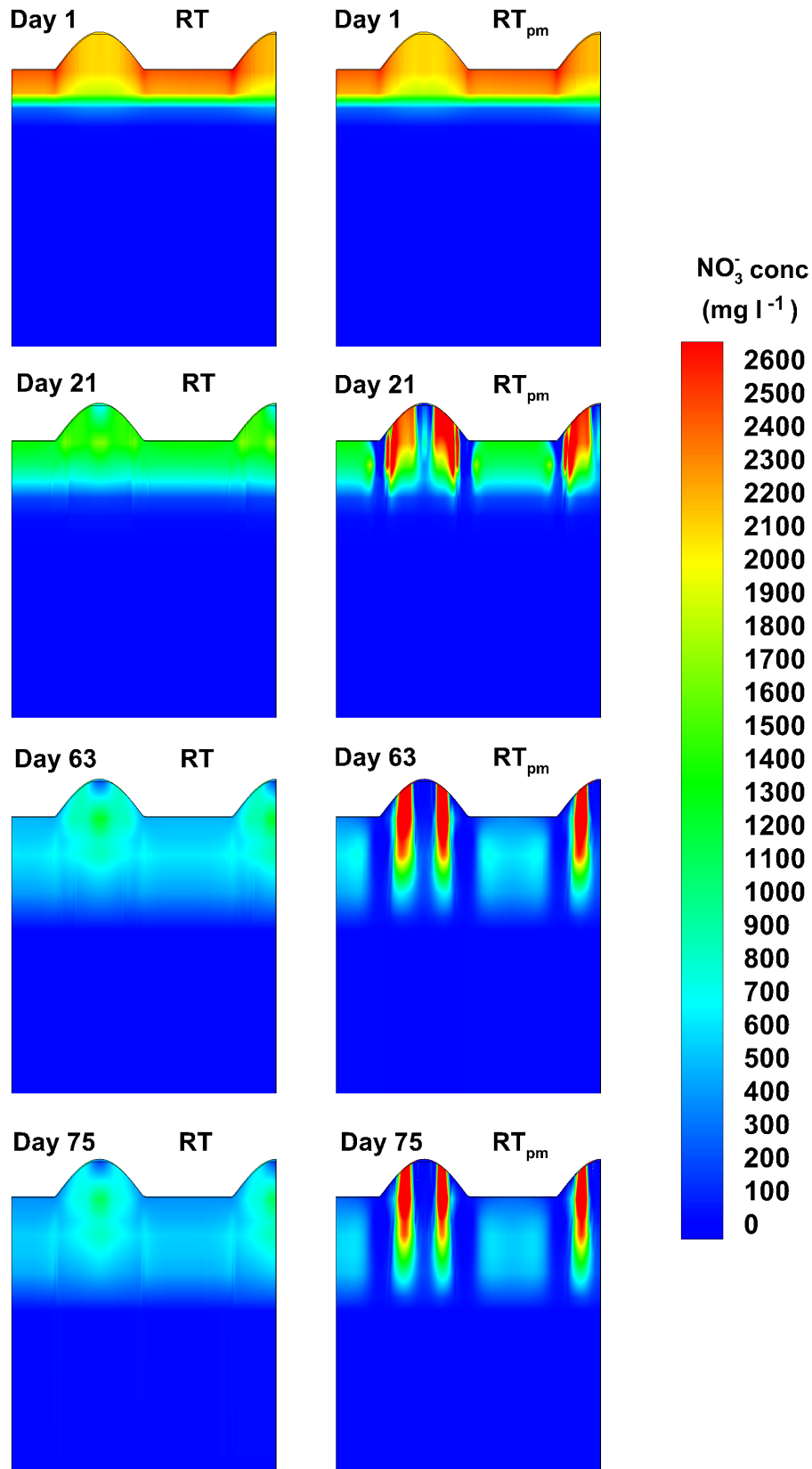


Figure 6.5: Comparison of simulated nitrate concentrations at days 1, 21, 63 and 75 under RT (ridge tillage without plastic mulch) and RT_{pm} (ridge tillage with plastic mulch).

6.3.3 The effect of plastic mulch on nitrate leaching loss

We further assessed the daily NO_3^- leaching loss in 45 cm in the soil profile for all fertilizer rates under RT and RT_{pm} (Figure 6.6). We assumed that this soil depth represents the zone, where nitrate was irreversibly lost for N uptake by radish crops. As expected, under both management strategies, the daily amount of leached NO_3^- increases with increasing fertilizer rates. High nitrate fluxes below the root zone are obviously associated with the heavy rainfall events. The simulation showed that peaks of NO_3^- leaching in 45 cm soil depth occurred with a time delay of 1-2 day after the respective rain event. The first two significant rain events occurred on day 20 and 23 both with a precipitation amount of approximately 40 mm d^{-1} . Considering the time shift, the total NO_3^- leaching loss from day 21 to day 25 was A ($2.98 \text{ kg NO}_3^- \text{ ha}^{-1}$) < B ($5.78 \text{ kg NO}_3^- \text{ ha}^{-1}$) < C ($8.58 \text{ kg NO}_3^- \text{ ha}^{-1}$) < D ($11.39 \text{ kg NO}_3^- \text{ ha}^{-1}$) under RT. In comparison to RT, the total NO_3^- leaching loss with plastic mulch (RT_{pm}) during this time period was 33.8% less. The heaviest monsoon event of the cropping season occurred from August 13 to August 15, 2010 (simulation days 62-64) with a total precipitation amount of 153.6 mm. This monsoon event led to nitrate leaching losses of A ($5.15 \text{ kg NO}_3^- \text{ ha}^{-1}$) < B ($10.0 \text{ kg NO}_3^- \text{ ha}^{-1}$) < C ($14.86 \text{ kg NO}_3^- \text{ ha}^{-1}$) < D ($19.71 \text{ kg NO}_3^- \text{ ha}^{-1}$) under RT below the root zone regarding the simulation days 63-66. Under RT_{pm} the leaching rates were 33.44% less compared to RT. In general, the highest daily NO_3^- leaching amount was simulated under RT with fertilizer rate D ($350 \text{ kg NO}_3^- \text{ ha}^{-1}$) on day 65 accounting for $6.04 \text{ kg NO}_3^- \text{ ha}^{-1} \text{ d}^{-1}$. Under dry weather conditions the leaching amounts were considerably lower ($< 0.1 \text{ kg NO}_3^- \text{ ha}^{-1}$).

After the simulation period of 76 days the cumulative amount of leached NO_3^- below the root zone under RT increased as follows: A ($23.61 \text{ kg NO}_3^- \text{ ha}^{-1}$) < B ($45.83 \text{ kg NO}_3^- \text{ ha}^{-1}$) < C ($68.09 \text{ kg NO}_3^- \text{ ha}^{-1}$) < D ($90.31 \text{ kg NO}_3^- \text{ ha}^{-1}$). Taking the basic fertilizer rate plus the fertilizer treatment rates into account, the total amounts of leached NO_3^- correspond to 22% of the total NO_3^- input. Plastic coverage of the ridges (RT_{pm}) resulted in lower cumulative leaching losses below the root zone with (A $17.56 \text{ kg NO}_3^- \text{ ha}^{-1}$) < B ($34.08 \text{ kg NO}_3^- \text{ ha}^{-1}$) < C ($50.66 \text{ kg NO}_3^- \text{ ha}^{-1}$) < D ($67.18 \text{ kg NO}_3^- \text{ ha}^{-1}$). This was equivalent to approximately 17% of the total NO_3^- input. Plastic mulching reduced the cumulative total NO_3^- leaching by 26% compared to RT.

This simulated nitrate leaching amounts corresponds to findings of Böhlke (2002), who reported in a literature review that commonly 10-50% of applied fertilizer N contributes to groundwater NO_3^- recharge under heavily fertilized and well-drained fields. Nevertheless, it has to be considered that the rain events in the observation period were only moderate compared to

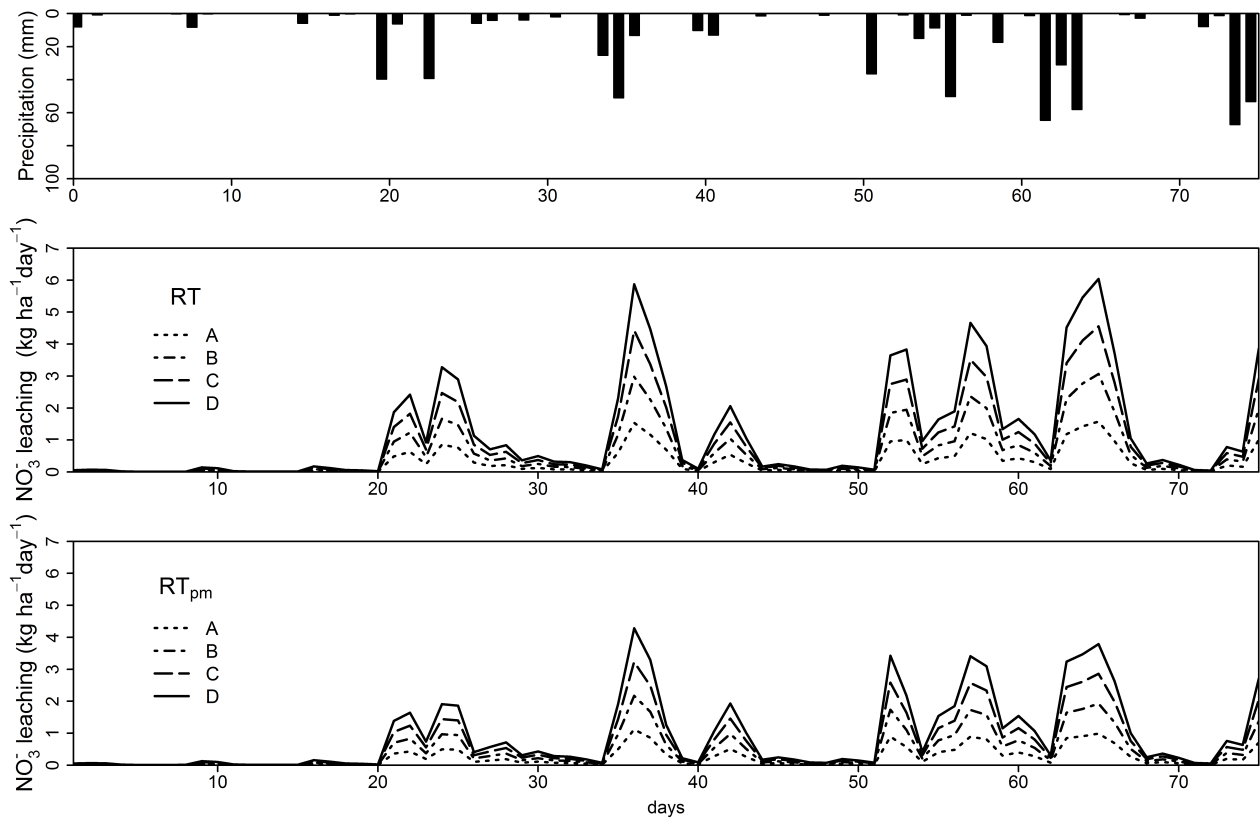


Figure 6.6: Precipitation rates and simulated daily nitrate leaching loss in 45 cm soil depth under RT (ridge tillage) and RT_{pm} (plastic mulched ridge tillage) and different fertilizer treatments (A: 50 kg NO₃⁻ ha⁻¹, B: 150 kg NO₃⁻ ha⁻¹, C: 250 kg NO₃⁻ ha⁻¹, D: 350 kg NO₃⁻ ha⁻¹).

other years. In the northeastern part of South Korea, rain events frequently exceed 100 mm d⁻¹ (Park et al., 2010). This supports the assumption that daily leached and cumulative leached NO₃⁻ can be even higher.

6.3.4 Fertilizer best management practices (FBMPs)

6.3.4.1 Enhanced fertilizer placement

Except of the primary tap root, the spreading root system of radishes is only weakly developed with dominating short fine roots. These conditions implicate that the fertilizer, which is distributed in the furrows, is most likely dispensable and irreversible lost for root water uptake. Therefore, we assumed that NO₃⁻ leaching loss can be reduced by an adapted fertilizer placement. We simulated NO₃⁻ leaching by placing the fertilizer only in ridges. Under RT, the treatment with fertilizer placed only in ridges led to cumulative NO₃⁻ leaching losses below the root zone in 45 cm depth of A (20.07 kg ha⁻¹) < B (38.96 kg ha⁻¹) < C (57.90 kg ha⁻¹) < D (76.9 kg ha⁻¹) after the simulation period of 76 days. Compared to the simulations with nitrate fertilizer uniformly distributed in ridges and furrows, the cumulative NO₃⁻ leaching loss was 15% lower

Table 6.4: Simulated cumulative NO_3^- leaching rates below the root zone as affected by plastic mulch and fertilizer placement. All values are given in $\text{kg NO}_3^- \text{ ha}^{-1}$.

	A	B	C	D
	50 kg ha^{-1}	150 kg ha^{-1}	250 kg ha^{-1}	350 kg ha^{-1}
$\text{RT}^{\text{a}} + \text{CF}^{\text{c}}$	23.61	45.83	68.09	90.31
$\text{RT}_{\text{pm}}^{\text{b}} + \text{CF}$	17.56	34.08	50.66	67.18
$\text{RT} + \text{FP}^{\text{d}}$	20.07	38.96	57.90	76.90
$\text{RT}_{\text{pm}} + \text{FP}$	11.19	21.71	32.27	42.79

^a ridge tillage without coverage

^b ridge tillage with plastic mulch

^c conventional fertilization in ridges and furrows

^d fertilizer placement only in ridges

and in total reduced by A (3.53 kg ha^{-1}) < B (6.86 kg ha^{-1}) < C (10.19 kg ha^{-1}) < D (13.52 kg ha^{-1}). Under RT_{pm} , the NO_3^- leaching loss below the root zone, when placing the fertilizer only in the ridges, was A (11.19 kg ha^{-1}) < B (21.71 kg ha^{-1}) < C (32.27 kg ha^{-1}) < D (42.79 kg ha^{-1}). The total reduction of NO_3^- leaching loss below the root zone by fertilizer application only to the ridges, was therefore A (6.38 kg ha^{-1}) < B (12.38 kg ha^{-1}) < C (18.39 kg ha^{-1}) < D (24.39 kg ha^{-1}), which is equivalent to 36% less leached NO_3^- (Table 6.4).

Our results revealed that a fertilizer placement restricted to the ridges is a valuable tool to considerably reduce NO_3^- leaching losses below the root zone. The results are in accordance with findings of Waddell and Weil (2006), who reported that the fertilizer application in the upper portion of the ridge in a corn cultivation led to lower N leaching losses and higher yields. Similar results were found by Clay et al. (1992), who investigated N fertilizer movement below ridges and furrows. They found that N placement in the ridge tops reduced N movement, while N movement in furrows increased due to the surface runoff from the ridges. Reduced nitrate leaching by placing nitrate only in the elevated portion of the ridges was further confirmed by Hamlett et al. (1990). These results have important economic and ecological implications. Firstly, farmers could benefit economically by fertilizer placement in the ridges. Secondly, this enhanced fertilizer placement could improve groundwater quality and might reduce environmental costs for amelioration of water quality and water purification caused by nitrate contamination.

6.3.4.2 Split applications

We developed the split application scenarios based on findings of the field experiment at the same field site (Kettering et al., unpublished data). The ^{15}N tracer experiment showed low fertilizer nitrogen use efficiencies (FNUE) at the beginning of the growing season because radishes had

Table 6.5: Fertilizer split application scenarios. All values are given in $\text{kg NO}_3^- \text{ ha}^{-1}$.

	Application 1	Application 2	Application 3
Scenario 1	150	-	-
Scenario 2a	75	75	-
Scenario 2b	50	100	-
Scenario 2c	30	120	-
Scenario 3a	50	50	50
Scenario 3b	30	60	60
Scenario 3c	20	80	50

not yet emerged. Accordingly, high fertilizer amounts during this early stage led to high nitrate leaching losses. This was confirmed by Bartsch, S. (unpublished data), who observed the highest NO_3^- concentrations of 31-33 mg l^{-1} in the groundwater next to the experimental field site from end of June to middle of July 2010. In the crop development stage, the FNUE increased significantly for all fertilizer rates. The highest FNUE with 30% was observed for the fertilizer rate B ($150 \text{ kg NO}_3^- \text{ ha}^{-1}$). Furthermore, the study showed that the biomass production at harvest time did not significantly differ for the fertilizer rates B (150 kg ha^{-1}), C (250 kg ha^{-1}) and D (350 kg ha^{-1}) so that fertilization above $150 \text{ NO}_3^- \text{ ha}^{-1}$ only increased the accumulation of NO_3^- in the radish root. Thus, Kettering et al. (unpublished data) recommended splitting the fertilizer application according to the plants N needs and suggested a maximum of $150 \text{ NO}_3^- \text{ ha}^{-1}$ in total. This was also proposed by Zhang et al. (1996), who stated that excessive fertilizer application should be prevented and more frequent, but smaller N applications during the rainy season with the additional use of slow-release fertilizer should help to maintain yield increase and minimize nitrate pollution of groundwater in northern China.

Hence, all split application scenarios (Table 6.5) were developed based on the total amount of $150 \text{ kg NO}_3^- \text{ ha}^{-1}$. The reference scenario (Scenario 1) refers to ridge tillage with plastic mulching (RT_{pm}) and a fertilizer application of $150 \text{ kg NO}_3^- \text{ ha}^{-1}$ at the beginning of the growing season distributed in ridges and furrows. The distribution of fertilizer in ridges and furrows for the first application was also characteristic for all other scenarios. For the scenarios 2a and 3a, we separated the fertilizer application into equal amounts. The other scenarios represent the application of successive reduced fertilizer amounts at the beginning of the growing season. Generally the second and third application was implemented after rainfall events.

In Figure 6.7a the cumulative nitrate leaching loss below the root zone for all scenarios are shown. As expected, the highest cumulative leaching loss was simulated for the reference scenario 1 ($34.1 \text{ kg NO}_3^- \text{ ha}^{-1}$). The other scenarios resulted in total cumulative NO_3^- leaching

loss per ha in the order of 2a (23.7 kg NO₃⁻ ha⁻¹) > 3a (19.4 kg NO₃⁻ ha⁻¹) > 2b (19.2 kg NO₃⁻ ha⁻¹) > 2c and 3b (15.7 kg NO₃⁻ ha⁻¹) > 3c (13.9 kg NO₃⁻ ha⁻¹). This was equivalent to a reduction of 30% (2a) < 44% (3a and 2b) < 54% (2c and 3c) < 59% (3c) of the total NO₃⁻ leaching loss in comparison to the reference scenario 1 (Table 6.6). The results indicated that a small application at the beginning of the growing season followed by a high application rate in the development stage of the crops and again a smaller application in the later season is most effective in reducing nitrate leaching loss to groundwater.

6.3.4.3 Combination of plastic mulching, fertilizer placement and split applications

All three management practices, namely plastic mulching of the ridges, fertilizer placement only in the ridges and split applications, showed that NO₃⁻ leaching loss to groundwater can be substantially reduced. Thus, we assumed that the combination of all management practices should lead to multiplicative effects in decreasing nitrate leaching below the root zone. Subsequently, we combined all management practices in our modeling study to assess the positive effect on NO₃⁻ leaching loss. Therefore, we placed the fertilizer for the first application solely in the plastic mulched ridges. For the second and third application we maintained the procedure of applying solved fertilizer in planting holes after the rain events.

In Figure 6.7b the cumulative NO₃⁻ leaching losses for all scenarios with combined management practices are shown. By taking the results of the simulation RT (ridge tillage without plastic coverage) and fertilizer rate B as the reference (cumulative total NO₃⁻ leaching loss of 45.83 kg NO₃⁻ ha⁻¹), the combination of the three management practices resulted in leached cumulative NO₃⁻ amounts of 14.25 kg NO₃⁻ ha⁻¹ (2a) > 12.25 kg NO₃⁻ ha⁻¹ (2b) > 11.3 kg NO₃⁻ ha⁻¹ (3a) > 9.99 kg NO₃⁻ ha⁻¹ (2c) > 9.13 kg NO₃⁻ ha⁻¹ (3b) > 8.14 kg NO₃⁻ ha⁻¹ (3c). Expressed as a percentage, NO₃⁻ leaching loss was 69% (2a) < 73% (2b) < 75% (3a) < 78% (2c) < 80% (3b) < 82% (3c) lower compared to the reference scenario (Table 6.6).

Consequently, the results verified the multiplicative effects of combined FBMPs. The local method of plastic mulched ridge cultivation is therefore a good step towards a sustainable management, which can be enhanced by additional FBMPs, when focusing solely on nitrate contamination of groundwater resources. Nevertheless, a differentiated view of the tillage practice on ecological impacts is necessary. Other studies showed that plastic mulching in highland agriculture vegetable production on hillslopes, especially during monsoon periods, have also negative effects by substantially increasing surface runoff (Ruidisch et al., 2012), Arnhold,

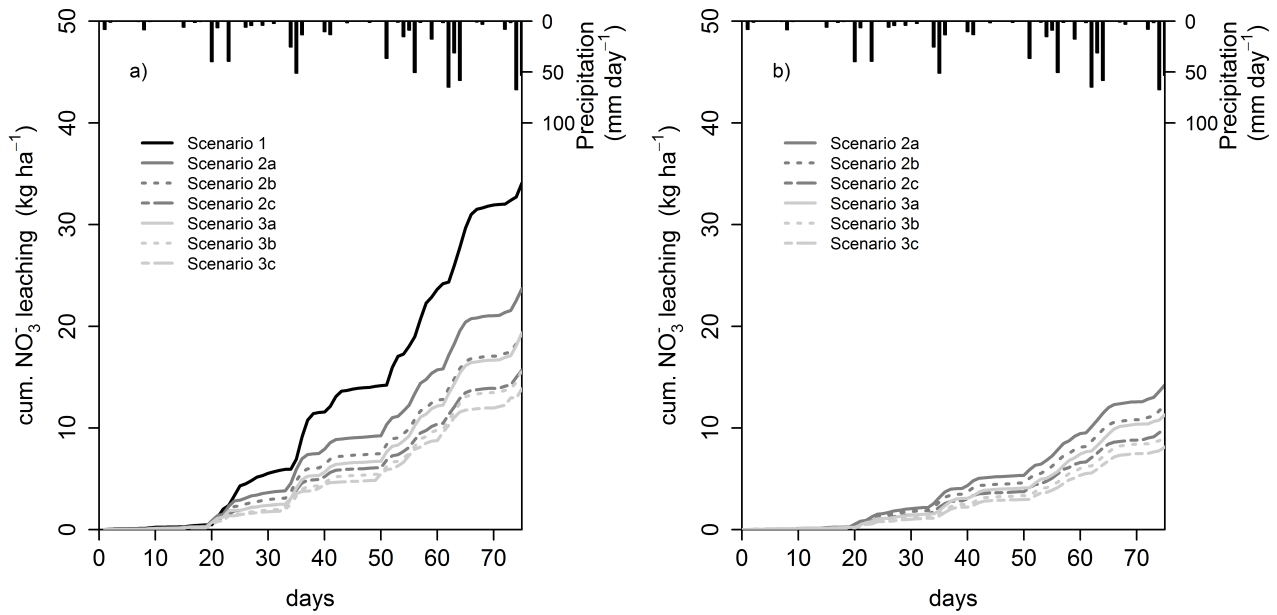


Figure 6.7: Simulated cumulative nitrate leaching after 76 days below the root zone for (a) split application scenarios only and (b) combination of enhanced fertilizer placement and split applications.

Table 6.6: Simulated cumulative NO_3^- leaching rates below the root zone as affected by plastic mulch, split applications and fertilizer placement. All values are given in $\text{kg NO}_3^- \text{ ha}^{-1}$.

	$\text{RT}_{\text{pm}}^{\text{a}} + \text{CF}^{\text{b}}$	$\text{RT}_{\text{pm}} + \text{FP}^{\text{c}}$
Scenario 1	34.1	21.71
Scenario 2a	23.7	14.25
Scenario 2b	19.2	12.25
Scenario 2c	15.7	9.99
Scenario 3a	19.4	11.3
Scenario 3b	23.7	9.13
Scenario 3c	13.9	8.14

^a ridge tillage with plastic mulch

^b conventional fertilization in ridges and furrows

^c fertilizer placement only in ridges

unpublished data), which causes high soil erosion rates and increased transport of nutrients, in particular phosphorous bounded on sediment particles, via surface runoff into water bodies (Park et al., 2010; Kim et al., 2001). In a different modeling study, the surface runoff in plastic mulched potato cultivation on hillslopes was increased up to 65%, whereas drainage water was reduced by 16% compared to ridge tillage without plastic coverage (Ruidisch et al., 2012). Based on these findings, it was concluded that the application of perforated plastic mulch supports the advantages of reducing drainage water, controlling weeds and earlier plant emergence and concurrently diminishes the negative effects such as excessive surface runoff.

In the presented modeling study, we assessed the impact of plastic mulching on N leaching losses in RT_{pm} in a flat terrain. Hence, an excessive runoff from fields to the river network is not expected. Moreover, water was observed to pond at the surface during monsoon events, when the infiltration capacity was exceeded, but percolated afterwards through the soil matrix and contributed to groundwater. This implicates that plastic mulching under these specific topographical conditions can be recommended, especially in combination with FBMPs such as fertilizer placement in ridges and split applications. Indeed, FBMPs seems to be promising also for the hillsloped dryland agricultural field, which makes up the largest part of the catchment. The given FBMPs implicate that high NO_3^- rates remain below the plastic cover unless the NO_3^- was not taken up by the plants during the cropping seasing. However, in the course of harvesting, plastic mulched ridges are destroyed, so that the protective function of the cropping system is not longer present. This conditions result in a higher leaching risk after harvest, especially if the rain fall variability is taken into account. In the growing season 2010 e.g., several heavy rainfall events occurred in the middle to late September after harvest. A rotating cropping system, which can benefit from the remaining NO_3^- in the soil, is another conceivably option, which would have several advantages. On the one hand it would improve N fixation in autumn, reduces the NO_3^- leaching risk after harvest and increases the N_{min} for the following growing season. On the other hand, the agricultural fields are currently prone to soil erosion after harvest due to the fallowness. A cover crop would therefore additionally help to reduce the erosion risk after harvest as well as to increase the organic carbon content (C_{org}) content of the soils.

6.4 Conclusion

Excessive mineral fertilizer application in combination with extreme rain event during East-Asian summer monsoon plays a key role in leaching agrochemical contaminants to aquatic systems. In view of the fact that high fertilizer inputs coincide with high economical cost, but

also cause negative ecological effects, a prior prevention of ecological damages or more specifically, the reduction of water quality degradation of groundwater and surface water bodies is therefore urgently needed.

The simulation results showed that ridge cultivation and plastic mulching of the ridges constitutes a valuable tool to decrease nitrate leaching in a flat terrain, where the precipitation contributes entirely to infiltration through the unsaturated zone. In hillslope areas, however, it increases surface runoff tremendously, which supports the transport of agrochemicals via surface runoff directly into the rivers. Thus, topographical aspects should be considered when plastic mulched ridge cultivation is practiced. Fertilizer best management practices (FBMPs) include an appropriate amount of total fertilizer input, right placement and right timing of fertilizer. Especially the timing is important in regions affected by extreme rain events, when daily leaching amounts can be considerably high. Thus, FBMPs can help increase the nutrient use efficiency of the crops and concurrently decrease nitrate leaching below the root zone. Our study revealed that the combination of FBMPs can minimize nitrate leaching considerably. Therefore, we suggest to

- reduce the total fertilizer amount to $150 \text{ kg NO}_3^- \text{ ha}^{-1}$
- apply plastic mulch in a flat terrain and perforated plastic mulch on hillslopes
- place the fertilizer only in ridges
- and apply fertilizer three times with e.g. $20 \text{ kg} / 80 \text{ kg} / 50 \text{ kg NO}_3^- \text{ ha}^{-1}$
- plant cover crops after harvest to improve N fixation, to reduce NO_3^- leaching, to increase C_{org} content and to prevent soil erosion loss in autumn.

Combining those management practices will lead to economical benefits in terms of decreasing fertilizer inputs as well as ecological benefits by reducing substantially the risk of groundwater pollution.

Acknowledgements

This study was carried out as part of the International Research Training Group TERRECO (GRK 1565/1) funded by the Deutsche Forschungsgemeinschaft (DFG) at the University of Bayreuth, Germany and the Korean Research Foundation (KRF) at Kangwon National University, Chuncheon, S. Korea. We would like to thank especially Mr. Park und Mrs. Kwon for their excellent support.

References

- Allen, R., L. Pereira, D. Raes, and M. Smith (1998). *Crop evapotranspiration. Guidelines for computing crop water requirements*. Rome, Italy: FAO. ISBN: 9789251042199.
- Bargar, B., J. B. Swan, and D. Jaynes (1999). "Soil water recharge under uncropped ridges and furrows". In: *Soil Science Society of America Journal* 63.5, pp. 1290–1299. ISSN: 0361-5995.
- Bear, J. (1972). *Dynamics of Fluids in Porous*. American Elsevier, New York.
- Benjamin, J., A. Blaylock, H. Brown, and R. Cruse (1990). "Ridge tillage effects on simulated water and heat transport". In: *Soil & Tillage Research* 18.2-3, pp. 167–180.
- Böhlke, J.-K. (2002). "Groundwater recharge and agricultural contamination". In: *Hydrogeology Journal* 10.1, pp. 153–179.
- Cannington, F., R. B. Duggings, and R. G. Roan (1975). "Florida vegetable production using plastic film mulch with drip irrigation". In: *Proceedings 12th Natl Agr Plastics Congr.*
- Choi, W.-J., G.-H. Han, S.-M. Lee, G.-T. Lee, K.-S. Yoon, and S.-M. Choi (2007). "Impact of land-use types on nitrate concentration and delta N-15 in unconfined groundwater in rural areas". In: *Agriculture, Ecosystems & Environment* 120.2-4, pp. 259–268.
- Clay, S., D. Clay, W. Koskinen, and G. Malzer (1992). "Agrichemical placement impacts onalachlor and nitrate movement through soils in a ridge tilled system". In: *Journal of Environmental Science and Health* B27.2, pp. 125–138.
- Danielopol, D. L., C. Griebler, A. Gunatilaka, and J. Notenboom (2003). "Present state and future prospects for groundwater ecosystems". In: *Environmental Conservation* 30.2, pp. 104–130.
- Doherty, J. (2005). *PEST Model- independent parameter estimation*. 5th. Watermark numerical computing.
- Gelhar, L. W., A. Mantoglou, C. Welty, and K. R. Rehfeldt (1985). *A review of field-scale physical solute transport processes in saturated and unsaturated porous media*. Final report. Cambridge, Massachusetts: Tennessee Valley Authority.
- Hamlett, J., J. Baker, and R. Horton (1990). "Water and anion movement under ridge tillage: a field study". In: *Transactions of the American Society of Agricultural Engineers* 33, pp. 1859–1866.
- Jaynes, D. and J. Swan (1999). "Solute Movement in Uncropped Ridge-Tilled Soil under Natural Rainfall". In: *Soil Science Society of America Journal* 63, pp. 264–269.
- Kettering, J., J.-H. Park, S. Lindner, B. Lee, J. Tenhunen, and Y. Kuzyakov (2012). "N fluxes in an agricultural catchment under monsoon climate: A budget approach at different scales".

- In: *Agriculture, Ecosystems & Environment* 161, pp. 101–111. DOI: 10.1016/j.agee.2012.07.027.
- Kim, B., J.-H. Park, G. Hwang, M.-S. Jun, and K. Choi (2001). “Eutrophication of reservoirs in South Korea”. In: *Limnology* 2, pp. 223–229. ISSN: 1439-8621. DOI: 10.1007/s10201-001-8040-6.
- Koh, D.-C., G.-T. Chae, Y.-Y. Yoon, B.-R. Kang, G.-W. Koh, and K.-H. Park (2009). “Baseline geochemical characteristics of groundwater in the mountainous area of Jeju Island, South Korea: Implications for degree of mineralization and nitrate contamination”. In: *Journal of Hydrology* 376.1-2, pp. 81–93.
- Koh, D.-C., K.-S. Ko, Y. Kim, S.-G. Lee, and H.-W. Chang (2007). “Effect of agricultural landuse on the chemistry of groundwater from basaltic aquifers, Jeju Island, South Korea”. In: *Hydrogeology Journal* 15, pp. 727–743.
- Kristensen, K. and S. Jensen (1975). “A model for estimating actual evapotranspiration from potential evapotranspiration”. In: *Nordic Hydrology* 6.3, pp. 170–188.
- Lament, W. J. (1993). “Plastic mulches for the production of vegetable crops”. In: *HortTechnology* 3.1, pp. 35–39.
- Leistra, M. and J. J. T. I. Boesten (2010). “Pesticide Leaching from Agricultural Fields with Ridges and Furrows”. In: *Water Air and Soil Pollution* 213.1-4, pp. 341–352. ISSN: 0049-6979. DOI: 10.1007/s11270-010-0389-x.
- Liu, G. D., W. L. Wu, and J. Zhang (2005). “Regional differentiation of non-point source pollution of agriculture-derived nitrate nitrogen in groundwater in northern China”. In: *Agriculture, Ecosystems & Environment* 107.2-3, pp. 211–220.
- Locascio, S. J., J. G. A. Fiskell, D. A. Graetz, and R. D. Hawk (1985). “Nitrogen accumulation by peppers as influenced by mulch and time of fertilizer application”. In: *Journal of the American Society for Horticultural Science* 110, pp. 325–328.
- Matson, P. A., W. J. Parton, A. G. Power, and M. J. Swift (1997). “Agricultural Intensification and Ecosystem Properties”. In: *Science* 277.5325, pp. 504–509.
- Min, J., S. Yun, K. Kim, H. Kim, J. Hahn, and S. Lee (2002). “Nitrate contamination of alluvial groundwaters in the Nakdong river basin, Korea”. In: *Geosciences Journal* 6, pp. 35–46.
- Moriasi, D. N., J. G. Arnold, M. W. van Liew, R. L. Bingner, R. D. Harmel, and T. L. Veith (2007). “Model evaluation guidelines for systematic quantification of accuracy in watershed simulations”. In: *Transactions of the ASABE* 50.3, pp. 885–900. ISSN: 0001-2351.

- Ongley, E. D. (1996). *Control of water pollution from agriculture*. Ed. by FAO. FAO Irrigation and Drainage Paper 55. Rome, Italy: FAO Food and Agriculture Organization of the United Nations.
- Park, J.-H., L. Duan, B. Kim, M. J. Mitchell, and H. Shibata (2010). “Potential effects of climate change and variability on watershed biogeochemical processes and water quality in Northeast Asia”. In: *Environment International* 36.2, pp. 212–225. ISSN: 01604120.
- Pickens, J. F. and G. E. Grisak (1981). “Scale-dependent dispersion in a stratified granular aquifer”. In: *Water Resources Research* 17.4, pp. 1191–1211.
- Rausch, R., W. Schäfer, R. Therrien, and C. Wagner (2005). *Solute transport modelling: An Introduction to Models and Solution Strategies*. Berlin, Stuttgart: Gebr. Borntraeger.
- Ruidisch, M., J. Kettering, S. Arnhold, and B. Huwe (2012). “Modeling water flow in a plastic mulched ridge cultivation system on hillslopes affected by South Korean summer monsoon”. In: *Agricultural Water Management*. DOI: 10.1016/j.agwat.2012.07.011.
- Schaap, M., F. Leji, and M. van Genuchten (2001). “ROSETTA: a computer program for estimating soil hydraulic parameters with hierarchical pedotransfer functions”. In: *Journal of Hydrology* 251, pp. 163–176.
- Spiertz, J. H. J. (2010). “Nitrogen, Sustainable Agriculture and Food Security: A Review”. In: *Agronomy for Sustainable Development* 30.1, pp. 43–55.
- Therrien, R., R. McLaren, E. Sudicky, and S. Panday (2010). *HydroGeoSphere: A Three-dimensional numerical model describing fully-integrated subsurface and surface flow and solute transport*. University of Waterloo. Waterloo, Canada.
- Tilman, D., K. G. Cassman, P. A. Matson, R. Naylor, and S. Polasky (2002). “Agricultural sustainability and intensive production practices”. In: *Nature* 418.6898, pp. 671–677. ISSN: 0028-0836. DOI: 10.1038/nature01014.
- Waddell, J. T. and R. R. Weil (2006). “Effects of fertilizer placement on solute leaching under ridge tillage and no tillage”. In: *Soil & Tillage Research* 90.1-2, pp. 194–204.
- Wallace, A. (1994). “High-precision agriculture is an excellent tool for conservation of natural resources”. In: *Communications in Soil Science and Plant Analysis* 25.1-2, pp. 45–49. DOI: 10.1080/00103629409369002.
- Zhang, W., Z. Tian, N. Zhang, and X. Li (1996). “Nitrate pollution of groundwater in northern China”. In: *Agriculture, Ecosystems and Environment* 59, pp. 223–231.

Declaration

Erklärung zur Promotionsarbeit: „Flow and transport processes as affected by tillage management under monsoonal conditions in South Korea“, eingereicht von Frau Marianne Ruidisch, geb. 18.03.1979.

Hiermit erkläre ich, dass ich die vorliegende Promotionsarbeit selbständig verfasst und keine anderen als die angegebenen Quellen und Hilfsmittel benutzt habe.

Bayreuth, 28.9.2012

Marianne Ruidisch

Hiermit erkläre ich, dass ich nicht bereits anderweitig versucht habe, diese Disseration ohne Erfolg einzureichen oder mich einer Doktorprüfung zu unterziehen.

Bayreuth, 28.9.2012

Marianne Ruidisch

Hiermit erkläre ich, dass ich die Hilfe von gewerblichen Promotionsberatern bzw. -vermittlern weder bisher in Anspruch genommen habe, noch künftig in Anspruch nehmen werde.

Bayreuth, 28.9.2012

Marianne Ruidisch